



**MECHANISMS AND NON-LINEAR  
PROBLEMS OF NUCLEATION AND  
GROWTH OF CRYSTALS AND  
THIN FILMS**

**2019**

# **BOOK OF ABSTRACTS**

**INTERNATIONAL CONFERENCE  
MECHANISMS AND NON-LINEAR  
PROBLEMS OF NUCLEATION AND  
GROWTH OF CRYSTALS AND  
THIN FILMS**

**1-5 JULY  
2019**

**SAINT-PETERSBURG  
RUSSIA**

**[WWW.MGCTF.RU](http://WWW.MGCTF.RU)**

# ORGANIZERS



Institute for problems  
in mechanical engineering  
(IPME RAS), Laboratory  
of structural and phase  
transitions in condensed  
matter



Saint-Petersburg  
Scientific Center RAS



Scientific and Technical Center  
– New Technologies” Ltd.



Monomax PCO

“New Silicon Technologies” Ltd.

# SPONSORS



General Sponsor  
"TESCAN Ltd."

## PREFACE



**VITALY VALENTINOVICH SLYOZOV**

09.03.1930—30.10.2013

International conference “Mechanisms and Non-linear Problems of Nucleation and Growth of Crystals and Thin Films” (MGCTF 2019) inherits traditions initiated by two international conferences devoted to an analysis of fundamental problems of phase transitions of the first kind. One of these conferences, “Nucleation and Non-linear Problems in First-order Phase Transitions” (NPT), was held in 1998 (NPT98) and 2002 (NPT2002) in Saint-Petersburg and was organized by the Laboratory of Structural and Phase Transformations in Condensed Matter of the Institute for Problems in Mechanical Engineering of the Russian Academy of Sciences (Prof. Sergey A. Kukushkin, Saint-Petersburg); another one is the research workshop “Nucleation Theory and Applications” that was carried out for 20 years (1997-2016) in Dubna and was organized by the Bogoliubov Laboratory of Theoretical Physics of the Joint Institute for Nuclear Research (Prof. Vyacheslav B. Priezhev, Dubna) in cooperation with the Institute of Physics of the University of Rostock (Prof. Jörn W.P. Schmelzer, Rostock, Germany). These two conferences covered practically all the major global trends and directions of the fundamental problems in the kinetic theory of phase transitions of the first kind.

Prof. Vitaly V. Slyozov (alternate spelling: Slezov) was the permanent plenary speaker and scientific “maestro” of both the mentioned conferences. Prof. V.V. Slyozov together with I.M. Lifshitz created the famous Lifshitz-Slyozov theory of Ostwald ripening, which describes one of the most fundamental processes in the kinetics of phase transformations, namely the late stage of phase transitions of the first kind. The Lifshitz-Slyozov law of evolution of ensembles of new-phase nuclei at the late stage has a universal appearance and describes behavior of the ensembles of new-phase grains in any system. The year 2018 marked the 60<sup>th</sup> anniversary of the Lifshitz-Slyozov theory, and the year 2020 will mark 90 years since the birth of Prof. V.V. Slyozov.

In recent years, the scope of application of phase transitions has significantly expanded. The fundamental problems of the formation of a new phase, which arise from the synthesis of new materials, nanostructures and nanowires, require the development of new thorough approaches based on the foundation of the theory of phase transitions that was created by the works of such “Titans” as J. Gibbs, M. Volmer and A. Weber, R. Becker and W. Döring, I. Lifshitz and V. Slyozov, Ya. Frenkel, Ya. Zeldovich, and F. Kuni.

The most important goal of this conference is to unite specialists working on the theory of phase transitions with technologists and experimenters who grow crystals and films. The conference will help to advance in obtaining new innovative materials for the creation of modern technologies. We hope that this conference will establish direct cooperation between leading scientists and research groups, create conditions for future joint work, discover and discuss new promising directions for the growth of films, crystals and structures of new semiconductor materials for their utilization in various

devices. Additional attention will be given to the processes occurring during phase transitions in the atmosphere and biology: formation of kidney stones, gallstones, blood clots is the problem concerning phase transitions of the first kind as well, and, in such systems, just like in any other ones, the evolution of the new-phase nuclei at the late stage of phase transitions obeys the Lifshitz-Slyozov law which is a guiding star for us as we move through the complex multi-factor processes of formation of a new phase.

I wish you fruitful discussions, new ideas and success in the work of the conference.

MGCTF-2019 Chair

*S. A. Kukushkin*

**SESSION “Mechanisms of crystal formation and growth in single- and multi-component systems: theoretical description of the process, numerical modeling, experimental results”**

**PHOTOPOLYMERIZATION PRODUCTS OF NEW DIACETYLENE ALCOHOL DERIVATIVES**

**Alekseev A.S.<sup>1</sup>, Domnin I.N.<sup>2</sup>, Ivanov A.B.<sup>1</sup>**

*1 - Prokhorov General Physics Institute Russian Academy of Sciences*

*2 - Saint Petersburg State University*

*alexanderalekseev@yandex.ru*

Photopolymerization of unsymmetrical diynes in Langmuir-Schaefer films with *N*-arylcarbamate groups in the hydrophobic part and hydroxymethylene groups in the hydrophilic part of the molecules was under the study. Colorless films transformed into intensely colored objects under UV irradiation due to the solid-state topochemical polymerization (STP) reaction. Usually the products of DA alcohol derivatives polymerization are the red phase PDAs. The result of new compounds photopolymerization (red, purple or blue phase PDA) was dependent on a number of methylene groups in hydrophobic (*m*) and hydrophilic (*n*) parts of studied molecules, and the type of aryl ring substituent (MeO group or hydrogen atom). The presence of hydrogen atom and the variation of *m* value from 5 to 6 changed the result of STP: instead of blue phase PDA observed for diyne with MeO group, the red phase PDA ( $\lambda_{\max} \sim 520$  nm) was appeared. The purple phase PDA film ( $\lambda_{\max} \sim 570-580$  nm) could be obtained, when the monolayer of compound with *m* = 9 and *n* = 2 UV irradiated. The films of molecules with *m* = 5 and *n* = 2, were transformed into blue phase polymeric films ( $\lambda_{\max} \sim 620-625$  nm), resistant to external influences. The addition of one methylene group at hydrophobic part of the molecule (*m* = 6) allowed to create the blue phase PDA film with the longest conjugation length of the polymeric chains. Since the discovery of STP reaction (Wegner, 1969), the blue phase polydiacetylene films were prepared on a basis of diacetylene alcohol derivatives for the first time. These new compounds with the unique optical and structural characteristics can be used in the design of thin-film devices for applications in molecular electronics.

## CRYSTALLISATION OF LAYERS IN PZT/LNO/Si HETEROSTRUCTURES

**Atanova A.V.<sup>1</sup>, Zhigalina O.M.<sup>1,2</sup>, Khmelenin D.N.<sup>1</sup>, Seregin D.S.<sup>3</sup>, Vorotilov K.A.<sup>3</sup>, Sigov A.S.<sup>3</sup>**

*1 - FSRC «Crystallography and Photonics» RAS, Moscow*

*2 - Bauman Moscow State Technical University, Moscow*

*3 - RTU MIREA, Moscow*

*atanova.a@crys.ras.ru*

Ferroelectric thin films based on  $\text{Pb}(\text{Zr}_x\text{Ti}_{1-x})\text{O}_3$  (PZT) have received great attention due to their low operating voltage and high switching rate [1 – 4]. However, the poor fatigue properties of structures with a Pt-electrode have led to the search of new materials for electrodes and approaches to improve their characteristics. One of the promising materials is lanthanum nickel oxide ( $\text{LaNiO}_3$ , LNO), which has pseudocubic perovskite structure with a lattice parameter close to PZT (3.84 Å for LNO, 4.04 Å for PZT). It is well known, that the structure of bottom layers has a great influence on the upper ones. It is of great importance to understand the interdependence between structure features of layers in these systems. Thus, the results of structural investigation of PZT-LNO-Si and PZT-LNO-SiO<sub>x</sub>-Si multilayer compositions are presented in this study.

To obtain heterostructures the chemical solution deposition technique was used. This method provides high-quality films with a uniform composition. To produce LNO-layer the precursor was deposited by means of layer-by-layer crystallization (seven times) on the silicon wafer in case of PZT-LNO-Si system or on the SiO<sub>x</sub> porous layer in case of PZT-LNO- SiO<sub>x</sub>-Si system with soft baking by infrared radiation and annealing at  $T = 650$  °C. The porous layer was supposed to reduce the stress in the system in order to improve fatigue properties and crack resistance. PZT films were formed by deposition of eight precursor sublayers with soft baking by infrared radiation, heat treatment in the muffle furnace at  $T = 400$  °C and annealing at  $T = 650$  °C of the whole volume simultaneously.

The structures were studied by transmission electron microscopy (TEM) techniques: bright field (BF) and dark field (DF) imaging, electron diffraction, scanning transmission electron microscopy (STEM) and energy dispersive analysis (EDX).

It has been shown, that the PZT film has a perovskite structure (P4mm space group) and the LNO layer is crystallized in a cubic phase (Pm-3m space group) in both systems. According to the DF-images, the heterogeneous nucleation mechanism at the interphase boundary occurs in the growth of PZT grains. The polycrystalline porous structure of LNO affects the PZT grains growth. Compared with Pt-based structures, the PZT columnar grains had a smaller width. In addition, some of perovskite grains that did not grow till upper film surface were found. The presence of the porous SiO<sub>x</sub>-layer causes decrease in the LNO grain size and increase in the layer porosity. However, it has been noted, that the SiO<sub>x</sub> – LNO interface does not have any porosity, meanwhile the Si – LNO interphase boundary is characterized by a continuous pore chain. The diffusion of titanium from PZT to LNO and lanthanum from LNO to PZT was observed by the elements mapping.

Electron microscopy investigations were carried out using equipment of the Shared Research Center of the Institute of Crystallography of Federal Research Centre " Crystallography and Photonics" of Russian Academy of Sciences.

### References

1. Seregin D. S., Baziruvikha A.-M., Kotova N. M., Vorotilov K. A., Delimova L. A., Zaitzeva N. V., Myakon'kikh A. V., Rudenko K. V., Lukichev V. F. Formation of PZT Structures on Silicon // Bulletin of the Russian Academy of Sciences: Physics. 2018. V. 82. № 3. P. 341–345.
2. Miyazaki H., Goto T., Miwa Y., Ohno T., Suzuki H., Ota T., Takahashi M. Preparation and evaluation of  $\text{LaNiO}_3$  thin film electrode with chemical solution deposition // Journal of the European Ceramic Society. 2004. V. 24. № 6. P. 1005–1008.
3. Vorotilov K. A., Zhigalina O. M., Vasil'ev V. A., Sigov A. S. Specific features of the formation of the crystal structure of lead zirconate titanate in the Si-SiO<sub>2</sub>-Ti(TiO<sub>2</sub>)-Pt-Pb(Zr<sub>x</sub>Ti<sub>1-x</sub>)O<sub>3</sub> systems // Physics of the Solid State. 2009. V.51. № 7. P. 1337–1340.
4. Zhao Q., Tan P., He G., Di J., Wang D., Qi L., Jin H. Cao M.. Effects of electrodes on ferroelectric properties of PNZT films prepared by sol-gel method //Journal of Sol-Gel Science and Technology, 2016, Vol. 78, № 2, p. 258-261.

# THEORETICAL STUDIES OF THE STRUCTURAL PECULIARITIES IN III/V SEMICONDUCTORS

**Baranovskii S.D.**

*Department of Physics, Philipps-University Marburg, D-35032 Marburg, Germany*

*baranovs@staff.uni-marburg.de*

By calculations in the framework of the valence force field method, we show that nitrogen atoms in diluted GaAs<sub>1-x</sub>N<sub>x</sub> tend to align along the [001] direction. In quaternary alloys Ga<sub>1-y</sub>In<sub>y</sub>As<sub>1-x</sub>N<sub>x</sub> this tendency is observed only in “as-grown” samples, while in the annealed samples nitrogen atoms build more energetically favorable bonds with indium<sup>1</sup>. It is shown that, if the structure factor of the Ga(NAs)/GaAs crystals is recalculated taking the static displacements of the Ga atoms into account, the composition derived from the transmission electron microscopy analysis appears in perfect agreement with that derived from the high-resolution x-ray diffraction<sup>2</sup>.

Density-functional theory and empirical energy functional calculations show that the reduction of the strain contribution to the alloy total energy functional is the driving force for the rearrangement in the nitrogen local environment upon annealing. It is shown that the entropy factor is not negligible and it plays a crucial role when determining the thermodynamically favorable atomic configuration. Particularly, the replacement of Ga-N bonds by In-N bonds upon annealing can account for the observed blueshift of the photoluminescence spectra and an enhancement of the photoluminescence quantum efficiency, as compared to the as-grown material. Annealing leads the increase of the band gap<sup>3</sup>.

The formation energies of {110}, {111}, {112}, and {113} antiphase boundaries in GaAs and GaP were studied theoretically using a full-potential linearized augmented plane-wave density-functional approach. Results of the study reveal that the stoichiometric {110} boundaries are the most energetically favorable in both compounds<sup>4</sup>.

Experimentally observed pyramidal structure formation at the interface between III/V semiconductors and silicon is reproduced by the kinetic Monte Carlo computer simulations and by first-principles computations. It is shown that a pyramidal interface structure is formed irrespective of the conditions applied during the growth of two semiconductors<sup>5</sup>.

Local fluctuations in the concentrations of chemically different components in the mixed crystals cause energy fluctuations for charge carriers. We provide a theory for this effect in multi-compound alloys containing more than two chemically different semiconductor species occupying sites in the same sublattice. A comparison between theoretical predictions and experimental data can be used to reveal compositional dependencies of such material parameters as the effective mass<sup>6</sup>.

1. O. Rubel et al., Appl. Phys. Lett. 85, 5908 (2004).
2. K. Volz et al., Appl. Phys. Lett. 88, 081910 (2006).
3. O. Rubel et al., Phys. Rev. B 74, 195206 (2006).
4. O. Rubel and S. D. Baranovskii, Int. J. Mol. Sci., 10, 5104 (2009).
5. A. Beyer et al., Chem. Mater. 28, 3265 (2016).
6. M. Wiemer et al., Phys. Stat. Sol. - Rapid Research Letters, 10, 911 (2016).

# THE MODEL FOR IN-PLANE AND OUT-OF-PLANE GROWTH REGIMES OF III-V NANOWIRES

**Berdnikov Y., Sibirev N.**

*ITMO University*

*yury.berdnikov@gmail.com*

Semiconductor III-V nanowires (NWs) and heterojunctions on their base are widely considered as the promising building blocks for novel photonic and optoelectronic applications. However, their use in the device applications are usually require the control on the direction of NW growth [1]. Nowadays, one of the most common approaches to synthesis of III-V NWs is the epitaxial growth via vapor-liquid-solid (VLS) mechanism [2]. In this work we present a model for in-plane and out-of-plane VLS NW growth and discuss the factors which determine the growth direction.

The model for VLS growth is based on the energies of liquid-solid ( $\gamma_{SL}$ ), liquid-substrate ( $\gamma_{SubL}$ ) and solid-substrate ( $\gamma_{SSub}$ ) interfaces. When  $\gamma_{SSub} - \gamma_{SubL} > \gamma_{SL}$ , the formation of the inclined facet is energetically preferable than the nucleation and growth in contact with the substrate. In this case, the inclined growth is expected. On the other hand,  $\gamma_{SSub} - \gamma_{SubL} < \gamma_{SL}$  corresponds to horizontal growth.

According to our model the in-plane and out-of-plane growth modes are strongly correlated with the composition of catalyst droplet. In turn, the values of the interface energies are different at different liquid compositions. In the specific case of GaAs growth, the droplet is ranged from pure gallium to AuGa alloy with the gallium content, which corresponds to the melting point for a given growth temperature. Besides the dependence on catalyst composition, the values of  $\gamma_{SSub}$  and  $\gamma_{SubL}$  also depend on the substrate material. In this work we compare the growth on graphite and Si(100) substrates.

In the estimations of interface energies, the AuGa catalyst is assumed to consist of 70% of gold and 30% of gallium. Foresaid Ga:Au ratio was observed in the in-situ X-ray energy dispersive spectroscopic measurements during the Au-catalysed growth of GaAs NWs at the temperatures similar to the sample growth temperature of 440°C [3]. However, the composition of the catalyst is sensitive to both growth temperature and precursor fluxes [3], and thus, the complete analysis require the extension for the cases of different Au content in the catalyst. Unfortunately, the exact dependences of interface energies on AuGa liquid composition are generally unknown. Nevertheless, the values of  $\gamma_{SL}$  and  $\gamma_{SubL}$  for pure gallium and gold-gallium composition during the growth can be found in the literature. Hence, we approximate the dependences of the interface energies by connecting the values for known liquid compositions with the straight lines. Figure 1\* shows the approximations for  $\gamma_{SL}$ ,  $\gamma_{SSi} - \gamma_{SiL}$  (labeled “Silicon”) and  $\gamma_{SG} - \gamma_{GL}$  (labeled “Graphite”) as the functions of gold concentrations in the catalyst. Both  $\gamma_{SSi} - \gamma_{SiL}$  and  $\gamma_{SG} - \gamma_{GL}$  larger than  $\gamma_{SL}$  at low Au concentrations and smaller than  $\gamma_{SL}$ .

Thus, generally, Au-rich particles promote the horizontal growth while Ga-rich particles induce the inclined growth. The boundary between inclined and horizontal growth modes is given by crossing point of  $\gamma_{SL}$  and  $\gamma_{SSub} - \gamma_{SubL}$  lines for arbitrary substrate and variable liquid composition. Particularly, within the model assumptions, the typical AuGa catalyst with Ga:Au ratio of 30:70 corresponds to horizontal growth on graphite and inclined growth on Si(100) surface. The purely gallium catalyst is expected to promote the out-of-plane growth on both substrates.

Acknowledgments:

The authors thank the Ministry of Education and Science of the Russian Federation for financial support under grant 14.587.21.0040 (project ID RFMEFI58717X0040).

Figure 1\*.  $\gamma_{SSub} - \gamma_{SubL}$  dependences on atomic concentration of gold in catalyst droplet approximated by straight lines for graphite and Si(100) substrates.

\*The abstract with figures is available at <http://2019.mgctf.ru/0100003506.doc>



# STRUCTURE AND PROPERTIES OF SiO<sub>x</sub> FILMS PREPARED BY CHEMICAL ETCHING OF AMORPHOUS METALLIC GLASS

Fedorov V.<sup>1</sup>, Berezner A.<sup>1</sup>, Beskrovnyi A.<sup>2</sup>, Fursova T.<sup>3</sup>, Pavlikov A.<sup>4</sup>

*1 - Tambov State University*

*2 - Joint Institute For Nuclear Research*

*3 - Institute of Solid State Physics (Russian Academy of Sciences)*

*4 - Moscow State University*

*qwert1009@mail.ru*

The structure and the physical properties of amorphous SiO<sub>x</sub> films prepared by chemical etching of an Fe-based amorphous ribbon alloy have been studied. The neutron diffraction and also the atomic-force microscopy show that the prepared visually transparent films have amorphous structure and their morphology is similar to that of opals. The samples have been studied by Raman and IR spectroscopy before and after their heat treatment. It is found that annealing of the films in air at a temperature of 1273 K leads to a change in their chemical compositions: an amorphous SiO<sub>2</sub> compound with inclusions of SiO<sub>2</sub> nanocrystals (crystalalite) forms.

## Results and discussion

The purpose of this work is to study the structure and the properties of SiO<sub>x</sub> films prepared by chemical etching of a Fe-based amorphous ribbon alloy. To prepare SiO<sub>x</sub> films, we have developed a new method of chemical etching. Ribbon-like amorphous 80×5×0.02-mm samples of the Fe-based metallic glass with the proportions of atomic masses 78.85% Fe, 15.40% Si, 1.09% Cu, 2.90% Nb, and 1.76% Al were placed into an etching solution consisting of 70% nitric acid and 90% medicine ethyl alcohol taken in the proportion one part acid and two parts ethanol. The chemical etching was performed in air for 1.5–2 h. Upon completing the etching, the sample was washed with distilled water and dried. As a result, we obtained the visually transparent 80×5×0.02-mm film. We can conclude by the neutron diffraction studies that the samples are in amorphous state. The atomic-force microscope demonstrates the existence of pores and also a globular (similar to opals) structure with a characteristic grain size of 200–300 nm. To analyze of the optical properties of the films, the reflectance and transmission IR-spectra of light were measured at T = 300 K. The study of the dielectric characteristics by the DC and AC four-probe methods indicates the existence of a high electrical resistance of the film. The reflectance spectrum of the annealed (1273 K) film does not contain the minimum, due to the vibrations of the C–H and O–H bonds. The spectrum of the annealed film has the wide X-ray diffraction peak with a maximum at  $2\theta \sim 22^\circ$  (without 520 cm<sup>-1</sup> Raman-maximum) against the background of the structureless band. This maximum demonstrates the appearance of nanosized inclusions (~7 nm) of the crystalline SiO<sub>2</sub> phase (crystalalite) in the amorphous matrix of the sample after annealing.

**Acknowledgements** This work was supported by the Russian Foundation for Basic Research (project No. 18-01-00513\_A).

**THE ORIGIN OF PHASE TRANSITION AND THE USUAL EVOLUTIONS  
OF THE UNIT-CELL CONSTANTS OF THE NASICON STRUCTURES OF THE SOLID  
SOLUTION  $\text{LiTi}_{2-x}\text{Ge}_x(\text{PO}_4)_3$**

**Bounar N.**

*LIME Laboratory, University of Jijel, BP 98 Jijel, 18000, Algeria*

*nedjmbounar@yahoo.fr*

The NASICON (Na Super Ionic CONductors)-type materials are good ionic conductors when serving as solid electrolytes for lithium-ion batteries. In this paper, Ge - doped  $\text{LiTi}_2(\text{PO}_4)_3$  has been synthesized by a conventional solid-state reaction. Compounds  $\text{LiM}_2^{\text{IV}}(\text{PO}_4)_3$  with LTP-type structure present a different behavior depending on nature of  $\text{M}^{\text{IV}}$ . For  $\text{M}^{\text{IV}} = \text{Ti}$  and Ge the structure shows the space group R-3c, whereas for  $\text{M}^{\text{IV}} = \text{Ge}$  the space group is R-3. Differences in behavior of  $\text{LiTi}_2(\text{PO}_4)_3$  -  $\text{LiGe}_2(\text{PO}_4)_3$  solid solutions are discussed in relation to the composition. Their structures  $\text{LiTi}_{2-x}\text{Ge}_x(\text{PO}_4)_3$  ( $0 \leq x \leq 1.6$ ) were determined from X-ray powder diffraction method (XRD) using Rietveld analysis. A sharp change in the lattice parameter "a" is observed between the compositions with  $x = 1$  and 1.2. The lattice parameter "c" increases as the Ge content increases in the whole range of composition. The space group R-3c becomes to R3 for the composition with  $x > 1$ . The SEM micrographs of the samples show relative porous microstructures due to the effect of the substitution.

## FORMATION OF WIDE-BANDGAP SEMICONDUCTORS ON $\text{Al}_2\text{O}_3$

**Bouravleuv A.<sup>1,2,3</sup>, Sobolev M.<sup>1</sup>, Ilkiv I.<sup>1</sup>, Pirogov E.<sup>1</sup>, Ubyivovk E.<sup>4</sup>, Sharofidinov S.<sup>3</sup>,  
Kukushkin S.<sup>5</sup>**

*1 - St Petersburg Academic University RAS*

*2 - Ioffe Institute*

*3 - Saint Petersburg Electrotechnical University*

*4 - St.Petersburg State University*

*5 - Institute of Problems of Mechanical Engineering RAS*

*bour@mail.ioffe.ru*

Up to day wide-bandgap semiconductor materials, such as III-N materials, first of all, attract increasing attention due to a diversity of their properties allowing to use them for the creation of different novel devices. Nonetheless, the relatively high price of native substrates or their absence makes of importance the synthesis of wide band-gap semiconductors on low-cost Si or  $\text{Al}_2\text{O}_3$  substrates [1-3]. However, it is accompanied by the formation of a large number of defects due to lattice and thermal coefficient mismatches usually. In order to solve this problem the different technological approaches can be applied. The most common is to create quite thick transition or buffer layers, which can lead to an increase in the thickness of the devices and inefficient consumption of materials.

Here we report on the alternative ways [4,5], which can be used for the formation of relatively thin transition layers, such as SiC, AlN, GaN, on  $\text{Al}_2\text{O}_3$  substrates. In our experiments, we used two-step procedure. First, Si layers were deposited on  $\text{Al}_2\text{O}_3$  substrate surface by molecular-beam epitaxy and then they were transformed into SiC. TEM investigation revealed the formation of suspended SiC layers. Another approached is based on atomic-layer deposition.

[1] O. Ambacher, J. Phys. D Appl. Phys. 31, 2653–2710 (1998).

[2] J. Millan, P. Godignon, X. Perpina, A. Perez-Tomas, J.A. Rebollo, IEEE Trans. Power Electron. 29, 2155–2163 (2014).

[3] G.H. Chung, T.A. Vuong, H. Kim, Results in Physics, 12, 83–84 (2019).

[4] S.A. Kukushkin, A.V. Osipov, A.V. Redkov, A.S. Grashchenko, N.A. Feoktistov, S.D. Fedotov, V.N. Statsenko, E.M. Sokolov, S.P. Timoshenkov, Rev. Adv. Mater. Sci. 57, 82-89 (2018).

[5] H. Seppänen, I. Kim, J. Etula, E. Ubyivovk, A. Bouravleuv, H. Lipsanen, Materials 12, 406 (2019).

## 2D MESOSCALE COLLOIDAL CRYSTAL PATTERNS COMPOSED BY MICROSPHERES ON SUBSTRATES

**Bredikhin V., Bityurin N.**

*Institute of Applied Physics of the Russian Academy of Sciences (IAP RAS) 46 Ul'yanov Street, 603950, Nizhny Novgorod, Russia*

*bredikh@appl.sci-nnov.ru*

The development of nanosphere lithography relies on the ability of depositing 2D colloidal crystals comprising micro- and nano-size elements on substrates of different materials. The most difficult problems here are deposition of coatings on hydrophobic substrates, e.g. polymers, from aqueous colloidal solutions and the formation needed 2D mesoscale colloidal crystal patterns. First problem is connected with hydro phobicity of polymer substrates, while water is a solvent in colloidal solutions frequently. To solve this problem we use UV photo oxidation for substrate hydro philization [1,2]. We developed a new method [2] of producing a two-dimensional ordered array of polymer microparticles (polystyrene microspheres  $\sim 1 \mu\text{m}$  in diameter) useable as for hydrofobic (polymer), as for hydro feeling (glass, semiconductors) substrates. With combination of UV hydrophyllization through appropriate mask and our new method of colloidal film deposit we demonstrated [2] an example of 2D composed periodic  $100 \cdot 100 \mu\text{m}^2$  squares formed of UV  $1 \mu\text{m}$  PS spheres on PMMA substrate. This achievement is based on the fact that during depositing colloidal film from solution the solution stays on irradiated places and remains not irradiated (hydrophobic) places intact. The considered technique allows using routine lithographic techniques and equipment technique.

For hydrofeeling substrate (glass) there is another situation. Without UV irradiation it is possible to produce homogeneous colloidal films (up to  $\sim 2.5 \cdot 2.5 \text{ cm}^2$  in our case) [1]. Due to UV irradiation action the glass substrate hydrophilicity is growing [1]. Due this effect under previous conditions of film deposition we shall obtain regular colloidal crystal film on non irradiated places, but, in opposite, irradiated paces will be coated by thick irregular coat. Such “inversed” technique can be used also in nanosphere technique using routine lithographic technology, for ex., by spraying metal on coated substrate, or irradiating it by laser beam, and chemically solving PS balls than.

Some processes of formation 2D regular structures from colloid solution are investigated in the report. Experimentally the growth of 2D pattern with  $10 \mu\text{m}$  PS balls when a drop of colloidal solution is drying under microscope was investigated. Visibly the process defined by Brown motion and attractive forces is very similar to formation of a surface of atomic crystal. Some growth parameters of colloidal crystal growth were defined.

In contrast to atomic crystal growth colloid solution are characterized by relatively large dispersion  $\sigma$  of sphere radii (of some percents). This lead to formation of closely packed  $N$  microspheres (grains) with the r.m.s. number of microspheres in a single grain equal  $N_\sigma \approx (2\sigma)^{-2}$  [2]. These grains define principal limit a quality of 2D colloidal film.

**Acknowledgements.** The research was performed with the financial support from the Russia Foundation for Basic Research (grant No. 18-02-00806 a).

### **Referencies**

1. Vladimir I. Bredikhin, Nikita M. Bityurin. Contact angle measurements with constant drop volume. Control of wettability of some materials by physico-chemical treatment. International Journal of Engineering Research & Science (IJOER) 2017 3, 82-87. <https://ijoer.com/Paper-November-2017/IJOER-NOV-2017-13.pdf>.
2. Vladimir Bredikhin and Nikita Bityurin. 2D mesoscale colloidal crystal patterns on polymer substrates Materials Research Express 2018, 5 (5), 055306, <https://doi.org/10.1088/2053-1591/aac1e9>.

# QUANTITATIVE STRAIN DISTRIBUTION IN ELECTROMECHANICALLY COUPLED IV-IV AND III-V SEMICONDUCTOR QUANTUM DOTS

**Cherkashin N.<sup>1</sup>, Nevedomskiy V.<sup>2</sup>, Sakharov A.<sup>2</sup>, Tsatsulnikov A.<sup>2</sup>, Nikolaev A.<sup>2</sup>, Ledentsov N.<sup>3</sup>, Shchukin V.<sup>3</sup>**

*1 - CEMES–CNRS, 29, rue Jeanne Marvig, BP 94347, 31055 Toulouse , France*

*2 - Ioffe Institute, Politekhnicheskaya 26, St. Petersburg 194021, Russia*

*3 - VI Systems GmbH, Hardenbergstr. 7, 10623 Berlin, Germany*

*nikolay.cherkashin@cemes.fr*

Quantum dots (QDs) are nanometer-sized structures which allow the 3D confinement of charge carriers leading to discrete atom-like energy levels. When electron and hole are confined in a QD, annihilation of exciton provides emission of a single photon. Such property allows QDs to be incorporated in semiconductor devices such as light emitting diodes, lasers, field effect transistors, single photon emitters etc. The emission properties of the devices can be adjusted by changing QD structure and by forming QD ordered chains and crystals. The effects of size quantization appear when the dimensions of the confining region are comparable to exciton Bohr radius which depends on the exact QD/matrix band structure. In contrast to most of the theoretical models developed so far, “real” QD crystals contain QDs of inhomogeneous size, composition and shape. In order to simulate the “real” band structure, quantitative data on the 3D strain fields and composition distributions in individual QDs and their configurations are essential but not provided so far.

In this work, we will demonstrate how advanced transmission electron microscopy (TEM) based methods adopted for strain measurements with a (sub)nanometer spatial resolution: geometric phase analysis (GPA) of high-resolution (HR) TEM images [1], HR dark-field electron holography (HR-DFEH) [2] and Moiré by specimen design (MoSD) [2, 3], bring value to this issue.

Four epitaxially grown structures will be considered. First structure contains a single layer of InAs/(001)GaAs QDs formed in Stranski-Krastanov mode. The second structure contains several layers of InGaAs QDs embedded within AlInGaP matrix and grown on high-index faceted (112)GaAs substrate. The third structure contains multiple layers of Ge/(001)Si islands formed in Volmer mode. The fourth structure contains several layers of InGaN/GaN islands formed after applying growth interruption which allowed a conversion of 2D InGaN layer into an array of 3D InGaN islands. We will demonstrate quantitative in-plane, out-of-plane and shear strain distributions in each spatially correlated system of QDs. In order to account for stress relaxation in a thin cross-sectional TEM lamella and to reconstruct composition distribution within the QDs, finite element method (FEM) modelling was applied. The structural data will be compared with electroluminescence measurements. The correlation between the resulting electro-optical properties and the predictions of numerical simulations will be discussed.

References:

1. N. Cherkashin et al., Appl. Phys. Lett. 102, 173115 (2013).
2. N. N. Ledentsov et al., Opt. Express 26 (11), 13985-13994 (2018).
3. N. Cherkashin et al., Scientific Reports 7, 12394 (2017).

# THE PROCESSES OF CRYSTALLIZATION AND DEGASSING OF METAL MELTS, QUENCHING FROM THE LIQUID STATE

Chernov A.A.<sup>1,2</sup>, Pil'nik A.A.<sup>1</sup>

*1 - Kutateladze Institute of Thermophysics SB RAS, Novosibirsk, Russia*

*2 - Novosibirsk State University, Novosibirsk, Russia*

*chernov@itp.nsc.ru*

The first-order phase transition occurs by way of random formation of new phase nuclei and their subsequent growth. It follows the process of metastability formation. Classical models often do not account for the changes in the metastability level of the initial state during the process of new phase formation. In order to keep the system in the stationary state, new phase nuclei are extracted from the system by artificial means. Then they are disassembled and returned to the system so that the initial metastable state can be maintained continuously. This approach is only a thought experiment aimed at examining the process of nuclei formation and the process of nuclei growth separately. In reality, the formation of even a small portion of a new phase can significantly change the initial metastable state of the system and it must be accounted for. The phase change process consists of two stages. The first one is the nucleation stage. During this stage the majority of new phase nuclei form. Due to a strong dependence of the nucleation rate on the supercooling, this stage is typically very rapid. The second stage is more long lasting. It consists of a further growth of the nuclei formed during the first stage. The nucleation stage is an object of great interest, but it is complicated as well. Studying it involves thermodynamics of small systems, nucleation kinetics, growth mechanisms of new phase nuclei in a wide range of parameters, adequate accounting for the effects of an ensemble of growing nuclei on the metastability of the system etc. Adding the factors responsible for the formation of metastability, we have a highly nonlinear mathematical problem in the form of a system of integro-differential equations, which has not been solved yet.

In the present work, the nonequilibrium model of the spherical crystal growth in a supercooled melt is presented. The model describes correctly the effect of melt heating near the phase boundary, which affects the growth rate of the crystal considerably. The analytical solution of the problem is found under the conditions of a strongly nonstationary process and large deviations from equilibrium. It has been demonstrated that near-equilibrium is achieved at the crystallization front after some time if the initial supercooling is below the thermal effect of the phase transition. In this case, the solution of the problem becomes self-similar. The crystal grows all the time under essentially nonequilibrium conditions if the initial supercooling is above the critical one. The effect of substance shrinkage on the growth rate of the crystal is investigated. The kinetic model of nucleation-mediated crystallization of a supercooled melt is presented. It correctly takes into account the change in supercooling of the initial phase in the process of formation and evolution of a new phase. The model makes it possible to find the characteristic time of the process, time course of the crystal phase volume, solidified material microstructure. The distinctive feature of the model is the use of the "forbidden" zones in the volume where the formation of new nucleation centers is suppressed.

The kinetic model of cavitation of the melt, brought rapidly into supercooled state, during its volumetric crystallization was developed. Time dependences of the crystalline mass and volumetric concentration of bubbles were derived. Essential dependence of the final size of crystalline grains and cavitation inclusions in the solidified melt on the cooling rate is shown. The analytical solution of the problem of dissolved gas segregation from melt during the crystallization process was found. The problem was solved using most commonly used geometries of crystal growth: plane, cylindrical and spherical. Shrinkage of the melt during crystallization was correctly taken into account. It was shown that in the case of equilibrium crystallization the solution becomes self-similar. The criteria allowing to predict the conditions for inevitable formation of cavities in solidified material is shown.

# EFFECT OF GROWTH CONDITIONS ON SURFACE MORPHOLOGY AND CONCENTRATION OF GROWTH DEFECTS OF CdTe/GaAs (100) EPITAXIAL LAYERS IN THE MOCVD PROCESS

**Chilyasov A.V., Evstigneev V.S., Moiseev A.N.**

*G.G. Devyatykh Institute of Chemistry of High-Purity Substances of RAS*

*tchilyasov@ihps.nnov.ru*

Cadmium telluride (CdTe) is a promising material for creating efficient thin-film devices – solar energy converters, X-ray and gamma-radiation detectors. Besides, the heteroepitaxial structures of CdTe/GaAs (100) are widely used as substrates for the preparation of IR-photosensitive layers based on  $\text{Hg}_{1-x}\text{Cd}_x\text{Te}$  ternary alloy. A particular feature of the growth of cadmium telluride layers on GaAs (100) substrates is the possibility of simultaneous deposition of CdTe (100) and CdTe (111) orientation layers. The choice of growth orientation is very sensitive to the substrate pre-growth treatment and the initial conditions for the nucleation and deposition of the layer. In addition, one of the main problems of MOCVD epitaxy of CdTe on GaAs (100) is the formation of a large number of growth macrodefects in the form of pyramidal hills (hillocks). Determination of the main factors affecting the occurrence of hillocks, which reduce the functional characteristics of the layers and the reduction of their surface density, is an important task.

In this work, the effect of temperature (550–630 °C) and duration (7–30 min.) of pre-growth annealing of epitaxially GaAs(100) $4^\circ \rightarrow \langle 110 \rangle$  substrates, temperature of the pre-decomposition zone of organometallic compounds (diethyltellurium and dimethylcadmium) and deposition temperature in MOCVD epitaxy ( $P=0.2$  atm) on the morphology, crystal quality of CdTe and the number of growth defects on its surface are studied.

It was found that the most significant effect of the studied factors on the surface morphology, crystalline quality, determined by the half-width of the rocking curve of X-ray diffraction, and the number of growth defects on the surface of the CdTe layers is provided by temperature and duration of annealing of the GaAs substrate in hydrogen flow before deposition. Annealing at temperatures below 550 °C results in preparation of polycrystalline CdTe layers. The crystal quality gradually improves with an increase in the substrate annealing temperature up to 600 °C (annealing time 15 min.) above which there is a sharp deterioration caused by etching of GaAs (100) surface. The surface roughness gradually decreases with an increase in the annealing temperature to 600 °C; however, the number of growth defects passing through the minimum of  $\approx 150\text{--}200 \text{ cm}^{-2}$  at 570–580 °C increases rapidly ( $> 10^3 \text{ cm}^{-2}$ ).

An increase in the CdTe deposition temperature in the range from 345 to 365 °C at a constant substrate annealing temperature slightly improves the crystalline quality of the layers; however, the concentration of the hillocks significantly increases. The temperature of the organometallic pre-cracking zone in the range of 290–320 °C produces a noticeable effect on the morphology of CdTe surface due to change in the composition of the gas mixture above the surface of the growing layer; however, it almost does not affect the surface density of growth defects.

Thus, the most probable place of origin of the hillock type macrodefects in the CdTe epitaxial layers is the interface between the substrate and the layer.

# MECHANISMS OF SILICON ALLOTROPES' CRYSTALLIZATION IN CONDENSED MEDIA BY IN SITU DIFFRACTION OF SYNCHROTRON RADIATION

Courac A.

*IMPMC Sorbonne université, 4 place Jussieu, 75005 Paris, France*

*alexandre.courac@upmc.fr*

HP research on Si started more than 50 years ago and since then several allotropes, displaying a wide variety of physical properties, have been reported.<sup>1-5</sup>

The narrow-bandgap semiconductor<sup>6</sup> Si-III<sup>4</sup> with BC8 structure (originally believed to be semimetal) can be obtained from the high-pressure tetragonal metallic phase, Si-II, formed during compression of common silicon according to **Si-I**→**Si-II** (Figure 1). Such a transformation during decompression can be either direct, **Si-II**→**Si-III**, or with an intermediate step **Si-II**→**Si-XII**→**Si-III**. Our in situ studies of pure Si in oxygen-free environment indicated that in the absence of pressure medium, **Si-I** remains metastable at least up to ~14 GPa, while the pressure medium allows reducing the onset pressure of transformation to ~10 GPa.

Upon heating Si-III at ambient pressure a hexagonal structure, named Si-IV, was observed. This allotrope was believed to be a structural analogue of the hexagonal diamond found in meteorites (called also lonsdaleite) with the 2H polytype structure. Calculations have predicted several hexagonal polytypes of Si and of other Group-IV elements to be metastable, such as 2H (AB), 4H (ABCB) and 6H (ABCACB). Exhaustive structural analysis, combining fine-powder X-ray and electron diffraction, afforded resolution of the crystal structure. We demonstrate that hexagonal Si obtained by high-pressure synthesis correspond to Si-4H polytype (ABCB stacking),<sup>5</sup> in contrast with Si-2H (AB stacking) proposed previously. The sequence of transformations **Si-III**→**Si-IV(4H)**→**Si-IV(6H)** has been observed in situ by powder X-ray diffraction. This result agrees with prior calculations that predicted a higher stability of the 4H form over 2H form. Further physical characterization, combining experimental data and ab-initio calculations, have shown a good agreement with the established structure. Strong photoluminescence emission was observed in the visible region, for which we foresee optimistic perspectives for the use of this material in Si-based photovoltaics.

The study of silicon allotropic transformation in Na-Si and K-Si systems at high pressure, high temperature conditions indicated new interesting results on the second-order character of **Si-II**→**Si-XI** transformation and will be discussed in the presentation. The impact of the second order character on the topology of the pressure-temperature phase diagram of silicon will be analyzed.

1. Kurakevych, O. O.; Le Godec, Y.; Strobel, T. A.; Kim, D. Y.; Crichton, W. A.; Guignard, J., Exploring silicon allotropy and chemistry by high pressure - high temperature conditions. *J. Phys.: Conf. Ser.* **2017**, *950*, 042049.
2. Kurakevych, O. O.; Le Godec, Y.; Crichton, W. A.; Strobel, T. A., Silicon allotropy and chemistry at extreme conditions. *Energy Procedia* **2016**, *92*, 839-844.
3. Kim, D. Y.; Stefanoski, S.; Kurakevych, O. O.; Strobel, T. A., Synthesis of an open-framework allotrope of silicon. *Nature Materials* **2015**, *14* (2), 169-173.
4. Kurakevych, O. O.; Le Godec, Y.; Crichton, W. A.; Guignard, J.; Strobel, T. A.; Zhang, H. D.; Liu, H. Y.; Diogo, C. C.; Polian, A.; Menguy, N.; Juhl, S. J.; Gervais, C., Synthesis of Bulk BC8 Silicon Allotrope by Direct Transformation and Reduced-Pressure Chemical Pathways. *Inorganic Chemistry* **2016**, *55* (17), 8943-8950.
5. Pandolfi, S.; Renero-Lecuna, C.; Le Godec, Y.; Baptiste, B.; Menguy, N.; Lazzeri, M.; Gervais, C.; Spektor, K.; Crichton, W. A.; Kurakevych, O. O., Nature of Hexagonal Silicon Forming via High-Pressure Synthesis: Nanostructured Hexagonal 4H Polytype. *Nano Letters* **2018**, *18* (9), 5989-5995.
6. Zhang, H. D.; Liu, H. Y.; Wei, K. Y.; Kurakevych, O. O.; Le Godec, Y.; Liu, Z. X.; Martin, J.; Guerrette, M.; Nolas, G. S.; Strobel, T. A., BC8 Silicon (Si-III) is a Narrow-Gap Semiconductor. *Physical Review Letters* **2017**, *118* (14).



# ROLE OF NUCLEATION IN THE VAPOR-LIQUID-SOLID GROWTH OF III-V SEMICONDUCTOR NANOWIRES

**Dubrovskii V.G.**<sup>1,2</sup>

1 - ITMO University, Kronverkskiy pr. 49, 197101 St. Petersburg, Russia

2 - Ioffe Institute RAS, Politekhnicheskaya 26, 194021 St. Petersburg, Russia

*dubrovskii@mail.ioffe.ru*

In this talk, we will discuss some interesting effects originating from self-regulated pulsed nucleation in vapor-liquid-solid (VLS) III-V nanowires (NWs). The Zeldovich nucleation rate in VLS NWs [1] will be considered, which determines the axial growth rate in the mononuclear regime and affects some important properties of NWs. It will be shown why and how the so-called nucleation antibunching in individual NWs leads to sub-Poissonian narrowing of the length distributions (LDs) within the ensembles of self-catalyzed NWs, as predicted theoretically in Ref. [2] and confirmed experimentally in Refs. [3,4]. It has been known for a long time [5,6] that the nucleation position (in the center of the liquid-solid interface or at the trijunction) determines the crystal structure of III-V NWs, which can be either wurtzite (WZ) or zincblende (ZB). More recently, *in-situ* studies revealed truncated growth interfaces which oscillate in synchronization with the nucleation pulses [7]. We will present the structural diagrams for VLS GaAs and GaP NWs revealing the preferred crystal phase as a function of the droplet contact angle. We will also consider how the stopping effect [8] originating from a limited amount of As dissolved in the droplet affects the VLS growth and properties of III-V NWs.

**Acknowledgements** The financial support of the Russian Foundation for Basic Research under Grants 17-52-16017, 18-02-40006, and 19-52-53031 is gratefully acknowledged.

## References

- [1] V. G. Dubrovskii and J. Grečenkov, *Cryst. Growth Des.*, 2015, 15, 340.
- [2] F. Glas and V. G. Dubrovskii, *Phys. Rev. Materials* 2017, 1, 036003.
- [3] E. Koivusalo *et al.*, *Nano Lett.*, 2017, 17, 5350.
- [4] T. Tauchnitz *et al.*, *Nanotechnology*, 2018, 29, 504004.
- [5] F. Glas, J. C. Harmand, G. Patriarche, *Phys. Rev. Lett.* 2007, 99, 146101.
- [6] V. G. Dubrovskii *et al.*, *Phys. Rev. B* 2008, 78, 235301.
- [7] D. Jacobsson *et al.*, *Nature* 2016, 531, 317.
- [8] V. G. Dubrovskii, *Cryst. Growth Des.* 2017, 17, 2544.

# INFLUENCE OF INDIUM ADDITION ON NUCLEATION AND GROWTH OF WHISKERS FROM TIN FILMS IN ELECTRONICS

**Dutta I.<sup>1</sup>, Das Mahapatra S.<sup>2</sup>**

*1 - Washington State University, Pullman, WA, USA*

*2 - Intel Corporation, Chandler, Arizona, USA*

*idutta@wsu.edu*

Copper components in electronic packages are often electroplated with 1-5  $\mu\text{m}$  thick tin film, from which long whiskers grow with passage of time, potentially causing electrical shorts between neighboring circuitry. Whisker growth from Sn coatings is a serious reliability concern in electronic packages, particularly when the required service life is over a decade, e.g., in medical, aerospace and defense applications. Here, we present the results of In-doping on whisker growth from electroplated Sn films and demonstrate that when Sn is alloyed 5-10% indium, whisker growth is completely eliminated. The reasons for the mitigation of whisker growth are discussed with respect to (1) the impact of In addition on the statistics of nucleation of protrusions (i.e., large hillocks) and whiskers, (2) influence of grain boundary diffusivity of Sn and hence the growth kinetics of whiskers, (3) the effect of In segregation at the surface-oxide layer and its role in driving whisker growth, (4) the role of grain shape and microstructure of Sn on whisker growth, and (5) the role of In in altering the intermetallic constitution at the Cu-Sn interface, and hence the driving force for whisker growth. These are explored numerically by MD and FEA simulations, as well as experimentally via SEM, FIB, AES, XPS and XRD. It is inferred that the observed mitigation due to In addition occurs due to a multitude of factors, the most important of which is the reduction of the driving force for whisker growth due to incorporation of In in the native Sn-oxide film on the surface of Sn. (Supported by NSF-CMMI-1335491).

## ION BEAM AND X-RAY METHODS OF THIN FILM COATING DIAGNOSTICS

**Egorov V.<sup>1</sup>, Egorov E.<sup>1,2</sup>, Afanas'ev M.<sup>2</sup>**

*1 - IMT RAS*

*2 - IRE RAS*

*egorov@iptm.ru*

The elements and structure diagnostics is a very important aspect of the thin film coating technology. Coating diagnostic problems can be solved by different analytical methods but best results can be achieved by use of ion beam and X-ray experimental procedures. It is known that the conventional X-ray spectrometry and diffractometry have little to offer as the element and structure diagnostic methods for the super thin film analysis owing to X-ray beam penetration into the studied target on great depth. At the same time, X-ray science has specific procedure for surface layers element and structure analysis. There are the X-ray fluorescence analysis at the exciting beam total external reflection (TXRF) [1] and the diffraction study at total external reflection condition [2]. The total external reflection phenomenon is characterized by excitation of the target surface layer with thickness 3-5 nanometers. In the result of this, total external reflection measurements are free from the matrix influence, demonstrate very low background intensities and allow to characterize peculiarities of coating structure and phase state. Base method of material ion beam analysis – the Rutherford backscattering spectrometry (RBS) presents possibilities to determinate the thin film coating thickness and to describe the depth element concentration profile with resolution up to 2 nanometers [3]. But chief feature of RBS method is its absoluteness. The method would not require standards and etalons. In combination of the ion beam channeling effect the RBS spectrometry can be used for study of the target monocrystallinity degree and the epitaxial quality in multilayer structures. RBS method allows to study diffusion and implanted profiles and isotopic depth distribution. The ion beam nuclear recoil method is the beautiful means for depth profile detection of hydrogen distribution in targets. In frame of the particle induced X-ray emission method (PIXE) we elaborated the unique procedure for surface layer element diagnostics with use the planar X-ray waveguide-resonator of specific design [4]. Its use allowed to bring nearer of the method to possibilities of mass spectrometry but without target destruction all positions are accompanied by exhaustive experimental data.

[1] R. Klockenkamper, A. von Bohlen. Total reflection fluorescence analysis and related methods. Wiley: New York. 2015. 519 p.

[2] A. Benedictovich, I. Feranchuk, A. Ulganenkov. Theoretical concepts of X-ray nanosize analysis. Springer-Verlag: Berlin. 2014. 318 p.

[3] J.R. Bird, J.S. Williams. Ion beams for material analysis. Academic Press: Sydney. 1989. 719 p.

[4] V.K. Egorov, E.V. Egorov, M.S. Afanas'ev. X-ray fluorescence material analysis initiated by high energy proton beams // IOP Conf. Ser.: J. of Phys. Conf. Ser. 1121 (2018) 012011.

# NONSTATIONARY NUCLEATION IN LAYERS OF GAS-SATURATED AMORPHOUS ICE IN THE PRESENCE OF ARTIFICIALLY INTRODUCED CRYSTAL CENTERS

**Faizullin M.Z., Vinogradov A.V., Tomin A.S., Koverda V.P.**

*Institute of Thermal Physics, Ural Branch of the Russian Academy of Sciences*

*faizullin@itp.uran.ru*

The stability of gas-saturated layers of amorphous ice prepared by condensation of supersonic molecular beams of rarefied steam and methane on a substrate cooled with liquid nitrogen has been experimentally investigated. Adiabatic expansion of a molecular beam of steam at the outlet of a supersonic nozzle leads to a decrease in temperature and the formation of crystalline nanoclusters in the flow. When nonequilibrium condensates were heated, glass transition and subsequent spontaneous crystallization were observed. The presence of water clusters introduced into nonequilibrium condensates artificially ensured conditions for the initiation of “hot” centers and a transition to an explosive regime of crystallization in an amorphous medium.

Several exothermic signals indicating crystallization from different centers and the random nature of their distribution in the volume of an amorphous medium were observed in DTA thermograms. The presence of crystal centers introduced into nonequilibrium amorphous condensates artificially shifts the beginning of crystallization to the region of low temperatures. The temperature corresponding to the final crystallization signal of an amorphous condensate increases from 158 K at zero methane content to 168 K at its 10 mass %. No noticeable effect of changes in the gas concentration on the glass transition temperature of gas-saturated amorphous ice was observed.

Crystallization of non-equilibrium gas-saturated layers of amorphous ice with artificially introduced crystallization centers leads to the formation of a gas hydrate. In conditions of deep metastability, a spontaneous crystallization regime is realized, which ensures the capture of gas molecules and does not lead to their displacement by the movement of the crystallization front.

The results of the investigation show the success of the method of condensation of supersonic molecular beams of rarefied steam and methane in producing gas hydrates. Condensation of gas-saturated layers of amorphous ice with supersonic velocities provided a multiple increase in the productivity of the hydrate formation process in comparison with condensation with subsonic velocities and traditional methods for producing gas hydrates under conditions close to equilibrium.

The work was supported by the Russian Foundation for Basic Research (Grant No. 18-08-00352a, 18-38-00443 mol-a) and the Program for Basic Research of the Ural Branch of the RAS (Grant No. 18-2-2-3).

# GROWTH OF CRYSTALS FROM THE GASEOUS PHASE ON THE SURFACES OF CLEAVAGE OF IONIC CRYSTALS UNDER CONDITIONS OF THERMO-ELECTRICAL SYNERGETIC INFLUENCE

**Fedorov V.A., Karyev L.G.**

*Tambov State University n.a. G.R. Derzhavin, city of Tambov, Russian Federation*

*fedorov@tsutmb.ru*

Experimental results of thermo-electrical synergetic influence on the surfaces of the ionic crystals' cleavages can be interpreted in the Concept of 1) appearance of thin films on the surface of sample crystals, and 2) growth of crystals from the gaseous phase.

In the **first case**, in all the experiments, the faceted crystals, with the surfaces {100} – NaCl, KCl, CaCO<sub>3</sub> – and {111}, {100}, {350}, {110} – LiF – were subjected to the heating and simultaneous influence of the electrical field.

The experiments were carried-out on the experimental stand, as per the Flat Capacitor scheme: one of the crystal faces was in secure contact with an electrode, the distance between the opposite face and the second electrode did not exceed ~ 0.1 mm. DC voltage of 400 V was supplied to the electrodes. The experiments were carried-out within the temperature range ( $T$ ) of 293 – 1073 K.

It was noted, that on the free surfaces {100} of the sample crystals NaCl, KCl and CaCO<sub>3</sub>, as well as on the surfaces {100}, {350}, {110}, {111} – LiF – there were detected changes in the form of droplets of jelly-type consistency or viscous fluid, wetting the crystal surface. New formations have characteristic dimensions of 3 – 300 micrometers (microns). In course of the heating (of the crystals) without the electrical field, such-type changes were not observed.

X-ray-diffraction studies reveal that the substance of the droplets is the amorph, the chemical composition of which is identical to the composition of the crystal. Formation of a new phase on the crystal surface after the thermal and electrical current treatment can be interpreted as appearance of a thin film from the crystal substance, with a stoichiometry different from the crystal [1].

In the **second case**, the thermal and electrical current treatment was applied to the crack of the crystal cleavage. In this case, both electrodes were in contact with the faces of the sample, parallel to the crack cavity. The experiments were carried-out within the temperature range of 293 – 893 K. The density of the ionic current reached ~ 27 A/m<sup>2</sup>. The experiments were performed in the air medium and in the vacuum (~ 0.01 Pa). The distance between the surfaces of the crack amounted to ~ 5·10<sup>-3</sup>–10<sup>-1</sup> mm.

Within the temperature range of intrinsic conductivity ( $T > 823$  K), there was observed the formation of local mono-crystalline outgrowths, of dimensions 4.4·10<sup>-2</sup>–3·10<sup>-1</sup> mm. Prior to formation of the outgrowths there appeared dislocation rosettes. In all the cases the outgrowths appeared on the positively-charges surfaces.

Formation of mono-crystalline outgrowths can be interpreted as the growth of crystals from the ion gas, originated in the crack cavity as a result of sublimation of the ions from the crystal's surface under the thermo-electrical influence.

## **Bibliography:**

L Karyev, V Fedorov. Healing of discontinuities in the ionic crystals under complex thermo-electric influence. IOP Conference Series: Materials Science and Engineering **168** (2017) UNSP 012065 doi: 10/1088/1757-899X/168/1/012065 P. 1-6

# EFFECT OF DOUBLE SOLID-PHASE EPITAXIAL RECRYSTALLIZATION ON THE DEFECT DENSITY IN ULTRATHIN SILICON-ON-SAPPHIRE LAYERS

**Fedotov S.D.<sup>1</sup>, Statsenko V.N.<sup>2</sup>, Golubkov S.A.<sup>3</sup>, Egorov N.N.<sup>3</sup>**

*1 - National Research University of Electronic Technology (MIET)*

*2 - Epiel JSC*

*3 - RIMST JSC (NIIMV)*

*fedotov.s.d@ya.ru*

Heteroepitaxial silicon-on-sapphire (SOS) wafers occupy a separate place among silicon-on-insulator technologies due to their utilization in the production of radiation-resistant space equipment, the nuclear industry and accelerators of elementary particles electronics, as well as in the production of microwave and RF electronics. The undeniable advantages of SOS are associated with the unique insulating properties of sapphire. Integrated circuits (ICs) on a SOS have low power consumption and high speed through low power dissipation and the absence of parasitic capacitances between the isolated elements. Today, for the creation of microwave ICs, the structures of SOS obtained by chemical vapor deposition (CVD) with ~300 nm submicron Si layers are used. However, the applying of SOS in the field of microwave ICs fabrication, intended for cellular communications and mobile devices of civil electronics, requires the formation of an ultrathin ( $\leq 100$  nm) layer of SOS. The high density of structural defects is a major barrier to the widespread use of ultra-thin SOS wafers. The method of solid-phase epitaxial recrystallization (SPER) is practically the only way to overcome this technological barrier. Single-crystal Si layers with a thickness of  $300 \pm 10$  nm were grown on R-cut 150 mm sapphire substrates using the combined CVD method (SOS No.1). For the purpose of the experiment, similar structures of imported SOS (SOS No.2) were also acquired. The SPER process with the implantation of Si<sup>+</sup> ions and thinning in oxygen (pyrogenic) was used. Crystal structures of the SOS No.1 and the SOS No.2 were measured by XRD in the  $\theta$ - $2\theta$  geometry for the symmetric diffraction reflection of Si(400). As can be noted, the position of the diffraction peaks for SOS No.1 is  $\theta_1 = 34.29 \div 34.33^\circ$  and is located to the left of the standard position of the unstressed Si(400) peak equal to  $\theta_0 = 34.56^\circ$ , which indicates the presence of compression stresses, the sum of the main lateral stresses ( $\sigma_1 + \sigma_2$ ) is in the range from -4.24 to -5.08 GPa. SOS No.2 had the position of the peaks  $\theta_1 = 35.31 \div 35.34^\circ$  which indicates the presence of tensile strain ( $\sigma_1 + \sigma_2$ ) in the range from 13.57 to 14.18 GPa. The layers of the SOS had a single crystal structure, the FWHM for the SOS No.1 was  $0.40^\circ$  before recrystallization (300 nm Si) and  $0, 27^\circ$  after SPER (100 nm Si), for foreign SOS No.2 the FWHM was  $0.48^\circ$  (300 nm Si) and  $0.30^\circ$  after SPER (100 nm Si). The study of transverse sections of ultrathin SOS using transmission electron microscopy (TEM) showed the presence of twin lamellae (twins) with twinning boundaries parallel to the (-11-1) and (-111) planes in the bulk of an ultrathin SOS layer that was not subjected to SPER. The linear density of twins for these samples was  $\sim 3 \times 10^5$  cm<sup>-1</sup>. Samples of ultra-thin SOS after SPER demonstrated the presence of part of twins and dislocations in the TEM dark-field image. The density of twins, determined by the secant method, was  $\sim 1 \times 10^4$  cm<sup>-1</sup>. RHEED patterns of Si(100), showing the presence of reflections from twins for slices of ultrathin SOS before SPER and the absence of these reflexes for ultrafine SOS after SPER. The authors believe that in this work the following are new provisions and results: the results of the joint work of the production chain «manufacturer of submicron SOS wafers → manufacturer of ultrathin SOS wafers» are reflected in the development of competitive manufacturing techniques for SOS structures with an ultrathin Si layer intended for the production of microwave electronics with low power consumption. A comparison of the structural characteristics of the Si device layer between the basic structures of domestic (JSC Epiel) and foreign production is made. The use of SPER made it possible to reduce the bulk density of defects in the ultrathin SOS layer by more than 2 orders of magnitude.

# CELLULAR NANO-STRUCTURING IN SiGe(Sn) ALLOY AFTER FAST CRYSTALLIZATION: A PLATFORM FOR HETEROEPITAXY

**Gaiduk P.**

*Department of Physical Electronics and Nanotechnology, Belarusian State University, Minsk, Belarus*

*gaiduk@bsu.by*

In this talk, a short review of structural changes, phase transition and segregation in SiGe(Sn) alloy layers during laser-induced melting and fast crystallization will be done. The structures of MBE grown eepitaxial SiGe(Sn) alloy layers are used as initial structures. The samples were then treated by pulsed laser beam (25-100 ns, 0.2-3.5 J/cm<sup>2</sup>). The structure, composition and optical properties of SiGe(Sn) layers are studied by transmission and scanning electron microscopy, RBS/Channelling, Raman spectrometry, time-resolved reflectivity, atomic force microscopy.

A special attention is devoted to fast crystallization of Si-based alloy layers and formation of cellular structure. We concentrate on segregation of dopant to a nanometer-scale cellular network; time-resolved reflectivity measurements of melting, crystallization and segregation. Optical properties of segregated cellular SiGe/Si structures are considered as well. The results of pulsed laser modification of Ge and GeSn nanodots are also be presented assuming that fast segregation is a powerful tool for production of non-equilibrium compounds, e.g. metastable Ge<sub>1-x</sub>Sn<sub>x</sub> dots with a direct tuneable energy band gap.

A new approach for nano-profiling of the surface is proposed and implemented. The approach consists of pulsed laser melting of SiGe(Sn) layers, self-organized formation of a cellular nanostructure followed by selective etching of Ge out of walls of the cells. The regimes of laser melting and anodic or thermal etching are achieved, in which the formation of epitaxial Si columns (200-300 nm in diameter and 500 nm in height), separated by grooves of 3-30 nm wide takes place. The nano-profiled SiGe/Si surface is finally applied for high-temperature growth of epitaxial SiC layers.

# CALCULATION OF THE SHAPE OF A MELT DROP LEAVING THE SHAPER WHEN GROWING A CRYSTAL BY THE STEPANOV METHOD

**Galaktionova N.E.<sup>1</sup>, Galaktionov E.V.<sup>2</sup>, Tropp E.A.<sup>2</sup>**

*1 - Peter the Great St. Petersburg Polytechnic University*

*2 - Ioffe Institute*

*nadyavk@mail.ru*

Theoretical studies of the shape of a liquid drop of small volume on a solid surface in the presence of a three-phase contact zone are necessary for solving many scientific and technological problems [1]. The equilibrium problems of capillary surfaces are the basis for studying the shape of liquid menisci in the process of single-crystal growth using the Stepanov method [2]. In [3], variational statements of the main tasks of this class were given: a drop on a solid surface, a drop on a drop of another liquid, a drop with a partially faceted surface.

In [4], the problems of the shapes of the surfaces of sessile and pendent drops were investigated taking into account the gravity force, their approximate solutions were found for the case of a small Bond number, and also a bibliography of works on this subject was given.

In this paper, we study a problem that is a symbiosis of two problems, namely, the problem of a capillary tube and the problem of a drop lying on a solid surface (the problem of a drop coming out of a shaper). We will take as a drop figure mushroom shape. In view of the axial symmetry, we will solve the problem in a cylindrical coordinate system. The mushroom stem is a cylinder, the shaper outer edge has a rounding along the arc of a circle, and the inner one has no rounding. The case when a melt drop goes beyond the outer edge of the shaper is considered.

We introduce into consideration the functional, which includes the surface energy and the energy of gravity force. The surface energy, in turn, consists of the part corresponding to the free surface of the drop and the part corresponding to the contact of the liquid with the solid. We solve the isoperimetric problem: find the minimum of the energy functional, provided that the functional describing the volume takes the given value. Varying the extended functional gives us the Euler equations and the transversality condition. Next, we reduce the problem to a dimensionless form. The right sides of the equations will contain the Bond number. Assuming its smallness, we look for the solution of the original problem in the form of a series in integer powers of the Bond number.

A zero approximation (which does not take into account the action of gravity force) and a first approximation (which takes into account the action of this force) are constructed. An algorithm for constructing the following approximations is given. It is shown that as the radius of curvature of the shaper tends to zero, the solution of the problem without rounding is obtained. A similar result holds for the case of rounding of the inner edge. It was found that the solution of the first approximation suffers a discontinuity (jump) of the first derivative at a point on outer edge of the shaper. The presence of rounding of the outer edge does not affect the existence of a jump in the first derivative of the solution. Thus, it is established that in the case under consideration there is no twice continuously differentiable solution of the original problem (the drop slips off the outer edge).

1. Finn R. Equilibrium Capillary Surfaces. Springer, New York, 1986. 236 p.
2. Antonov P.I., Zatulovskii L.M., Kostygov A.S. et al. Fabrication of Profiled Single Crystals and Articles by the Stepanov Method. / Ed. by V.R. Regel' and S.P. Nikanorov. L.: "Nauka", 1981. 280 p.
3. Galaktionova N.E., Galaktionov E.V., Tropp E.A. // Izv. Ross. Akad. Nauk, Ser. Fiz. 2009. **73**, P. 1393.
4. Galaktionov E.V., Galaktionova N.E., Tropp E.A. // Tech. Phys. 2016. **61**, P. 1781.



# VERTICAL LIQUID BRIDGES AND CRYSTAL GROWTH BY THE STEPANOV METHOD

Galaktionov E.V.<sup>1</sup>, Galaktionova N.E.<sup>2</sup>, Tropp E.A.<sup>1</sup>

*1 - Ioffe Institute*

*2 - Peter the Great St. Petersburg Polytechnic University*

*evgalakt@mail.ru*

Recently, the theory of liquid bridges between various surfaces attracts the attention of researchers. In one of the first works devoted to the study of liquid bridges [1], the author proposes to consider two types of objects, namely, bridges with a fixed contact contour ( $r$ - bridges) and bridges with a fixed contact angle ( $\theta$  – bridges). In [2], the authors distinguish two main areas of research: the study of the shape of liquid bridges and the study of their stability. In conducting these studies, both asymptotic and numerical methods for solving equations are used. In [3] and [4], asymptotic representations for the forms of the lateral surfaces of the horizontal and vertical  $\theta$  – bridges with small Bond numbers are constructed. The bibliography is presented in [2], [3].

The practical application of this theory is the study of the profile curves of meniscus cylindrical single crystals grown from the melt by the Stepanov method [5]. In this paper, a special case of a liquid bridge - an axisymmetric vertical liquid bridge of small volume between two parallel solid planes that are separated from each other on a preset distance is considered. Such a liquid bridge simulates a drop of melt between the shaper and the crystal in the steady-state growth process.

We introduce into consideration the functional, which includes the surface energy and the energy of gravity force. The surface energy, in turn, consists of the part corresponding to the free surface of the drop and the part corresponding to the contact of the liquid with the solid. We reduce the initial problem to an isoperimetric problem: finding the minimum of this functional subject to the constancy of the volume of the liquid bridge. Next, we perform the variation of the extended functional and as a result we obtain the Euler equation and two transversality conditions. These conditions determine the contact angles (the angles between the curve describing the lateral surface of the liquid bridge and the bottom (top)) in terms of the given surface tension coefficients.

After reducing the problem to a dimensionless form, the parameter - Bond number, appears in the right side of the equation. The approximate solutions of the problem are found under the assumption that this parameter is small.

Different variants of boundary conditions are considered, namely: at the bottom and the top - the conditions of transversality; at the top – the growth angle [5] and at the bottom – the transversality condition; at the top – the growth angle, at the bottom – the condition of engagement for the edge of the shaper (the bottom radius is set).

An algorithm for the iterative process of finding a solution to the original problem is proposed. A non-uniqueness of the solution is detected. The dependence of the solutions number on the liquid bridge height has been analyzed. It is shown that the maximum number of different profiles of the lateral surface of the bridge is four. The critical height value is found. There are no solutions for liquid bridge heights exceeding the critical one.

1. Fortes M.A. // J. Colloid Interface Sci. 1982. **88**, N 2, P. 338.
2. Fel L.G., Rubinstein B.Y. // Z. Angew.Math. 2016. **66**, P. 3447.
3. Haynes M., O'Brien S.B.G., Benilov E.S. // Phys. Fluids. 2016. **28**, P. 042107.
4. Galaktionov E.V., Galaktionova N.E., Tropp E.A. // Tech. Phys. 2017. **62**, P. 1482.
5. Antonov P.I., Zatulovskii L.M., Kostygov A.S. et al., Fabrication of Profiled Single Crystals and Articles by the Stepanov Method. Ed. by V.R. Regel' and S.P. Nikanorov. L.: "Nauka", 1981. 280 p.

# ON GROWTH OF SbSI FILMS BY THE QUASI-CLOSED VOLUME TECHNIQUE AND THEIR PROPERTIES

Garmashov S.

*Southern Federal University*

*garmashov@sfedu.ru*

Antimony sulfoiodide (SbSI) is attractive as a material with piezoelectric, semiconductor and ferroelectric properties. Growth of thin films of SbSI is of interest for creating infrared radiation sensors, memory elements, and other devices [1, 2].

One method of forming SbSI films is based on the evaporation of the source-compound in a quasi-closed volume and the condensation of a vapor substance on a substrate with a lower temperature. For the first time such method of producing SbSI films was proposed in [3] and further investigated in [4, 5].

Since SbSI evaporates incongruently with decomposition into two components: an easily evaporating  $SbI_3$  compound and a weakly volatile  $Sb_2S_3$  compound, it is important to ensure that the temperature and duration of the growth process are such that these compounds could form a stoichiometric SbSI film on the substrate. For this purpose, a series of *in-situ* experiments was organized with monitoring of the state of condensate on a glass substrate using a digital video camera. The temperature control of the source and the substrate was carried out automatically and was synchronized with the video. SbSI was used as a source in the form of crystals grown in an ampoule and in the form of a powder synthesized from aqueous solutions [6].

The use of video has been allowed to observe the evolution of condensate on the substrate and to fix the moment of formation of the SbSI film.

The report provides information on the optimal temperature regime for producing SbSI films of stoichiometric composition, X-ray diffractometry, electron microscopy, and the absorption spectra of these films.

1. S. Surthi, S. Kotru, R.K. Pandey, *J. Mater. Sci. Lett.*, 2003, **22**, 591– 593.
2. K. C. Goedel, U.Steiner. *Nanoscale*, 2016, **8**, 15920.
3. V.Yu. Gershanov, E.G. Merinova, E.D. Rogach, *Abstracts of II All-Union Conf. on the Physical-Chemical Principles of the Technology of Ferroelectric and Related Materials*, Zvenigorod, 1983, 185.
4. S.I. Garmashov, V.Yu. Gershanov, I.N. Rybina, S.N. Svirskaya, I.N. Zakharchenko, A.A. Sverdlov, D.A. Kakichev, *Abstracts of VIII International Conference “Kinetics and mechanism of crystallization”*, Ivanovo, 2014, 134.
5. S.I. Garmashov, E.S. Druzhinina, *Abstracts of X International Conference “Kinetics and mechanism of crystallization”*, Suzdal, 2018, 335-336.
6. T.G. Lupeiko, S.N. Svirskaya, I.N. Rybina, E.S. Medvedeva, A.S. Pakhomov, *Materialy III mezhvuzovskoy nauchno-practicheskoy ezhegodnoy konferentsii “Novye technologii i innovatsionnye razrabotki”*, Tambov, 2010, 102-105.

# NUCLEATION STATISTICS AND LENGTH DISTRIBUTIONS FOR WURTZITE AND ZINC BLENDE III-V NANOWIRES GROWING FROM LIQUID NANODROPLETS WITH VERY LOW GROUP V CONTENT

Glas F.

*Centre for Nanoscience and Nanotechnology, CNRS, Université Paris-Sud, Université Paris-Saclay*

*frank.glas@c2n.upsaclay.fr*

The growth of semiconductor nanowires (NWs) in the vapor-liquid-solid (VLS) mode offers a unique opportunity to study individual and sequential nucleation events in a nanosized medium. In VLS growth, the formation of the solid NW from the external vapor fluxes is mediated by an apical liquid catalyst nanodroplet. This can now be observed at high spatial resolution and in real time in dedicated electron microscopes, and such *in situ* experiments have indeed confirmed that NWs grow monolayer by monolayer (ML) [1,2,3], the formation of each ML being triggered by a single nucleation event occurring at the solid-liquid interface [3].

We consider specifically the growth of NWs of III-V compounds. The volatile group V elements (P or As) are present at very low concentration (on the order of a percent) in the liquid nanodroplet. This means that the formation of even a single ML may significantly deplete the droplet in group V element. We demonstrated experimentally and theoretically that this has a strong impact on the statistics of nucleation, which become sub-Poissonian [4,5]: depletion makes a new nucleation less likely after a first one than before, so that the nucleation events become anti-correlated in time. In turn, this "nucleation antibunching" [4] has important consequences on the length distributions of ensembles of NWs, which may be much more uniform than in the case of Poisson statistics [6].

This picture is valid when the time for ML completion (after nucleation) is short compared with the interval between successive nucleations. This requires in particular enough group V atoms in the droplet to complete rapidly the solid ML. However, another regime is possible, whereby the number of group V atoms in the liquid at nucleation is even lower, namely less, and possibly well below, the group V content of a ML. Such a regime is easily achievable and is actually realized in some of our *in situ* experiments: the ML then advances slowly since the system has to wait for the external fluxes to refill the droplet.

In this case, the kinetics and statistics of nucleation are deeply modified. We have simulated NW growth sequences corresponding to such conditions and calculated numerically and analytically the nucleation statistics. We investigated the distributions of the "growth times" (between nucleation and completion of a ML) and waiting times (between ML completion and next nucleation). We find two extreme regimes, depending on group V desorption from the liquid droplet (and hence on temperature). We also studied the length distributions of ensemble of NWs in this previously unexplored regime.

III-V NWs are known for their cubic/hexagonal polytypism. The results summarized above apply to the formation of MLs in the hexagonal structure, where the solid-liquid interface remains planar. In the cubic structure, growth may involve the formation of a truncated interface: material from the already grown NW may then be used to feed ML propagation. We will discuss how the nucleation kinetics and statistics and the length distributions of ensembles of NWs are then modified.

- [1] C.-Y. Wen, J. Tersoff, M. C. Reuter, E. A. Stach, F. M. Ross, *Phys. Rev. Lett.* **105**, 195502 (2010).
- [2] D. Jacobsson, F. Panciera, J. Tersoff, M. C. Reuter, S. Lehmann, S. Hofmann, K. A. Dick, F. M. Ross, *Nature* **531**, 317 (2016).
- [3] J.-C. Harmand, G. Patriarche, F. Glas, F. Panciera, I. Florea, J.-L. Maurice, Y. Ollivier, *Phys. Rev. Lett.* **121**, 166101 (2018).
- [4] F. Glas, J.-C. Harmand, G. Patriarche, *Phys. Rev. Lett.* **104**, 135501 (2010).
- [5] F. Glas, *Phys. Rev. B* **90**, 125406 (2014).
- [6] F. Glas, V. G. Dubrovskii, *Phys. Rev. Mater.* **1**, 036003 (2017).

## TWO APPROACHES TO FORMATION OF THIN Mg<sub>2</sub>Si FILMS ON Si SURFACE: ULTRA-FAST DEPOSITION AT 400 C AND ROOM TEMPERATURE DEPOSITION ON AMORPHOUS Si

**Gouralnik A.S.<sup>1</sup>, Shevlyagin A.V.<sup>1</sup>, Chernev I.M.<sup>1</sup>, Gerasimenko A.V.<sup>2</sup>, Gutakovskii A.K.<sup>3</sup>**

*1 - Institute of Automation and Control Processes, Far-Eastern Branch RAS, Vladivostok, Russia*

*2 - Institute of Chemistry, Far-Eastern Branch of RAS, Vladivostok, Russia*

*3 - Institute of Semiconductor Physics, Siberian Branch RAS, Novosibirsk, Russia*

*fun\_era@mail.ru*

Mg and Si are abundant, ecologically friendly and relatively cheap elements. The silicide Mg<sub>2</sub>Si looks naturally compatible with traditional silicon technology. It is a narrow gap semiconductor suitable for production of infrared photodetectors for the wavelengths of ~1.5 micrometers (the best for optoelectronics fiber cables). There are perspectives of significant improving of solar cell performance in IR region *via* applications of Mg<sub>2</sub>Si layers.

Till now, it has been believed that growth of Mg<sub>2</sub>Si on Si at  $T > 200$  °C is impossible since at such temperatures Mg re-evaporates from the surface without condensation. This has been formulated *via* the *condensation coefficient*  $\alpha_c$  which is zero for  $T > 200$  °C [Mahan et al., Phys. Rev. **B 54** 16965 (1996)]. It can be suggested that the Mg atoms' binding energy on the Si surface is so low that they evaporate before they have chance to interact. We analyzed the Mg concentration on the surface during the early stage of deposition,  $C_{Mg/Si}$ , in terms of *mean residence time* before re-evaporation,  $\tau_{Mg/Si}$ , and found that the  $C_{Mg/Si}$  value saturates with time,  $t$ :  $C_{Mg/Si} = R\tau_{Mg/Si} (1 - \exp(-t/\tau_{Mg/Si}))$ , where  $R$  is the deposition rate. At  $T > 200$  °C the residence time  $\tau_{Mg/Si}$  is so short that for the usual deposition rates (0.001 – 5 nm/sec) the saturation value  $R\tau_{Mg/Si}$  is very low. Unlike molecules, the formula units (f.u.) Mg<sub>2</sub>Si need to be surrounded by similar units to self-arrange stereo-chemically. That means that large amounts of interacting atoms are required for silicide nuclei formation. Since the dependences of Mg condensation and silicide nucleation rates on  $C_{Mg/Si}$  are essentially non-linear, the non-condensation problem can be circumvented by radical increase of the Mg deposition rate  $R$  [Gouralnik et al., Appl. Surf. Sci. **439**, 282 (2018)]. Here we demonstrate the Mg<sub>2</sub>Si films successfully grown by deposition of Mg on silicon at  $T \approx 400$  °C, at the rates of ~100 – 1000 nm/second. Such rates were implemented by discharging a capacitor through the foil onto which Mg was pre-deposited [Russian Federation Patent №116859]. The films have the best crystal quality. The silicide growth mechanism is discussed. Perspectives of applications of such Mg<sub>2</sub>Si layers for improving solar cell performance in IR region are considered.

Intermixing of components is the inherent part of the any compound synthesis process. Amorphous silicon has ~ (5–15)% lower density than crystalline Si, this promotes deeper intermixing. During intermixing, nuclei of new phases occur and grow inside a solid mixture having some finite hardness. The chemical interactions of reagents can cause internal strains due to phase transformations, volumetric effects and lattice misfits at the interface. The strains can contribute into the reaction energetics and thus influence the product formation. Since these spontaneous strains can get high values without application of external pressure (that is a difficult and expensive procedure), intermixing systems represent an attractive field of investigations [Alloys and Compounds **778**, 514 (2019)]. We report on formation of the metastable (at normal pressure) orthorhombic phase Mg<sub>2</sub>Si by Mg deposition onto amorphous Si.

# FORMATION AND COMPOSITION FEATURES OF SELF-SCROLLING HYDROSILICATE CRYSTALS

**Krasilin A.A., Khrapova E.K., Gusarov V.V.**

*Ioffe Institute*

*ikrasilin@mail.ioffe.ru*

Some of the layered hydrosilicates (1:1 phyllosilicates) possess a possibility to form particles with wavy or scrolled morphology. This feature originates from size difference between the sheets constituting the phyllosilicate layer. The brightest representatives of these materials are  $\text{Mg}_3\text{Si}_2\text{O}_5(\text{OH})_4$  with chrysotile structure and  $\text{Al}_2\text{Si}_2\text{O}_5(\text{OH})_4$  with halloysite structure scrolled in opposite direction (with silica sheet inside of outside) with respect to each other. Driving forces of scrolling are, on the one hand, compensation of size difference, and on the other hand – difference in specific surface energies on the opposite sides of the layer. Resulting nanoscrolls could be found in mineral form or synthesized at hydrothermal conditions.

This talk will cover experimental aspects of replacing of Mg and Si cations by different d-elements thus changing the nanoscrolls morphology and other properties as well as modelling of the scrolling process. The developed energy model helped to estimate preferable diameter of multiwalled  $\text{Mg}_3\text{Si}_2\text{O}_5(\text{OH})_4$  and  $\text{Ni}_3\text{Si}_2\text{O}_5(\text{OH})_4$  nanoscrolls of certain estimated mass. It has been revealed that simultaneous presence of  $\text{Mg}^{2+}$  and  $\text{Ni}^{2+}$  yields increase of conical scrolls content, which may be related with unequal value of internal stress in the hydrosilicate layer. Energy model predicts that there is option additional to the scrolling for size difference compensation between the sheets, which is arranging of “isomorphous” cations in accordance with change of the layer curvature. Comparison of modeling results and experimental STEM/EDS data for  $(\text{Mg}_{1-x}, \text{Ni}_x)_3\text{Si}_2\text{O}_5(\text{OH})_4$  for conical and cylindrical nanoscrolls are considered. In particular, it is shown that Ni cations tend to concentrate at the outer wraps of the multiwalled scroll, whereas Mg cations concentrate at the inner ones.

The research was supported by Russian Science Foundation grant 16-13-10252.

# DYNAMICS OF ATOMIC STEPS AND SHAPE TRANSFORMATIONS OF NANOWIRES

**Filimonov S.N., Hervieu Yu.Yu.**

*National Research Tomsk State University*

*ervye@mail.tsu.ru*

Formation and propagation of monoatomic steps govern morphology of a growing crystal surface. Here we discuss how the shape evolution of nanowires (NWs) is affected by the step dynamics. We have developed a model of lateral growth of NWs via sequential formation of monoatomic steps at the NW base and their propagation along the nanowire sidewall [1]. The elongation rate of the NW and step velocities are determined from the solution of the surface diffusion equation subject to the boundary conditions at the steps, NW base, NW top, and on the substrate surface. The 2D growth on the substrate surface is taken into account within the mean-field approach [2,3]. The model reproduces the NW shapes with an abrupt change of the NW diameter observed in the experiment. We show that propagation of the steps approaching the NW top might be suppressed because of the positive supersaturation at the step relatively to the NW top. Therefore, the sidewall becomes unstable against step bunching. This explains the transition from cylindrical to syringe-like NW shape observed in the experiments on the Au-assisted MBE growth of InAs and GaAs [4].

We use this approach to describe the early stage of the NW growth on top of the pyramid-like pedestals formed under the catalyst droplet during the pre-growth annealing [5]. It is assumed that the top pedestal facet grows layer-by-layer by nucleation and spreading of 2D islands under the droplet. When the edge of the 2D island crosses the triple phase line it continues growing as the atomic step at the pedestal sidewall. The sidewall step is unstable against dissolution in favor of the next 2D island nucleated on top of the pedestal because of the difference of the specific energies of the step and the edge of the 2D island under the catalyst droplet. However, the step might run away from the pedestal top due to attachment of the sidewall and substrate adatoms. In this case, the step moves along the sidewall downward to the pedestal base and the pedestal grows in size without changing the pedestal shape. However, with the increasing pedestal size the new layers are nucleated at the pedestal top before the sidewall step reaches the pedestal base. The growing sidewall step cuts off the upward flux of sidewall and substrate adatoms, therefore the next step cannot come off the 2D island, so that a segment of the vertical sidewall forms, preventing the lateral growth of new layers generated by the droplet. The pedestal growth ceases, giving rise to the growth of the NW on top of the pedestal. The numerical modeling of the step dynamics demonstrates that the transition to the formation of the vertical sidewall may be delayed considerably with the decreasing supersaturation at the step relatively to the NW top and with the increasing density of steps (the edges of 2D islands) on the non-activated substrate surface.

- [1] S.N. Filimonov, Yu.Yu. Hervieu, *J. Cryst. Growth* 427 (2015) 60.
- [2] G.S. Bales, A. Zangwill, *Phys. Rev. B* 55 (1997) R1973.
- [3] Yu.Yu. Hervieu, *J. Cryst. Growth* 493 (2018) 1.
- [4] M. C. Plante, R. R. LaPierre, *J. Appl. Phys.* 105 (2009) 114304.
- [5] Z.M. Liao et al, *Appl. Phys. Lett.* 102 (2013) 063106.

# RELAXED STRUCTURE OF INTERPHASE BOUNDARIES IN TWO-LAYER METAL FILMS: MOLECULAR DYNAMICS

**Ievlev V.M.<sup>1,2</sup>, Prizhimov A.S.<sup>2</sup>**

*1 - Lomonosov Moscow State University*

*2 - Voronezh State University*

*rnileme@mail.ru*

Relaxed structure of interphase boundaries in epitaxial thin-film Ni/Pd, Ni/Ag, Cu/Ag heterostructures and in the heterostructures nanoparticles (semi-spherical islands) of Ni or Cu on the surface of the Pd monocrystal, Pd nanoparticles on the surface of Ni or Cu monocrystals was investigated.

1. On the example of epitaxial film Ni/Pd, Ni/Ag, Cu/Ag heterostructures it is shown that the compensation of the dimensional discrepancy occurs through the formation of a monolayer solid-state phase and the occurrence of mismatch dislocations, i.e. there is a two-stage compensation of the dimensional mismatch, manifested in the splitting of the interfacial boundary.

2. The orientation dependence of the type of growth of Ni films on the surface of a Pd monocrystal: on the (001) and (110)Pd surfaces – by Frank and van der Merwe with compensation of the size discrepancy through the formation of packing defects (partial dislocations at the interface), as well as full dislocations in the case of growth on (110)Pd; on the surface (111)Pd – by Folmer and Weber mechanism.

3. In the models of nanoparticle – monocrystal Ni/Pd, Pd/Ni, Cu/Pd, Pd/Cu the size effect is established: during annealing the islands of subcritical size are rotated to orientation, corresponding to the coincidence orientation (lattice of coincident nodes) with the formation of a relaxed atomic structure of a special interface consists of the structural units corresponding to the nearest lattice of coincident nodes; the rotation of the nanoparticle to that position confirms the existence of local energy minima on the orientation dependence of the energy of the interfaces. The orientation of the islands that larger than the critical size does not change, the relaxed structure of the boundaries is organized by structural elements and boundary dislocations (analogue of grain boundary dislocations) which compensating the deviation from the special orientation.

4. The general pattern of the structure of interfaces is asymmetry. In epitaxial heterostructures defects are formed in a growing film, in nanoparticle – monocrystal heterostructures an atomic rearrangements occur in a system component with a larger lattice parameter.

The work is supported by the Russian Scientific Foundation, the project 19-19-00232.

# DETERMINATION OF CRYSTALLISATION TEMPERATURE OF MULLITE BY LUMINESCENCE SPECTRA OF EUROPIUM AND CHROMIUM IONS

Igo A.V.

*Ulyanovsk state university*

*igoalexander@mail.ru*

Crystallization from the amorphous state occurs when the temperature rises above a certain limit, when diffusion processes become essential. Crystallization occurs when it becomes possible for a phase to exist with less energy than the energy of the amorphous phase. In the process of temperature rise, it is possible to form intermediate crystalline states or transition phases. The report is related to the study of the process of formation of mullite crystals by heating aluminosilicates.

In the experiment, the temperatures of formation of the transition phase and stable phase of the crystalline state of mullite was estimated. Mullite is certainly one of the most important oxide materials for both conventional and advanced ceramics [1]. The luminescence spectra of kaolin samples fired at temperatures from 600 to 1200 °C were measured [2]. Before firing, chromium and europium oxides were added to the samples.

Electronic structures of Cr<sup>3+</sup> and Eu<sup>3+</sup> ions as an impurity centers in the surrounding crystalline field are known and calculated in detail in the forms of a Tanabe - Sugano diagrams. On the luminescence spectrum, the narrow spectral line of the <sup>2</sup>E<sub>g</sub>-<sup>4</sup>A<sub>2g</sub> transition corresponds to octahedral position of Cr<sup>3+</sup> ion in the mullite crystals, and a wide spectral line of the <sup>4</sup>T<sub>2g</sub>-<sup>4</sup>A<sub>2g</sub> transition corresponds to a tetrahedral position of Cr<sup>3+</sup> in the mullite crystals. At the spectra of samples fired at temperatures above 890 °C the luminescence of <sup>2</sup>E<sub>g</sub>-<sup>4</sup>A<sub>2g</sub> transition is observed, but only at the temperatures of firing above 920 °C both spectral lines are observed in the spectra.

Some transition forms of sillimanite-type have a crystal lattice similar to mullite, but in them impossible to introduce Cr<sup>3+</sup> ions into the tetrahedral position. Contrary to them, the crystal structure of the stable phase of the mullite contains a certain distribution of oxygen vacancies, which allows Cr<sup>3+</sup> ions to penetrate into tetrahedral positions. Since the temperature of 920 °C and above, the spectra show a stable ratio of the intensities of the two spectral lines.

The optical transition <sup>5</sup>D<sub>0</sub>-<sup>7</sup>F<sub>2</sub> of Eu<sup>3+</sup> ion has a high sensitivity to the symmetry of the surrounding crystal field. In the cubic symmetry field (the initial state of the oxide), the level <sup>7</sup>F<sub>2</sub> is split into two sublevels, the upper three times degenerate and the lower two times. When the ion Eu<sup>3+</sup> is placed in the octahedral position the splitting of the level into two sublevels remains, only the upper one becomes twice degenerate and the lower one three times. In the luminescence spectra level splitting is observed clearly, and the degeneracy is manifested in the intensity of the line. From the firing temperature of 600 to 920 °C the intensity ratio of the sublevels is of the order of 0.75, and above 920 °C the intensity ratio of the order of 1.5. A sharp change in the symmetry of the crystal field suggests the formation of a new crystalline phase (phase transition).

The intensity of Cr<sup>3+</sup> luminescent lines depends on the impurity concentration and the amount of mullite formed and can be used to estimate them [3].

1. H. Schneider, R. X. Fischer, J. Schreuer // J. Am. Ceram. Soc. 2015, V. 98, pp. 2948–2967
2. A.V. Igo // Optics and Spectroscopy, 2017, V. 122, pp. 912-918
3. A.V. Igo, A.E. Kozhevnikov // Glass and Ceramics, 2017, V.74, pp.23-25



## SILICON NANO-CRYSTALLITES FOR ADVANCED APPLICATION

**Ivanda M., Gebavi H., Mikac L., Đerek V., Baran N., Ristić D., Životkov D.**

*Center of Excellence for Advanced Materials and Sensing Devices, Ruđer Bošković Institute, Bijenička cesta 54, Zagreb, Croatia*

*ivanda@irb.hr*

The presented research addresses basic properties and application of silicon/hybrid nanostructures for surface enhanced Raman spectroscopy (SERS), infrared light detection and gas sensing. The silicon nanostructuring were performed by anodisation process, chemical etching and low pressure chemical vapor deposition (LPCVD).

Today there is an increased demand for the development of stable, sensitive, reproducible and portable SERS-active substrates. Some of the most broadly used SERS substrates are noble metal colloids. During the preparation of colloidal suspensions, the size and shape of the particles can be well controlled. However, the use of colloids for SERS has some disadvantages, like problems with reproducibility and stability. Other popular types of substrates are rough or nanoporous surfaces. Porous silicon (PSi) is a semiconducting material fabricated by electrochemical etching in hydrofluoric acid (HF) that has high surface-to-volume ratios and is, therefore, interesting materials for sensing devices, drug delivery systems and for use in SERS. Here we present the SERS substrates produced by different synthesis methods.

Silver nanoparticles on different porous silicon nanostructures have been prepared by the immersion plating in AgNO<sub>3</sub>. This procedure enable preparation of SERS substrates based on p-type pSi and for ultra-low concentration detection of R6G with dilution up to 10<sup>-15</sup> M.

Another approach is to develop SERS optical fiber probe by growing horizontal silicon nanowires on the optical fiber by vapour-liquid-solid growth by using LPCVD technique. The SERS sensitivity were tested on silver nanoparticles decorated substrates and the detection concentration limit of 10<sup>-9</sup> M of rhodamine 6G molecules was reached. The Ag decorated nanowires shown on Fig. 1 are proved to be sensitive substrates for SERS only if the silicon nanowires thickness, length, volume density as well as metal nanoparticle size and distribution are carefully designed.

Figure 1\*. SiNWs on optical fiber obtained by VLS method decorated with AgNPs during various sputtering times: 1, 2, and 4 min.

Silicon based alternatives are of interest to replace expensive low band-gap materials, like InGaAs, in telecommunications and imaging applications. Herein, we report on the significant enhancement in NIR photodetector performance afforded by nano- and microstructuring of p-doped silicon (p-Si) and, thereafter, deposition of a layer of the organic semiconductor Tyrian Purple (Fig.2). Among different silicon structures produced by electrochemically etching, metal-assisted chemical etching, the micro-pyramids produced by anisotropic chemical etching are shown the strongest effective increase of the NIR response of p-Si/TyP heterojunction diodes. In all cases, the structured interfaces were found to give photodiodes with superior characteristics as compared with planar interface devices, providing up to 100-fold improvement in short-circuit photocurrent, corresponding with responsivity values of 1–5mA/W in the wavelength range of 1.3–1.6 micrometers.

Finally, as a third example, we will present the sensitivity of oxidized nano- porous silicon in detection of ammonia by resistivity measurements.

Figure 2\*. J-V characteristics of Al/p-Si/TyP/Al in dark and under illumination with a 1.48 lm laser diode (200 mW/cm<sup>2</sup>) of planar silicon and silicon micropiramids: (a); SEM images of 30–40nm TyP films grown on planar p-Si (scale bar200 nm): (b).

**\*The abstract with figures is available at <http://2019.mgctf.ru/0100003626.doc>**

# MATHEMATICAL MODELING OF DENDRITIC CRYSTAL GROWTH IN MUSHY ZONE OF METALLIC ALLOYS

Ivanova A.

*Institute of Applied Mathematics and Mechanics*

*ivanova.iamm@mail.ru*

During metallic alloys solidification the planar solid/liquid interface transforms to a disturbed surface. As the result the mixed zone containing the liquid and solid phases appears between the liquid and solid metal. It is called mushy zone. The crystals in mushy zone can be oriented columnar and nonoriented equiaxed. Thus, the crystalline structure of the casting ingot is formed. Groups of crystals of the same type can be separated by a sharp boundary, but also mixed transitions from one to another group can take place. Different industrial technologies require determination of alloy semi-finished product structure with more or less accuracy.

It is difficult to predict the ingot structure because it is determined through the complicated crystallization process, that involves many physical phenomena such as heat and mass diffusion, dendritic morphology, capillary effects, etc. These phenomena interact with each other and predominate at different conditions. In order to control structure formation in practice means understanding the connection between process parameters and microstructure evolution. The understanding of such physical relation can only be complete in case it can be explained mathematically.

The columnar into equiaxed structure transformation (CET) was the subject of the mathematical modelling method [1] that takes into account the extreme points (minima and maxima) and also points of inflection of some considered/simulated functions.

The temperature field simulation [2] allowed for initial suggesting of columnar structure disappearing, equiaxed dendrites appearing and CET localization in term of solidification time.

This paper devoted to mathematical modeling of dendritic crystal growth in mushy zone of metallic alloys. The growth of the columnar dendrites starts from the chill zone of the ingot and is carried out in the direction opposite to the heat extraction (perpendicular to the crystallization front). When the temperature of liquid alloy falls below a certain value, the process of nucleation and growth of equiaxed nonoriented crystals begins. In both cases the nucleation and growth of crystals occur when the melt is supercooled below the equilibrium liquidus point [3].

The model takes into account that the liquidus temperature depends on the concentration of the alloying components and impurities and in turns, the faster the speed of advance of the phase change boundary, the more the liquidus temperature "slides" before it since diffusion has not time to align the melt composition near the front.

Calculations are made on a rectangular grid. The temperature distribution is determined using the method presented in [4]. The method for recalculating the concentrations and fraction of solidified/melted substance in the cells has been proposed.

[1] Wołczyński W. (2016) Large Steel Ingots: Microstructure Mathematical Modeling. Rafael Colas & George E. Totten, (Eds.), Volume III: Heat Treatment: Special – Molten of the Encyclopedia of Iron, Steel, and Their Alloys (1910-1924), London, New York: CRC Press, Taylor & Francis Group.

[2] Louhenkilpi S., Miettinen J., and Holappa L. (2006) Simulation of Microstructure of As-cast Steels in Continuous Casting. ISIJ International, Vol. 46, No. 6, pp. 914–920.

[3] Samoylovich Yu.A. (1983) Sistemny analiz kristallizatsii slitka. Kiev: Nauk. dumka.

[4] Kurganskyy A.N., Maksimova A.Yu. (2016) The entropy of a thermodynamic graph. Trudy Instituta Prikladnoj Matematiki i Mechaniki V.30, pp. 96–108.

# THE SCALING OF SUBNANOMETER EOT GATE DIELECTRICS FOR ULTIMATE NANO CMOS TECHNOLOGY

**Iwai H.I.**

*Tokyo Institute of Technology*

*iwai.h.aa@m.titech.ac.jp*

The progress of microprocessors or logic integrated circuits in the past 50 years has been accomplished by the downsizing of MOSFETs with the scaling scheme [1]. In that scheme, the lateral and vertical dimensions and supply voltage for MOSFETs are reduced by the same factor in principle. By the scaling, the cost, performance and power consumption per MOSFET have been improved constantly. Gate oxide is a key component of the MOSFET, and its equivalent oxide thickness (EOT) has been decreased continuously from 110 nm in early 1970's to recent sub-1.0 nm. With decreasing the gate length MOSFETs, thinning the gate oxide is necessary to enhance the controllability of the gate bias to the channel current so as to cut-off the subthreshold leakage current between the source and drain. SiO<sub>2</sub> based gate oxide had been used almost 40 years for PMOS, NMOS and then CMOS integrated circuits from early 1970's to late 2010's, because of their extraordinary good properties at the Si channel interface. However, when the gate oxide thickness approached to 1 nm, we had to change the oxide to 'high dielectric constant' or 'high-k' ('k' is 'dielectric constant') materials to suppress the huge direct-tunneling leakage current through the gate oxide. With increasing the k value, the same capacitance of the MOS gate can be obtained with a physically thick gate oxide film, and the direct-tunneling leakage can be suppressed. The requirements for the high-k material are i) high k value, ii) high band offset value between Si and high-k oxide to suppress the tunneling leakage, iii) chemical stability at Si interface during high temperature (several-100 to 1,000 degree C) process for integrated circuit manufacturing, iv) good electrical property at the Si interface. Among many candidates, La<sub>2</sub>O<sub>3</sub> had been regarded as the best, and HfO<sub>2</sub> was the second candidates. However, because of the hygroscopicity of La<sub>2</sub>O<sub>3</sub>, HfO<sub>2</sub> based gate oxide was chosen and introduced into products in 2007 with 1.0 nm EOT for several 10 nm gate length MOSFETs. Then, the pace of oxide EOT thinning has been slow because of many difficulties related to ultra-thin gate film, such as remote scattering of channel carriers by fixed charge and roughness at the interface between that gate oxide and electrode. For the moment, EOT used for the most advanced generation is around 0.8 nm for 20 nm gate length MOSFETs in production. It is expected that the downsizing the MOSFETs will reach its limit at the gate length of about 12 nm with supply voltage of about 0.55 V about 10 years from now. For 12 nm gate length, about 0.5 nm EOT is supposed to be required for the normal operation of MOSFETs. In this presentation, future high-k gate stack technology including that of La silicate is explained. Good MOSFET operation with La silicate gate oxide with EOT = 0.4 nm is demonstrated.

[1] R. Dennard et. al, IEEE J. SSC, vol. 9, no. 5, pp.256 – 268, 1974

# THE INFLUENCE OF ARGON GAS FLUX AND DEPOSITION RATE ON OPTICAL AND PHYSICAL PROPERTIES OF DC MAGNETRON SPUTTERED ITO THIN FILM

**Kadivar E., Moshabaki A.**

*Department of Physics, Shiraz University of Technology, Shiraz, 71555-313, Iran*

*erfan.kadivar@sutech.ac.ir*

## **Introduction**

Indium tin oxide (ITO), which is a highly degenerate n-type semiconductor with a wide band gap (about 3.7eV), high optical transparency and electrical conductivity, is widely used as transparent conductive oxide (TCO) films. The ITO transparent conductive thin films have been applied in a variety of optoelectronic devices such as organic light emitting diodes, gas sensors, electrochromic devices, heat mirror, photovoltaic solar cells, etc. The ITO thin film has been deposited by a variety of techniques such as electron beam evaporation, thermal evaporation, direct current sputtering (DC), radio frequency (RF) magnetron sputtering and etc [1-2].

Affecting factors on surface quality and electrooptical properties of a prepared thin film by sputtering technique are chamber pressure, material purity, substrate temperature, sputtering power, layer thickness and ratio of oxygen gas flux to argon gas flux [3-5]. The surface roughness and figure of merit are two significant factors for determining the quality of ITO thin film [6]. The aim of this work is to produce the ITO thin films with low surface roughness and high figure of merit. Unlike previous works [7-8], in this work, ITO thin films have been prepared on the glass substrates by DC magnetron sputtering at zero oxygen gas flux. We investigate the effect of argon gas flux and deposition rate on the morphology and electrooptical characteristics of thin films.

## **Result**

<see full text\*>

Table 1\*. Influence of argon gas flow on the physical properties of ITO thin film in the absence of oxygen gas flow.

Table 2\*. The influence of deposition rate on the resistivity and surface roughness.

Figure 1\*. FESEM images of ITO films deposited at different values of argon gas flow: a) 5 sccm and b) 10 sccm.

Figure 2\*. Hall mobility as well as the carrier concentration of the ITO films at different argon gas flow.

## **Conclusion**

The ITO thin film was deposited on BK7 glass substrate by DC magnetron sputtering method at zero oxygen gas flow rate. The effect of argon gas flux, and deposition rate on the morphology and electrooptical characteristics of thin films have been analyzed. Our experimental results indicate that the surface roughness increases by decreasing the argon and rate deposition. The result revealed that the lowest surface roughness of 1.07nm was achieved at argon gas flow 20 sccm and deposition rate 0.5 Å/s.

## **References**

- [1] S. Boycheva, A.K. Sytchkova, M.L. Grilli, A. Piegari, *Thin Solid Films* 515 (2007) 8469.
- [2] S.H. Kim, N.M. Park, T.Y. Kim, G.Y. Sung, *Thin Solid Films* 472 (2005) 262.
- [3] F. Niino, H. Hirasawa, K. Kondo, *Thin Solid Films* 411 (2002) 28.
- [4] D. Kim, Y. Han, J.S. Cho, S.K. Koh, *Thin Solid Films* 377 (2000) 81.
- [5] Y. Han, D. Kim, J.S. Cho, S.K. Koh, *Thin Solid Films* 473 (2005) 218.
- [6] T. Yang, Z. Zhang, S. Song, Y. Li, M.S. Lv, Z. Wu, S. Han, *Vacuum*, 83 (2009) 257.
- [7] C. Guill'en, J. Herrero, *Vacuum* 80 (2006) 615.
- [8] J Xu, Y Yuan, F Wang, K Zhang, *ECS Transactions* 44 (2012) 1311.

\*The full abstract with figures and tables is available at <http://2019.mgctf.ru/0100003152.doc>

# CRYSTAL GROWTH AT SPONTANEOUS CRYSTALLIZATION IN NON-INERTIAL SYSTEMS IN SPACE STATION AND EARTH CONDITIONS BY THE EXAMPLE OF SYNTHESIS AND GROWTH OF CRYSTALS FROM SOLUTION-MELT

**Kalashnikov E.V.<sup>1,2</sup>, Gurin V.N.<sup>2</sup>, Nikanorov S.P.<sup>2</sup>, Derkatchenko L.I.<sup>2</sup>, Yagovkina M.A.<sup>2</sup>**

*1 - Moscow State Regional University, Mitishy of Moscow Region, V.Voloshina street, 24, Russia*

*2 - A.F. Ioffe Physical-Technical Institute of Russian Academy of Science, Saint-Petersburg, Politechnicheskaya street, 26. Russia*

*ekevkalashnikov1@gmail.com*

At the experimental study of the gravitational field influence on the spontaneous growth of crystals from melt, three situations were studied:

- (1). Synthesis and crystal growth of from the melt of at force of gravity condition, (on Earth)
- (2). Synthesis and crystal growth of from the melt at absence of gravity force (on the space station, SS)
- (3). Behavior of grown crystals obtained by the previous two methods on Earth.

The main results of this study were:

at the absence of gravity (at SS) formed crystals

- a) have sizes about ~2 times larger than isometric crystals of the same compound grown in terrestrial conditions
- b) get new additional faces
- c). differ in composition from stoichiometric composition
- d). Over time (relaxation time), in terrestrial conditions, "cosmic" crystals return to their original size and composition, characteristic of terrestrial conditions.

It is shown that the reason for the difference between the crystals that arose in the conditions of "Earth" and "space" is the pressure of the reaction forces of the support in the melt (in the conditions of "Earth"), and their absence (in "space"). It is the absence of pressure of the reaction forces of the support in the melt (SS) that leads to the fact that the crystals grown on the SS have the properties specified in (a, b, c) and grow with excess stress. This excess stress is numerically equal to the pressure of the reaction forces of the support in the melt on the Earth.

# OPTICAL PROPERTIES OF SPATIALLY INDIRECT EXCITONS IN ZINC BLENDE GaSb/GaAs QD STRUCTURE

**Kang H.-K.<sup>1,2</sup>, Kim J.-H.<sup>2</sup>, Lee E.-H.<sup>2</sup>, Baik M.<sup>1,2</sup>, Song J.-D.<sup>2</sup>, Cho M.-H.<sup>1</sup>**

*1 - Department of Physics, Yonsei University*

*2 - Center of Opto-Electronic Materials, KIST*

*mh.cho@yonsei.ac.kr*

We report the optical and growth properties of GaSb/GaAs QD type-II structure by molecular beam epitaxy. X-Ray and SEM images confirmed that the QD has zinc blende crystal structure with hexagonal disk shape. From The TEM results, the base and height image of the GaSb QDs are measured as 60nm and 4nm, respectively. The PL from the 80 nm capped GaAs sample have two peaks at 1.1eV assigned to QD, and WL peak energy at 1.26 eV at temperature 14K and 30 mW excitation laser power. The integrated PL intensity of QDs is much stronger than the WL, where the ratio  $I_{\text{QD}}/I_{\text{WL}}$  of the integral intensities changes with temperature. The QD and WL peaks shift to higher energy by 5.8 meV and 9.17 meV respectively with increasing excitation laser power. This behavior suggests type-II band lineup, in which holes are confined in the QD, while electrons are loosely bound around the QD by coulomb attractive force of the holes. Moreover, we investigated the temperature dependence of the PL peak energy and intensity. The energy difference between QD and WL is around 156 meV and hence thermal excitation of exciton from QD to WL should be taken into account. In order to investigate carrier dynamics of type-II GaSb/GaAs QD structure, we performed time-resolved photoluminescence experiment. The GaSb/GaAs QD shows a long decay performance for the QD peak with single-exponential function, which has a decay time constant of  $\tau = 9$  ns. In contrast, the WL PL decay has a two step decay process, which is composed of initial fast component and a slower tail component. The initial faster decay time constant of  $\tau = 0.8$  ns indicates the carrier transfer process from the WL to the GaSb/GaAs QDs.

# THREE-CATION SCANDOBORATES: SYNTHESIS, STRUCTURE, PROPERTIES AND CRYSTAL GROWTH

**Kokh A.<sup>1</sup>, Kononova N.<sup>1</sup>, Kuznetsov A.<sup>1</sup>, Kokh K.<sup>1,2</sup>, Shevchenko V.<sup>1</sup>, Uralbekov B.<sup>3</sup>, Bolatov A.<sup>3</sup>, Svetlichnyi V.<sup>4</sup>**

*1 - Sobolev Institute of Geology and Mineralogy SB RAS*

*2 - Novosibirsk State University*

*3 - Al-Farabi Kazakh National University*

*4 - Tomsk State University*

*a.e.kokh@gmail.com*

Complex orthoborates with the general formula  $RX_3(BO_3)_4$ , where  $R = Y, Ln$ ;  $X = Al, Ga, Sc, Cr, Fe$  are practically important and interesting in the view of crystal chemistry. One of the important properties of these compounds is the ability to form a non-centrosymmetric structure, which is called huntite-like. Such a structure causes, for example, non-linear optical properties. The presence of active laser cations in the structure also implies the use of these crystals as active elements with self-frequency doubling.

The stabilization of the huntite-like structure can occur if an additional isomorphous cation is introduced into the  $LaSc_3(BO_3)_4$  structure. That was shown for the first time in

$Nd_xLa_{1-x}Sc_3(BO_3)_4$  [Li et al., 2001], which initiated the study of new class of three-cation scandoborates with the huntite-like structure. Further, in a number of works by adding a third cation R nonlinear optical crystals  $R_xLa_ySc_z(BO_3)_4$  ( $x+y+z=4$ ) with a stable huntite-like structure were obtained: with  $R = Y$  [Ye et al., 2005], Lu [Li et al., 2007], Bi [Xu et al., 2009] and Gd [Xu et al., 2011].

In this work complex orthoborates of rare earth metals with the general chemical formula  $R_xLa_{1-x}Sc_3(BO_3)_4$  ( $R = Sm, Tb$ ) have been obtained by solid state synthesis and spontaneous crystallization. These crystals belong to the huntite family with the space group  $R32$  and for  $x=0.5$  have unit cell parameters  $a=9.823(6)\text{\AA}$ ,  $c=7.975(3)\text{\AA}$  (SLSB) and  $a=9.803(3)\text{\AA}$ ,  $c=7.960(4)\text{\AA}$  (TLSB). The formation of a huntite-like structure in the systems  $R_xLa_{1-x}Sc_3(BO_3)_4$ , ( $R = Sm, Tb$ ), as well as the dependence of the compositions stable in the required structure depending on the production method is shown. Volumetric SLSB and TLSB crystals with dimensions about  $30\times 30\times 10$  mm with a transparent area of about  $5\times 5\times 5$  mm were grown by TSSG method.  $LiBO_2$ -LiF compound was used as a solvent [Fedorova et al., 2013].

This work presents absorption, Raman and luminescence spectra for SLSB and TLSB crystals. Spectral characteristics confirm the potential of using crystals as luminescent materials.

The effective nonlinearity of these crystals was estimated by Kurtz-Perry powder SHG test.

*Acknowledgements:* This work is supporting by RFBR project #19-05-00198a, state contract of IGM SB RAS and partially by Project GF MES RK IRN AP05130794.

## *References:*

- Fedorova M. V., Kononova N. G., Kokh A. E., and Shevchenko V. S., 2013. Growth of  $MBO_3$  ( $M = La, Y, Sc$ ) and  $LaSc_3(BO_3)_4$  crystals from  $LiBO_2$ -LiF fluxes. *Inorganic Materials*. 49, 482-486.
- Li Y., Aka G., Kahn-Harari A., and Vivien D., 2001. Phase transition, growth, and optical properties of  $Nd_xLa_{1-x}Sc_3(BO_3)_4$  crystals. *J. Materials Research*. 16, 38-44.
- Li W., Huang L., Zhang G., and Ye N., 2007. Growth and characterization of nonlinear optical crystal  $Lu_{0.66}La_{0.95}Sc_{2.39}(BO_3)_4$ . *J. Crystal Growth*. 307, 405-409.
- Xu X., Wang Sh., Ye N., 2009. A new nonlinear optical crystal  $Bi_xLa_ySc_z(BO_3)_4$  ( $x + y + z = 4$ ). *Journal of Alloys and Compounds*. 481, 664-667.
- Xu X., Ye N., 2011.  $Gd_xLa_{1-x}Sc_3(BO_3)_4$ : A new nonlinear optical crystal. *J. Crystal Growth*. 324, 304-308.
- Ye N., Stone-Sundberg J.L., Hruschka M.A., et al., 2005. Nonlinear Optical Crystal  $Y_xLa_ySc_z(BO_3)_4$  ( $x + y + z = 4$ ). *Chem. Mater.* 17. 2687-2692.

## PHASE COMPOSITION AND ELECTRICAL TRANSPORT IN THIN FILMS SYNTHESIZED BY EVAPORATION OF Bi<sub>2</sub>Se<sub>3</sub> ON MICA

**Kokh K.A.<sup>1,2,3</sup>, Nebogatikova N.A.<sup>2,4</sup>, Tereshchenko O.E.<sup>2,3,4</sup>, Kustov D.A.<sup>4</sup>, Antonova I.V.<sup>2,4,5</sup>**

*1 - Sobolev Institute of Geology and Mineralogy SB RAS, Novosibirsk 630090, Russia*

*2 - Novosibirsk State University, Novosibirsk 630090, Russia*

*3 - Saint Petersburg State University, Saint Petersburg, 198504, Russia*

*4 - Rzhanov Institute of semiconductor physics SB RAS, Novosibirsk 630090, Russia*

*5 - Novosibirsk State Technical University, Novosibirsk, 630087, Russia*

*kokh@igm.nsc.ru*

Bi<sub>2</sub>Se<sub>3</sub> is a layered semiconductor, which has good chemical stability, the band gap (~ 0.3 eV) and demonstrates the properties of a topological insulator (TI) [1]. The practical application of TI is limited by the bulk conductivity of the crystals. The preparation of thin films (with a thickness of less than 100 nm) is supposed to significantly reduce the bulk conductivity and form the surface states with spin polarized conductivity [2]. Present methods for producing bismuth chalcogenide include mechanical, liquid-phase, or electrochemical exfoliation. Due to the brittleness of these materials the produced films usually are limited in size of the order of several tens of microns [3].

In this work, epitaxial growth of Bi<sub>2</sub>Se<sub>3</sub> films from the gas phase on mica was carried out. In the heated end of the quartz reactor, a boat with fragment of the Bi<sub>2</sub>Se<sub>3</sub> crystal was placed. The opposite end was connected to a vacuum pump. Substrates of technical mica were put in the center of the reactor, where the temperature gradient was created.

According to X-ray diffraction, van der Waals epitaxy with an oriented growth of the single-crystal Bi<sub>2</sub>Se<sub>3</sub> layer was realized. Maxim lengths of 3–6 cm of material were obtained at 500 °C. In the range of deposition time 4.5–26 hours, films were obtained, according to AFM, with a thickness of 20–300 nm. When the growth temperature decreased to 450 °C, the growth slows down considerably. There are grains 300–500 nm in size, and 1 nm in relief (Se-Bi – Se – Bi – Se quintet) Conductivity measurements at room temperature showed that films ~ 20 nm thick exhibit a layer resistance of 10<sup>3</sup>-10<sup>4</sup> Ohm/sq, and more thick films (~ 120-200 nm) layer resistance drops to 10 Ohm/sq. The saturation of the resistance at the level of 10<sup>3</sup>–10<sup>4</sup> Ohm/sq may indicate a predominant contribution to the conductivity by topological surface states. Similar levels of resistance were achieved on thin BiSbTeSe<sub>2</sub> films with a thickness of less than 100 nm [4]. We also investigated the films obtained by exfoliation from a bulk Bi<sub>2</sub>Se<sub>3</sub> crystal. The resistance of the films was 10<sup>3</sup> - 10<sup>4</sup> Ohm/sq which was thickness independent at the values of less than 80 nm.

Surface morphology studies using SEM showed the presence of an extraneous phase with a nontriangular shape. Its presence probably makes a contribution to the defectiveness of the film and a decrease in conductivity in some points of measurements. We estimate this phase as Bi<sub>2</sub>SeO<sub>2</sub>, which was confirmed using Raman spectroscopy on the films obtained at 600 and 700 °C. The probable source of oxygen is thermal decomposition of mica. The presence of globules of elemental selenium is noted in the cold part of the substrates. We explain their presence by low oxygen activity in the presence of Bi<sub>2</sub>Se<sub>3</sub>/Bi<sub>2</sub>SeO<sub>2</sub> buffer, which is insufficient for the oxidation of selenium.

*Acknowledgements:* This work is supported by RFBR (19-05-00198) and SPbSU (15.61.202.2015).

1. Hsieh D et al. Nature 460 1101 (2009).
2. Mo D. L. et al. Nanoscale research letter 11 354 (2016).
3. Chiatti O. et al. Scientific reports 6 27483 (2016).
4. Xu Y. et al. Nature Physics 10 956 (2014).



# QUARTZ GLASS OBTAINED ON THE PLASMATRON OF JSC "DINUR" FROM RAMENSKOYE SAND. FEATURES OF CRYSTALLIZATION ON A POLISHED SURFACE

**Kolobov A.Yu.<sup>1,2</sup>, Sycheva G.A.<sup>1,2</sup>**

*1 - JSC "DINUR", 623103, city of Pervouralsk, Sverdlovsk region, Ilyich street, 1*

*2 - Grebenshchikov Institute of Silicate Chemistry, Russian Academy of Sciences, 199034, St. Petersburg, nab. Makarova 2*

*art.kolobov@yandex.ru*

The main raw material for melting quartz glass at JSC "DINUR" is quartz sand production Ramenskoye mining and processing plant. Sand melting is carried out in plasmatrons. The operating current of the arc of the reactor is 1300 A at a voltage of 300-400 V. The characteristics of the melting process depend on the specific reactor and the content of impurities in the sand of aluminum and iron oxides. The ingot obtained as a result of melting is a cylinder several meters long, about half a meter in diameter and weighing more than 600 kg. The product of melting quartz sand with a high content of impurities is characterized by reduced resistance to crystallization [1-2].

In the Central factory laboratory of JSC "DINUR" conducted a comprehensive study of the properties of quartz glass and its products. According to chemical analysis, the  $\text{Al}_2\text{O}_3$  content is 0.25% and  $\text{Fe}_2\text{O}_3$  0.05%. Radiographs obtained quartz glass have a distinctive look, indicating the amorphous sample - wide halo with angular width  $2\Theta$  about  $20^\circ$ . For quartz glass is characterized by the presence of only near order — the regularity of the position of the particles in the interatomic units (1-10 Å), the presence of regularities in the arrangement only for neighboring atoms or molecules. Since quartz glass does not have a pronounced crystal lattice, there is no periodicity in the arrangement of atoms, there is no clear diffraction pattern and individual x-ray diffraction reflections. When calculating the content of the crystalline phases of cristobalite and quartz from the x-ray spectra, the most correct values can be obtained from the integral intensities of the maxima in the region with the maximum signal/noise ratio. Line of quartz on the radiograph indicates not completely melted piece of rock and the occurrence of cristobalite is due to the peculiarities of the regime of melting.

According to XRD data, the largest amount of quartz (10-12%) was found in a dense crust on the surface of the ingot, while the content of cristobalite did not exceed 2.0%. The mineralogical composition of the majority of the studied samples of quartz glass, purified from the surface crystalline crust, is represented by pure silica glass. Quartz and cristobalite were not identified by XRD and microscopy in most of the samples.

In those samples where the presence of cristobalite was established by XRD (in some cases up to 1.0%), petrographic study confirmed the appearance and nucleation of crystals on gas bubbles, cracks, along the piles or at the boundary of foreign inclusions. As such inclusions can act, for example, particles of electrode graphite or hardware metal.

1. Y.E. Pivinskii, P.V. Dyakin, A.Yu. Kolobov. *Refractories and Industrial Ceramics*, 2016, T. 57. № 1, 27-32.

2. A.I. Nepomnyashchikh, A.A. Shalaev, T.Yu. Sizova, A.N. Sapozhnikov, A.S. Paklin. *Geography and natural resources*, 2016, № 6, 60-64.

# STUDY OF PHASE EQUILIBRIA IN THE CsHSO<sub>4</sub>-CsH<sub>2</sub>PO<sub>4</sub>-NH<sub>4</sub>H<sub>2</sub>PO<sub>4</sub>-H<sub>2</sub>O SYSTEM

**Komornikov V.A., Timakov I.S., Grebenev V.V., Zajnullin O.B., Makarova I.P., Selezneva E.V.**

*Shubnikov Institute of Crystallography, Federal Scientific Research Centre "Crystallography and Photonics," Russian Academy of Sciences, Moscow, 119333 Russia*

*v.a.kom@mail.ru*

Many acid salts of singly charged cations are promising proton conductors, which, along with other ion-conducting compounds, attract the attention of researchers. This group includes compounds with the general formula  $M_mH_n(AO_4)_{(m+n)/2} \cdot xH_2O$  ( $M = NH_4, K, Rb, Cs; A = S, Se, HP, HAs$ ). Their distinctive feature is structural phase transitions occurring at elevated temperatures (preceding the melting point).

When a phase transition occurs, conductivity  $\sigma$  in superprotonic crystals significantly increases (to values comparable with the conductivity of the melt), whereas the aggregate state of the compound remains solid. The high proton conductivity of these crystals is primarily due to their structural features and the structural changes upon heating [1].

The combination of high proton conductivity ( $\sigma \approx 10^{-3} \Omega^{-1} \text{ cm}^{-1}$ ) in the solid aggregate state at moderate (140–230°C) temperatures attracts the attention of researchers to crystals of the aforementioned family as promising materials for the proton-exchange membranes of fuel cells [2].

Previously, the authors have already investigated the phase equilibria in the pseudo-termed system CsHSO<sub>4</sub> – CsH<sub>2</sub>PO<sub>4</sub> – H<sub>2</sub>O [3], determined the conditions for obtaining crystals-superprotonics Cs<sub>4</sub>(HSO<sub>4</sub>)<sub>3</sub>(H<sub>2</sub>PO<sub>4</sub>) and Cs<sub>6</sub>H(HSO<sub>4</sub>)<sub>3</sub>(H<sub>2</sub>PO<sub>4</sub>)<sub>4</sub>. The work [4] shows the prospects for using these compounds as proton-exchange membranes of hydrogen-air fuel cells. Further modification of the properties of the compounds Cs<sub>4</sub>(HSO<sub>4</sub>)<sub>3</sub>(H<sub>2</sub>PO<sub>4</sub>) and Cs<sub>6</sub>H(HSO<sub>4</sub>)<sub>3</sub>(H<sub>2</sub>PO<sub>4</sub>)<sub>4</sub> was performed by the method of cationic ammonium substitution.

In this paper we report the results of studying the phase equilibria in the CsHSO<sub>4</sub> – CsH<sub>2</sub>PO<sub>4</sub> – NH<sub>4</sub>H<sub>2</sub>PO<sub>4</sub> – H<sub>2</sub>O system and determining the conditions for obtaining complex ammonium and cesium hydrogen sulfate–phosphates in the form of single crystals and single-phase fine-grained powders by growth from aqueous.

As a result of studying the phase equilibria in the CsHSO<sub>4</sub> – CsH<sub>2</sub>PO<sub>4</sub> – NH<sub>4</sub>H<sub>2</sub>PO<sub>4</sub> – H<sub>2</sub>O system, the crystallization conditions for the following compounds were determined: the initial components – CsHSO<sub>4</sub>, CsH<sub>2</sub>PO<sub>4</sub>, NH<sub>4</sub>H<sub>2</sub>PO<sub>4</sub>; solid solutions – Cs<sub>1-x</sub>(NH<sub>4</sub>)<sub>x</sub>H<sub>2</sub>PO<sub>4</sub>, (Cs<sub>1-x</sub>(NH<sub>4</sub>)<sub>x</sub>)<sub>4</sub>(HSO<sub>4</sub>)<sub>3</sub>(H<sub>2</sub>PO<sub>4</sub>) and Cs<sub>1-x</sub>(NH<sub>4</sub>)<sub>x</sub>(HSO<sub>4</sub>)(H<sub>2</sub>PO<sub>4</sub>); stoichiometric compounds – Cs<sub>3</sub>NH<sub>4</sub>(HSO<sub>4</sub>)<sub>3</sub>(H<sub>2</sub>PO<sub>4</sub>) and CsNH<sub>4</sub>(HSO<sub>4</sub>)(H<sub>2</sub>PO<sub>4</sub>). Wherein, the Cs<sub>3</sub>NH<sub>4</sub>(HSO<sub>4</sub>)<sub>3</sub>(H<sub>2</sub>PO<sub>4</sub>) and CsNH<sub>4</sub>(HSO<sub>4</sub>)(H<sub>2</sub>PO<sub>4</sub>) phases, as well as (Cs<sub>1-x</sub>(NH<sub>4</sub>)<sub>x</sub>)<sub>4</sub>(HSO<sub>4</sub>)<sub>3</sub>(H<sub>2</sub>PO<sub>4</sub>) and Cs<sub>1-x</sub>(NH<sub>4</sub>)<sub>x</sub>(HSO<sub>4</sub>)(H<sub>2</sub>PO<sub>4</sub>) obtained for the first time.

The reported study was funded by RFBR according to the research project № 18-32-20050.

The experiments were performed using the equipment of the Shared Research Center of the Institute of Crystallography, Russian Academy of Sciences, and supported by the Ministry of Education and Science of the Russian Federation (project no. RFMEFI62114X0005)

1. A. I. Baranov, *Crystallogr. Rep.* 48 (6), 1012 (2003).

2. M. H. Sossina, A. B. Dane, R. I. Calum, *et al.*, *Nature* 410, 910 (2001).

3. Makarova I., Grebenev V., Dmitricheva E., Vasiliev I., Komornikov V., Dolbinina V., Mikheykin A. // *Acta Cryst B.* 72, 133 (2016).

4. V. A. Komornikov, A. M. Grechikhina, V. V. Grebenev, I. S. Timakov, O. B. Zajnullin, and V. G. Zinoviev, *Crystallogr. Rep.*, 63 (3), 806–811 (2018).

# PROTON-CONDUCTING COMPOSITE MATERIALS BASED ON SUPERPROTONIC CRYSTALS

**Komornikov V.A., Grebenev V.A., Timakov I.S., Zajnullin O.B.**

*Shubnikov Institute of Crystallography, Federal Scientific Research Centre "Crystallography and Photonics," Russian Academy of Sciences, Moscow, 119333 Russia*

*v.a.kom@mail.ru*

One of the lines of development of environmentally friendly energy technologies is the design of hydrogen-based fuel cells (hydrogen power engineering). The most important component of any hydrogen fuel cell is the proton-exchange membrane with properties specified by certain technical requirements: high ionic conductivity at the operation temperature, low gas permeability, and low dielectric loss tangent. Note that conductivity is the crucial parameter for the membrane material, which directly affects the fuel cell energy efficiency.

With the use of a special method of preparative synthesis  $x\text{CsH}_2\text{PO}_4 - (1-x)\text{AlPO}_4$ ;  $x\text{Cs}_4(\text{HSO}_4)_3(\text{H}_2\text{PO}_4) - (1-x)\text{AlPO}_4$ ;  $x\text{Cs}_6(\text{HSO}_4)_3(\text{H}_2\text{PO}_4)_4 - (1-x)\text{AlPO}_4$  composite materials over a wide range of compositions was obtained. A special feature of the approach used in the synthesis is the formation of a proton-conducting phase and an aluminophosphate component *in one volume*. The application of this technique at the macro level allows obtaining these materials in the form of relatively thin transparent films with the necessary geometry.

At the microlevel, the application of this approach leads to the production of materials with a higher density and a larger interphase boundary area (in comparison with proton-conducting composites on oxide additives of the type  $x\text{M}_m\text{H}_n(\text{XO}_4)_{(m+n)/2} - (1-x)\text{SiO}_2/\text{TiO}_2/\text{SnO}_2$ , ( $\text{M}=\text{K}, \text{Rb}, \text{Cs}, \text{NH}_4$ ;  $\text{XO}_4 = \text{SO}_4, \text{SeO}_4, \text{HPO}_4$ )). This feature is realized due to the filling of the space between in the first place formed crystallites of the conducting phase to a largely amorphous phase of polyaluminophosphate (conditionally -  $\text{AlPO}_4$ ).

A comparative analysis of the temperature dependence of the conductivity for the materials studied revealed increased (in comparison with the single-phase superprotonic crystal) meanings, while the intrinsic conductivity of the polyaluminophosphate component decreases the activation energy of the conductivity.

The initial tests of the obtained membrane materials under the conditions of the hydrogen atmosphere showed the possibility of obtaining the potential on the cell up to values of 1.1 V (with a maximum theoretical value of 1.23 V). In this case, the phase composition of materials does not undergo noticeable changes even under the conditions of cyclic operation of the fuel cell.

Thus, tests of the materials obtained in a hydrogen atmosphere showed the fundamental applicability of both the technology used to produce membrane materials and the materials themselves for hydrogen-air fuel cells.

The reported study was funded by RFBR according to the research project № 18-32-20050.

The experiments were performed using the equipment of the Shared Research Center of the Institute of Crystallography, Russian Academy of Sciences, and supported by the Ministry of Education and Science of the Russian Federation (project no. RFMEFI62114X0005).

## REVERSIBLE 2D-3D TRANSITION IN THIN GAN LAYER FORMED ON THE AlN (0001) SURFACE

Mansurov V.G., Galitsyn Yu.G., Malin T.V., Milakhin D.S., Konfederatova K.A., Zhuravlev K.S.

*Rzhanov Institute of Semiconductor Physics*

*kseniya.konfederatova@gmail.com*

The formation of quantum dots (QDs) by epitaxial growth is usually carried out using the Stranski-Krastanov growth mode. A nontrivial effect is observed when GaN QD is formed on the AlN (0001) surface by the ammonia MBE method. The effect is as follows: after growing an ultrathin two-dimensional GaN layer on AlN (0001), the system remains two-dimensional under ammonia flux. However, the interruption of ammonia flux results in spontaneous formation of three-dimensional (3D) GaN islands. This effect has been studied in several works, and the review of these works is given in the article [1]. It was assumed that the relaxation of elastic stresses in the GaN layer plays a significant role in the 2D-3D transition, when the ammonia flow is interrupted. The formation of 3D islands was explained as interplay of the surface free energy changes and the elimination of kinetic impediments for the diffusion of growth components. However, this 2D-3D transition was studied only as a function of temperature, and the role of ammonia pressure was not taken into account. Moreover, a possibility of migration of Ga-N atomic pairs was assumed, that is questionable.

In this work, a spontaneous 2D-3D transition (in other words, a phase transition) on the surface of a thin layer of gallium nitride on the AlN(0001) was studied as function of the surface temperature and ammonia pressure. It was shown that with an increase in temperature (at a given ammonia pressure) or with an increase in ammonia pressure (at a given temperature), the equilibrium concentration of the 3D islands decreases. It was experimentally shown that this 2D-3D phase transition is reversible.

In our opinion, such a transition should be described as the dependence of the surface coverage by the 3D islands ( $\theta$ ) as function of temperature ( $T$ ) and ammonia pressure ( $P$ ), i.e. in terms of an equation of state  $\theta=f(P, T)$ . Then, interrupting of ammonia flux is an extremal case when the  $\theta=f(0, T)$ .

Decreasing of the ammonia pressure over the GaN surface, including interruption of the flow, leads to a change in the surface composition, namely, enrichment of the surface with gallium, that is, to an increase in the chemical potential of gallium atoms. In this case, the surface energy will increase, and its subsequent relaxation (reduction of the surface energy) results in a change in the morphological state of the surface, that is, to the formation of 3D islands. The concentration of the 3D islands will be determined by the so-called fugacity  $z$ , where  $z=(2\pi mkT/h^2)^{3/2}\exp(\mu(P,T)/kT)$ . In this work the state equation of the GaN 3D islands ensemble is considered in framework of the lattice gas model. This model was successfully used in the analysis of GaAs nucleation on the GaAs(001) surface [2,3], and also of the InAs QDs formation on the GaAs(001) surface [4] etc. In the present work a three-parameter isotherm (equation of state) was used, that was derived in frame of the lattice gas model [3,4].

This work was supported by the Russian Foundation for Basic Research (grants No. 17-02-00947, 18-52-00008).

[1] Damilano B, Brault J, Massies, J. Appl. Phys.;118, 024304. (2015).

[2] V.P.LaBella, Z. Ding, D.W.Bullock, et al, Int. J. Mod. Phys.B,15,2301 (2001).

[3] Yu.G. Galitsyn, D.V. Dmitriev, V.G. Mansurov et al. JETP Letters, 86, 482 (2007).

[4] Yu. G. Galitsyn; A. A. Lyamkina; S. P. Moshchenko et al., in: Self-assembly of Nanostructures, edited by S. Belucci, The INFN Lectures, Springer, 3, chap. 3. (2012).

# FORMATION OF AgInS<sub>2</sub>/ZnS COLLOIDAL NANOCRYSTALS AND THEIR PHOTOLUMINESCENCE PROPERTIES

**Korepanov O.A., Mazing D.S., Aleksandrova O.A., Moshnikov V.A.**

*Saint Petersburg Electrotechnical University "LETI"*

*okrpnv@gmail.com*

Ternary metal chalcogenides nanocrystals is a prospective group of material for a wide range of potential applications such as solar cells, bioimaging, lighting and sensorics [1, 2]. Compared to much more ubiquitous and well-studied binary cadmium and lead chalcogenide nanocrystals ternary systems such as CuInS<sub>2</sub>, AgInS<sub>2</sub>, CuInSe<sub>2</sub>, AgInSe<sub>2</sub> are considered to be less toxic and environmentally friendlier. Photoluminescence mechanisms in these nanocrystals are thought to be connected to internal defects which leads to universally large Stokes shifts, broad emission with long lifetimes. The most developed synthesis techniques are hot-injection or heating-up methods carried out in non-polar solvents using aliphatic thiols (commonly 1- Dodecanethiol) as complexing agents and ligands [3]. Even though these techniques produce good results alternative aqueous approach is of interest too [4], especially given potential biomedical applications where the non-polar method necessitates additional hydrophilization of hydrophobic nanocrystals. Moreover, aqueous techniques are generally cheaper and environmentally more benign.

In this work, colloidal nanocrystals of AgInS<sub>2</sub> were synthesized in aqueous solution using biocompatible L-Glutathione as a ligand. Wider bandgap semiconductor shell ZnS was deposited on the cores in order to enhance luminescence properties and stability. Thus prepared nanocrystals generally had an asymmetric multiple band emission spectrum which can be decomposed using Gaussian function. Variation of cation ratio [Ag<sup>+</sup>] to [In<sup>3+</sup>] led to a variation of the spectrum so that raising indium content caused an intensity increase of longer wavelength emission band [5].

In order to reveal the crystal structure, morphology and origins of the photoluminescence properties the nanocrystals were characterized by means photoluminescence and absorption spectroscopies, transmission electron microscopy, X-ray diffractometry, X-ray photoelectron spectroscopy, dynamic light scattering.

## References

- [1] Korepanov, O. A., Mazing, D. S., Aleksandrova, O. A., & Moshnikov, V. A. (2019, January). Synthesis and Study of Colloidal Nanocrystals Based on Ternary Chalcogenides for Active Media of Heavy Metal Ions Sensors. In 2019 IEEE Conference of Russian Young Researchers in Electrical and Electronic Engineering (EIConRus) IEEE, 771-773.
- [2] Istomina M. S., Pechnikova N. A., Korolev D. V. , Pochkayeva E. I. , Mazing D. S. , Galagudza M. M., Moshnikov V. A. , Shlyakhto E. V. "ZAIS-based colloidal QDs as fluorescent labels for theranostics: physical properties, biodistribution and biocompatibility." Bulletin of Russian State Medical University 6 (2018), 94-101.
- [3] Aldakov, D., Lefrançois, A., & Reiss, P. (2013). Ternary and quaternary metal chalcogenide nanocrystals: synthesis, properties and applications. Journal of Materials Chemistry C, 1(24), 3756-3776.
- [4] Jing, L., Kershaw, S. V., Li, Y., Huang, X., Li, Y., Rogach, A. L., & Gao, M. (2016). Aqueous based semiconductor nanocrystals. Chemical reviews, 116(18), 10623-10730.
- [5] Mazing, D. S., Chernaguzov, I. S., Shulga, A. I., Korepanov, O. A., Aleksandrova, O. A., & Moshnikov, V. A. (2018, June). Synthesis of ternary chalcogenide colloidal nanocrystals in aqueous medium. In Journal of Physics: Conference Series (Vol. 1038, No. 1, p. 012050). IOP Publishing.

# VAPOR–SOLID–SOLID MECHANISM OF Au-CATALYZED III-V NANOWIRE GROWTH

**Koryakin A.A.<sup>1,2</sup>, Kukushkin S.A.<sup>1,2,3</sup>, Kotlyar K.P.<sup>1</sup>, Ubyivovk E.D.<sup>2,4</sup>, Reznik R.R.<sup>2</sup>,  
Cirilin G.E.<sup>1,2</sup>**

*1 - St. Petersburg Academic University, St.Petersburg 194021, Russia*

*2 - ITMO University, St. Petersburg 197101, Russia*

*3 - Institute of Problems of Mechanical Engineering RAS, St. Petersburg 199178, Russia*

*4 - St. Petersburg State University, Petrodvorets, St.Petersburg 198504, Russia*

*alexkorya@gmail.com*

The wire-like nanocrystals (nanowires) of semiconductor compounds are promising candidates for the creation of new high-performance electronic and optoelectronic devices [1]. Nowadays, epitaxial methods of the growth of semiconductor nanowires using catalysts (for example, gold, silver, copper, gallium) are most widely spread. In the classic Wagner and Ellis study [2] devoted to the investigation of the catalytic growth of silicon whiskers (wire-like microcrystals), it was assumed that the crystals grow by the vapor–liquid–solid (VLS) mechanism. According to the VLS mechanism, crystal growth proceeds at a temperature higher than the eutectic one for this pair of materials and, consequently, a catalyst liquid droplet is located at the crystal tip. In further investigations, it was found that the growth of Au-catalyzed III–V nanowires (for example, GaAs, InAs, InP, GaInAs) is possible at temperatures both higher than the eutectic temperature and lower than this value. The eutectic temperature in these studies was determined on the basis of binary phase diagrams for gold and group III elements. Such an approximation when analyzing phase diagrams can be used because the concentration of arsenic and phosphorus atoms in the catalyst is insignificant (~1% or less). To explain nanowire growth at temperatures below the eutectic temperature, the vapor–solid–solid (VSS) mechanism was proposed. The catalyst material in the VSS growth mechanism is in the solid state. Also, it was assumed that III–V nanowires can grow by the VLS mechanism even at temperatures below the eutectic temperature. Actually, it is difficult to make an unambiguous conclusion about the physical state of a catalyst. This is associated, first, with the presence of hysteresis cycle with melting temperature of the catalyst; second, if the nanowire radii are small (less than 5–10 nm), the surface energy of the catalyst droplet can affect the melting point of the catalyst; third, ternary or quaternary phase diagrams should be considered instead of binary phase diagrams; fourth, the surrounding environment can influence on the melting temperature of the catalyst, etc. Therefore, the problem of the physical state of the catalyst during the growth of semiconductor nanowires currently remains open.

The purpose of this study was to investigate the possibility of Au-catalyzed III–V nanowire growth by the VSS mechanism. A new theoretical model of the VSS growth of nanowires was developed on the basis of the nucleation theory in solid. For the first time, the effect of elastic stresses caused by the lattice mismatch between the catalyst and nanowire material on the solid-phase nucleation rate was considered. The VSS growth mechanism of Au-catalyzed GaAs [3] and InAs nanowires growing along the [111] crystallographic direction was investigated theoretically. It was shown that the growth of III–V nucleus on the catalyst-nanowire interface is limited by the diffusion of group V elements on the interface. The experimental series on the Au-catalyzed InAs nanowire growth on the Si(111) substrate at the temperature of 270 °C by MBE method was obtained. The morphology of InAs nanowires was studied by scanning electron microscopy (SEM). The crystal structure of InAs nanowires and the catalyst composition were investigated by analytical methods of transmission electron microscopy (TEM). The analysis of the catalyst particle state proved the existence of VSS growth mechanism. The theoretical results are in agreement with the experimental results on the nanowire growth rate.

A.A.K acknowledges financial support of the Russian Foundation for Basic Research under the research project № 18-32-00559.

[1] N. P. Dasgupta, J. Sun, C. Liu *et al.*, *Advanced Materials* **26**, 2137–2184 (2014)

[2] R. S. Wagner, W. C. Ellis, *Appl. Phys. Lett.* **4**, 89 (1964).

[3] A.A. Koryakin, S.A. Kukushkin, N.V. Sibirev, *Semiconductors* **53**, 350–360 (2019)

# ON THE FORMATION OF AXIAL HETEROSTRUCTURES IN CATALYTIC TERNARY III-V NANOWIRES

**Koryakin A.A.<sup>1,2</sup>, Leshchenko E.D.<sup>2,3</sup>, Kotlyar K.P.<sup>1</sup>**

*1 - St. Petersburg Academic University, St. Petersburg 194021, Russia*

*2 - ITMO University, St. Petersburg 197101, Russia*

*3 - Solid State Physics and NanoLund, Lund University, Lund Box118, S-22100, Sweden*

*alexkorya@gmail.com*

Ternary III-V nanowires with axial heterostructures are promising nanomaterials for optoelectronic applications [1]. A wide range of semiconductors can be combined into the nanowire without the formation of defects due to high lattice mismatch. At present, III-V nanowires are often synthesized by the vapor-liquid-solid (VLS) method during MBE or MOCVD growth. The VLS method requires the use of foreign material (e.g. gold, silver, copper) for catalyst-assisted growth or group III material (e.g. gallium) for self-assisted growth. This method is a relatively easy growth method that facilitates the formation of homogeneous nanowire arrays. However, there are two technological problems of axial heterostructure formation in nanowires via the VLS method. The first problem is the formation of abrupt heterojunctions. The second problem is the obtaining of nanowire arrays with a high yield of vertical nanowires. The characteristics of optoelectronic devices depend strongly on the heterojunction width. It is usually desirable for devices with high-performance characteristics to form a nanowire array with a high yield and narrow heterojunctions.

This work is devoted to the investigation of axial heterojunction formation in ternary III-V nanowire grown via the VLS method. We have developed the theory of nanowire growth and modeled the formation of axial BD/A<sub>x</sub>B<sub>1-x</sub>D/BD heterojunction in A<sub>x</sub>B<sub>1-x</sub>D nanowires, where A and B are group III(V) elements, D is group V(III) element. The nanowire was considered as a set of monolayers that differ, in general, in the composition. This is in contrast to the previous models [2,3] where the nanowire composition can change continuously along the nanowire axis. Also, we assumed that the composition of *i* ML depends on the droplet composition,  $y_i, c_{tot}$ , and on the composition of previous monolayers  $x_{i-1}, x_{i-2}, \dots$ :  $x_i = x_i(y_i, c_{tot}, x_{i-1}, x_{i-2}, \dots)$ . This function was found in the frame of two approaches. In the first approach, the composition of the growing monolayer is assumed to be the same as in case of thermodynamic equilibrium for atoms in the droplet and monolayer [2]. The second approach is based on the nucleation theory and required the finding of critical nucleus composition on the catalyst-nanowire interface [3]. The both approaches lead to the identical or similar results. The chemical potentials of species in the monolayer were calculated taking into account the elastic stresses due to the lattice mismatch between consequent monolayers. The total elastic energy stored in nanowire was calculated by the finite element method. The composition profiles of axial heterostructures were obtained for different growth conditions by solving the equations of thermodynamic equilibrium or the equations for the saddle point conditions and the material balance equation for species in droplet. We have shown that the elastic stresses can be neglected in the case of very thin nanowires (radius less than 3 nm). The presence of elastic stresses lead to the suppression of the miscibility gap [3]. We have performed the comparison of the theoretical and experimental composition profiles for heterostructured III-V nanowires. The results obtained can be used for the optimization of III-V nanowire growth with axial heterostructures.

A.A.K acknowledges financial support of the Russian Foundation for Basic Research under the research project № 18-32-00559.

[1] N.P. Dasgupta *et al.*, *Adv. Mater* **26**, 2137–2184 (2014)

[2] F. Glas, M.R. Ramdani, G. Patriarche, J.C. Harmand, *Phys. Rev. B* **88**, 195304 (2013)

[3] V.G. Dubrovskii, A.A. Koryakin, N.V. Sibirev *Mater. Des.* **132**, 400–408 (2017)

# THE GROWTH AND PROPERTIES OF GUANYLUREA(1+) HYDROGEN PHOSPHATE (GUHP) CRYSTAL

**Kaminskii A.A.<sup>1</sup>, Manomenova V.L.<sup>1</sup>, Rudneva E.B.<sup>1</sup>, Sorokina N.I.<sup>1</sup>, Grebenev V.V.<sup>1</sup>,  
Kozlova N.N.<sup>1</sup>, Angeluts A.A.<sup>2</sup>, Ozheredov I.A.<sup>2,3</sup>, Solyankin P.M.<sup>2,3</sup>, Denisjuk I.Yu.<sup>4</sup>,  
Fokina M.I.<sup>4</sup>, Zulina N.A.<sup>4</sup>, Shkurinov A.P.<sup>2,3</sup>, Voloshin A.E.<sup>1</sup>**

*1 - Shubnikov Institute of Crystallography FSRC «Crystallography and Photonics» Russian Academy of Sciences, Moscow*

*2 - Physical Faculty and International Laser Center, M. V. Lomonosov Moscow State University, Moscow*

*3 - Institute on Laser and Information Technologies of Russian Academy of Sciences — Branch of Federal Scientific Research Center “Crystallography and Photonics” RAS, Shatura*

*4 - ITMO University, Saint-Petersburg*

79647099102@yandex.ru

Presently the need for materials with desired nonlinear optical (NLO) properties has led to intensive research in this area. Such materials can be used in physical, biological and medical devices (confocal microscopy, endoscopic devices). As the requirements for each particular application are different, it becomes necessary to develop new materials with an unusual combination of physical and chemical properties. Highly promising groups of crystalline compounds for NLO are hydrogen-bonded salts of organic bases and inorganic acids [1]. Novel and promising NLO guanylurea(1+) hydrogen phosphite crystal (GUHP)  $(\text{NH}_2)_2\text{CNHCO}(\text{NH}_2)\text{H}_2\text{PO}_3$ , which belongs to the monoclinic crystallographic space group Cc, can be successfully used for nonlinear optical conversion through the generation of second and third optical harmonics IR laser radiation [2-5], converting femtosecond radiation to the terahertz frequency range. The GUHP semi-organic crystal has high mechanical and laser durability; it is not inferior to an LBO crystal in terms of the laser damage threshold, and is superior to the well-known KDP crystal in terms of the efficiency of nonlinear optical conversion of laser radiation.

In this work, we obtained the temperature dependence of the equilibrium concentration of guanylurea(1+) hydrogen phosphite in water solutions. The change of density in water solutions of GUHP with a change in their concentration was investigated. The results obtained allowed the growth of GUHP crystals in various temperature and hydrodynamic mode. The effect of the pH of the solutions on the habit of the grown crystals was studied. It was revealed that with a decrease in the acidity of the initial solution to pH = 4.6 ( $\text{pH}_{\text{init}} = 3.6$ ), a relative decrease in the growth rate of the face (010) is observed. With an increase in acidity to pH = 2.6, no change in the ratio of the growth rates of the faces of the GUHP crystal was observed.

The crystal structure was refined and the nonlinear properties of the second order of the growing crystals were investigated. Absorption and generation spectra of the obtained single-crystal samples in the visible and near-IR range were also obtained.

This work was supported by the Russian Foundation for Basic Research (Grant No. 18-29-20104).

1. I. Matulkova', I. Neřmec, I. Cı'sarřova', P. Neřmec, and Z. Micřka, Inorganicsalts ofbiguanide – Searching for new materials for second harmonicgeneration, J. Mol. Struct. 886(2008), pp. 103–120.
2. Kroupa J. // J. Opt. 2010. V. 12. 045706 (3pp).
3. Kroupa J., Fridrichova M. // J. Opt. 2011. V. 13. 035204 (7pp).
4. Fridrichova M., Kroupa J., Nemeć I. et al. // Phase Transitions. 2010. V. 83, №. 10–11, P. 761.
5. Kaminskii A.A., Becker P, Rhee H. et al. // Phys. StatusSolidi. 2013. V. B 250. № 9. P. 1837.



# THE FINGERPRINTS OF HOMOGENEOUS NUCLEATION AND CRYSTALLIZATION IN POLYAMID-66 AS STUDIED BY COMBINED INFRARED (IR) SPECTROSCOPY AND FAST SCANNING CHIP CALORIMETRY

Anton A.M.<sup>1</sup>, Zhuravlev E.<sup>2</sup>, Kossack W.<sup>1</sup>, Andrianov R.<sup>2</sup>, Schick C.<sup>2</sup>, Kremer F.<sup>1</sup>

1 - University of Leipzig

2 - University of Rostock

*kremer@physik.uni-leipzig.de*

Employing a novel calorimetry chip accomplished with an InfraRed (IR) transparent SiN membrane enables one to carry out IR spectroscopic measurements and Fast Scanning Chip Calorimetry (FSC) on the *identical* sample of poly(amide-66) having an amount of material as small as ~ 100 ng. By that it is possible to achieve cooling rates as fast as 5000 K/s and to quench the sample in the fully amorphous state. Annealing the sample for a certain time  $\tau_i$  at a given temperature T allows to determine the onset of nucleation and crystal growth based on FSC and to unravel the *molecular* interactions from the analysis of the IR – spectra. A wealth of findings is observed, such as different molecular moieties of poly(amide-66) show a *specific* performance in the course of homogeneous nucleation and crystal growth or interactions leading to homogeneous nucleation are hierarchically ordered. Far reaching interactions (H-bonding) are earlier involved than short-range steric ones as exemplified for the  $\sigma(\text{CH}_2)$  scissors vibration.

# HIGHLY-LUMINESCENT CRYSTALS OF A NOVEL LINEAR PI-CONJUGATED THIOPHENE-PHENYLENE CO-OLIGOMER WITH BENZOTHIADIAZOLE FRAGMENT

Postnikov V.A.<sup>1</sup>, Kulishov A.A.<sup>1</sup>, Lyasnikova M.S.<sup>1</sup>, Sorokina N.I.<sup>1</sup>, Voloshin A.E.<sup>1</sup>, Borshchev O.V.<sup>2</sup>, Surin N.M.<sup>2</sup>, Svidchenko E.A.<sup>2</sup>, Ponomarenko S.A.<sup>2</sup>

1 - Shubnikov Institute of Crystallography of FSRC "Crystallography and Photonics" RAS

2 - Enikolopov Institute of Synthetic Polymeric Materials RAS

*adakyla1255@gmail.com*

Linear co-oligomers containing benzothiadiazole, thiophene and phenylene fragments in the structure of the conjugated core are a relatively new and poorly studied class of organic semiconductor materials. These substances are distinguished by high heat resistance, a large absorption cross section, and a rather small width of the forbidden band, which makes them promising for use in organic electronics and photonics [1]. However, the growth and structure of single-crystal samples of linear oligomers with a benzothiadiazole fragment are not yet described in the literature. This abstract is devoted to the study of growth processes from solutions of crystals of a new linear co-oligomer with a central benzothiadiazole fragment in the conjugate core and terminal trimethylsilyl groups (-Si(CH<sub>3</sub>)<sub>3</sub>): 4,7-bis{4-[5'-(trimethylsilyl)-2,2'-bithien-5-yl]phenyl}-2,1,3-benzothiadiazole ((TMS-2T-Ph)2-BTD). Terminal groups -Si(CH<sub>3</sub>)<sub>3</sub> were embedded in the compound to improve solubility.

For the first time, results are presented on the synthesis, growth from solutions and the structure of crystals of a new linear oligomer (TMS-2T-Ph) 2-BTD. The parameters of melting and liquid-crystalline phase transition were established by the DSC and in situ optical microscopy observation methods. Single crystalline samples of (TMS-2T-Ph) 2-BTD were grown in the form of needles up to 7 mm long. The crystal structure was resolved by single crystal X-ray diffraction at 85 K and 293 K. It has been established that the habit of crystals is mainly determined by the growth anisotropy along the [001], [100] and [010] directions with speeds in decreasing order, respectively. Just as for a number of linear oligophenyls and thiophene-phenylene co-oligomers, the crystal structure (TMS-2T-Ph) 2-BTD is shaped as a stack of monomolecular layers in orientation (010). However, the tendency to nucleation and growth of 2D crystals in the geometry of the (010) plane under the experimental conditions at the liquid – air interface is not observed.

The optical absorption and photoluminescence spectra of solutions and crystals (TMS-2T-Ph) 2-BTD were obtained, and the kinetics of their photo-degradation under the action of UV radiation was studied.

Work was supported by Russian Foundation for Basic Research (Project No. 18-33-20050) in part «synthesis, crystal growth and photoluminescence of novel co-oligomers», Ministry of Science and Higher Education within the State assignment FSRC "Crystallography and Photonics" RAS" in part «crystal structure studies». This work was made in the framework of Leading Science School (grant NSh-5698.2018.3).

M.S. Skorotetckiy et al. Influence of the structure of electron-donating aromatic units in organosilicon luminophores based on 2,1,3-benzothiadiazole electron-withdrawing core on their absorption-luminescent properties. *Dyes and Pigments*, 2018, 155 284–291.

# INVESTIGATION OF THERMOELECTRIC PROPERTIES OF THIN-FILM NANOSTRUCTURES MnSi

**Kuznetsov Y.<sup>1,2</sup>, Dorokhin M.<sup>2</sup>, Erofeeva I.<sup>2</sup>, Demina P.<sup>2</sup>, Lesnikov V.<sup>2</sup>**

*1 - Нижегородский государственный университет им. Н.И. Лобачевского*

*2 - Нижегородский физико-технический институт*

*yurakz94@list.ru*

## **1. Introduction**

Modern environmental problems raise great interest in the field of creation of thermoelectric energy converters. The efficiency of conversion of thermal energy into electrical one is characterized by the dimensionless thermoelectric figure of merit  $ZT = \alpha^2 \sigma T / \lambda$ , where  $\alpha$  is the Seebeck coefficient,  $\sigma$  is electrical conductivity,  $\lambda$  is thermal conductivity,  $T$  is average temperature. Achieving the competitive  $ZT$  values  $ZT(1 \div 3)$  allows the energy conversion efficiency to compete with other alternative sources, for example, with solar batteries. To solve this problem, nanoscale SiMn films, which, according to [1], have a low thermal conductivity, were used as the structures under study.

## **2. Experimental**

The studied SiMn films were obtained by pulsed laser deposition in vacuum using Nd:YAG laser. The substrates for the films were sapphire plates, which are good dielectric materials with monocrystalline structure. The requirement for dielectric isolation of the substrate is necessary to eliminate the influence of the substrate on the measured value of thermo-voltage. The composition of the films was chosen close to the manganese monosilicide MnSi and to the higher manganese silicide MnSi<sub>1.73</sub>. The targets for sputtering were high-purity silicon (Si) and manganese (Mn), as well as compound targets of a given composition (MnSi<sub>1.73</sub>). In the case of using individual targets, the Mn vs Si composition was set by the selection of sputtering time of Mn and Si targets [2] In the case of using a compound target, the composition was determined by the target itself. To control the composition of the structures and the targets used, an X-ray microanalysis was carried out. The thickness of the structures was determined by the sputtering time.

The investigated structures were two films deposited from Si and Mn targets and two films deposited from a compound manganese silicide target. Structures 1 and 2 differ in composition (MnSi<sub>1.5</sub> and MnSi<sub>1.7</sub> respectively), but have the same thickness and temperature of growth. Such a structure would provide lower values of the thermal conductivity due to the lattice structure of higher manganese silicide [4]. Films 3 and 4 have the same composition (MnSi<sub>1.73</sub>), the same deposition temperature, but different thickness due to the different sputtering times (90 and 150 nm respectively). For the thermoelectric measurements the samples were mounted on two graphite tables, which can be heated independently by incandescent lamps located under the tables. In the structures under study, the temperature dependences of the Seebeck coefficient, the thermal conductivity coefficient by the  $3\omega$  [3] method, and the specific resistance by the standard four-probe method were recorded.

In the course of the research it was shown that the maximum  $ZT$  of structure 1 (MnSi<sub>1.5</sub>) was 0.03 at 450 °C, which is too small value unable order to compete with other thermoelectric materials. The thermoelectric efficiency of structure 2 (MnSi<sub>1.7</sub>) turned out to be higher than that of structure 1. The maximum value has reached 0.055, which is, however, also far from a typical result from bulk manganese silicides. It was experimentally shown that the Seebeck coefficient of this structure turned out to be the largest of the materials we studied which is due to the largest resistivity of the film. Such a sharp decrease in electrical conductivity is explained by the inhomogeneity of the film, which arises from sputtering of two different targets. To increase the homogeneity of the film and, subsequently, decrease the resistance, structures 3 and 4 were made. These structures were deposited from a compound manganese silicide target, as discussed above. The maximum value of  $ZT$  was over 0.1, which is a good value of thermoelectric figure of merit for thin-film structures.

## **In conclusion**

The paper shows that manganese silicide films are a promising material for the creation of thermoelectric energy converters with increased efficiency coefficients. It has been established that the value of thermoelectric parameters strongly depends on the composition of the structure. It was shown that the use of compound manganese silicide targets for laser sputtering allows increasing film homogeneity, which may be accompanied by an increase in  $ZT$ .

## **Acknowledgments**

This study was supported by the Russian Science Foundation (project 17-79-20173).

## **References**

- [1]. Ivanova L.D./ Materials Journal of Thermoelectricity №3, 2009. p.60 – 66
- [2]. Nevolin N.V./ Technical Physics Journal, 2009. - v.79.-P.120-127
- [3]. Maize K. / Department of Electrical Engineering, USA. – P.1-6
- [4]. Dharov A / Fundamental Research. – 2014. – V.8. - P.1345-1350

# GROWTH FROM SOLUTIONS, STRUCTURE AND PROPERTIES OF CRYSTALLINE FILMS OF LINEAR OLIGOPHENYLS AND THEIR DERIVATIVES WITH END SUBSTITUENTS

**Lyasnikova M.S.<sup>1</sup>, Postnikov V.A.<sup>1</sup>, Kulishov A.A.<sup>1</sup>, Grebenev V.V.<sup>1</sup>, Sorokina N.I.<sup>1</sup>,  
Lebedev-Stepanov P.V.<sup>2</sup>, Stepko A.S.<sup>1,2</sup>, Borshchev O.V.<sup>3</sup>, Surin N.M.<sup>3</sup>, Svidchenko E.A.<sup>3</sup>,  
Ponomarenko S.A.<sup>3</sup>, Voloshin A.E.<sup>1</sup>**

*1 - Shubnikov Institute of Crystallography of FSRC "Crystallography and Photonics" RAS*

*2 - Photochemistry Center of FSRC "Crystallography and Photonics" RAS*

*3 - Enikolopov Institute of Synthetic Polymeric Materials RAS*

*mlyasnikova@yandex.ru*

Among the various families of semiconductor organic oligomers, linear oligophenyls (nP) are known as highly stable phosphors with a high quantum yield of luminescence. In particular, para-terphenyl (3P) crystals are in demand as one of the most effective organic scintillators. Oligophenyls with the number of aromatic rings in the structure of a molecule with  $n \geq 4$  are effective blue emitters and possess semiconductor properties. To obtain single-crystal films and plates, the most attractive from the point of view of simplicity and the implementation of the approach of applying thin crystalline layers directly on a substrate are the methods of growth from solutions. Unfortunately, the applicability of these methods for producing large single-crystal films with an increase in the number of conjugated units (phenyl rings) in the linear structure of the oligomer molecule is limited by a significant decrease in solubility. The introduction of terminal groups of substituents into the structure of the molecule significantly increases the solubility, thereby contributing to the improvement of growth characteristics.

This report presents the result of investigations of the influence of terminal trimethylsilyl ( $-\text{Si}(\text{CH}_3)_3$ ) and tert-butyl ( $-\text{C}(\text{CH}_3)_3$ ) groups of para-terphenyl and para-quaterphenyl (4P) molecules on the growth characteristics, structure and optical-luminescent crystal properties.

The thermogravimetric data of the crystals was investigated by DSC and TGA. Based on these studies, the melting parameters for 3P and 4P were refined, and for their derivatives were established for the first time, including polymorphic transitions.

To obtain single-crystal films and plates, the growth method from solvent-anti-solvent solutions as the most effective was generally used [1-2]. Under the conditions of the applied method growth of crystal films with high probability is carried out on interphase border liquid-air. For this reason, the upper face of crystals is much smoother (in some cases with roughness at the level of monomolecular layers) than the lower one wetted with a solution. The thickness of the films grown under these conditions can vary from hundreds of nanometers to hundreds of microns, and their length can exceed 20 mm. The morphology and quality of the surface of the crystals was investigated by the methods of optical, scanning laser confocal and atomic force microscopy. The structure of the obtained crystalline samples at 85 K and 293 K by X-ray single-crystal diffraction was investigated.

For the first time the solubility of derivatives of 3P and 4P in toluene at 293 K by the spectrophotometric method [3] was studied. Based on the constructed dependence of optical density on concentration, the boundaries of the existence of aggregated solutions are established.

Theoretical estimates of the binding energy of crystal molecules 3P, 4P and their derivatives when these molecules are attached to the crystallographic planes (001), (010) and (100) were carried out by the atomic force field OPLS method. The calculation of the values of the surface energies of the corresponding faces is carried out. On the basis of the obtained data, conclusions are made about the relative growth rate of these faces. The calculation results are compared with the experiment.

Optical absorption and photoluminescence spectra of solutions and crystals of oligophenyls and their derivatives are investigated.

This work was supported by the Ministry of Science and Higher Education within the State assignment FSRC «Crystallography and Photonics» RAS

[1] V. A. Postnikov et. al. *Crystallography Reports*, 2018, **63**, 1, 152-162.

[2] V. A. Postnikov et. al. *Crystallography Reports*, 2018, **63**, 5, 819-831.

[3] V. A. Postnikov et. al. *Russian Journal of Physical Chemistry*, 2019, 9, is accepted for printing.

# IN SITU INVESTIGATIONS OF THE GROWTH KINETICS OF THE PRISM AND PYRAMID FACES OF KDP CRYSTAL AT ULTRAHIGH SUPERSATURATIONS

**Lyasnikova M.S., Kovalyov S.I., Grebenev V.V., Rudneva E.B., Voloshin A.E., Manomenova V.L.**

*Shubnikov Institute of Crystallography of FSRC "Crystallography and Photonics" RAS*

*mlyasnikova@yandex.ru*

The kinetics of the growth of the faces of the prism and the pyramid of the KDP crystal by laser interferometry *in situ* at ultrahigh supersaturation using a cell and a solution supply system based on the temperature drop scheme was investigated.

Earlier X-ray diffraction studies of KDP crystals [1] showed that in the supersaturation interval  $\sigma = 0.22 \div 0.47$ , where  $\sigma = \ln(c/c_0)$  ( $c$  and  $c_0$  – the real and equilibrium salt concentration in the solution, respectively), the crystals grow by the mechanism of two-dimensional nucleation. One of the main problems that arise when growing crystals from solutions with large supercooling is the instability of the solution, which leads to spontaneous nucleation, instantly reducing supersaturation and making it impossible for the further growth of the crystal.

The stability of the solutions depends on their pretreatment, namely on the filtration of solutions, which allows to remove mechanical impurities and undissolved particles, on the duration and absolute value of the solution overheating and the solution cooling rate before the experiment. In addition, the resistance of solutions to supercooling depends significantly on the design of a particular growth crystallizer.

For studying of crystals growth at high supersaturation developed the technique of the experiment, allowing *in situ* investigations of the growth kinetics of KDP crystal faces. To stabilize the solution, a structurally independent thermostatic tank with a volume of 5 l is used, which allows overheat the solution to high temperatures and sufficiently slow, natural cooling to supersaturation  $\sigma \leq 0.5$  without forced mixing. The method of fastening the used tank allows to exclude the influence of vibrations affecting at the stability of the solution.

It is shown that the stability of the solution achieved in this way allows to exclude spontaneous nucleation during the experiment.

A cell used as a part of a laser interferometer was developed and manufactured for research. The experimental facilities for the study of KDP crystal growth kinetics at supersaturation  $\sigma > 0.2$  consists of two parts: optical and growth. The optical part is a Michelson interferometer, in one of the arms of which there is a growth cell with the crystal under study.

At the preparatory stage of the experiment, the KDP crystal face is being regenerated until several (ideally one) dislocation growth hillocks. After regeneration, the crystal is supplied with a supercooled working solution. The time of the experiment to study the kinetics of crystal face growth at  $\sigma \leq 0.5$  is  $\approx 5$  min.

The obtained results showed the possibility of studying the kinetics of crystal growth at significant supersaturation. In this paper the kinetics of crystal growth at supersaturation of the solution to  $\sigma \sim 0.5$  was studied. It was found that at the beginning of the experiment at high supersaturation on the investigated face of the crystal a large number of competing growth hillocks formed. As a result of competition one growth hillock with the least power is on the surface.

[1] V.L. Manomenova, S.S. Baskakova, E.B. Rudneva, A.E. Voloshin, S.E. Shmelyov. Influence of Some Factors on the Stability of  $\text{KH}_2\text{PO}_4$  Aqueous Solutions // Crystallography Reports, 2018, Vol. 63, No. 4, pp. 677–681

This work was supported by the RFBR grant № 16-29-11785.

# THIN FILMS OF BISMUTH: PREPARATION METHODS AND STRUCTURAL CHANGES UNDER THE INFLUENCE OF LASER RADIATION

Makarova E.S.<sup>1</sup>, Kablukova N.S.<sup>2,3</sup>, Novotelnova A.V.<sup>1</sup>, Tukmakova A.S.<sup>1</sup>, Khodzitsky M.K.<sup>4</sup>, Demchenko P.S.<sup>4</sup>

*1 - ITMO University, Faculty of Cryogenic Engineering*

*2 - Herzen State Pedagogical University of Russia, Faculty of Physics,  
Department of General and Experimental Physics*

*3 - Saint-Petersburg State University of Industrial Technologies and Design*

*4 - ITMO University, Terahertz Biomedicine Laboratory*

*makarova\_helena\_2011@mail.ru*

Nowadays, the study of interaction of high-frequency emission with different materials becomes an actual topic. The significance of such research is due to the rapid development of scientific and technological applications of femtosecond lasers. Femtosecond emission leads to the generation of wideband terahertz (THz) pulses. In accordance to this fact, the study and development of THz antennas and sensors is widely presented in the world.

Bismuth and its solid solutions are of great interest as the materials for devices working in THz range. The study of semimetals like bismuth under the THz emission has been presented in [1]. It was shown that there is the correlation between response time and material structure: monocrystal or polycrystal.

The need of devices miniaturization leads to the necessity of low dimensional objects and thin films usage. Thin films development is associated with the line of various difficulties. The discrepancy between film and the substrate crystal structures leads to additional mechanical stresses manifestation. The difference in the linear coefficient of thermal expansion of the film and the substrate leads to the uniaxial deformation [2]. In bismuth crystals and films a strong properties sensitivity to mechanical deformations is observed.

Thin films structure also depends on deposition method, deposition rate, substrate temperature during the film formation, annealing temperature and time.

A line of methods of bismuth thin films obtaining and treatment was considered: thermal evaporation and zone recrystallization under the coating.

The crystallites structure and orientation were investigated using the method of chemical etching with the atomic force microscopy. The dependences of crystallites size on the deposition method and substrate type were obtained.

Thin monocrystalline bismuth films obtained by zone recrystallization have a crystallographic axis orientation  $C_3$  perpendicular to the plane of the substrate. The crystallites size of annealed films depends on the substrate type. The films on polyimide substrate have a crystallite size up to 5-6 microns. The films on mica substrate have the crystallites of irregular form, interwoven one into another, the crystallite size ranges from 20 to 100 microns.

Structural changes appeared in bismuth thin films due to the THz radiation has been studied.

## References:

1. Terahertz radiation from bismuth surface induced by femtosecond laser pulses / I. E. Ilyakov, B. V. Shishkin, D. A. Fadeev, I. V. Oladyshkin, V. V. Chernov, A. I. Okhapkin, P. A. Yunin, V. A. Mironov, R. A. Akhmedzhanov // Optics Letters. — 2016. — Vol.41, №18. — P. 4289—4292
2. Grabov V M, Komarov V. A, Kablukova N. S. Galvanomagnetic properties of thin films of bismuth and bismuth-antimony alloys on substrates with different thermal expansions // Physics of the Solid State. — 2016. — T. 58. № 3. — C. 622-628.

## FEATURES OF KDP CRYSTAL GROWTH AT ULTRAHIGH SUPERSATURATION

**Manomenova V.L., Rudneva E.B., Kovalyov S.I., Voloshin A.E.**

*Shubnikov Institute of Crystallography of Federal Scientific Research Centre "Crystallography and Photonics" of Russian Academy of Sciences*

*manomenova.vera@mail.ru*

The potassium dihydrogen phosphate  $\text{KH}_2\text{PO}_4$  (KDP) crystal, like other crystals of the KDP group, is widely used for the manufacture of nonlinear optical elements. These crystals have high resistance to laser radiation and are not subject to various induced effects (such as photorefractive). The combination of these properties ensures their wide use in quantum electronics and laser technology. The stability of the  $\text{KH}_2\text{PO}_4$  in a wide temperature range and relative simplicity of growing and processing the KDP crystal make it a convenient model object for the study of growth processes from the solution.

With the method of growing KDP crystals at high supersaturation  $\sigma$  appeared the crystal growth rate is significantly increased. The maximum  $\sigma$  that now used for industrial growth of KDP crystals is less than 0.2 [1, 2]. The search for conditions for the stable growth of crystals at higher supersaturation and the study of the peculiarities of their growth are of great scientific and practical interest.

It is known that the crystal growth from aqueous solutions at high  $\sigma$  is accompanied by spontaneous heterogeneous nucleation that cause a sharp drop of  $\sigma$  and leads to crystal growth rates decreasing. To solve this problem we have studied the influence of a number of factors on KDP supersaturated solutions stability to spontaneous secondary nucleation. Such factors as the solution hydrogen index value, the rate of temperature decreasing, the presence of impurity particles were checked.

The temperature and hydrodynamic conditions that provide the stable growth of crystals at high  $\sigma$  was determined. A number of KDP crystals at  $\sigma > 0.38$  were grown. X-ray diffraction studies have revealed their structural features: for example the crystal growth at  $\sigma > 0.34$  often accompanied by the extensive inclusions formation in the bipyramid growth sector. As a result the growth speed of {101} sector significantly increasing in comparison with the speed of the {100} growth sector. This phenomenon may be associated with a change in the growth mechanism of the bipyramid surface [3]. For some applications the doped KDP crystals may be required. However, the production of KDP crystals with a concentration of the doping impurity of  $\text{Me}^{2+}$  and  $\text{Me}^{3+}$  exceeding few ppm is possible only if supersaturation is ultrahigh.  $\text{FeCl}_3$  was used as doping additive. To increase the  $\text{Fe}^{3+}$  concentration in the {100} prism sector from 5 to 100 ppm it was required to increase the solutions supersaturation from 0.03 to 0.4.

At  $\sigma \leq 0.43$  and different temperature and hydrodynamic modes a series of  $\text{KDP:Fe}^{3+}$  crystals up to  $\sim 20 \times 20 \times 20 \text{ mm}^3$  in size has been grown. The X-ray topography studies of the grown crystals real structure helped us to choose the preferable conditions for the growth of  $\text{KDP:Fe}^{3+}$  crystals with a high content of  $\text{Fe}^{3+}$ . The values of  $\text{Fe}^{3+}$  effective distribution coefficients for both growth sectors of KDP crystals grown from high-doped (up to 55 ppm) solutions in the wide supersaturation range 0.1-0.4 were established for the first time. The spectral characteristics of {100} growth sector of  $\text{KDP:Fe}^{3+}$  crystals with  $\text{Fe}^{3+}$  content from 1 to 100 ppm were studied. It was found that the concentration of  $\text{Fe}^{3+}$  above 60 ppm leads to a steady shift of the absorption band edge to 330-340 nm.

The work was supported by grant RFBR No. 16-29-11785 ofi-m.

1. J.J. De Yoreo, Z.U. Rek, N.P. Zaitseva et al. // J. Cryst. Growth. 166. (1996) 291.
2. N.P. Zaitseva, J.J. De Yoreo, M.R. Dehaven et al. // J. of Crystal Growth. 180 (1997) 255.
3. A.E. Voloshin, S.S. Baskakova, E.B. Rudneva // J. Cryst. Growth. 457 (2017) 337.

# CRYSTALLIZATION OF HYDROXYAPATITE ON WATER-SOLUBLE POLYMER. A BIOMIMETIC APPROACH TO HYBRID MATERIALS

**Mizutani T., Okuda K.**

*Doshisha University, Kyoto, Japan*

*tmizutan@mail.doshisha.ac.jp*

Crystallization of inorganic crystals in the presence of water-soluble polymers attracts interests since the polymers can act as a heterogeneous nucleation site, and control the crystal phase, crystal size, and morphology by the interactions of the functional groups of the polymers and inorganic ions/the surface of the crystals. The study would also shed light on the mechanism of biomineralization, where the inorganic crystals nucleate and grow on the surface of biopolymers. In this paper, we present experimental studies on the coprecipitation<sup>1)</sup> of hydroxyapatite in the presence of natural and synthetic water-soluble polymers with functional groups such as carboxylate, phosphate, and hydroxy groups, to clarify the effects of the functional groups of polymers on the nucleation and crystal growth of hydroxyapatite. We found that quantitative coprecipitation occurs in the case of most water-soluble polymers, and the resultant precipitates were nano-meter sized polymer-hydroxyapatite hybrids. We also report that these hybrids exhibited mechanical properties comparable to those of commodity plastics materials.

In a typical process of coprecipitation, polyethylene terephthalate having carboxylate groups in the benzene ring with the substitution degree of 10-20%, provided by Goo Chemical Co., Ltd. Japan, was dissolved in water, and aqueous Na<sub>2</sub>HPO<sub>4</sub> and NaOH were added. To this homogeneous solution was added an aqueous solution of CaCl<sub>2</sub>, and coprecipitation occurs spontaneously. The coprecipitates were collected by filtration, and subjected to X-ray diffraction, and thermogravimetric analysis.

XRD patterns showed that the crystalline phase of the precipitates was hydroxyapatite. The crystallite size estimated with the Scherrer equation along the *c*-axis was 23-28 nm, comparable to those of natural bone (12-17 nm).<sup>2)</sup> The weight percent of inorganic components in the coprecipitated powder determined by thermogravimetry was 37, 53, and 62%, and agreed with those calculated from the feed ratios. Therefore, both organic phase and inorganic phase were coprecipitated in a quantitative manner. The coprecipitated powder was densified at 120 °C under the pressure of 120 MPa for 5 min. Three-point bending test of the specimen showed that the bending strength was 37-43 MPa, the elastic modulus was 1.3-1.8 GPa, and the strain at break was 4-9%.

Similar coprecipitation process was applied to other water-soluble polymers, both synthetic and natural ones. Comparative studies were carried out to clarify the relationship between the structure of polymers and the properties of the hybrid powders.

## References

1. Gordon, L.; Salutsky, M. L.; Willard, H. H. *Precipitation from homogeneous solution*; John Wiley & Sons, Inc.: New York, 1959.
2. Aoba, T. *Japanese J. Oral Biol.* 1978, 20, 616-627.



# NANOSCALE ELECTROLESS SILVER PLATING WITH CONTROLLED NUCLEATION AND GROWTH CHARACTERISTICS

**Muench F.<sup>1,2</sup>, Vaskevich A.<sup>2</sup>, Ensinger W.<sup>1</sup>**

*1 - Department of Materials and Earth Sciences, Technische Universität Darmstadt,  
64287 Darmstadt, Germany*

*2 - Department of Materials and Interfaces, Weizmann Institute of Science,  
7610001 Rehovot, Israel*

*muench@ma.tu-darmstadt.de*

Electroless plating represents a compelling synthetic option for depositing metal nanomaterials: It can be used to homogeneously metallize work pieces of almost arbitrary shape by simply immersing them in aqueous plating baths, operates at low temperatures, is compatible with various substrate materials, and is easily scalable. However, the method traditionally is employed for producing dense coatings, lacks nanoscale precision, and heavily focuses on few metals such as nickel. In order to reach its full nanofabrication potential, these structural and compositional limitations must be overcome.

In this contribution, we show how the seeding and deposition chemistries of electroless plating can be tuned to create silver films of greatly differing architecture and desired functionality. First, by moderating the plating kinetics and ensuring a high areal nucleation density, free-standing nanoscale silver films can be deposited with outstanding conformity. Combining this reaction with ion-track templates enables the fabrication of high aspect ratio silver nanowires and nanotubes in the form of arrays<sup>1</sup> and networks,<sup>2</sup> which can be applied as miniaturized flow reactors<sup>1</sup> and electrochemical sensors.<sup>2</sup> Contrarily, in our second example, the silver nuclei are purposefully spread out to avoid percolation during growth. This provides an efficient, fast and flexible route toward silver nanoparticle films of defined particle density and size, which exhibit localized surface plasmon resonance and represent a promising transducer platform for optical biosensors.<sup>3</sup> Third, electroless plating can be adapted to avoid random 3D nucleation and achieve directed growth. Using this strategy, thermodynamically unfavorable, anisotropic and defect-rich products can be realized,<sup>4-6</sup> such as films composed of disrupted nanoplates,<sup>5</sup> which exhibit excellent catalytic properties.<sup>6</sup>

[1] F. Muench, M. Rauber, C. Stegmann, S. Lauterbach, U. Kunz, H.-J. Kleebe, W. Ensinger, *Nanotechnology* 22 (2011) 415602.

[2] F. Muench, E.-M. Felix, M. Rauber, S. Schaefer, M. Antoni, U. Kunz, H.-J. Kleebe, C. Trautmann, W. Ensinger, *Electrochim. Acta* 202 (2016) 47–54.

[3] F. Muench, A. Solomonov, T. Bendikov, L. Molina-Luna, I. Rubinstein, A. Vaskevich, *ACS Appl. Bio Mater.* 2 (2019) 856–864.

[4] F. Muench, B. Juretzka, S. Narayan, A. Radetinac, S. Flege, S. Schaefer, R. W. Stark, W. Ensinger, *New J. Chem.* 39 (2015) 6803–6812.

[5] F. Muench, A. Vaskevich, R. Popovitz-Biro, T. Bendikov, Y. Feldman, I. Rubinstein, *Electrochim. Acta* 264 (2018) 233–243.

[6] F. Muench, R. Popovitz-Biro, T. Bendikov, Y. Feldman, B. Hecker, M. Oezaslan, I. Rubinstein, A. Vaskevich, *Adv. Mater.* 30 (2018) 1805179.

# POROUS CARBON NANOMATERIALS PRODUCED AS INVERSE OR DIRECT REPLICA OF ION-TRACK ETCHED POLYMER MEMBRANES

**Muench F., Ensinger W.**

*Department of Materials and Earth Sciences, Technische Universität Darmstadt,  
64287 Darmstadt, Germany*

*muench@ma.tu-darmstadt.de*

Template-assisted syntheses of carbon nanomaterials are commonly based on the pyrolysis of organic precursors, such as can be seen in the prominent example of carbon nanocasting in porous silica.<sup>1</sup> Due to the limited thermal stability of most polymers, this concept is difficult to transfer to ion-track etched polymer templates.

In this contribution, we summarize different strategies how the exceptional structural tunability of this template class can be harnessed for fabricating tailored carbon nanomaterials. As shown in the pioneering work of Lausevic et al., non-melting polyimide foils can be transformed to carbon under full retention of the pores previously created by ion-track etching.<sup>2</sup> The pore architecture and crystallinity of such carbon membranes can be controlled by the irradiation, etching and pyrolysis conditions, enabling one to independently adjust the properties of the carbon matrix and the artificially introduced channels.<sup>3</sup> At lower pyrolysis temperatures, the carbon formed from polymer decomposition remains amorphous and microporous, while the size of the ion-track channels can be freely adjusted from few tens of nanometers upwards, allowing the fabrication of free-standing carbon membranes possessing a well-defined hierarchical porosity. At elevated temperatures, the polyimide can be converted to highly oriented pyrolytic graphite, while the ion-track channels partially close due to recrystallization. Combined with exfoliation, this approach could be used for producing porous graphene with defined pore size and density. While the aforementioned method yields direct carbon replica of ion-track etched polymer membranes, inverse replica are accessible with an organic sol-gel strategy.<sup>4</sup> To this end, the ion-track channels are first filled with a phenolic resin, which in a second step is cross-linked to render it insoluble. The solubility mismatch of the linear template polymer and the infiltrated resin makes it possible to selectively remove the template matrix with organic solvents. After template dissolution, the resin-filled channels are pyrolyzed, providing access to carbon nanofiber arrays and networks.

[1] A.-H. Lu, F. Schüth, *Adv. Mater.* 18 (2006) 1793–1805.

[2] Z. Lausevic, P. Y. Apel, I. V. Blonskaya, *Carbon* 49 (2011) 4948–4952.

[3] F. Muench, T. Seidl, M. Rauber, B. Peter, J. Brötz, M. Krause, C. Trautmann, C. Roth, S. Katusic, W. Ensinger, *Mater. Chem. Phys.* 148 (2014) 846–853.

[4] X. Zhao, F. Muench, S. Schaefer, C. Fasel, U. Kunz, S. Ayata, S. Liu, H.-J. Kleebe, W. Ensinger, *Mater. Lett.* 187 (2017) 56–59.

# SYNTHESIS OF TiN, Ti AND TiSi<sub>2</sub> THIN FILMS FOR THE CONTACT SYSTEM OF SOLAR CELLS

**Nussupov K.Kh., Beisenkhanov N.B., Bakranova D.I., Keinbay S., Turakhun A.A., Sultan A.A.**

*Kazakh-British Technical University*

*rich-famouskair@mail.ru*

The use of copper plating has advantages over aluminum plating due to its low resistivity. However, the diffusion of copper atoms into silicon leads to a decrease in the service life of solar cells. Copper atoms form deep levels in the forbidden zone of silicon to which charge carriers are captured, leading to a decrease in the lifetime of minority charge carriers. It is necessary to create diffusion barriers between the copper metallization and the silicon substrate. Titanium nitride (TiN) is a well-known extremely hard material with low electrical resistivity and high thermal and chemical stability. It is widely used in semiconductor technology as a diffusion barrier, adhesive layer, etc. [1,2]. In this work, the synthesis and study of the structure of titanium and titanium nitride thin films deposited by magnetron sputtering on a Magna-200 unit were carried out. TiN<sub>x</sub> films were synthesized for use as a diffusion barrier to the front and rear of silicon solar cells. The influence of the deposition conditions on the thickness, density and composition of the deposited films is considered. Such parameters varied as magnetron power in the range of 690–1400 W; the temperature of the silicon substrate in the range of 23–170 °C; N<sub>2</sub> gas flow rate in the range of 0.9–3.6 l/h; Ar gas flow rate in the range from 0.06 to 3.6 l/h; N<sub>2</sub>/Ar gas flow ratio in the range of 1–60. The maximum density of the film was 5.247 g/cm<sup>3</sup>, corresponding to the composition TiN<sub>0.786</sub> = Ti<sub>56</sub>N<sub>44</sub>, with the following deposition parameters: power – 1200 W; N/Ar = 1.8/0.06 l/h = 30; pressure – 0.8 Pa; duration – 320 s; substrate temperature – 100 °C. On the X-ray diffraction pattern, the lines TiN (111), (200), (220) from the layer 67.9 nm thick are observed. Atomic force microscopy shows the granular structure of the surface of a titanium nitride film. Using X-ray reflectometry, it was shown that annealing in a stream of argon at a temperature of 700 °C for 30 minutes caused a decrease in the film density to 4.46 g/cm<sup>3</sup> and an increase in thickness from 90 nm to 150 nm. The results are interpreted by the mutual diffusion of Ti and Si atoms and the formation of titanium silicides. Titanium disilicide TiSi<sub>2</sub>, which has a low resistivity (12–20 μOhm·cm), is widely used as a material for metallization. In order to analyze the electrical properties of the contact layers, we synthesized films of titanium and titanium nitride on the silicon surface, followed by annealing at temperatures of 700, 750, or 800 °C for 30 minutes in an Ar atmosphere. Using sensitive X-ray diffraction, the formation of Ti<sub>5</sub>Si<sub>3</sub>, Ti<sub>5</sub>Si<sub>4</sub>, TiSi and TiSi<sub>2</sub> nanocrystals was observed. The stability of the films and the mutual diffusion of Si and Ti atoms in Si-Ti and Si-TiN systems were analyzed. The necessary conditions for the formation of TiSi<sub>2</sub> nanocrystals are discussed, in particular, the presence of a sufficiently thick titanium layer on the silicon surface. A change in the texture of titanium nitride nanocrystals after annealing is observed. The sizes of titanium nanocrystals, titanium nitride, and titanium silicides after deposition and annealing are estimated (3.3–9.1 nm). The mechanism of their changes is considered and by diffusion processes is explained. The effect of fast annealing for 1–5 min in vacuum at a temperature of 720 °C on the formation of structural phases TiSi<sub>x</sub> and on the phase composition of two-layer Ti-TiN<sub>x</sub> films with a total thickness of 50 nm on the silicon surface is considered. Intensive X-ray lines of TiN from a layer of even 25 nm thick are observed. The stabilizing effect of the titanium nitride film on the titanium film is shown. The influence of magnetron sputtering parameters for MAGNA 29 unit on the thickness of Cu films (0.2–10 μm) on a c-Si plate (Taiwan, d=150 mm) is considered. For the Cu-Ti-TiSi<sub>y</sub>-Si and Cu-TiN<sub>x</sub>-TiSi<sub>y</sub>-Si systems, the current-voltage characteristics of p-n-junctions were measured and the I<sub>dir</sub>/I<sub>rev</sub> ratio up to 3000 of the direct and reverse currents was determined.

1 N.K. Ponon, D.J.R. Appleby, E. Arac, P.J. King, et al. Thin Solid Films. 578, 2015, 31-37.

2 K.Kh. Nussupov, N.B. Beisenkhanov et al. Materials Today: Proceedings. 4(3), 2017, 4534-41.

## EFFECTS OF AMORPHOUS STRUCTURES ON EXPLOSIVE CRYSTALLIZATION OF SPUTTER-DEPOSITED AMORPHOUS GERMANIUM THIN FILMS

**Okugawa M.<sup>1</sup>, Nakamura R.<sup>2</sup>, Numakura H.<sup>2</sup>, Heya A.<sup>3</sup>, Matsuo N.<sup>3</sup>, Yasuda H.<sup>4</sup>**

*1 - Mathematics for Advanced Materials Open Innovation Laboratory, National Institute of Advanced Industrial Science and Technology c/o Advanced Institute for Materials Research, Tohoku University, 2-1-1, Katahira, Aoba-ku, Sendai, Miyagi 980-8577, Japan*

*2 - Department of Materials Science, Graduate School of Engineering, Osaka Prefecture University, Gakuen-cho 1-1, Naka-ku, Sakai 599-8531, Japan*

*3 - Department of Materials and Synchrotron Radiation Engineering, University of Hyogo, Himeji, Hyogo 671-2280, Japan*

*4 - Research Center for Ultra-High Voltage Electron Microscopy, Osaka University, Ibaraki, Osaka 567-0047, Japan*

*masayuki.okugawa@aist.go.jp*

In amorphous germanium (a-Ge) and amorphous silicon films, extremely rapid crystallization, called explosive crystallization, is known to occur by instantaneous processes such as mechanical stimulation, laser irradiation, and electron irradiation. In this study, we investigated the crystallization behavior of a-Ge films by non-thermal and thermal rapid crystallization techniques, namely, low-energy electron irradiation and flash-lamp annealing (FLA). We have found that the mode of crystallization depends on the amorphous state: explosive crystallization occurred by both electron irradiation and FLA in pristine films, while it did not occur in those aged at room temperature for over 6 months. In a previous paper [Okugawa et al., J. Appl. Phys. 119, 214309 (2016)], it was reported that liquid-like high-density amorphous (HDA) regions were formed in a-Ge films by the long-term aging. The explosive crystallization observed in pristine a-Ge films is suggested to occur via liquid-like HDA interfaces at the growth front.

To understand the relationship between the crystallization behaviour and atomic arrangements, molecular dynamics a-Ge models were prepared by simulating sputter-deposition processes. The result will also be presented.

## 2D ISLAND NUCLEATION CONTROLLED BY NANOCUSTER DIFFUSION DURING Si AND Ge EPITAXY ON Si(111)-(7×7) SURFACE AT ELEVATED TEMPERATURES

**Petrov A.<sup>1</sup>, Rogilo D.<sup>1</sup>, Sheglov D.<sup>1</sup>, Latyshev A.<sup>1,2</sup>**

*1 - Rzhanov Institute of Semiconductor Physics SB RAS, 630090 Novosibirsk, Russia*

*2 - Novosibirsk State University, 630090 Novosibirsk, Russia*

*alexey\_petrov@isp.nsc.ru*

The growth of epitaxial germanium layers on silicon surfaces has received much attention during the last decades due to the application of SiGe self-organized nanostructures in microelectronics and infrared optoelectronics [1]. The comprehension of fundamental processes proceeding in Ge/Si epitaxial system is required for fabrication of nanostructures of high perfection. A particular interest is attracted to the Si(111) surface having complicated (7×7) surface reconstruction, which strongly transforms surface diffusion and two-dimensional (2D) island nucleation in comparison with non-reconstructed Si(111)-“1×1” surface [2]. The epitaxial growth of Ge and Si on the Si(111)-(7×7) surface starts from the formation of non-epitaxial clusters consisting of 7–8 atoms within half unit cell [3]. While Si nanoclusters have been shown to control surface mass transport during Si/Si(111)-(7×7) growth at elevated temperatures [4], the role of such nanoclusters in surface mass transport in the case of Ge/Si(111)-(7×7) growth has not been addressed yet.

We have studied two-dimensional (2D) island nucleation at the initial stages of Si and Ge epitaxial growth near monatomic steps and on wide (up to 10 μm) terraces on the Si(111)-(7×7) surface in 500–750°C interval by *in situ* ultrahigh vacuum reflection electron microscopy (UHV REM) and *ex situ* atomic force microscopy (AFM). Concentrations of 2D islands nucleated on the terraces and depletion zone widths near the steps have been measured as functions of deposition rate and substrate temperature.

Having analyzed depletion zone width, it has been shown that high concentration of step kinks being effective sinks for diffusing species provides growth kinetics limited by surface diffusion only near the steps both during Si and Ge epitaxy. In contrast to Si/Si(111)-(7×7) epitaxy [5], the negligible energy barrier for attachment to the island edges preserves diffusion limited kinetics during Ge/Si(111)-(7×7) growth on the large-scale terraces far from the steps. We have demonstrated that Ge–Si and Si nanoclusters are dominating diffusion species providing surface mass transport on the Si(111)-(7×7) surface during Ge and Si epitaxial growth at temperatures above 500°C and 600°C, respectively; the activation energy of Ge–Si nanocluster diffusion has been first estimated at 1.3–1.4 eV. Within atomistic rate-equation theoretical framework [6], a critical nucleus of 2D island near the steps (both for Si and Ge epitaxy) and on the wide terraces (for Ge epitaxy) consists of  $\gg 18$  nanoclusters.

This work was supported by the project RFMEFI58117X0026 and performed on the equipment of CKP “Nanostruktury.”

- [1] J.-N. Aqua et al., Phys. Rep., 522, 59 (2013).
- [2] S. Filimonov et al., Phys. Rev. B., 76, 035428 (2007).
- [3] B. Voigtländer, Surf. Sci. Rep., 43, 127 (2001).
- [4] D.I. Rogilo et al., Surf. Sci., 667, 1 (2018).
- [5] D.I. Rogilo et al., Phys. Rev. Lett., 111, 036105-1 (2013).
- [6] J.A. Venables, Philos. Mag., 27, 697 (1973).

# PHENOMENOLOGICAL MODELS OF NUCLEATION AND GROWTH OF METAL ON A SEMICONDUCTOR

**Plusnin N.I.**

*IACP FEB RAS, Vladivostok*

*plusnin@iacp.dvo.ru*

A way of deposition of metal vapors on a substrate in vacuum to reduce the influx of thermal energy from the source to the surface of the substrate has been proposed. In this way, nonequilibrium layers on Si (111) and Si (001) with a composition close to pure Cr, Co, Fe, and Cu were obtained. The composition (AES), morphology (AFM) and density (EELS) of these layers were studied depending on the thickness. The report discusses the phenomenological models of metal nucleation and growth on silicon during the deposition taking into account the experimental results obtained.

# CRYSTALS OF PI-CONJUGATED LINEAR CO-OLIGOMERS: NUCLEATION AND GROWTH FROM SOLUTIONS

**Postnikov V.A.<sup>1</sup>, Kulishov A.A.<sup>1</sup>, Lyasnikova M.S.<sup>1</sup>, Sorokina N.I.<sup>1</sup>, Ostrovskaya A.A.<sup>2</sup>, Borshchev O.V.<sup>3</sup>, Ponomarenko S.A.<sup>3</sup>**

*1 - Shubnikov Institute of Crystallography of FSRC "Crystallography and Photonics" RAS*

*2 - Moscow Technological University (MITHT)*

*3 - Enikolopov Institute of Synthetic Polymeric Materials RAS*

*postva@yandex.ru*

The linear conjugate co-oligomers are of great interest for Organic Electronics and Photonics as materials on the basis of which it is possible to grow high-quality crystals with a low density of defects. High structural perfection of crystals provides high performance of optoelectronic devices. To obtain relatively large single-crystal samples, the methods of growing crystals from solutions appear to be most attractive because of their relative simplicity, low cost and efficiency. Solution crystal growth techniques are also promising for the technology of forming ultrathin single-crystal films of semiconductor co-oligomers directly on substrates under conditions of slow drying of the solvent. This report presents the results of studying the features of crystallization from solutions of a number of pi-conjugated linear co-oligomers from the families of oligoacens, oligophenyls, thiophene-phenylenes, and also new substances with a central benzothiadiazole fragment.

The morphological features of the grown crystals were investigated by means of optical and scanning laser confocal microscopy. The structure of the obtained crystalline samples at 85 K and 293 K and the crystallographic orientation of their faces were investigated by single crystal X-ray diffraction analysis. The crystal structure of co-oligomers with terminal substituents (-Si(CH<sub>3</sub>)<sub>3</sub> and -C(CH<sub>3</sub>)<sub>3</sub>) and the central benzothiadiazole fragment was resolved for the first time. The presence of terminal substituents in the structure of the molecule significantly increases the solubility, thereby improving the growth characteristics of the forming crystals. Due to the considerable anisotropy of intermolecular bonds, linear pi-conjugated co-oligomers are inclinable to 1D- or 2D-crystallization in the form of needles or films, respectively. For the crystals of the studied substances, the structure is in the form of a stack of monomolecular layers. However, the nature of the molecular packing inside the monomolecular layer, apparently, determines the pounding of the co-oligomers to one or another type of crystallization. The regularities of linear co-oligomers 2D-crystallization at the liquid-air interface are discussed in the report.

The thermodynamic model of nucleation and growth of a flat crystalline nucleus at the liquid-air interface under the conditions of the "solvent-antisolvent" method [1] is considered. To analyze the model, experimental data on the solutions surface tension at the interphase boundaries and the calculated values of the surface energy of various faces of organic crystals [2] were used. The analysis of the ratio of the geometric dimensions of the formed single crystalline films was carried out on the basis of model estimates and experimental data obtained for real crystals. The mechanisms of layered growth of flat crystals are discussed.

With work was supported by Ministry of Science and Higher Education within the State assignment FSRC "Crystallography and Photonics" RAS" in part «crystal growth and structure studies», Russian Foundation for Basic Research (Project No. 18-33-20050) in part «studies of co-oligomers with benzothiadiazole and oxazole fragments».

1. V. A. Postnikov and S. V. Chertopalov. Crystallography Reports, 2015, **60**, 4, 594–600.
2. H.-G. Rubahn et al. Interface Controlled Organic Thin Films. Springer-Verlag, 2009. Pp. 3-10.

# SURFACE MORPHOLOGY, MICROSTRUCTURE AND PIEZOELECTRIC RESPONSE OF PEROVSKITE ISLANDS DURING THE PYROCHLORE TO PEROVSKITE PHASE TRANSFORMATION IN THIN PZT FILMS

**Pronin I.P.<sup>1,2</sup>, Kaptelov E.Y.<sup>1,2</sup>, Senkevich S.V.<sup>1,2</sup>, Kiselev D.A.<sup>2,3</sup>, Osipov V.V.<sup>1,2</sup>, Pronin V.P.<sup>2</sup>**

*1 - Ioffe Institute, St. Petersburg, 194021, Russia*

*2 - Herzen State Pedagogical University of Russia, St. Petersburg, 191186, Russia*

*3 - National University of Science and Technology MISiS, Moscow, 119049, Russia*

*Petrovich@mail.ioffe.ru*

Thin ferroelectric films of lead zirconate titanate (PZT) are widely used in various fields of microelectromechanics, infrared technique, microwave electronics, multiferroics. Films of compositions corresponding to the morphotropic phase boundary (MPB), where the electromechanical parameters of solid solutions reach their maximum values, are most in demand. A necessary condition is also the use of practically important silicon substrate with a platinum electrode, as well as the formation of unipolar (self-poled) PZT films. It was previously shown that the piezoelectric response of individual islands or local (isolated) regions of the perovskite phase exceeds the analogous response of continuous films and depends on the transverse size of the islands [1-2]. In this regard, the purpose of this work was to study the microstructure and local properties of perovskite islands in thin PZT films.

Thin films were formed on a platinized silicon substrate (Pt/TiO<sub>2</sub>/SiO<sub>2</sub>/Si). A two-stage method was used, including RF-magnetron sputtering of a ceramic target and the subsequent synthesis of films in air. To obtain individual perovskite islands in the matrix of the low-temperature nonferroelectric pyrochlore phase, either the synthesis temperature was varied (530–570 °C) or the working gas (Ar+O<sub>2</sub>) pressure in the range of 2–8 Pa. The composition of the ceramic target corresponded to the MPB region. SEM, AFM and PFM methods were used to diagnose film surface, microstructure, composition and piezoresponse.

AFM indicated a complex morphological configuration of the phase boundary of perovskite islands situated in the matrix of pyrochlore phase. The thickness of the pyrochlore layer at the boundary increased by several percent, then, at the phase boundary, a sharp shrinkage of the material occurred, and the thickness of the perovskite island increased towards its center. This phase transformation was accompanied by an increase in the porosity of the film in the region of the interface. It is shown that the perovskite islands had unipolarity (self-polarization), the vector of which was oriented to the lower (platinum) electrode. The effect of inhomogeneous distribution of the piezoresponse over the surface of the perovskite island, from the maximum response near its boundary to the minimum to the center of the island, was discovered. It is assumed that the observed effect is caused by the difference in the mechanical clamping of the crystal grains in the periphery of the islands and in the center. The radial inhomogeneity of the piezoelectric response increased with decreasing size of perovskite islands.

When the pressure of the working gas mixture was changed, a significant change in the lead content in the PZT amorphous films was revealed — from substantially higher than the stoichiometric content to below the stoichiometric one. In the latter case, this strongly affected the possibility of crystallization of the perovskite phase, when the formation of the perovskite phase occurred through the nucleation and growth of individual islands. It was found that the mean value of self-polarization in individual islands was almost twice as high as self-polarization in single-phase perovskite films.

The work was partly supported by the Ministry for Education and Science (Russian Federation) (Grant No 16.2811.2017/4.6).

1. Bühlmann S., Dwir B., Baborowski J., and P. Muralt. *Appl. Phys. Lett.* **80**, 3195 (2002).
2. Sun F., Tian G., Chen C., et al. *Ceramics International.* **44**, 21725 (2018).



# PECULIARITIES OF GROWTH OF A NON-KOSSEL CRYSTAL VIA CHERNOV'S MECHANISM

**Redkov A.V.<sup>1</sup>, Kukushkin S.A.<sup>1,2</sup>, Gangrskaya E.S.<sup>2</sup>**

*1 - Institute for Problems in Mechanical Engineering RAS*

*2 - Saint-Petersburg Academic University RAS*

*avredkov@gmail.com*

The work is devoted to extension of existing theory on mechanisms of crystal growth onto the so-called non-Kossel crystals, which are complex crystalline compounds whose cell contains several different types of atoms in nonequivalent positions. The problem of growth of such crystals is one of the important tasks which we need to solve in order to grow defect-free multicomponent crystals, which are in demand in modern industry. One of the well-developed for single crystals growth mechanisms is the Chernov mechanism [1]. The key idea of this mechanisms is that the component diffuses in bulk gas (or solution) directly towards the steps and kinks on the surface and incorporate directly into them. The difference between the Chernov's mechanism and classical Burton-Cabrera-Frank mechanism [2] is that in BCF surface diffusion takes place, whereas in Chernov's mechanisms surface diffusion is suppressed and only volume diffusion governs the process. In paper [1] Chernov developed a theory, which describes exactly this mechanism and allows one to find growth rate of a simple Kossel crystal depending on growth conditions (supersaturation etc.). Despite that this theory was modified many times taking into account different effects [3], as far as we know, there is no generalization of the theory for multicomponent systems, which would allow one to fully describe the growth of an arbitrary multicomponent non-Kossel crystal from its own vapors. This work is aimed at the extension of Chernov's theory onto multicomponent system and it considers the growth of a non-Kossel crystal due to diffusion of components from vapor or solution directly towards the steps on the surface. Some peculiarities of this process are discussed and analytical expressions are found for the rate of advance of a single step, and the rate of advance of a group of equidistant steps.

[1] Chernov, A. A. (1961). Crystal growth from the solution and from the melt. *Sov. Phys. Usp*, 4, 129.

[2] Burton W. K., Cabrera N., Frank F. C. (1951). The growth of crystals and the equilibrium structure of their surfaces. *Philosophical Transactions of the Royal Society of London. Series A, Mathematical and Physical Sciences*, 243(866), 299-358.

[3] Gilmer G. H., Ghez R., Cabrera, N. (1971). An analysis of combined surface and volume diffusion processes in crystal growth. *Journal of Crystal Growth*, 8(1), 79-93.

## ANOMALIES OF PROPERTIES IN KCNSH MIXED CRYSTALS

**Rudneva E.B.<sup>1</sup>, Manomenova V.L.<sup>1</sup>, Koldaeva M.V.<sup>1</sup>, Sorokina N.I.<sup>1</sup>, Voloshin A.E.<sup>1</sup>,  
Grebenev V.V.<sup>1</sup>, Verin I.A.<sup>1</sup>, Lyasnikova M.S.<sup>1</sup>, Vasilyeva N.A.<sup>1</sup>, Masalov V.M.<sup>2</sup>, Zhokhov A.A.<sup>2</sup>,  
Emelchenko G.A.<sup>2</sup>**

*1 - Shubnikov Institute of Crystallography of Federal Scientific Research Centre "Crystallography and Photonics" of Russian Academy of Sciences*

*2 - Institute of Solid State Physics of Russian Academy of Sciences*

*rudneva.lena@inbox.ru*

Devices based on the principle of solar-blind technology are actively used for remote diagnostics of power lines, environmental monitoring and medical diagnostics. Their principle of operation is based on the registration of radiation in the wavelength range 250-290 nm, where the solar radiation is almost completely suppressed by the ozone layer of the Earth, and suppression of other non-working ranges of the spectrum. Now crystals used for this purpose are  $\alpha$ -NiSO<sub>4</sub>·6H<sub>2</sub>O ( $\alpha$ -NSH), Me<sub>2</sub>Ni(SO<sub>4</sub>)<sub>2</sub>·6H<sub>2</sub>O and K<sub>2</sub>Co(SO<sub>4</sub>)<sub>2</sub>·6H<sub>2</sub>O (KCSH). A significant disadvantage of all these crystals is the presence of transmission peaks in the visible region that reduce the filtration efficiency and sensitivity of the devices. The K<sub>2</sub>Co<sub>x</sub>Ni<sub>1-x</sub>(SO<sub>4</sub>)<sub>2</sub>·6H<sub>2</sub>O (KCNSH) mixed crystals are a promising material for optical UV filters because they suppress transmission in the visible spectrum.

KCNSH crystals were grown from solutions with the mass fraction ratio KCSH:KNSH = 0:1 (I); 1:4 (II); 1:2 (III); 1:1 (IV); 2:1 (V); 3.7:1 (VI), 19:1 (VII), 39:1 (VIIa), 99:1 (VIIb), 1:0 (VIII).

The measurement of KCNSH crystals dehydration temperature showed that in addition to the absolute maximum of  $T_{deg}$  for crystals with KCSH content  $c_{Co}$  of about 10%, there is a local maximum at  $c_{Co} \approx 90\%$ . During indentation of KCNSH crystals by Vickers pyramid the maxima of microhardness in the sectors {001} and {110} with  $c_{Co} \approx 10-15$  wt. % were found.

The study of the Co/Ni ratio in the crystals showed that the  $c_{Co}$  not equal for the growth sectors {110} and {001} and the difference between them  $\Delta c_{Co} = c_{Co}\{110\} - c_{Co}\{001\}$  varies depending on the solution composition. The  $\Delta c_{Co}$  is minimal for crystals II and III, as well as for VIIa and VIIb and maximal for the V and VI crystals.  $\Delta c_{Co}$  determines the sectorial inhomogeneity of crystals: in crystals II and III defects are practically absent and the most imperfect were crystals VI that had a large number of defects observed in the optical microscope and the lowest transmittance in the UV region. The crystals V were a little bit less defective. The IV and VII ones had only a few inclusions. However, this dependence does not exactly explain existence of maxima of properties for crystals III and VII-VIIa. A more accurate answer is given by the X-ray diffraction data analysis of both growth sectors – {110} and {001}.

The unit cell volume  $V$  of {110} growth sector is larger than in {001} sector, that is consistent with the fact that the growth sector {001} contains less Co than the {110} sector. However, the change in  $V$  is determined not only by the content of Co, since the dependence of  $V(c_{Co})$  is different for the two growth sectors.

This feature can be explained only by an additional, rather noticeable effect of impurities on the lattice parameters, that, in particular, is confirmed by the fact that for the extreme members of the series (KNSH and KCSH), the parameters and volumes of the unit cell also different in different growth sectors. The dependence of  $\Delta V$  on  $c_{Co}$  has two minima corresponding to crystals III and VII, the maximum volume difference is observed for crystals VI that generally correlates with the observed crystal defects. So it is the difference of the lattice parameters, rather than various Co content in different sectors has a decisive influence on the anomalies of properties in KCNSH crystals: elastic stresses arising because the mismatch of lattice parameters at the sectorial boundaries lead to the inclusions formation during the growth of the crystal that reduces its thermal stability and microhardness [1].

The work is supported by grant RSF № 15-12-00030.

[1] M. S. Grigor'eva, A. E. Voloshin, E. B. Rudneva et al. A study of the mechanisms of defect formation in K<sub>2</sub>Ni(SO<sub>4</sub>)<sub>2</sub>·6H<sub>2</sub>O/K<sub>2</sub>Co(SO<sub>4</sub>)<sub>2</sub>·6H<sub>2</sub>O bicrystals grown from aqueous solutions. Crystallography Reports. 2009. Vol. 54. P. 637–644.

# FILIFORM POLYCRYSTALLINE PHOSPHOR $Cd_{0.1}Zn_{0.9}S$ : Cu, Ag ON THE SURFACE OF THE NEW MATERIAL Si/(NANO-SiC)

**Sergeeva N.M., Bogdanov S.P.**

*St. Petersburg state Institute of Technology (Technical University), Moskovsky prospect 26,  
St. Petersburg, 190013, Russia*

*Alnserg41@mail.ru*

Promising is the use of zinc-cadmium-sulfide phosphors (P) as a film coating surface templates (substrates) with a buffer layer Si/(nano-SiC) -a new material grown by the method of substitution of atoms [1] to create a new generation of light-emitting devices. In the framework of the comprehensive plan study of the properties of P were grown polycrystalline films  $Cd_{0.1}Zn_{0.9}S$ : Cu, Ag in an aqueous colloidal solution containing a compound of zinc acetate, cadmium nitrate and sodium sulfide on the surface of the substrate by means of crystallization under normal conditions. Films P were studied by physical and chemical methods of surface analysis. X-ray phase analysis (XRD) method established the phase composition: solid solution  $Cd_{0.1}Zn_{0.9}S$  cubic symmetry (main phase) P, impurities: sodium sulfate ( $Na_2SO_4$ ), sodium cadmium sulfide ( $Na_6Cd_7S_{10}$ ). The morphology and chemical (elemental) composition of the P film were studied by scanning electron microscopy (SEM) in the modes of formation of electron microscopic images in the signals of secondary and reflected electrons (SE, RE), respectively. In the signals of the SE contrast of the SEM image it is shown that the films are polycrystalline, on the crack surface, the average thickness of the layers is ~ 100 microns. On its surface are visible areas of crystals of various morphological forms: filamentous (1D structure), needle and oval. Moreover, the particles of these forms are not chaotic, but are concentrated in certain areas on the surface of the P film. In RE signals, the contrast of the SEM image is determined by the characteristic X-ray spectrum of the concentrations of the elements in situ of the film generated by the electron beam (sensor). In situ EDRS energy dispersive X-ray spectroscopy the elemental composition of the film (at.%): zinc, cadmium, sulfur and sodium. 1D filament and needle, plate represented solid solutions of  $Cd_{0.1}Zn_{0.9}S$  and  $Cd_{0.23}Zn_{0.77}S$  respectively. It is confirmed that 1D filament of crystals are formed in voids, at the edges of the substrate, in slightly opening cracks, where the heat sink is better. Assume a mechanism of self-Assembly of 1D crystals of P “bottom-up” orientation: the diffusion of Si from the substrate, the formation of voids, the introduction of vacancy  $Cd_{0.1}Zn_{0.9}S$ , evaporation of water molecules creates the directed movement and growth of 1D ( $Cd_{0.1}Zn_{0.9}S$ )/Si( $SiO_2$ ). One-dimensional 1D crystals of P containing copper, silver can be of interest as promising materials for the creation of new high-performance electronic and optoelectronic sensors and light guides, directed transmission of light energy.

## References

1. Kukushkin S.A., Osipov A.V. // J. Phys. D.: Appl. Phys. 2014. v. 47.P. 313001.
2. Kukushkin S.A., Slezov V.V. Disperse systems on the surface of solids: mechanisms of thin film formation (evolutionary approach). St.Petersburg: Science. 1996. 304 p.
3. Sergeeva N.M. Self-organization of dispersed particles during deposition on the surface of Si/nano SiC heterostructure in aqueous colloidal solution.// Science-intensive technologies of functional materials: thesis of reports V international scientific and technical conference, 10-12 oct. 2018. St.Petersburg: St.PbSI of Film and Te, 2018. 90p., P.11.

# CRYSTAL GROWTH AND UNIQUE MORPHOLOGY OF HETEROSTRUCTURED ALUMINUM HYDROXIDE FILM FORMED ON ALUMINUM ALLOYS USING STEAM

**Serizawa A., Kanasugi K., Tanabe M.**

*Shibaura Institute of Technology*

*serizawa@shibaura-it.ac.jp*

The novel formation method of anticorrosive film on metallic materials using steam, steam process, was applied to Al alloys. The anticorrosive film was generated with a chemical reaction of steam and Al during steam process. The resultant film was characterized, and then and evaluated by electrochemical measurements. FE-SEM images of the film surfaces showed that plate-like nanocrystals were densely formed over the entire surface. Cross-sectional view of the film revealed that the film had a two-layer structure in which a plate-like nanocrystals layer was formed on an extremely dense amorphous structure. XRD patterns indicated that the film was composed mainly of AlOOH crystals. The potentiodynamic polarization curves revealed that the corrosion current density of the film-coated substrates significantly decreased. The appearance of the surface of the film-coated specimen exhibited no damage at all, even after saltwater immersion for 168 h. In contrast, considerable pitting corrosion was observed on the as-received specimen. In summary, the corrosion resistance of the film-coated Al alloys was improved because of a unique morphology with two-layer structure of AlOOH film. Acknowledgements: This research was supported by JST under Industry-Academia Collaborative R&D Program "Heterogeneous Structure Control" (No. 20100120) and Program on Open Innovation Platform with Enterprises, Research Institute and Academia (OPERA) (No. 18072116), and JSPS KAKENHI (No. 19H02482).

# GROWTH AND CHARACTERIZATION OF ALKALI-EARTH HALIDE SCINTILLATOR CRYSTALS

**Shalaev A., Shendrik R., Rusakov A., Rupasov A., Myasnikova A.**

*Vinogradov Institute of Geochemistry SB RAS*

*alshal@mail.ru*

The work motivated by a necessity of searching new materials for detection of ionizing radiation. The ternary alkali earth-halide systems doped with rare-earth ions are promising scintillators showing high efficiency and energy resolution. Aspects of crystal growth and optical properties of BaBrI, BaClI and SrBrI single crystals with rare-earth doping are reported.

The crystals have been grown by the vertical Bridgman method in sealed quartz ampoule in vacuum. The compounds of alkaline earth halides are hygroscopic. Therefore, much attention is paid to drying raw materials before crystal growth. The thermogravimetric method and differential scanning calorimetry were used to determine the melting points, the level of hydration and the possible dehydration temperature of the charge materials. We describe processing procedures that, when combined with our molten salt filtration methods, have led to advances in achieving a significant reduction of cracking effects during the growth of single crystals. In addition, we have developed a procedure to grow BaBrI crystals using the Czochralski method. The resulting crystal has a length of 3 cm and is free of cracks.

Scintillation properties and luminescence mechanisms of these crystals are reported. Emission, excitation and optical absorption spectra as well as luminescence decay kinetics are studied under excitation by X-ray, vacuum ultraviolet and ultraviolet radiation. The energies of the first 4f-5d transition in  $\text{Eu}^{2+}$  and band gap of the crystals are obtained. It is shown that electron-hole and exciton mechanisms are possible to transfer energy to the luminescence centers in these crystals.

This work was partially supported by grant from the Russian Science Foundation, RSF project 18-72-10085. The reported study was performed with the equipment set at the Centres for Collective Use "Isotope-geochemistry investigations" at A.P. Vinogradov Institute of Geochemistry SB RAS.

# MORPHOLOGY EVOLUTION DURING EARLY STAGE OF SINGLE CRYSTAL DIAMOND HOMOEPITAXIAL GROWTH BY MICROWAVE PLASMA CHEMICAL VAPOR DEPOSITION

**Shu G.<sup>1,2</sup>, Ralchenko V.<sup>1,2</sup>, Bolshakov A.<sup>1,2</sup>, Komlenok M.<sup>2</sup>, Khomich A.<sup>2,3</sup>, Ashkinazi E.<sup>2</sup>, Dai B.<sup>1</sup>, Zhu J.<sup>1</sup>**

*1 - National Key Laboratory of Science and Technology on Advanced Composites in Special Environments, Harbin Institute of Technology, Harbin 150001, P.R. China*

*2 - General Physics Institute RAS, Moscow 119991, Russia*

*3 - Institute of Radio Engineering and Electronics RAS, Fryazino 141190, Russia*

*sgy1161@163.com*

Epitaxial growth of single crystal diamond (SCD) by microwave plasma assisted chemical vapor deposition (MPCVD) technique allows production of high quality films and crystals for advanced applications, including electronics. While the step growth mode is well established for the most typical growth condition for SCD [1,2], less information is known about the development of the surface relief with steps and terraces at the beginning of the epitaxy process. Here, we report on the observations of surface morphology features during the earliest stages of SCD synthesis, with the evolution from the nucleation on substrate till the complete formation of growth steps. Epitaxial diamond growth was carried out with a MPCVD reactor (2.45 GHz) on well-polished nanoscale smooth surface HPHT diamond substrates with (100) oriented face, under the typical process parameters: pressure of 120 Torr, MW power of 3 kW and 3% CH<sub>4</sub> mixed with H<sub>2</sub> with total flow rate 400 sccm. The growth was interrupted periodically, in times of a few minutes to 2 hours for the surface inspection. The as-grown samples were characterized with SEM, AFM and laser scanning microscopy (LSM). Microscopic appearance gradually changed with time from independent hill-like nucleation islands to parallel terraces by accumulation and connection from many isolated islands (Fig. 1). Raman and photoluminescence spectra of the epilayers were also analyzed.

Fig.1\*. LSM images of the surface relief for the early growth stage (a), and completely formed growth steps after a longer deposition time (b).

## References:

- [1] Van Enckevort W.J.P., et al. Step-related growth phenomena on exact and misoriented {001} surfaces of CVD-grown single-crystal diamonds, *Diamond Relat. Mater.* 1995, 4: 250-255.
- [2] Lee S.T., et al. CVD diamond films: nucleation and growth, *Mater. Sci. Eng. R: Reports*, 1999, 25: 123-154.

\*The abstract with figures is available at <http://2019.mgctf.ru/01000034a8.doc>

## MICROSTRUCTURE OF BARIUM-STRONTIUM TITANATE BASED GLASS CERAMICS

Turygin A.P.<sup>1</sup>, Abramov A.S.<sup>1</sup>, Alikin D.O.<sup>1</sup>, Chezganov D.S.<sup>1</sup>, Baturin I.S.<sup>1</sup>, Song X.<sup>2</sup>, Zhang T.<sup>2</sup>, Zhang Y.<sup>2</sup>, Hu K.<sup>2</sup>, Zhao Z.<sup>2</sup>, Shur V.Ya.<sup>1</sup>

1 - School of Natural Sciences and Mathematics, Ural Federal University, Ekaterinburg, Russia

2 - Beijing Key Laboratory of Fine Ceramics, State Key Laboratory of New Ceramics and Fine Processing, Institute of Nuclear and New Energy Technology, Tsinghua University, Beijing 100084, PR China

vladimir.shur@urfu.ru

Glass-ceramics comprising of ferroelectric grains surrounded by glass matrix are of significant interest for power electronics applications due to enhanced energy storage capabilities [1]. Barium strontium titanate (BST) ferroelectric glass-ceramics is one of the most promising candidates due to dielectric constants and high breakdown strengths [2,3]. In spite of macroscopic properties of BST ceramics are well known, there is still lack of studies on local distribution of ferroelectric phase and its evolution during ceramics cycling.

We have studied microstructure and surface morphology of  $(\text{Ba}_{0.25}, \text{Sr}_{0.75})\text{TiO}_3$  based glass-ceramics with composition  $25.95\text{BaO}-8.65\text{SrO}-(29.4-x)\text{TiO}_2-22\text{SiO}_2-12\text{Al}_2\text{O}_3-2\text{BaF}_2-x\text{MnO}_2$  and different amount of Mn additive ( $x = 0-0.5$  mol%), prepared from melted and quenched mixed powders. The as-quenched glass was annealed and subjected to controlled crystallization in air for 2 h in temperature range from 850 to 950°C.

Scanning electron microscopy allows us to reveal dendrite-like clusters of crystalline phase with sizes from 3 to 6  $\mu\text{m}$  in samples crystallized at 850°C with width of individual branches below 100 nm. Crystalline phase possesses dense branching morphology, which formed due to tip splitting growth. Value of fractal dimension  $D = 1.96$  obtained by box counting is sufficiently larger than typical fractal dimension for DLA clusters ( $D = 1.70$ ) [4]. All investigated samples BST-Mn-850°C with different Mn concentration demonstrated similar values of fractal dimension.

Ceramics with higher crystallization temperature (950°C) consisted of conventional faceted-shape grains with typical sizes about 50-200 nm. The observed microstructures play the key role in dielectric properties of glass-ceramics.

Acknowledgements: The research was made possible by Russian Foundation for Basic Research (Grant 18-52-53032-NNSF-a). The equipment of the Ural Center for Shared Use “Modern nanotechnology” Ural Federal University was used.

[1] Q. Tan, P. Irwin, Y. Cao, *IEEJ Trans. FM* **126**, 1153 (2006).

[2] Y. Zhang, J.J. Huang, T. Ma, X.R. Wang, C.S. Deng, X.M. Dai, *J. Am. Ceram. Soc.* **94**, 1805 (2011).

[3] X. Wang, Y. Zhang, I. Baturin, T. Liang, *Mat. Res. Bull.* **48**, 3817 (2013).

[4] E. Ben-Jacob, *Cont. Phys.*, **34**, 247 (1993).

# INFLUENCE OF ELASTIC STRESS ON CRYSTAL PHASE OF GaP NANOWIRES

**Sibirev N.V.<sup>1,2</sup>, Berdnikov Y.S.<sup>1</sup>, Sibirev V.N.<sup>3</sup>**

*1 - ITMO University*

*2 - Saint-Petersburg State University*

*3 - Saint Petersburg Mining University*

*NickSibirev@corp.ifmo.ru*

Crystal structure is one of the basic characteristics of a material which strongly influences its physical properties, such as symmetry, modulus of elasticity, density, band gap, Fermi level, surface energies etc. Most of III-V compounds except nitrides in the bulk phase form a face-centered cubic lattice, so called zinc blende crystal structure. In contradiction to it, metal catalyst III-V nanowires frequently demonstrates metastable hexagonal crystal structure, named wurtzite.

Usually such nanowire growth in metastable phase is explained by crystallization at the triple-phase line [1]. The explanation requires, that nanowire growth proceeds in monocentric layer-by-layer growth, sidewalls surface energy is less for metastable wurtzite phase and nucleation at the triple line is more favorable than in the center. This conditions look diameter independent. The diameter dependence is recovered by considering a purely geometrical effect [2]. Nanowire growth rate in monocentric regime is the product of nucleation rate and available nucleation area. It is clear that nucleation in the center is possible on the whole facet, while triple line nucleation is possible only in the perimeter of nanowire [2]. Also increasing nanowire radius leads to transition from monocentric growth regime to polycentric one [3]. So there is a certain critical value of nanowire radius above which nanowire always should grow in zinc blende crystal phase. Yet there are a lot of papers where experimentally observed thick GaP nanowires with wurtzite crystal phase [4].

Here we discuss another opportunity to stabilize the metastable phase in nanowires — the accumulation of elastic energy. It is well known that during the deposition of III-V materials on different substrates, large elastic stresses lead to the formation of quantum dots and, further, to a three-dimensional growth of bulk material in stable crystal phase. In nanowires elastic stresses could be effectively relaxed on the sidewalls [5], so nanowire growth usually proceeds in a different way. They grow in layer-by-layer mode, when growth of each layer starts only when the formation of a previous layer is fully completed [1,6]. Even more, most nanowires grow in the so-called mononuclear mode, when each layer formed only from one nucleus. Typically this new layer nucleus forms coherently on previous layer. If nucleus have different crystal structure it would be strongly affected by elastic stress from nanowire stem [7] and it is energetically favorable if nucleus adopt crystal structure of previous layer.

Lattice mismatch between face-centered cubic (sphalerite) and hexagonal (wurtzite) phase could reach several percent, and for GaP elastic stress of the formation of stable phase on metastable layer reaches value of 12 meV per pair. This is greater than the difference in the energy of the formation of the cubic and hexagonal phase. So GaP nanowires could grow in wurtzite phase for any radius.

- [1] Glas F., Harmand J.C., Patriarche G. // 2007. Phys. Rev. Lett. V. 99. Iss.14. P. 3–6.
- [2] Sibirev N.V., Dubrovskii V.G. // 2004. Tech. Phys. Lett. V. 30. Iss.9. .
- [3] Ren X., Huang H., Dubrovskii V.G., Sibirev N. V, Nazarenko M. V, Bolshakov A.D., Ye X., Wang Q., Huang Y., Zhang X., Guo J., Liu X. // 2011. Semicond. Sci. Technol. V. 26. Iss.1. P. 014034.
- [4] Halder N.N., Cohen S., Gershoni D., Ritter D. // 2018. Appl. Phys. Lett. V. 112. Iss.13. P. 133107.
- [5] Glas F. // 2006. Phys. Rev. B V. 74. Iss.12. P. 2–5.
- [6] Dubrovskii V.G., Soshnikov I.P., Cirilin G.E., Tonkikh A.A., Samsonenko Y.B., Sibirev N.V., Ustinov V.M. // 2004. Phys. Status Solidi Basic Res. V. 241. Iss.7. .
- [7] Glas F., Daudin B. // 2012. Phys. Rev. B V. 86. Iss.17. P. 1–8.



# DIAMOND NUCLEATION FROM ACTIVATED VAPOR PHASE

**Spitsyn B.V.**

*A.N.Frumkin Institute of Physical Chemistry and Electrochemistry RAS, Moscow, Russia*

*bvspitsyn@gmail.com*

The study of the origin of a new phase formation from a supersaturated initial medium still represents a complex theoretical and applied problem. The simplest case should be the nucleation under isothermal conditions of a new liquid or solid phase from a gas phase derived from thermodynamic equilibrium, i.e. in one component system. According to classical theory [1], the frequency of homogeneous nucleation,  $J$ , is determined by the relation

$$J = A \exp(-\Delta G_a/kT) \exp(-16\pi\Omega^2\alpha^3/3kT\Delta\mu^2) \quad (1)$$

where  $J$  - the number of nuclei in unit volume per unit time,  $\Omega$ - specific volume per particle in the crystal; pre-exponential term,  $A$ , is proportional to the particles density in a mother phase,  $k$  - Boltzmann constant;  $\alpha$ - specific free energy at crystal environment boundary,  $G_a$ - free activation energy at the new particle addition to the nucleus;  $\Delta\mu$  - in chemical potential difference between the initial and final phases. General view of (1) shows that it appears to be one of the strongest known in physics and physical chemistry functional dependency, because the surface energy,  $\alpha$ , appeared in the 3-rd power under the sign of the exponent. More complex will be thenucleation in a multi-component system. And finally, the following complication should be expected in the processes of diamond nucleation from highly excited gaseous media, developed and used for the synthesis of diamond in the region of its thermodynamic metastability [2]. It would seem that the well-known high value of the surface energy of diamond leaves no hope for its spontaneous nucleation. However, due to the presence in the gas phase of atomic hydrogen in superequilibrium concentration, the surface of critical diamond nuclei and diamond layers growing from them will be predominantly covered not by unsaturated “dangling” carbon bonds, but by strong C – H bonds, which will drastically reduce the value of both non-equilibrium and equilibrium surface energy. This ensures the selective synthesis of metastable diamond, not accompanied by parallel nucleation and growth of graphite [2]. The report will consider the features of homogeneous [3] and heterogeneous diamond nucleation, the disequilibrium of the surface of critical embryos, their electric charge and the role of “wetting” with a nascent diamond on the surface of a non-diamond substrate.

1. A A Chernov, Modern Crystallography, V. 3. Crystal Growth, Berlin, Springer Verlag, 1984. Crystallization, Ann Rev Sci. 1973.
2. B.V.Spitsyn, L.L.Builov, B.V.Deryagin, J Cryst Growth 52 (1981) 219.
3. S. Mitura, et al., Thin Solid Films 128(3-4) (1985)353.

# FORMATION OF STEPS AT THE THREE-PHASE LINE OF CONTACT UNDER THE GROWTH VAPOR-LIQUID-SOLID NANOWIRES

Nebol'sin V.A., Swaikat N.

Voronezh State Technical University

*nada.s84@mail.ru*

As shown by Wagner and Ellis [1], the mechanism of whisker growth in the absence of screw dislocations is easy to understand in the case of the well-known vapor–liquid–solid (VLS) process. According to the generally accepted views [2, 3], the physics of VLS growth is related to the properties of the vapor–liquid and liquid–solid interface. VLS growth has been extensively studied with application to basic semiconductor materials [4]. At the same time, the activating role of the liquid droplet and the mechanism by which it moves upward from the substrate through the VLS process, “pulling” the crystal, are still unclear. Nor has been the origin of the well-known paradox understood: the pronounced tendency, e.g., in the case of silicon whiskers, for the most densely packed faces {111} to grow very rapidly (characteristically, these faces of diamond-like crystals grow very slowly by the layer mechanism). Silicon nanowires also grow along {111} [2]. In addition, the epitaxy temperature is 200–800 K higher than the temperature of nanowire growth with the participation of liquid droplets. The observed Si nanowhisker growth and the kinetic data obtained are in conflict with kinetic control and exponential rate law of Si epilayers in similar chemical processes. The shapes of the nanowires, round in cross section, indicate that the liquid in the droplet wets the (111) singular face of the solidification interface along the perimeter, without wetting the lateral surface.

The purpose of this work was to clarify the physicochemical mechanism of quasi-1D vapor phase growth of Si, Ge, GaAs, GaP, et. al. nanowires (nucleation at the wetting perimeter of the droplet, etc.) and to gain detailed insight into the physics of the activation of nanowire growth by the liquid, which substantially reduces the activation barrier. As metal solvents, we used Au, Cu, Sn and Ga particles.

The formation of steps at the three-phase line of contact under the droplet is shown to be a factor of 2–3 easier compared to nucleation at the solid–liquid and solid–vapor interface. Equations were derived for the shape, radius, and formation energy of a critical nucleus at the three-phase line of contact under the droplet and were used to evaluate these parameters. The formation energy of critical nuclei along the three-phase line of contact,  $dF$ , is on the order of  $kT$ , and the formation of steps at the growth interface from its closed boundary to the wetting perimeter of the droplet is quite plausible thermodynamically. The physical nature of nanowire growth process is the reduction in activation barriers to crystal growth via the release of the excess surface energy by the spheroidizing droplet at the three-phase line of contact, the decrease in the supersaturation needed for the growth of the singular face of the nanowire at a preset rate, and the stable equilibrium of the droplet on this face.

1. Wagner, R.S. and Ellis, W.C. Vapor–Liquid–Solid Mechanism of Single Crystal Growth, *Appl. Phys. Lett.* 1964. V. 4. № 5. P. 89–90.
2. Nebolsin V.A., Dolgachev A.A., Dunaev A.I. On the general laws of growth of oil companies // *News of the Russian Academy of Sciences. Ser. Phys.* 2008. V.72. №9. P.1285-1288.
3. Nebol'sin V.A., Shchetinin A.A., Natarova E.I. Variation in silicon whisker radius during unsteady-state growth // *Inorg. Mater.* 1998. V.34. № 2. P. 87-89.
4. Nebol'sin, V.A., Dunaev, A.I., Tatarenkov, A.F., Shmakova, S.S. Scenarios of stable Vapor-Liquid Droplet-Solid Nanowire Growth // *J. Cryst. Growth.* 2016. №. 450. P. 207-214.

# GLASS FORMATION AND NUCLEATION KINETICS IN THE MeO-B<sub>2</sub>O<sub>3</sub>-P<sub>2</sub>O<sub>5</sub> SYSTEM, WHERE Me=Ca, Sr, Ba

Sycheva G.A.

*Grebenshchikov Institute of Silicate Chemistry, Russian Academy of Sciences, 199034, St. Petersburg,  
nab. Makarova 2*

*sycheva\_galina@mail.ru*

There are the following main reasons making the study of glass formation and homogeneous and heterogeneous nucleation kinetics in borophosphate glasses fairly important. The first reason lies in the fact that controlled crystallization of glasses can lead to a wide range of glass-ceramics having unusual microstructures and properties. The second reason results from the fact that the high viscosity of silicate glasses makes it possible to “freeze” any stage of the crystallization process. Therefore, the glasses are very convenient objects for the experimental study of nucleation. These investigations can serve as basis for verifying and further development of the crystallization theory. No previous work has been reported regarding the glass formation regions and crystallization kinetics in the systems MeO-B<sub>2</sub>O<sub>3</sub>-P<sub>2</sub>O<sub>5</sub>, where Me=Ca, Sr, Ba and so, in this work, the homogeneous and heterogeneous nucleation of MeO-B<sub>2</sub>O<sub>3</sub>-P<sub>2</sub>O<sub>5</sub> glasses are investigated. The choice of this system was dictated by several interrelated factors. First, MeO borophosphate glasses are of practical importance, as the basis of the production of stillwellite glass-ceramics. Second, for these glasses, not only the surface crystallization, but also volume nucleation is observed. To obtain the number of crystals  $N(T,t)$  nucleated at the temperature  $T$  vs the nucleation time  $t$  and then to calculate the nucleation rate  $I(T,t)=dN(T,t)/dt$ , the following method is usually used depending on whether the temperature maximum of  $I$  overlaps that of crystal growth rate  $U$ . When the value of  $U$  at the nucleation temperature  $T$  is too low to observe the crystal after a lapse of reasonable time, it is possible to apply the “development” method, also known as Tamman’s method. Its basic idea consists in the crystal “development” at a temperature  $T_d > T$  to sizes visible in a microscope. In choosing  $T_d$  the following conditions should be met:  $I(T) \gg I(T_d)$  and  $U(T) \ll U(T_d)$ . In this work, the effects of varying the water content of Ba borophosphate glasses on the number of crystals  $N(T,t)$  nucleated at the temperature  $T_m$ , where the stationary nucleation rate has maximum, has been also studied. It is known that the water content of phosphate glasses greatly depends on the ratio M/P, M being the concentration of alkali metal ion and P the concentration of phosphorus. The water content in phosphate glasses is described by an exponential-like dependence, which rapidly decreases with decreasing P<sub>2</sub>O<sub>5</sub> content. When the P<sub>2</sub>O<sub>5</sub> content is lower than 45 mol %, the water content becomes negligible. In the case of BaO-B<sub>2</sub>O<sub>3</sub>-P<sub>2</sub>O<sub>5</sub> system, the water content depends on the ratio M/(P+B), P+B being the sum of the concentrations of phosphorus and boron oxides. As for the phosphate glasses investigated the water content of BaO-B<sub>2</sub>O<sub>3</sub>-P<sub>2</sub>O<sub>5</sub> glasses depends on the melting temperature, the melting time and on the rate of flow of water vapor through the melt. A study of the crystallization kinetic in borophosphate systems has been made. The degree of crystallinity has been determined in the glasses as a function of temperature and RO content in the interval 40-50 mol %. The observed phenomena have been explained in terms of the crystal nucleation theory for complex glasses. Since the glasses in the Ca and Sr borophosphate systems were produced in thin layers it was impossible to study their crystallization kinetics by development technique. Due to the above reason, the crystallization process was also studied by x-ray phase quantitative analysis. The estimation of the amount of the formed crystalline phase was carried out on the basis of the use of a standard (maximally crystallized at a given temperature of the sample) and data on both the magnitude of the integral intensity and the height of the diffraction peak determined for glasses at a certain scattering angle.

# **SURFACE ENERGY AT THE CRYSTAL NUCLEUS-GLASS INTERFACE, THE SIZE OF THE CRITICAL NUCLEUS OF CRYSTALS AND THE ENERGY BARRIER FOR THE FORMATION OF A STABLE CRYSTALLINE NUCLEUS IN ALKALI SILICATE GLASSES**

**Sycheva G.A.**

*Grebenshchikov Institute of Silicate Chemistry, Russian Academy of Sciences, 199034, St. Petersburg, nab. Makarova 2*

*sycheva\_galina@mail.ru*

The results of studying of the surface energy at the crystal nucleus-glass interface, the size of the critical nucleus of crystals and the energy barrier for the formation of a stable crystalline nucleus from the kinetics of homogeneous (spontaneous) and heterogeneous (catalyzed) crystal nucleation in silicate glass is presented for alkali silicate glasses. Nucleation is catalyzed via the photosensitive mechanism by adding poorly soluble impurities, shifting the glass composition towards the higher content of one of the components (autocatalysis), and by passing steam through the glass melt. The fundamental characteristics of crystal nucleation are obtained. The composition ranges with the maximum and minimum steady-state crystal nucleation rates are identified. There has been keen interest in the fundamental problems of crystal nucleation and growth in glass due to the development of new glass ceramic materials. The fabrication of these materials is based on the controlled crystallization of glass with tailored compositions, which would be impossible without knowing the general regularities of crystal nucleation and growth in glass. A quantitative description of the experiment is a major challenge when studying the homogeneous and heterogeneous crystal nucleation and amorphization and crystallization processes in glass. The key characteristics are the steady-state nucleation rate, the time of unsteady-state nucleation, and the temperature dependences of these parameters. By knowing the temperature dependence between the steady-state nucleation rates, we can control the crystallization process by exposing the glass samples to a temperature close to the maximum nucleation rate. In order to produce the glass crystalline material (photoceram glass), we need to keep the initial glass in the region where the steady state nucleation rate is maximum.

In this study, we investigated the surface energy at the crystal nucleus-glass interface, the size of the critical nucleus of crystals and the energy barrier for the formation of a stable crystalline nucleus from the kinetics of homogeneous (spontaneous) and heterogeneous (catalyzed) crystal nucleation in silicate glass is presented for alkali silicate glasses.

Glass was synthesized at 1450°C using lithium carbonate, hydrated and anhydrous silica, silver nitrate, and gold(III) chloride (all reagents were of pure for analysis grade). The melt was poured onto a monolithic metal plate. The composition of the synthesized glass is listed in Table 1. The castings were colorless and transparent. H<sub>2</sub>O was added to the composition of 26Li<sub>2</sub>O · 74SiO<sub>2</sub> glass (mol %) by bubbling with the vapor of distilled water for different time intervals. Chemical analysis showed three quantities of H<sub>2</sub>O: 0.05, 0.12, and 0.20 wt % above 100%. Glass with hollow bubbles was produced using anhydrous SiO<sub>2</sub> as the initial reagent. The use of hydrated SiO<sub>2</sub> (with the water contained in the initial reagent) resulted in the formation of bubbles within the minuscule water droplets inside. Photosensitive Ag and Au impurities were added to the lithium disilicate glass of stoichiometric composition using the sol-gel method.

The range of compositions (23.4–46.0 mol % Li<sub>2</sub>O) characterized by the maximum difference in the rates of the homogeneous and heterogeneous steady state nucleation is determined. The values of the energy barrier of nucleation that a crystal nucleus needs to overcome so that crystal nucleation could take place in glass were obtained for the first time.

# CRYSTAL GROWTH OF LARGE CZTS SINGLE CRYSTAL BY VERTICAL GRADIENT FREEZE

**Tablaoui M., Khelfane A., Ziane M.-I.**

*Centre de Recherche en Technologie des Semi-conducteurs pour l'Energétique (CRTSE), 02, Bd. Frantz FANON BP 140 Les 07 Merveilles, Algiers, Algeria*

*tablaouimeftah@yahoo.com*

CZTS compound is drawing attention for over a decade thanks to its interesting photovoltaic (PV) properties [1]. However, in PV applications it has not exceeded more than 13% efficiency. This is likely due to the grain boundaries in the thin film material. Furthermore, CZTS is being attractive for thermoelectric application (TE) because of its large band gap compared to conventional TE materials [2]. The TE efficiency depends on thermal and electrical conductivities and Seebeck coefficient. However, it is difficult to accurately measure these parameters on samples with voids or grain boundaries. Thus, we suppose that a single crystal is required. It is difficult to grow bulk CZTS single crystal from the melt as it exhibits melts incongruently and crystallizes through a peritectic reaction [3].

Herein, we report on the crystal growth of CZTS single crystal via Vertical Gradient Freeze Technique. We used a thermal gradient of about 18°C/cm (Fig.1\*, Left) to grow a large sized (up to 15 mm) CZTS single crystal. The external surface of the as-grown ingot was free of cracks, voids or grain boundaries (Fig.1, Medium). In this presentation, we will show that it is possible to grow CZTS single crystal from the melt with a very low cooling rate and a medium temperature gradient. The flat liquid-solid interface we got was favorable to obtain a large crystal (Fig.1\*, Right).

Figure 1\*. Left: Temperature profile with growth ampoule. Medium: Grown ingot. Right: View of a slice from the top of the ingot.

[1] Siebentritt, S. Schorr, S. Prog. Photovolt: Res. Appl, 2012. 64(a1), 59-60

[2] H. Yang, L. A. Jauregui, G. Zhang, Y. P. Chen, and Y. Wu, Nano letters 12, 540.

[3] I.D. Olekseyuk, I.V. Dudchak, L.V. Piskach, Journal of Alloys and Compounds, 368 (2004), 135–143.

**Acknowledgments:** This work was funded by the Research Center in Semiconductors Technology for Energies under the Algerian Directorate of Scientific Research and Technology carried out thanks to DGRSDT/MESRS (Algeria).

\*The abstract with figures is available at <http://2019.mgctf.ru/01000031a8.doc>

## THE CALCIUM CARBONATE CASE STUDY. FROM IONS TO THE AMORPHOUS PHASE. CLASSICAL OR NON-CLASSICAL NUCLEATION?

Testino A., Carino A., Mohammed A.S.A., Cervellino A.

*Paul Scherrer Institut*

*andrea.testino@psi.ch*

The formation mechanism of calcium carbonate from ions to amorphous calcium carbonate (ACC) in diluted solution was studied experimentally (in-situ) and computationally (using a thermodynamic-kinetic model). The thermodynamic model includes a complete speciation package; the kinetic mode is based on the discretized population balance approach and the classical nucleation theory.

The early stage of the precipitation pathway (i.e., before the critical conditions for ACC nucleation) was studied in-situ by Small-Angle X-ray Scattering (SAXS) at constant pH, T and saturation level, using a liquid jet setup. Undersaturated conditions were investigated as well. The data were modelled using parametric statistical models providing insight about the size distribution of denser matter in the liquid jet. The experimental results are consistent with the presence of a broad size distribution of entities (superclusters) with variable density and highly hydrated, which were postulated by previous computational model. Simultaneously, a population of clusters of about 2 nm, identified in literature using cryoTEM and analytical ultracentrifugation, were qualitatively detected and are mainly aggregate in the superclusters.

Analytical equipment were used to collect the experimental data of the overall process, applying the controlled composition approach, up to the ACC formation. At the critical saturation conditions, primary and secondary nucleation events occur and the experimental results are consistent with a grow model limited by the diffusion of calcium and carbonate ions. Therefore, clusters act as spectator species in the growth process.

The experiments and computational results indicate specific features that can addressed to both the classical and the non-classical formation pathway. These two views of the solid formation mechanism are often associated to a well-defined landscape of the Gibbs free energy vs. embryo/nucleolus size, which –in the non-classical view– admits more than one point where its derivative is zero, e.g. at least a minimum before the critical size.

Our results demonstrated that the saturation level largely influence the nature of the denser matter before the nucleation events. Therefore, the Gibbs free energy cannot be represented as a 2D plot and the fundamental definition of what is “non-classical” should be reconsidered. Moreover, the equations associated to the classical nucleation theory are unaffected by undercritical events and they can still be used to estimate the nucleation rate, even if a population of clusters exist.

## SYNTHESIS OF COMPLEX HYDROSULPHATES OF SINGLY CHARGED CATIONS

**Timakov I.S., Grebenev V.V., Komornikov V.A., Zainullin O.B., Selezneva E.V.**

*Federal Scientific Research Centre "Crystallography and Photonics" of Russian Academy of Sciences*

*selos93@mail.ru*

A large number of acidic salts of singly charged cations are promising protonic conductors and attract the attention of researchers along with other ion-conducting compounds. The effect of abnormally high proton conductivity was first discovered at the Institute of Crystallography in the study of proton transport processes in CsHSO<sub>4</sub> and CsHSeO<sub>4</sub> crystals [1]. This group includes compounds with the general formula  $M_mH_n(AO_4)_{(m+n)/2} \cdot xH_2O$  ( $M = K, Rb, Cs, NH_4$ ;  $A = S, Se, P, As$ ). Their distinctive feature is structural phase transitions at elevated temperatures before melting. During the phase transition, the conductivity values  $\sigma$  in these crystals significantly increase and reach values comparable to the conductivity in the melt, while the compound itself remains solid according to the state of aggregation.

The combination of the properties of high proton conductivity ( $\sigma \approx 10^{-3} \Omega^{-1}cm^{-1}$ ) in a solid state of aggregation at moderate temperatures (140–230°C) makes these compounds attractive for use, for example, as fuel cell membranes [2, 3].

To obtain new compounds belonging to the  $M_mH_n(AO_4)_{(m+n)/2} \cdot xH_2O$  family, we studied the phase equilibria in the quaternary water–salt system  $K_2SO_4 - Rb_2SO_4 - H_2SO_4 - H_2O$ , which was not investigated previously. The conditions for obtaining large single crystals of complex hydrosulfates are determined.

The results obtained allowed us to present a phase equilibrium diagram for these conditions. Single crystals of solid solutions with the general formulas  $(K_xRb_{(1-x)})_9H_7(SO_4)_8$ ,  $(K_xRb_{(1-x)})_3H(SO_4)_2$  and  $(K_xRb_{(1-x)})_2SO_4$  were obtained. In addition, the obtained single crystals of solid solutions of the  $K_3H(SO_4)_2 - Rb_3H(SO_4)_2$  series were investigated by the methods of differential scanning calorimetry and thermogravimetric analysis.

The work was supported by the Ministry of Science and Higher Education within the State assignment FSRC "Crystallography and Photonics" RAS.

[1] A. I. Baranov, L. A. Shuvalov, and N. M. Shchagina, JETP Lett. 36(11), 459 (1982);

[2] T. Norby, Nature 410, 877 (2001);

[3] R. Fitzgerald. Phys. Today 54, 22 (2001).

# DIFFERENT MORPHOLOGIES OF SILICOALUMINOPHOSPHATE SAPO-11: EXPERIMENT AND THEORY

**Tiuliukova I.A.<sup>1</sup>, Parkhomchuk E.V.<sup>1,2</sup>**

*1 - Boreskov Institute of Catalysis SB RAS, Novosibirsk, Russia*

*2 - Novosibirsk State University, Novosibirsk, Russia*

*i.tiuliukova@gmail.com*

SAPO-11 is a silicoaluminophosphate molecular sieve, one of the structures of the important zeolite-like materials. It is used as an acid catalyst in a selective skeletal isomerization process of paraffins and olefins. Catalytic and adsorption properties are determined by the size, morphology, and texture of crystals, which in turn depend on the way of material preparation. SAPO-11 structure is usually obtained by hydrothermal synthesis (HTS) in an aqueous medium at 200°C for 24 hours and typically represents spherical aggregates of 5-20 micrometers consisting of small crystallites. However, some curious changes in the crystal morphology and porosity are observed when the reaction medium type changes.

To study the evolution of morphological and textural properties the following media were used for HTS: water, the equimolar mixture of water and ethanol, ethanol. Precursor suspensions of aluminum isopropoxide, orthophosphorous acid, dipropylamine and amorphous SiO<sub>2</sub> were transferred into a stainless steel autoclave to undergo the HTS. Conventional hydrothermal crystallization at 200 °C for 24 h in ethanol medium doesn't result in SAPO – 11 phase, but non-porous aluminium phosphate in the form of β-cristobalite was obtained, the required phase was not formed even during the prolonged period for 160 hours. We succeeded in producing SAPO-11 crystals in ethanol medium only by the two-stage hydrothermal approach, which implied the separation of nucleation and crystal growth stages. The first crystallization stage lasted for 3 hours (5 hours in the presence of ethanol) at 200°C. The second stage proceeded at 120 °C for the various time from 24 to 160 hours. These results may indicate the higher nucleation energy of β-cristobalite AlPO<sub>4</sub> in ethanol medium compared to that one of SAPO-11.

SAPO-11 crystals, synthesized in the ethanol medium, have previously unobservable screw-like morphology compared to crystals, synthesized in water medium (see the authors' publication: Tiuliukova I.A., et.al. Screw-like morphology of silicoaluminophosphate-11 (SAPO-11) crystallized in ethanol medium // *Mater. Lett.* 2018. V. 228. P. 61–64). Possibly, these screw-like crystals result from special non-classical crystal growth, realized through the aggregation and the oriented attachment of particles into an iso-oriented crystal with further formation a single crystal upon the fusion of nanoparticles. As a result of direct aggregation, these crystals have a well-defined hexagonal shape in the middle of the crystal. Most likely, plate-like nanocrystals composing the crystal were formed by the sorption of ethanol molecules on the particular crystal face of growing crystallites that do not allow the crystallites to develop along one of growth directions. This effect was observed by using other organic additives in literature for metal-substituted microporous aluminophosphate – MeAlPO-5.

The work was financially supported by the Ministry of Education and Science of the Russian Federation (RFMEFI60417X0159, the title of the agreement: "Development of methods for hydrotreating of vacuum residue into high-quality marine fuels on macroporous catalysts"), the presentation is supported by PJSC Gaz-prom Neft project.



# ORIENTED GROWTH OF BaSrTiO<sub>3</sub> THIN FILMS ON SEMI-INSULATING SILICON CARBIDE

**Tumarkin A., Odinets A., Zlygostov M.**

*Electrotechnical University "LETI"*

*avtumarkin@yandex.ru*

Ferroelectric (FE) films in a paraelectric state have received much attention as promising materials for the development of voltage controlled microwave (MW) tunable devices due to their high dielectric non-linearity. The most extensively studied ferroelectric (FE) materials for the use at microwave frequencies are solid solutions of barium and strontium titanates Ba<sub>x</sub>Sr<sub>1-x</sub>TiO<sub>3</sub> (BST) because of the good combination of high tunability and low MW losses. One of the main parameters of MW devices is power handling capability (PHC) i.e. the capability to process the high power MW signal without the deviation of working parameters. The total deviation generally can be divided to the electrical effect and the overheating due to the dissipation of MW power. The problem of the overheating of the FE MW elements is partially caused by the poor thermal conductivity of the dielectric substrate. So, the usage of the silicon carbide (SiC) substrate with high thermal conductivity as a heat sink can effectively improve PHC of FE MW devices.

Therefore, our study aims to carry out investigation of the structural properties of BST films on semi-insulating SiC substrates prepared by the multi-step RF deposition technique with an intermediate annealing (IA) of the layers at a temperature higher than that of growth. This approach allows us to correct defects of the crystal lattice during the film growth. Thus, we expect that it would improve the crystallinity of a film, opening up a practical application of BST/SiC heterostructures in high-power nonlinear elements operating in the microwave range.

Thin BST films on SiC substrates were obtained by RF magnetron sputtering of a ceramic target with Ba<sub>0.4</sub>Sr<sub>0.6</sub>TiO<sub>3</sub> composition. The phase composition of obtained BST films was studied by X-ray diffraction (XRD). The microstructure and surface morphology were studied by atomic force microscopy. The component composition of the BST films was evaluated using the medium energy ion scattering method.

According to XRD analysis, the multi-layer BST thin film structured by IA shows highly (h00) oriented perovskite structure while the single-layer film is polycrystalline. The difference in crystal lattice between the multi-layer and the single-layer BST film can be explained by the fact that during the intermediate annealing, the density of flux of sputtered atoms is radically changed, supersaturation is decreased, and, therefore, a growth mechanism of a film is varied. In this case, the flow of matter is formally transformed from the category of a strong source to the category of a weak one. Thus, with the weak source, under conditions close to equilibrium, the film will be more oriented. Moreover, the each annealed layer begins to play the role of a new substrate heated to a temperature that higher than the deposition one. In this case, there are two reasons for the oriented growth: the low supersaturation and the absence of an interphase energy barrier, since the new layer is formed on its own material.

So, the usage of an intermediate annealing at a temperature higher than that of growth, allows us to decrease the strength of source of deposited atoms during the formation of the layers and create the conditions for the oriented nucleation and growth of each new layer. This approach makes the film more ordered and less defective, hence promising better electrical characteristics.

This work was supported by the RFBR projects 16-29-05147, 18-37-00348 and the Ministry of Education and Science of the Russian Federation (3.3990.2017/4.6).

# GLYCINE-NITRATE SYNTHESIS OF CRYSTAL SOLID SOLUTIONS OF BARIUM-STRONTIUM TITANATE

Belysheva D.N.<sup>1</sup>, Sviridov S.I.<sup>1</sup>, Sinelshchikova O.Y.<sup>1</sup>, Tumarkin A.V.<sup>2</sup>, Tyurnina N.G.<sup>1</sup>,  
Tyurnina Z.G.<sup>1</sup>

1 - Institute of Silicate Chemistry  
2 - Electrotechnical University "LETI"

avtumarkin@yandex.ru

Barium-strontium titanate is a crystal electroceramic material that has ferroelectric and piezoelectric properties. Today, there are both industrial and laboratory methods for its production. Most low-temperature methods are associated with deposition and hydration processes and require additional high-temperature treatment to form the perovskite crystal structure and decomposition of precursors.

Currently, there is an increased interest in multiferroics – composite materials, including glass-based, combining ferroelectric and ferromagnetic properties. The relevance of the development of methods for the synthesis of BaTiO<sub>3</sub> and its solid solutions by burning organo-salt compositions is due to the fact that their use can significantly reduce the temperature and duration of temperature treatment, and the original compositions can be used to impregnate a porous ferromagnetic glass matrix to form a multiferroic material.

The aim of this work was to determine the optimal parameters of synthesis of crystal solid solutions of barium-strontium titanate by the method of combustion of glycine-nitrate compositions for future development of glass-ceramic composite multiferroic materials.

Preparation of the initial mixtures was carried out on the basis of hydrated titanium dioxide, the required amount of which was dissolved in 1.4M nitric acid solution to form a solution of TiO(NO<sub>3</sub>)<sub>2</sub>. Aqueous solutions of nitrates or barium and strontium acetates were introduced into the resulting solution of titanium-nitrate in accordance with the stoichiometry of the resulting complex oxide, as well as glycine. The ratio of Ba<sub>1-x</sub>Sr<sub>x</sub>TiO<sub>3</sub> : C<sub>2</sub>H<sub>5</sub>NO<sub>2</sub> was chosen based on the equations of redox reactions and varied in the range from 0.9 to 2.4. The phase composition of obtained barium-strontium titanate samples was studied by X-ray diffraction (XRD).

According to the XRD, during the calcination of glycine-nitrate compositions in the temperature range 550-650°C, the formation of nanocrystalline barium-strontium titanate occurs, as well as a small number of undecayed impurities were found, the presence of which depended on the nature of the combustion of the obtained gels. According to the results of a comprehensive thermal analysis, the combustion process of all glycine-nitrate compositions begins at 180°C and, depending on the glycine content, has a different character, either volumetric combustion or self-propagating synthesis. The optimal condition for the formation of single-phase products in this case is the volumetric combustion mode, in which the firing at 550°C allows to obtain single-phase nanoscale powders of solid solutions Ba<sub>1-x</sub>Sr<sub>x</sub>TiO<sub>3</sub> (0 ≤ x ≤ 0.4).

Thus, we can assume that the developed method of synthesis is suitable for impregnation of porous glass materials in order to form barium-strontium titanate crystal nanoparticles in the pore space and on the surface of ferromagnetic glass matrices.

This work was supported by the RFBR project 19-07-00600.

# GROWTH OF HIGH-PERFECT MIXED COBALT NICKEL POTASSIUM SULFATE HEXAHYDRATE CRYSTALS BY THE TEMPERATURE DIFFERENCE TECHNIQUE WITH CONTINUOUS SOLUTION FEEDING

**Vasilyeva N.A.<sup>1</sup>, Rudneva E.B.<sup>1</sup>, Manomenova V.L.<sup>1</sup>, Masalov V.M.<sup>2</sup>, Zhokhov A.A.<sup>2</sup>,  
Emelchenko G.A.<sup>2</sup>, Voloshin A.E.<sup>1</sup>**

*1 - Shubnikov Institute of Crystallography, FSRC "Crystallography and Photonics", Russian Academy of Sciences*

*2 - Institute of Solid State Physics, Russian Academy of Sciences*

*Natalie5590@mail.ru*

The material based on the mixed  $K_2Ni_xCo_{(1-x)}(SO_4)_2 \cdot 6H_2O$  crystal is promising for solar-blind technology devices [1, 2]. Its use as flame sensors and corona discharge will improve the quality and performance characteristics of devices by an order of magnitude. However, due to the distribution coefficients of the isomorphous components are different for different face growth sectors, mixed  $K_2Ni_xCo_{(1-x)}(SO_4)_2 \cdot 6H_2O$  crystals are characterized by an increased composition inhomogeneity compared to single-component crystals [3]. This circumstance does not allow to obtain the crystals of high optical quality, suitable for practical use as UV optical filters, by the standard growth method for water-soluble crystals - by the cooling solution technique.

The report describes the growth method of high structural perfection mixed  $K_2Ni_xCo_{(1-x)}(SO_4)_2 \cdot 6H_2O$  crystals by the temperature difference technique with continuous solution feeding. In order to eliminate sectorial inhomogeneity, the mixed  $K_2Ni_xCo_{(1-x)}(SO_4)_2 \cdot 6H_2O$  crystals were grown in cylindrical shapers. To eliminate the zonal inhomogeneity of the crystals, the feeding of mother liquor was calculated and implemented, taking into account the change in the solution composition both in the stationary growth mode due to different distribution coefficients of isomorphous components and due to formation of the diffusion boundary layer in the initial transient. The crystal growth rate was determined by the initial value of the solution supercooling and the feeding rate.

The real structure of mixed  $K_2Ni_xCo_{(1-x)}(SO_4)_2 \cdot 6H_2O$  crystals grown by the temperature difference technique with continuous solution feeding in shapers was studied by X-ray topography. It was found that such crystals do not contain inclusions and dislocations, do not have noticeable internal stresses.

The transmission spectra of the obtained  $K_2Ni_xCo_{(1-x)}(SO_4)_2 \cdot 6H_2O$  mixed crystals were studied. All samples have high (85 - 87%) transmission in the UV region, peaks in the visible region are almost absent, and the peaks in the IR region do not exceed 10%. This makes it possible to successfully use  $K_2Ni_xCo_{(1-x)}(SO_4)_2 \cdot 6H_2O$  crystals as zone optical filters. Optical elements with a diameter of 20 mm and a thickness of 10 mm were made from the grown crystals.

The work has been supported by the Russian Science Foundation (project No. 15-12-00030).

1. N. A. Vasil'eva, M. S. Grigor'eva, V. V. Grebenev, and A. E. Voloshin, *Crystallogr. Rep.* 58 (4), 646 (2013).
2. Zhuang X., Genbo S., Youping H., Zheng G. *Cryst. Res. Technol.*, 41 (10), 1031 (2006)
3. N. A. Vasilyeva, D. S. Nuzhdin, M. A. Faddeev, V. V. Grebenev, V. A. Lykov, A. E. Voloshin, *Crystallogr. Rep.* 61 (2), 304 (2016).

# THE PROBLEM OF GROWING MIXED CRYSTALS AND HIGH-EFFICIENCY $K_2(\text{Co, Ni})(\text{SO}_4)_2 \cdot 6\text{H}_2\text{O}$ OPTICAL FILTERS

**Voloshin A.E.<sup>1</sup>, Rudneva E.B.<sup>1</sup>, Manomenova V.L.<sup>1</sup>, Vasilyeva N.A.<sup>1</sup>, Kovalev S.I.<sup>1</sup>,  
Grigorieva M.S.<sup>1</sup>, Emelchenko G.A.<sup>2</sup>, Masalov V.M.<sup>2</sup>, Zhokhov A.A.<sup>2</sup>**

*1 - Shubnikov Institute of Crystallography, FSRC «Crystallography and Photonics» RAS*

*2 - Institute of Solid State Physics RAS*

*voloshin@crys.ras.ru*

The growth of mixed crystals from solutions until today has met irresistible difficulties due to their catastrophic defect structure. For this reason, so far there have been no examples of their use for practical purposes. A systematic study of the mechanisms of defect formation in such crystals that we have carried out allowed us to solve this problem for the first time and to develop a fundamental approach to obtaining perfect mixed crystals from water solutions.

In a three-component system (water and two salts) under  $P, T = \text{const}$ , there is a continuous series of saturated solutions and crystals equilibrium to them. In the case of contact of a crystal with a solution whose composition is not in equilibrium with the crystal composition, complicated processes begin to occur on the crystal surface, leading to an intense generation of defects. The other, more obvious problems of growing mixed crystals are associated with their strong zonal and sectorial heterogeneity and, as a result, a high level of internal stresses, the presence of cracks, a large number of inclusions.

As a result of the studies, the general mechanism of the interaction of a crystal with a non-equilibrium to it solution of isomorphous salt components (an isomorphous substitution reaction) was determined, which results in transforming the crystal surface into a mosaic of local areas where multidirectional processes (the dissolution and the growth) occur simultaneously. An analytical description of the process is given; it is shown that it can be suppressed by creating a certain additional supercooling in the system [1, 2]. A new type of composition inhomogeneity, mosaic micro-inhomogeneity, was investigated. A new mechanism for mismatch stresses relaxation in heterostructures of brittle crystals obtained from low temperature solution, when formation of mismatch dislocations is impossible, is found: in this case, stress relaxation occurs due to the formation of numerous inclusions at the interface, the probability of their formation decreases as the mismatch decreases [3]. Optical filters transparent in the wavelength range of 200 - 300 nm are key elements of the devices for solar-blind technology. Crystals of simple and complex sulfates of nickel and cobalt, traditionally used for this purpose, have parasitic transmission peaks in the visible region that significantly reduces the efficiency of radiation filtering. Therefore, the creation of an optical filter based on a solid solution of nickel and cobalt salts, which mutually absorb the parasitic peaks of each other, was of great practical interest.

Crystals  $(\text{Co, Ni})K_2(\text{SO}_4)_2 \cdot 6\text{H}_2\text{O}$  were chosen as objects for the study. As a result of comprehensive studies, the general concept of growing mixed crystals of high structural perfection from solutions was formulated and implemented [4]: 1) the growth in the shapers to eliminate sectorial inhomogeneity; 2) feeding the solution according to a special law to eliminate the initial transient region; 3) growth at a constant temperature to reduce zonal inhomogeneity and under supercooling sufficient to suppress exchange processes in the system.

The  $K_2\text{Co}_x\text{Ni}_{(1-x)}(\text{SO}_4)_2 \cdot 6\text{H}_2\text{O}$  crystals of high structural perfection, having optimal optical and mechanical properties and thermal stability 15 ° C higher than the crystals of the individual components, have been grown. The optical filters from these crystals perform UV transmission comparable to that of an  $\alpha\text{-NiSO}_4 \cdot 6\text{H}_2\text{O}$  crystal (~ 87%) that indicates the absence of the scattering centers, while transmission in the visible range is suppressed by an order of magnitude.

The work was supported by the grant of Russian Science Foundation No. 15-12-00030 in part of the development of  $K_2\text{Co}_x\text{Ni}_{(1-x)}(\text{SO}_4)_2 \cdot 6\text{H}_2\text{O}$  optical filters; the study of the crystal structure was carried out with the support of Ministry of Science and Higher Education of Russian Federation in the framework of the State Task of FNITS " Crystallography and photonics " RAS.

[1] A.E. Glikin, S.I. Kovalev, E.B. Rudneva et al. *J. Cryst. Growth.* **255** (2003) 150.

[2] A.E. Voloshin, S.I. Kovalev, E.B. Rudneva, A.E. Glikin. *J. Cryst. Growth.* **261** (2004) 105.

[3] M.S. Grigor'eva, A.E. Voloshin, E.B. Rudneva et al. *Crystallography Reports* **54** (2009) 637.

[4] A.E. Voloshin, V.L. Manomenova, E.B. Rudneva et al. *J. Cryst. Growth,* **500** (2018) 98.

## A MATHEMATICAL MODEL OF FINITE-SIZE EFFECTS IN THIN FILM CRYSTALLIZATION

Kozyukhin S.<sup>1</sup>, Vorobyov Y.<sup>2</sup>, Lazarenko P.<sup>3</sup>, Sybina Yu.<sup>3</sup>, Ermachikhin A.<sup>2</sup>, Sherchenkov A.<sup>3</sup>

1 - Kurnakov Institute of General and Inorganic Chemistry, RAS, 119991 Moscow, Russia

2 - Ryazan State Radio Engineering University, 390005 Ryazan, Russia

3 - National Research University of Electronic Technology, 124498 Zelenograd, Russia

*vorobjov.y.v@rsreu.ru*

Phase change materials, in particular,  $\text{Ge}_2\text{Sb}_2\text{Te}_5$ , are the basis for one of the most promising memory technologies—phase change memory, or PCM. In PCM information is stored in the form of phase state of a phase change material. Two states of active material, crystalline and non-crystalline, possess strikingly different electrical and optical properties making phase change materials perfectly suitable for binary storage of information. Moreover, partial crystallization of the active volume inside a memory cell leads to the formation of an intermediate state of the latter. Thus, it is possible to achieve the multi-bit storage of information in PCM.

Two processes govern the functioning of a PCM device—crystallization and reverse one, amorphization. The latter is performed through the process of melt quenching, thus forming the vitreous state of a phase change material. Both processes occur due to local heating, but the melt quenching is very fast and can take less than ten nanoseconds to complete in phase change materials. Crystallization, on the contrary, is a remarkably time-consuming process involving processes of nucleation and growth. In connection with the necessity of long heating stimulation, this makes crystallization also the most energy-consuming procedure in PCM.

In order to facilitate the development of PCM devices, an adequate mathematical model of the crystallization process in a memory cell is essential. Generally, the Kolmogorov-Johnson-Mehl-Avrami (KJMA) model is widely used. However, the finite-size effects attributed to the small volume of a memory cell are often out of consideration thus violating the original KJMA model assumptions. The more complicated crystallization behavior of finite-size systems, in particular, the possibility of heterogeneous nucleation at the boundaries, leads to the non-uniform distribution of the crystalline fraction over the system volume. The abovementioned non-uniformity inside a memory cell, in turn, will determine the value of its electrical resistance.

The purpose of this study is to reveal the finite-size effects that film geometry introduce into the crystallization process of the film material.

On the basis of the KJMA approach, a mathematical model for the thin film crystallization was developed. Two nucleation mechanisms are involved in the model. First, homogeneous nucleation is described by emerging of spherical crystallization centers inside the film. Second, the heterogeneous nucleation on the film boundaries is taken into account using the simple spherical-cap model. Exact close form solutions were obtained for some simple steady-state cases.

Calculations show that in the case of homogeneous nucleation the film boundaries inhibit crystallization process in the near surface layers. Crystallization by means of the heterogeneous nucleation, producing the opposing influence, is an apparently two-stage process. Initially, the nucleation dominates but since the surface is fully covered by the crystalline phase only the growth of previously emerged crystalline grains comprises the crystallization process.

### **Acknowledgements**

Yu.V. acknowledges the support of Russian Foundation for Basic Research and Ministry of Industry and Economic Development of Ryazan Region (grant № 18-42-623003). P.L. thanks RFBR (project № 18-33-20237\18).

# FORMATION MECHANISMS OF HEMATITE CONCAVE NANOCUBES

Wang Z.

*College of Chemistry and Chemical Engineering, Xiamen University, Xiamen, China*

*zawang@xmu.edu.cn*

Nanocrystals (NCs) enclosed by high energy facets have attracted much attention due to their high activities in many processes such as heterogeneous catalysis, energy conversion, and gas sensing. However, the surfaces with high energy are thermodynamically unstable and usually disappear during the growth of NCs. Therefore, it is a big challenge to synthesize NCs with high-index facets. In most cases, these NCs are polyhedra encased by convex surfaces. Despite great successes having been achieved in the synthesis of NCs with convex surfaces, the synthesis of NCs with concave surfaces, however, is still in an embryonic stage which may draw more attention since the concave structures are expected to show unexplored or substantially enhanced properties relative to their convex counterparts. There has few report on concave metal oxides except for  $\text{Cu}_2\text{O}$ . It should be pointed out that  $\text{Cu}_2\text{O}$ , as well as noble metals, are all in cubic systems, and the fabrication of other concave metal oxides that do not crystallize in cubic crystalline systems is still limited. Hematite ( $\alpha\text{-Fe}_2\text{O}_3$ ), as an important n-type semiconductor with a band gap of 2.2 eV, has been widely used in catalysis and sensors. To date, the synthesis of  $\alpha\text{-Fe}_2\text{O}_3$  NCs with high-index facets exposed still remains a big challenge. Here, we report a simple copper ion-assisted hydrothermal route based on kinetically controlled overgrowth to the synthesis of  $\alpha\text{-Fe}_2\text{O}_3$  concave ‘nanocubes’ bound by high-index {1344} and {1238} facets. Different from noble metals and some metal oxides (e.g.  $\text{Cu}_2\text{O}$ ) with cubic crystalline systems,  $\alpha\text{-Fe}_2\text{O}_3$  belongs to the trigonal system, thus the exposed high-index facets of concave nanocubes are very special.

Fig. 1\*(a) TEM images recorded at different tilting angles and (b) the corresponding geometric models of a hematite concave nanocube. (c) TEM image of an individual hematite concave nanocube, (d) corresponding SAED pattern and (e) HRTEM image of the region indicated by the square in (c).

In a typical synthesis of concave nanocubes, a mixture of  $\text{Fe}(\text{NO}_3)_3$ , cupric acetate ( $\text{CuOAc}_2$ ), and ammonium hydroxide was kept at 140 °C under hydrothermal conditions for 16 h. Fig. 1a shows the TEM images obtained from a single concave nanocube at different tilting angles. Deep dents on the surfaces of the nanocubes can be clearly observed, supporting the formation of a concave rather than a flat surface on each lateral face. The images observed are also consistent with the proposed geometric models (Fig. 1b). Fig. 1c shows a high resolution TEM image of an individual concave nanocube viewed along the [2201] direction, as conformed by the corresponding selected area electron diffraction (SAED) pattern (Fig. 1d). It can be seen that eight lateral facets of the concave nanocube were projected edge-on. For rhombohedral hematite structures, if a crystal facet of the concave nanocube is already given, then the Miller indices of its adjacent crystal facets can be derived from the projection angles along a selected crystallographic axis. By comparing the measured and calculated values of projected angles, the eight edge-on facets can be indexed as {1344} and {1238} planes. The high resolution TEM (HRTEM) image of an edge of an individual concave nanocube is shown in Fig. 1e. The lattice spacing was measured to be 0.37 nm, which is in agreement with the {0112} lattice spacing of rhombohedral hematite, indicating the single crystalline nature of the as-obtained product.

Fig. 2\* SEM images of the nanocrystals collected at different reaction times: (a) 1 h, (b) 2 h, (c) 6 h, (d) 10 h, and (e) 16 h. Scale bars: 200 nm. (f) Schematic diagram of the kinetically controlled overgrowth (when  $V_2$  is much larger than  $V_1$ ) of concave nanocubes evolved from pseudonanocubes.

To gain insight into the details of morphological evolution during the growth of the  $\alpha\text{-Fe}_2\text{O}_3$  concave nanocubes, time-dependent experiments were carried out (Fig. 2\*). In the first 6 h, the transformation of dense aggregates of primary nanoparticles into nanocubes can be attributed to <...>\*

\*The full abstract with figures is available at <http://2019.mgctf.ru/01000030f3.doc>

# FINITE SIZE AND PROXIMITY EFFECTS IN ULTRA THIN EPITAXIAL TRANSITION METAL SUPERLATTICES

Wolff M.

*Uppsala University*

*max.wolff@physics.uu.se*

The similarities in lattice parameter and crystal structure of iron, chromium and vanadium allows the growth of epitaxial single crystalline thin films on MgO substrates with exceptional quality. However, usually epitaxial growth is limited by strain relaxation at a critical thickness resulting in an increasing number of defects. In this talk I will show how this limitation is overcome by combining iron or chromium and vanadium layers with a certain thickness ratio to minimise the internal strain in the layered structure. The well defined and carefully controlled strain in the resulting superlattices allows the investigation of finite size and proximity effects. While iron is magnetic, vanadium has the tendency to absorb hydrogen, which opens the opportunity to study thermodynamics and kinetics in ultra thin films. I will show the finite size scaling of the critical point in the vanadium-hydride phase diagram down to the monolayer limit. Additionally, the influence of strain on the diffusivity in ultra thin vanadium layers will be discussed as well as proximity effects when replacing the iron layers by chromium.

## RELATIONSHIP OF Mg<sub>2</sub>Si PHASE-CONTENT AND THERMAL EXPANTION PROPERTIES OF Mg-Si AND Mg-Si-Ca ALLOYS

**Wu Sh., Guo T., An P., Zhou X., Lü Sh.**

*State Key Laboratory of Materials Processing and Die & Mould Technology, Huazhong University of Science and Technology, Wuhan 430074, China*

*ssw636@hust.edu.cn*

The thermal expansion properties of Mg- $x$ Si ( $x = 1$  wt.%, 1.38 wt.%, 2 wt.%, 3 wt.%, and 4 wt.%) binary alloys and Mg-4Si- $y$ Ca ( $y = 0.2$  wt.%, 0.4 wt.%, 0.6 wt.%, 0.8 wt.%, and 1.0 wt.%) alloys over the temperature range of 25–300 °C were systematically studied. The results show that the Mg-Si binary alloys, which solidified under normal gravity casting conditions, consisted of  $\alpha$ -Mg and Mg<sub>2</sub>Si phases. The volume fraction of Mg<sub>2</sub>Si phase increases with the increase of Si content in Mg-Si alloys, from 30.72% to 46.50% when Si content increases from 1 wt.% Si to 4wt.% Si. The thermal expansion coefficients of the alloys have very close relationship with the volume fraction of Mg<sub>2</sub>Si phase in the alloys. The thermal expansion coefficient of Mg- $x$ Si binary alloys decreases with the increase of Mg<sub>2</sub>Si volume fraction. The addition of Ca element to Mg-4Si alloys has an obvious modification effect on the Mg<sub>2</sub>Si phase. When the Ca content increases constantly, the thermal expansion coefficient of the Mg-4Si-Ca alloys increases at first, then it continues to decline. The mechanism is mainly related to the precipitation of the CaMgSi phase.



# MOLECULAR DYNAMICS SIMULATION OF Ti CRYSTAL GROWTH PROCESS WITH CRYSTAL-LIQUID CONFIGURATION METHOD

Yang X.

*Huazhong University of Science and Technology*

*yangxinh@hust.edu.cn*

The computation models were created with the crystal-liquid configuration method. They were divided into three parts: upper, middle and lower. The upper and lower parts are liquid but the middle one is crystalline, hexagonal close packed (HCP) or face-centered cubic (FCC). The molecular dynamics simulations with the embedded atom potential were performed to exhibit the whole Ti crystal growth process in the models. It includes two steps. The first step is the relaxation process in the NVT ensemble and the second step is the crystal growth process in the NPT ensemble. In the simulation, the atomic energy variation and configuration evolution were tracked, and both the average atomic energy and pair correlation function were recorded.

The following conclusions can be obtained.

- (1) The Ti atoms in the middle part crystallize gradually from the two solid-liquid interfaces to the center of the model until the upper and lower interfaces shake hands. Compared with the HCP model, the FCC model has a greater crystal growth velocity.
- (2) The variation of average atomic energy can be divided into three stages. When the temperature falls, the atomic energy sharply decreases in the first stage, slowly decreases in the second stage, but finally enters a steady state after a sudden drop in the third stage. They correspond to initiation, development and termination of Ti crystal growth, respectively.
- (3) With time elapsing, all the peaks of the pair correlation curves increase remarkably, and some new peaks take place, which is obviously an important crystal character.

**Acknowledgment:** This work was supported by the National Natural Science Foundation of China (Grant numbers: 11572135 and 11772137).

# INFLUENCE OF PREFORMED NUCLEI ON CRYSTAL NUCLEATION KINETICS IN SODA-LIME-SILICA GLASS

Yuritsyn N.S.

*Grebenshchikov Institute of Silicate Chemistry, Russian Academy of Sciences 199034, St.Petersburg, nab. Makarova 2*

*yuritsyn@gmail.ru*

An unusual stepped form of the time-dependence of the number  $N(t_n)$  of crystals nucleated at a temperature  $T_n$  was obtained for a soda–lime–silica glass of the composition  $22.4\text{Na}_2\text{O}\cdot 28.0\text{CaO}\cdot 49.6\text{SiO}_2$ , mol.%. The crystals were solid solutions based on the  $\text{Na}_2\text{O}\cdot 2\text{CaO}\cdot 3\text{SiO}_2$  compound. The investigation of the nucleation kinetics was performed for nucleation temperatures  $T_n = 500$  and  $515^\circ\text{C}$  located well below the glass transition temperature  $T_g = 540^\circ\text{C}$  and the temperature of the maximum of the steady-state crystal nucleation rate  $T_{\max} = 571^\circ\text{C}$ .

To determine the number of nucleated crystals, the development method was used. After heat treatment of the samples for various periods of time at the nucleation temperature  $T_n$ , an additional short heat treatment was carried out at a temperature  $T_d > T_n$ , at which the crystal nuclei were grown to the size visible in an optical microscope. It is usually assumed that crystal nuclei are practically absent in the initial glass and their formation occurs at  $T_n$ . However, in the synthesis of glasses with high steady-state nucleation rates, when a melt of glass cools in the glass transition range, a noticeable amount of crystal nuclei can form. We call them preformed nuclei (pf-nuclei). They form the size distribution  $n_{\text{pf}}(g)$ . At low nucleation temperatures  $T_n < T_{\max}$  pf-nuclei can significantly change the shape of the curve  $N(t_n)$  [1].

It was established that already at  $t_n = 0$ , after development of the initial sample at  $T_d$ , a significant number of crystals were observed. These crystals grew from the nuclei of the distribution  $n_{\text{pf}}(g)$ , the size of which exceeded the critical size  $g_d^*$ , corresponding to the temperature  $T_d$ . With an increase in the time of heat treatment at  $T_n$ , after the development of samples at  $T_d$ , an increase in the number of crystals was observed in the  $N(t_n)$  dependence. This growth is explained by the growth of nuclei of crystals  $n_{\text{pf}}(g)$  at  $T_n$  from the size range  $g_n^* - g_d^*$  ( $g_n^*$  is the critical size of the nucleus at the temperature  $T_n$ ) to a size exceeding  $g_d^*$ . We note that almost all pf-nuclei with sizes  $g < g_n^*$  at a temperature  $T_n$  dissolve. After all the pf-nuclei from the interval  $g_n^* - g_d^*$  exceeded the size of  $g_d^*$  at time  $t_{\text{ns}}$ , the dependence  $N(t_n)$  showed the saturation level  $N_s$  of the pf-crystals. The dependence  $N(t_n)$  for a short time interval remained constant,  $N_s$ . With a subsequent increase in the heat treatment time  $t_n$ , an increase in the number of crystals was observed due to usual crystal nucleation in glass at temperature  $T_n$ . The induction period of nucleation of such crystals at low temperatures is large, greater than  $t_{\text{ns}}$ . As a result, it was possible to clearly observe the stepped form of the  $N(t_n)$  dependence due to pf-nuclei.

The appearance of a step on the dependence  $N(t_n)$  was clearly observed when the maximum number of crystals in the experiment  $N_{\max}$  after the maximum duration of nucleation heat treatment did not greatly exceed  $N_s$ . This situation is typical for temperatures significantly lower than  $T_{\max}$ , at low values of the steady-state nucleation rate  $I_{\text{st}}$ . When studying crystal nucleation at temperatures close to  $T_{\max}$ , usually the maximum number of crystals in the experiment  $N_{\max}$  substantially exceeds the value of  $N_s$ . Therefore, in such experiments, the step due to pf-nuclei on the  $N(t_n)$  dependences is practically not observed.

After subtracting from the  $N(t_n)$  curves of the pf-crystals, the induction periods  $\tau$  and the steady-state nucleation rates  $I_{\text{st}}$  of the crystals formed at temperatures  $500$  and  $515^\circ\text{C}$  were determined. The obtained data made it possible to clarify the temperature dependence of the stationary rate of nucleation in the investigated glass at low temperatures. Such data is important for the development of the theory of nucleation. The classical theory of nucleation qualitatively explains a maximum on a temperature dependence  $I_{\text{st}}(T)$  at a temperature  $T_{\max}$ . However, a quantitative discrepancy between theory and experiment is observed at temperatures  $T < T_{\max}$ , which quickly increases with decreasing temperature [2]. Therefore, for a deeper understanding of the nucleation process, reliable data on the rate of nucleation of crystals in glasses are needed, especially at low temperatures  $T_n < T_{\max}$ .

1. N.S. Yuritsyn. J. Non-Cryst. Solids. 2015. V. 427. P. 139–145.
2. A.S. Abyzov, V.M. Fokin, N.S. Yuritsyn, A.M. Rodrigues, J.W.P. Schmelzer. J. Non-Cryst. Solids. 2017. V. 462. P. 32–40.

# NUCLEATION AND GROWTH OF CRYSTALS IN SODA-LIME-SILICA GLASSES

Yuritsyn N.S.

*Grebenshchikov Institute of Silicate Chemistry, Russian Academy of Sciences 199034, St.Petersburg,  
nab. Makarova 2*

*yuritsyn@mail.ru*

Soda-lime-silica glasses of the metasilicate section  $\text{CaO}\cdot\text{SiO}_2 - \text{Na}_2\text{O}\cdot\text{SiO}_2$  are convenient objects for studying the nucleation and growth of crystals. Glasses of this section are basic in fabrication of glass ceramic materials used in medicine. The crystal nucleation was investigated in the range of glass compositions  $\text{Na}_2\text{O}\cdot 2\text{CaO}\cdot 3\text{SiO}_2 - 2\text{Na}_2\text{O}\cdot\text{CaO}\cdot 3\text{SiO}_2$  by development method. In the range  $\text{Na}_2\text{O}\cdot 2\text{CaO}\cdot 3\text{SiO}_2 - \text{Na}_2\text{O}\cdot\text{CaO}\cdot 2\text{SiO}_2$  (1) crystals of solid solutions based on  $\text{Na}_2\text{O}\cdot 2\text{CaO}\cdot 3\text{SiO}_2$  are formed. In the range  $\text{Na}_2\text{O}\cdot\text{CaO}\cdot 2\text{SiO}_2 - 2\text{Na}_2\text{O}\cdot\text{CaO}\cdot 3\text{SiO}_2$  (2) crystals of two phases are formed: solid solutions based on  $\text{Na}_2\text{O}\cdot 2\text{CaO}\cdot 3\text{SiO}_2$  (real composition  $\text{Na}_2\text{O}\cdot\text{CaO}\cdot 2\text{SiO}_2$ ) and  $2\text{Na}_2\text{O}\cdot\text{CaO}\cdot 3\text{SiO}_2$  crystals. The classical theory of nucleation qualitatively explains the maximum on the temperature dependence of the steady state nucleation rate  $I_{st}(T)$  at a temperature  $T_{max}$ . However, a quantitative discrepancy between theory and experiment is observed at temperatures  $T < T_{max}$ , which quickly increases with decreasing temperature [1]. Therefore, for a deeper understanding of the nucleation process, reliable data on the rate of crystal nucleation in glasses are needed at low temperatures  $T < T_{max}$ . The interest in low-temperature measurements of the nucleation rate is also related to the fact that at these temperatures the size distribution of crystalline clusters in the original glass can significantly influence the time-dependence of the number  $N(t)$  of nucleated crystals. The results for a glass of composition from range 1 are presented.

The temperature dependences  $I_{st}(T)$  for glasses from ranges 1 and 2 are determined. The maximal stationary rate of crystal nucleation in the composition range 1 increases substantially with the increase of the sodium oxide content. It is assumed that in this range, along with nucleation of crystals of solid solutions based on  $\text{Na}_2\text{O}\cdot 2\text{CaO}\cdot 3\text{SiO}_2$ , nucleation of crystals  $2\text{Na}_2\text{O}\cdot\text{CaO}\cdot 3\text{SiO}_2$  could occur as well [3].

Nucleation of crystals of the two phases  $\text{Na}_2\text{O}\cdot\text{CaO}\cdot 2\text{SiO}_2$  and  $2\text{Na}_2\text{O}\cdot\text{CaO}\cdot 3\text{SiO}_2$  in glass of the composition  $28.4\text{Na}_2\text{O}\cdot 21.2\text{CaO}\cdot 50.4\text{SiO}_2$  (mol.%) from the middle of the range 2 was studied.

The crystal growth rates were measured along the polished surface and in the glass volume of the stoichiometric composition of  $\text{Na}_2\text{O}\cdot 2\text{CaO}\cdot 3\text{SiO}_2$  in the temperature range of  $600 - 750^\circ\text{C}$ , above the glass transition temperature  $T_g = 572^\circ\text{C}$  [4]. It was established that the growth rate of crystals along the surface is higher than in the volume of glass. The difference between these rates increases rapidly with decreasing temperature, so that the growth rate on the surface exceeds the growth rate in the volume by more than two orders of magnitude at a temperature of  $600^\circ\text{C}$ . This experimental fact shows that at low temperatures the coefficient of effective diffusion of structural units determining the growth kinetics along the glass surface is much higher than in the volume, but with increasing temperature gradually approaches the latter.

In a glass of composition  $28.4\text{Na}_2\text{O}\cdot 21.2\text{CaO}\cdot 50.4\text{SiO}_2$  (mol.%) (glass transition temperature  $510^\circ\text{C}$ ), the growth of crystals of two phases was studied:  $\text{Na}_2\text{O}\cdot\text{CaO}\cdot 2\text{SiO}_2$  (I) and  $2\text{Na}_2\text{O}\cdot\text{CaO}\cdot 3\text{SiO}_2$  (II). In the initial period of crystallization of glass at  $639^\circ\text{C}$ , an approximately linear with time growth of crystals in the form of spherulites of approximately spherical shape was observed. As the crystals grew at a constant temperature, in the vicinity of the crystals I a calcium deficiency was formed, and around crystals II there was a deficiency of sodium. The crystal growth rates decreased, and conditions were created at the crystal boundary for the nucleation and growth of another phase. In photographs of sections of glass samples obtained with an optical microscope in reflected light, after heat treatments, layers of different colors can be observed around spherical crystals, corresponding to the successive formation of layers of crystals of two phases.

1. A.S. Abyzov, V.M. Fokin, N.S. Yuritsyn, A.M. Rodrigues, J.W.P. Schmelzer. *J. Non-Cryst. Solids*. 2017. V. 462. P. 32–40.
2. N.S. Yuritsyn. *J. Non-Cryst. Solids*. 2015. V. 427. P. 139–145.
3. N.S. Yuritsyn. *Glass Physics and Chemistry*. 2015. V. 41. N1. P. 112–115.
4. N.S. Yuritsyn, A.S. Abyzov, V.M. Fokin. *J. Non-Cryst. Solids*. 2018. V. 498. P. 42–48.

## PREPARATION AND STUDY OF WATER-SOLUBLE COBALT AND NICKEL SALTS

**Zainullin O.B., Komornikov V.A., Timakov I.S.**

*Shubnikov Institute of Crystallography FSRC «Crystallography and Photonics» Russian Academy of Sciences, Moscow*

*Evil\_hamster@mail.ru*

In modern instrumentation optical filters are an important component. At the Institute of Crystallography methods are developed for growing crystals with a narrow optical transmission band in various regions of the optical spectrum.

Filters with a narrow bandwidth in the UV range are used in devices "solar-blind technology" [1]. These studies are carried out with the use of double sulfates of transition elements, the so-called Tutton salts [2]. However, optical filters obtained from the crystals of these substances have an optical transmission region in the visible zone, which negatively affects the technical characteristics of the instruments produced with their use.

This paper is devoted to determining the conditions for obtaining crystals of water-soluble cobalt and nickel salts with the required spectral characteristics. Cobalt and nickel chlorides attract attention with similar optical properties and prospects for increasing the temperature range of operation.

In this work, phase equilibria of  $\text{NiCl}_2\text{-CoCl}_2\text{-H}_2\text{O}$ ,  $\text{NiCl}_2\text{-HCl-H}_2\text{O}$  water-salt systems are investigated. Based on the experimental data obtained, it was possible to obtain a relatively large crystal of  $\text{NiCl}_2\cdot 6\text{H}_2\text{O}$ , the dimensions of which made it possible to study its optical as well as thermal properties. The results of microscopy of the surface of the obtained crystals unambiguously indicate the mechanism of layer-by-layer growth of the face of a crystal with the participation of vicinal mounds. Based on the research results,  $\text{NiCl}_2\cdot 4\text{H}_2\text{O}$  crystalline hydrate is a more promising material due to the wider temperature range of existence compared with  $\text{NiCl}_2\cdot 6\text{H}_2\text{O}$ . Next, the conditions for the formation of  $\text{NiCl}_2\cdot 4\text{H}_2\text{O}$  with the minimum necessary concentration of hydrochloric acid at  $25^\circ\text{C}$  were determined to further obtain a single-crystal sample of this crystalline hydrate and study its properties.

The fields of crystallization of solid solutions with the general formula  $\text{Ni}_x\text{Co}_{(1-x)}\text{Cl}_2\cdot 6\text{H}_2\text{O}$  at  $25^\circ\text{C}$  were also determined. Under the conditions of the joint presence of  $\text{NiCl}_2\cdot 6\text{H}_2\text{O}$  and  $\text{CoCl}_2\cdot 6\text{H}_2\text{O}$ , a series of solid solutions is formed in a wide range of compositions at  $0 < x < 1$ . The crystallization range of the starting components is very limited and amounts to only a few mole percent.

The optical transmission spectra of solutions of these compounds with a concentration close to saturated solutions, as well as the optical transmission spectra of crystalline samples, were studied. Both the solutions and the resulting crystalline samples have two transmission bands, one of which is located in the ultraviolet region, and the other in the visible part of the spectrum. However, the position of the bands varies and depends on the specific composition of the test substance.

The data obtained as a result of research allow us to develop methods for growing large single crystals from aqueous solutions suitable for practical use in optics.

The equipment used in the CCU of the Russian Academy of Sciences was used (Ministry of Education and Science, project RFMEFI62114X0005).

This work was supported by the Ministry of Science and Higher Education in the framework of the work on the State task of the Federal Research Center "Crystallography and Photonics" of the Russian Academy of Sciences.

1. А.Э. Волошин, Е.Б. Руднева и др. Патент на изобретение RU 2417388 от 24.11.2006
2. В.Л. Маноменова, Е.Б. Руднева и др. Кристаллография, 50, 937-942, (2005).

**SESSION “New methods and approaches to the description of growth and the investigation of different properties of wide-bandgap semiconductors”**

**LOW-TEMPERATURE SYNTHESIS OF  $\alpha$ -SiC NANOCRYSTALS**

**Nussupov K.Kh., Beisenkhanov N.B., Bakranova D.I., Keiinbay S., Turakhun A.A., Sultan A.A.**

*Kazakh-British Technical University*

*beisen@mail.ru*

Crystalline SiC/Si substrates find use at growing a number of heteroepitaxial films of wide-gap semiconductors, such as SiC, AlN, GaN, AlGaIn, for the manufacture of a wide class of micro- and optoelectronic devices [1,2].

In this work, the structure of silicon carbide films synthesized by magnetron sputtering, atom substitution, and ion implantation techniques was studied and compared the results obtained. The Magna-200 magnetron sputtering unit has been upgraded and two of the three targets have been tuned to high-frequency mode. A high-frequency mode of 13.56 MHz of magnetron sputtering of both targets, silicon and graphite, were used. The deposition mode was as follows: power (rf) – 150 W, frequency – 13.56 MHz; Ar – 2.4 l/h, 0.4 Pa; Si substrate temperature is 100 °C, duration is 10800 s. A thick amorphous SiC<sub>x</sub> film with a high density of ~ 3.52 g/cm<sup>3</sup> containing nanoclusters with a predominance of shortened SiC bonds was obtained. A new phenomenon is shown in this work – the prevalence of shortened Si–C-bonds in an amorphous silicon carbide film, which led to a shift of the maximum of the IR spectrum to a region above 800 cm<sup>-1</sup> – up to 870 cm<sup>-1</sup>. The results can be interpreted by the action of a high-frequency field in the process of deposition of Si and C ions by magnetron sputtering, which contributes to the compaction of the film. For the first time, there was observed a reverse shift of the maximum of the SiC peak of the IR spectrum from 870 cm<sup>-1</sup> to the region of lower frequencies (820 cm<sup>-1</sup>) of the spectrum after rapid annealing at a temperature of 970 °C for 5 minutes. The decomposition of the SiC peak of the IR spectrum into components indicates a significant concentration of dilatation dipoles absorbing at ~ 960 cm<sup>-1</sup>, compared with the area of this component for films obtained by the atomic substitution and ion implantation techniques. Basing on the data of IR spectroscopy, X-ray diffraction and X-ray reflectometry on the phase composition and density of the film (3.522 and 3.397 g/cm<sup>3</sup> before and after annealing, respectively), it was concluded that rapid annealing leads to a partial decomposition of clusters, improvement of the film structure, the formation of nanocrystals  $\alpha$ -SiC,  $\beta$ -SiC and Si and reduction the density of the film. An assumption is made on the presence of diamond inclusions and dense clusters. X-ray diffraction for films synthesized by ion implantation after annealing at temperatures of 1000–1200 °C shows the formation of nanocrystals of only  $\beta$ -SiC [1].  $\beta$ -SiC nanocrystals are also formed in the transition layer "SiC film – Si substrate" after high-temperature synthesis (1250-1330 °C) by the atom substitution method [2]. The low-temperature formation of  $\alpha$ -SiC (1250 °C) in silicon carbide layers obtained by the atomic substitution method was shown by IR spectroscopy [2]. It is known that  $\beta$ -SiC is transformed into  $\alpha$ -SiC at temperature of ~ 1700 °C. The low-temperature formation of  $\alpha$ -SiC (970 °C) in layers synthesized by magnetron sputtering was repeatedly identified on silicon substrates by X-ray diffraction and requires more detailed studies by other methods. The same mode of magnetron sputtering using two silicon targets did not lead to the appearance of any x-ray lines after annealing the films at 700 °C, except for three lines of Si. Subsequent annealing at a temperature of 970 °C for 120 min resulted in complete recrystallization of the surface and the disappearance of poly-Si lines, which indicates the absence of impurities. Thus, the reliability of low-temperature synthesis (970 °C) of  $\alpha$ -SiC is shown.

1 S.A. Kukushkin and A.V. Osipov. J. of Phys. D: Appl. Phys. 47 (2014) 313001-313041.

2 Kukushkin S.A., Nussupov K.Kh., Osipov A.V., Beisenkhanov N.B., Bakranova D.I. Superlattices and Microstructures. 111 (2017) 899-911.

3 Nussupov K.Kh., Beisenkhanov N.B., Valitova I.V., Mit' K.A., Mukhamedshina D.M., Dmitrieva E.A. J. of Materials Science: Materials in Electronics. 19 (2008) 254–262.

# AROMATIC-LIKE CARBON NANOSTRUCTURES CREATED ON THE VICINAL SiC SURFACES

**Benemanskaya G.<sup>1</sup>, Timoshnev S.<sup>2</sup>, Kukushkin S.<sup>3</sup>**

*1 - Ioffe Institute of the Russian Academy of Sciences*

*2 - Saint-Petersburg National Research Academic University of the Russian Academy of Sciences*

*3 - Institute of Problems of Mechanical Engineering of the Russian Academy of Sciences*

*galina.benemanskaya@mail.ioffe.ru*

Silicon carbide (SiC) is a wide-gap semiconductor, fortunate when the use of this material for the making of semiconductor devices with unique electronic properties. In this work, the electronic properties of a several SiC/Si(111)-4° and 8° vicinal surfaces are investigated. It is studied also the Cs and Ba adsorption on these SiC vicinal surfaces for the first time. The epitaxial SiC/Si(111)-8° nanolayers were grown using the original atomic substitution method [1–3]. The method is based on the idea of chemical substitution of half of the Si atoms in the Si unit cell with exactly the same number of C atoms. Note that the presence of carbon vacancy clusters leads to the formation of (111) faces of SiC. An important factor is also the priority of the vicinal surfaces with terraces and steps, as well as unusual electronic and morphological features of surface C atoms.

Electronic structure of the ultrathin Cs/SiC(111)-4°, Ba/SiC(111)-8° interfaces are studied *in situ* in an ultrahigh vacuum using soft X-ray photoelectron spectroscopy. Experiments are carried out at BESSY II, Helmholtz Zentrum Berlin via synchrotron radiation with photon energies in the range of 80–450 eV. Photoemission studies are performed using submonolayer Cs or Ba deposition. The spectra of the C 1s, Si 2p, Ba 4d and Cs 5p core levels were measured for the clean SiC nanolayers and for the SiC with Ba or Cs adsorbed atoms. It is found that the C 1s spectrum for the clean SiC nanolayer consists of two distinct components B and S1. The peak B observed at the energy of ~283.7 eV is attributed to carbon bound to silicon (C-Si) in the bulk SiC substrate. The peak S1 observed at the higher energy of ~285.5 eV is indicated the *s-p*<sup>2</sup> hybridized C-C bonds. Thus, the peak S1 can be considered as an evidence for the C-enriched surface.

The Ba or Cs adsorption on the SiC(111)-4° or 8° nanolayers is found to cause a drastic change in the C 1s core level spectrum. The emergence of additional surface component S2 at the binding energy of ~286 eV is evident. It is found the step-by-step arising of a new peak SU at energy of ~290.5 eV on the highest binding energy side of the B, S1 and S2 peaks. The binding energies of S1, S2 and SU components show a weak dependence on the Ba coverage and the relative intensities being equally modified with the increasing Ba coverage. On the other hand, S2 component indicates a stronger degree of interaction between C-C atoms and increase of the C ionicity. The presence of S1 and emergence of S2 component are widely identified a surface phase transition on a corrugation of the vicinal SiC(111)-8° surface and appearance of an additional adsorption sites induced by Ba adsorption. The shake-up satellite SU is distinctly revealed. The stabilizing Ba atoms adsorbed on the SiC nano-layer initiate a specific 2D phase transition in the surface system, with the formation of a new type of carbon nanostructure composed of six-membered carbon rings, in which the chemical bonding between carbon atoms are close in nature to the bonding in the aromatic-like compounds. Additional evidence of successful creation of a carbon nanostructure composed of carbon rings is presented using Raman spectroscopy.

Thus, the clusters of aromatic-like carbon rings are formed on the surface of inorganic SiC compound due to effect of adsorption of the Cs or Ba atoms. The Raman spectroscopy data unambiguously supports the conclusion that, upon adsorption of metal atoms on the vicinal SiC nanolayers, a new, previously unknown carbon nanostructure involving carbon rings structurally similar to aromatic-like compounds is formed.

The authors thank Synchrotron BESSY II and Russian-German Beamline, Synchrotron BESSY II, Helmholtz Zentrum Berlin for providing the facilities to perform the experiments.

## References

- [1] S.A. Kukushkin, A.V. Osipov, N.A. Feoktistov. *Phys. Solid State* 56 (2014) 1507.
- [2] S.A. Kukushkin, A.V. Osipov. *J. Phys. D: Appl. Phys.* 50 (2017) 464006.
- [3] G.V. Benemanskaya, P.A. Dementev, S.A. Kukushkin, M.N. Lapushkin, A.V. Osipov, S.N. Timoshnev. *Tech. Phys. Lett.* 42 (2016) 1145.

# **BULK GROWTH OF GaN. HOW TO OVERCOME THE EQUILIBRIUM CRYSTAL SHAPE?**

**Bockowski M.**<sup>1,2</sup>

*1 - Institute of High Pressure Physics Polish Academy of Sciences, Sokolowska 29/37, 01-142  
Warsaw, Poland*

*2 - Center for Integrated Research of Future Electronics, Institute of Materials and Systems for  
Sustainability, Nagoya University, C3-1 Furo-cho, Chikusa-su, Nagoya 464-8603, Japan*

*bocian@unipress.waw.pl*

A current status of bulk GaN crystal growth technology will be described. Today, there are three main technologies applied for GaN crystal growth. Two of them, sodium flux (growth in the mixture of gallium and sodium under nitrogen pressure of approximately 5 MPa and at temperature of 900°C with MOCVD-GaN/sapphire templates as seeds) and ammonothermal (crystallization on native seeds in supercritical ammonia under pressure up to 0.6 GPa and temperatures from 400°C to 750°C), belong to the group of solution growth methods. Both ammonothermal and sodium flux growth result in high structural quality, large crystals (at least 2 inch diameter), and can be doped n-type. Ammonothermal growth has also demonstrated semi-insulating crystals. The third method, halide vapor phase epitaxy (HVPE), involves crystallization from gas phase (due to reaction between gallium chloride and ammonia at 1100°C and ambient pressure) and has high growth rates required for thick substrate growth. Since HVPE-GaN is mainly deposited on foreign substrates (sapphire, gallium arsenide), it enables growth of large GaN crystals (up to 6 inch). However, they are of poorer structural quality as crystallographic planes are often bent and the wafers obtained from crystals can be plastically deformed. Therefore, it is impossible to misorient them uniformly across the entire wafer surface, which is a critical requirement for device-quality wafers. The way to overcome this problem is to use GaN crystals of very high crystallographic quality as seeds for HVPE growth. Recently, it has been presented that GaN crystal grown by the sodium flux method can be applied as seed material as can ammonothermally grown crystals. This allowed crystallization of HVPE-GaN with a low threading dislocation density ( $\sim 10^5 \text{ cm}^{-2}$ ) and absolutely flat crystallographic planes. Doping with donors (silicon, germanium) and acceptors (carbon, manganese, iron) is possible via HVPE to obtain any required electrical properties of GaN. However, it should be remarked that all of these methods allow thicknesses of only a few millimeters thick GaN, which only produce one new wafer from one seed when losses from sawing and polishing are considered. Therefore, they represent a wafer-to-wafer technology. Up to now, no one has demonstrated real bulk GaN crystal and convenient technology for growing it. It will be discussed in the paper in detail. It will be shown that due to anisotropy of the growth and crystallization occurring in the lateral directions during the growth process in the chosen direction, real bulk growth of GaN is difficult, even if native high structural quality seeds are used. The main goal is to design a new process wherein only one growth facet is stabilized and grown out during a long time. It can be achieved by controlling a thermal field around the growing crystal. The crystal has to reach its final shape by adapting to the thermal field rather than taking its equilibrium habit.

## GROWTH AND STUDY OF ALLOYED GaP NANOWIRE HETEROSTRUCTURES

**Bolshakov A.<sup>1</sup>, Fedorov V.<sup>1</sup>, Mozharov A.<sup>1</sup>, Sibirev N.<sup>2</sup>, Kryzhanovskaya N.<sup>1</sup>, Cirlin G.<sup>1,2</sup>, Mukhin I.<sup>1,2</sup>**

*1 - St Petersburg Academic University*

*2 - ITMO University*

*bolshakov@live.com*

From the 1960s III-phosphide semiconductors, namely GaP and its alloys such as GaP<sub>1-x</sub>As<sub>x</sub> attract attention in optoelectronics and photonics due to several reasons. First of all, compare to other III-V zinc-blende (ZB) semiconductors, GaP is nearly lattice matched (0.37% mismatch) with Si and can be used as a buffer layer material for integration of polar III-V direct bandgap materials (e.g. GaAs) on Si platform. Due to their morphology, A<sub>3</sub>B<sub>5</sub> nanowires (NWs) can be synthesized epitaxially on highly mismatched substrates, such as Si.

In this work MBE synthesis and characterization of heterostructured GaP NWs with GaP<sub>1-x</sub>As<sub>x</sub> NDs with controllable composition are demonstrated. Structural investigation reveals cubic ZB structure of GaP segments with lamellar twinning along the growth direction, while GaP<sub>1-x</sub>As<sub>x</sub> ternary alloy tends to growth in WZ crystal structure. EDX analysis of the heterostructure chemical composition shows that even at high As/P BEP ratio of 10, the maximum achieved content of As in the ND is nearly 60%. The observed phenomenon is discussed within the self-consistent theoretical model. Experimental data on the NDs composition was fitted with high accuracy using the developed model demonstrating potential of the approach for controlled synthesis of GaP<sub>1-x</sub>As<sub>x</sub> alloyed NWs. PL studies demonstrate broadband PL response centered at 660 nm. Fabry-Pérot type equidistant axial resonances in PL spectra of synthesized NWs were observed.

We also report on molecular beam epitaxy synthesis of large scale ordered arrays of A<sub>3</sub>B<sub>5</sub> NWs on Si. We present the method for fabrication of the growth masks via etching of the pre-deposited SiO layer through the resist pattern obtained with projection photolithography through array of silica microspheres.



## **BORON NITRIDE EPILAYERS GROWN ON $\text{AlO}_x\text{N}_y$ AND $\text{Al}_2\text{O}_3$ BUFFER LAYER**

**Caban P.A.<sup>1</sup>, Michalowski P.<sup>1</sup>, Gaca J.<sup>1</sup>, Wojcik M.<sup>1</sup>, Ciepielewski P.<sup>1</sup>, Mozdzonek M.<sup>1</sup>,  
Teklinska D.<sup>1</sup>, Dumiszewska E.<sup>1</sup>, Firek P.<sup>2</sup>, Baranowski J.M.<sup>1</sup>**

*1 - Lukasiewicz Research Network - Institute of Electronic Materials Technology, Warsaw, Poland*

*2 - Institute of Microelectronics and Optoelectronics, Warsaw University of Technology, Warsaw,  
Poland*

*piotr.caban@itme.edu.pl*

Boron nitride films were epitaxially grown by MOCVD method. Triethylborone (TEB) and ammonia ( $\text{NH}_3$ ) were applied as a precursor gases. The growth was performed at  $1050^\circ\text{C}$  temperature and 400mbar pressure which indicates self-terminated growth mode. As a result very thin (2nm) BN films with atomic smooth surfaces was grown.

Structural properties of BN grown directly on the  $\text{Al}_2\text{O}_3$ ,  $\text{AlO}_x\text{N}_y/\text{Al}_2\text{O}_3$ ,  $\text{AlO}_x\text{N}_y/\text{Si}$  and  $\text{Al}_2\text{O}_3/\text{Si}$  substrates were investigated. The measurements techniques used for investigation of the grown BN films involved SIMS, ATR spectroscopy, XRR, Raman and XPS.

The ATR method revealed an in-plane infrared active mode due to a transverse optic phonon  $\text{E}_{1u}$  of the  $\text{sp}^2$  bonded BN at wavelength  $1373\text{cm}^{-1}$  for BN grown on the  $\text{Al}_2\text{O}_3$  and  $\text{AlO}_x\text{N}_y/\text{Al}_2\text{O}_3$  substrates. The FWHM was respectively  $25\text{cm}^{-1}$  for  $\text{BN}/\text{Al}_2\text{O}_3$  and  $27\text{cm}^{-1}$  for  $\text{BN}/\text{AlO}_x\text{N}_y/\text{Al}_2\text{O}_3$ .

SIMS measurements revealed fluctuation of BN for Si substrate diffusion of Si through  $\text{AlO}_x\text{N}_y$  into BN were observed. Whereas uniformity of grown thin films for both sapphire substrates was observed. The advantage of  $\text{Al}_2\text{O}_3$  buffer layer instead of  $\text{AlO}_x\text{N}_y$  was confirmed.

*This work was supported by the European Union's Horizon 2020 research and innovation program under grant agreement No 785219*

## III-V NANOWIRES GROWN BY MBE ON Si AND SiC SUBSTRATES

**Cirlin G.**<sup>1,2</sup>

*1 - Academic University RAS*

*2 - ITMO University*

*george.cirlin@mail.ru*

Vertical nanowires (NWs), having a high length/diameter ratio and a diameter of several tens of nanometers, are a new attractive object in modern nanotechnology due to an interesting physics of quasi-1D systems and their potential applications in electronics, biology, field-emission devices etc. In this work, we report on the molecular beam epitaxial (MBE) growth of different A<sub>3</sub>B<sub>5</sub> semiconductor nanowires on different substrates, including silicon and SiC/Si either catalyzed by gold particles or grown in self-catalyzed mode. We show that MBE has several advantages in NWs formation, in particular due to the high ad-atom diffusivity and diffusion-induced mechanism of NWs growth. We present the detailed examination of the growth conditions influence on the structural and optical properties of the NWs. Reflection high-energy electron diffraction, scanning electron microscopy, transmission electron diffraction, scanning probe microscopy and photoluminescence techniques are applied to shed more light on NWs growth mechanism study. Additionally, we present a systematic study of different nanoinclusions embedded in the nanowires body, like InAsP/InP or GaAs/AlGaAs. Optical properties combined with TEM study supports zero-dimensional behavior of these inclusions. Possible applications of the NWs are considered.

# MBE GROWTH, STRUCTURAL AND OPTICAL PROPERTIES OF GALLIUM ARSENIDE PHOSPHIDE NITRIDE HETEROSTRUCTURES ON SILICON

**Fedorov V.<sup>1,2</sup>, Bolshakov A.<sup>1,2</sup>, Koval O.<sup>1</sup>, Sapunov G.<sup>1</sup>, Kirilenko D.<sup>3,2</sup>, Mozharov A.<sup>1</sup>, Mukhin I.<sup>1,2</sup>**

*1 - St. Petersburg Academic University, Khlopina 8/3, 194021, St. Petersburg, Russia*

*2 - ITMO University, Kronverkskij 49, 197101, St. Petersburg, Russia*

*3 - Ioffe Institute, Politekhnicheskaya 29, 194021, Saint Petersburg, Russia*

*vfedorov@fl.ioffe.ru*

A specific feature of dilute III–V nitride quaternary alloys is a wide tunability of lattice constants and bandgap energy, which make them promising materials for optoelectronic applications and their monolithic integration on silicon. GaP itself is an indirect III-V semiconductor ( $E_g = 2.26$  eV) closely lattice mismatch with Si ( $\Delta a/a \sim 0.37\%$ ) notable for its broad transparency range (0.6–11  $\mu\text{m}$ ) and high second-order nonlinear optical susceptibility [1]. Incorporation of nitrogen into in GaPN leads to dramatic bandgap shrinking ( $\sim 100$  meV%), accompanied with decrease of lattice parameter. Moreover, indirect to direct bandgap transition at the N concentration higher than 0.4% occurs, while at 2% GaPN becomes lattice matched to Si [2]. In turn, incorporation of arsenic in quaternary GaPNAs alloys with nitrogen content higher than 2% allows to compensate changes in lattice parameter keeping it lattice-matched to the Si allowing to independently tune the bandgap. However, III-V epitaxy on silicon faces the problem of surface energy mismatch leading to the 3D island growth and problem of polar-on-nonpolar nucleation leading to the formation of antiphase domains (APDs) growing out of phase in terms of lattice occupation with group-III and -V elements [3]. Thus, special seeding and buffer layers are used to obtain uniform III-V nucleation on Si [4].

This report aims to provide details on growth and properties of dilute nitride GaPNAs/GaP/Si heterostructures with an achieved nitrogen concentration up to the 5%. Role of substrate miscut and buffer layer preparation technique on the APD formation is regarded. Dilute nitride phosphide heterostructures were grown with solid source plasma assisted molecular beam epitaxy system equipped with valved phosphorus and arsenic cracker sources and RF-plasma nitrogen source. Structure of synthesized samples was studied by X-ray diffraction (XRD) and transmission electron microscopy (TEM) while its morphology was investigated by scanning electron (SEM) and atomic-force microscopy (AFM). Concentrations of the incorporated nitrogen in the ternary GaPN alloy was calculated according to Vegard's law, while composition of lattice matched quaternary GaPNAs alloys was evaluated by Raman spectroscopy. Effect of growth temperature and V/III ratio on nitrogen incorporation was studied: most effective incorporation was achieved at growth temperature reduced by 40 °C in compare to the GaP growth (600 °C) and stoichiometric P/Ga ratio. It was found that during the growth of GaPN layer with more than 0.4% of incorporated nitrogen APD boundaries change their orientation from vertical  $\{110\}$  to inclined  $\{111\}$  and  $\{112\}$  planes and self-annihilates. This results in formation of completely APD free dilute nitride layer even in case of antiphase disordered GaP buffer. Thus, lattice matched GaPN layers can be used as buffer layer for defect free growth of quaternary GaPNAs alloys. Optical properties of synthesized heterostructures was studied by photoluminescence (PL) spectroscopy. Broadband PL response exhibiting red shift with increase of N concentration was found. Highest PL intensity was found for the ternary GaPN alloy lattice matched with Si indicating its strong dependence on film crystal quality.

This work was supported by the Russian Science Foundation grants № 18-72-00231 and № 18-72-00219.

- [1] Gudovskikh A.S., Zelentsov K.S. et al., Energy Procedia, 102, 56–63, (2016)
- [2] Miyoshi S., Yaguchi H., Onabe K., et al., Appl. Phys. Lett., 63, 3506–3508, (1993)
- [3] Lucci I., Charbonnier S., Pedesseau L., et al., Phys. Rev. Mater. 2, 060401, (2018)
- [4] Beyer A., Ohlmann. J, Liebich S., et al., J. Appl. Phys., 111, 083534 (2012)

# IMPROVEMENT OF CRYSTALLINE QUALITY OF AlGaN BY NUCLEATION GROWTH AND ULTRAVIOLET LASER APPLICATION

**Iwaya M.<sup>1</sup>, Sato K.<sup>1,2</sup>, Takeuchi T.<sup>1</sup>, Kamiyama S.<sup>1</sup>, Akasaki I.<sup>1,3</sup>, Miyake H.<sup>4</sup>**

*1 - Department of Materials Science and Engineering, Meijo Univ.*

*2 - Asahi Kasei*

*3 - Akasaki Reserch Center, Nagoya Univ.*

*4 - Grad. Sch. of RIS1, Grad. Sch. of Eng. 1, SPORR3, Mie Univ.*

*iwaya@meijo-u.ac.jp*

AlGaN-based UV-LEDs and LDs have a wide range of applications in medical, industrial and environmental fields. High performance AlGaN-based UV LEDs have been demonstrated. The emission wavelength is also realized almost physical property limit of 210 nm. In contrast, the realization of UV LDs is also very important. UV LDs have a great potential in the fields of laser processing especially surface processing, medical, biotechnology and so on. So far, there are many reports of UV-A LDs. To our best knowledge, the report of the shortest wavelength of AlGaN-based UV LD is 326 nm under pulsed current injection. There are two major issues, such as laser oscillation with low injection carriers and injection of a current to the extent of population inversion, to realize its target. Among them, we have achieved high current operation in UV-B region exceeding 45 kA/cm<sup>2</sup> with pn junction using p-type AlGaN with average AlN molar fraction of 0.55 and film thickness of 300 nm, respectively. This p-type AlGaN can form an optical resonator sufficiently in the UV-B region. In contrast, high current density operation has not been obtained so far in the UV-C region. It is also many reports by using a photoexcitation method also as a low threshold value of carrier required for laser oscillation. To summarize these results, very low oscillation threshold power densities such as several kW/cm<sup>2</sup> are obtained for lasers in the UV-C region. On the other hand, the most laser oscillation threshold power densities of the UV-B region are still high about several hundred kW/cm<sup>2</sup>. This reason is that AlN is used as a template and an active layer is formed thereon to fabricate a laser structure in these studies. However, there is a large lattice mismatch between AlGaN active layer in the UV-B region and AlN template. Therefore, it is thought that this large lattice mismatch introduces some defects and increases the threshold power density. Therefore, it is very important to realize high crystalline quality and relaxed AlGaN underlying layer. Also, it is considered preferable that the AlN molar fraction be around 0.6 if we aim at the UV-B region. In this presentation, we investigated the AlGaN with AlN molar fraction of 0.55 underlying layer film thickness dependence of threshold power density in UV-B lasers on sputtered AlN template with high temperature annealing treatment. We confirmed that initial growth of AlGaN becomes nucleation growth by inserting a homoepitaxial AlN layer between AlN template and AlGaN, and it shifts to two-dimensional growth. We also confirmed that by using such a growth mode it is possible to reduce the dislocation in AlGaN. We investigated the dependence of AlGaN film thickness and AlN template dependence on samples with homoepitaxial AlN layer inserted. It was confirmed that the threshold power density in UV-B laser and dark spot density were reduced as the film thickness increased. By optimization of crystal growth condition, the threshold power density in UV-B laser and dark spot density have been reduced to 36 kW/cm<sup>2</sup> and  $7.5 \times 10^8$  cm<sup>-2</sup>, respectively.

# CONSTITUENTS OF THE GROWTH OF GaN NANOWIRE ARRAYS: NUCLEATION, RADIUS SELF-REGULATION, HEIGHT SELF-EQUILIBRATION, BUNDLING, ELASTIC AND PLASTIC RELAXATION

**Kaganer V.<sup>1</sup>, Fernández-Garrido S.<sup>1,2</sup>, Sabelfeld K.<sup>3</sup>, van Treeck D.<sup>1</sup>, Geelhaar L.<sup>1</sup>, Brandt O.<sup>1</sup>**

*1 - Paul Drude Institute for Solid State Electronics*

*2 - Universidad Autónoma de Madrid, Madrid, Spain*

*3 - Institute of Computational Mathematics and Mathematical Geophysics, Russian Academy of Sciences, Novosibirsk, Russia*

*kaganer@pdi-berlin.de*

The growth of GaN and ZnO nanowires (NWs) is fundamentally different from the vapor-liquid-solid (VLS) approach used for the synthesis of the majority of semiconductor NWs. Whereas VLS growth is initiated by a metal droplet, GaN NWs form spontaneously on a wide variety of substrates. Decisive advantages of this spontaneous formation is the absence of polytypism induced in VLS growth by the metal droplet as well as the possibility to synthesize abrupt axial heterojunctions on the cation sublattice. A disadvantage of the spontaneous NW formation is that the NW density cannot be easily controlled. On most substrates, including Si and glass, the GaN NW density is so high that adjacent NWs coalesce after reaching a certain length [1]. An exception is crystalline TiN, on which GaN NW ensembles with a low density and a negligible coalescence degree can be obtained [2].

Here, we present a comprehensive overview of the phenomena governing the spontaneous formation and growth of GaN NWs ranging from their nucleation and coalescence to the height equilibration at the later stages of growth.

Insight in the nucleation of NWs is obtained by studying the distribution of the distances between nearest neighbor NWs at the initial stages of growth. GaN NWs on Si possess initially a Poisson distribution of distances, which points to their independent nucleation that is not restricted by Ga adatom diffusion on the substrate. Nucleation is terminated when the substrate is shadowed from the Ga atom flux by growing NWs [1]. In contrast, the nearest neighbor distance distribution of GaN NWs on TiN does not contain short distances, because Ga adatom diffusion to the already nucleated NWs forms zones with reduced Ga adatom density. In this case, nucleation is terminated when these zones overlap [2].

As a result of the high mobility of Ga adatoms on the NW sidewall facets, NWs grow in height due to Ga fluxes impinging onto both the top and the sidewall facets. Despite the nominally N-rich conditions during growth, the finite amount of active N available for growth limits the axial growth rate. An excess of Ga adatoms at the NW tip gives rise to radial growth, which is self-regulated and ceases after reaching an equilibrium NW diameter [3].

The growth kinetics of dense arrays of GaN NWs involves the exchange of Ga atoms between adjacent NWs: Ga atoms desorbed from the side surfaces of NWs readsorb on neighboring ones. This process favors the growth of shorter NWs and gives rise to a narrow NW height distribution during the late stages of growth [4].

In dense arrays of spontaneously formed GaN NWs, NWs coalesce by bundling: adjacent NWs bend and merge at their top, thus reducing their surface energy at the expense of the elastic energy of bending [1]. The bending energy can be substantially reduced by the creation of dislocations at the coalescence joints. A comparison of experimental and calculated x-ray diffraction profiles from ensembles of bundled NWs demonstrates that a large part of the bending energy is indeed relieved by plastic deformation [5].

[1] V. Kaganer, S. Fernández-Garrido, P. Dogan, K. Sabelfeld, O. Brandt, *Nano Lett.* **16**, 3717 (2016).

[2] D. van Treeck, G. Calabrese, J. Goertz, V. Kaganer, O. Brandt, S. Fernández-Garrido, L. Geelhaar, *Nano Res.* **11**, 565 (2018).

[3] S. Fernández-Garrido, V. Kaganer, K. Sabelfeld, T. Gotschke, J. Grandal, E. Calleja, L. Geelhaar, O. Brandt, *Nano Lett.* **13**, 3274 (2013).

[4] K. Sabelfeld, V. Kaganer, F. Limbach, P. Dogan, O. Brandt, L. Geelhaar, H. Riechert, *Appl. Phys. Lett.* **103**, 133105 (2013).

[5] V. Kaganer, B. Jenichen, O. Brandt, *Phys. Rev. Applied* **6**, 064023 (2016).

# FORMATION AND STUDY OF THE PROPERTIES OF INGAN POLYTYPE STRUCTURES GROWN BY LOW-TEMPERATURE MOLECULAR-BEAM EPITAXY

**Kotlyar K.**<sup>1,2</sup>, **Reznik R.**<sup>1,2,3,4</sup>, **Lihachev A.**<sup>5</sup>, **Kirilenko D.**<sup>5</sup>, **Soshnikov I.**<sup>1,3,5</sup>, **Cirlin G.**<sup>1,3,4</sup>

1 - St. Petersburg Academic University, Khlopina st. 8/7, St. Petersburg 194021, Russia

2 - St. Petersburg State University, Universitetskaya nab. 7-9, St. Petersburg 199034, Russia

3 - Institute for Analytical Instrumentation of the RAS, Rizhsky pr. 26, St. Petersburg 190103, Russia

4 - ITMO University, Kronverkskiy pr. 49, St. Petersburg 197101, Russia

5 - Ioffe Physical-Technical Institute of the RAS, Politekhnicheskaya ul. 26, St. Petersburg 194021, Russia

*konstantin21kt@gmail.com*

The polymorphic (polytype) structures of materials (III-N) is interest for different optoelectronic application, such as fabrication of nano-optoelectronics devices [1], renewable energy sources [2]. In this work, we demonstrate the perspective of the synthesis of InGaN structures with different morphology using low-temperature molecular beam epitaxy.

The InGaN structures are grown by molecular beam epitaxy on Si (111) substrates. Characterization of samples morphology using SEM methods shows that in the region adjacent to the substrate, a layer of closely spaced nanotubes is grown. The typical height of nanotubes is about 400 nm, external and internal diameter is about 65 nm and 25 nm respectively. In the area above the nanotube layer, an array of 3D structures (so-called "nanoflowers") is grown. The typical size of single "nanoflower" in the vertical and lateral directions is about 4,5 and 1  $\mu\text{m}$  respectively.

TEM shows that a single "nanoflower" structure consists of blocks of nanocrystals at the hexagonal and/or cubic crystal phase. The typical size of the nanocrystals is about 100-500 nm. The growth mechanism of the structures is associated at the formation of a 3D InGaN nanocrystal at the cubic phase at the site of a stacking fault and following growth of InGaN crystal in hexagonal phase on the faces of cubic nanocrystal. The analysis of the nanocrystals composition using the EDX technique shows a higher indium content for the hexagonal phase (~20-30%) than in the cubic phase (~5-10%). The photoluminescence spectra of the samples demonstrate the emission band at the range of 500-600 nm.

The work (epitaxial growth and characterization) is supported by the Ministry of Education and Science of Russian Federation (State task 16.9791.2017/8.9). SEM characterization was performed using equipment owned by the Federal Joint Research Center "Material science and characterization in advanced technology" with financial support by Ministry of Education and Science of the Russian Federation (id RFMEFI62117X0018).

[1] M. Monavarian, A. Rashidi and D. Feezell, A Decade of Nonpolar and Semipolar III-Nitrides: A Review of Successes and Challenges, *Phys. Status Solidi A*, 1800628 (1-22), (2018).

[2] J. Li, J. Y. Lin and H. X. Jiang, Direct hydrogen gas generation by using InGaN epilayers as working electrodes, *Appl. Phys. Lett.*, vol. **93**, 162107, (2008).

## SITE-SPECIFIC MICRO CROSS SECTIONING BY A FIB-SEM. ADVANTAGES FOR INVESTIGATION OF THIN FILMS

**Lukashova M.V., Dergachev A.I.**

*TESCAN Russian office*

*LukashovaMV@tescan.ru*

Up-to-date complicated materials and devices require more sophisticated tools for their development and inspection in order to reach the area of interest and analyze it. Scanning electron microscopy (SEM) in combination with focus ion beam methods (FIB) is an appropriate technique for keeping up with the rapid evolution of material sciences by offering analytical capabilities with high level of precision.

Approach with using of a FIB-SEM microscope consists of several steps:

- **Searching of an area of interest** by scanning across a sample surface with SEM; commonly 5 – 15 minutes for sample positioning, pumping of a FIB-SEM chamber and searching.
- **Deposition of a Pt-mask** in a site-specific place on a sample for protection of the highest layers of a sample. Typical size of the Pt-mask is 5 mkm × 30 mkm; approximately 5 minutes for deposition. A FIB-SEM should be completed with a gas injection system (GIS) with a Pt-nozzle as a frequent option for this type of SEMs.
- **FIB milling** in order to make a micro cross-section through the Pt-mask to deeper areas of a sample. Duration depends on size of a cross-section and usually takes 20 – 60 minutes for a cross-section 40 mkm × 20 mkm.
- **Investigation** of a site-specific local cross-section with a SEM column; all time you want.

The advantages of the FIB-SEM cross sectioning are:

- A conventional scanning electron microscope is an instrument for investigation of sample surface only. With a FIB-SEM you have a possibility to see not only surface but internal structures also.
- The level of visualization of received results is very good. Thin layers on a cross-section looks like an AutoCAD design file.
- As a rule, FIB cross-sections are very smooth.
- It is very site-specific methodic. A user chooses position for a cross-section or TEM lamellae preparation ideally precisely comparing with methods, which deals with macro-samples. You could clearly visualize multilayer structures.
- Very thin films on a sample surface can be observed. For example, in TESCANA Russia laboratory practice we have faced with investigation of ~ 7 nm films. The film thickness ~ 30 nm is common. The thinnest and nearest surface layer does not disappear on a FIB cross-section because of protection with a Pt-mask.
- Observation of internal cracks, pores, other sub-surface cavities is very convenient with a FIB, because all voids remain in their original form on a FIB cross-section after ion polishing. There are no jamming of voids and no debris stays in voids to confuse results.
- Making of local FIB cross-sections is almost non-destructive method comparing with traditional epoxy mounting and polishing. Therefore, you can investigate museum exhibits or forensic evidences without their destruction.
- One of modifications of described before method is used for preparation of site-specific lamellas for a transmission electron microscope (TEM).

The described method is presented in TESCANA demonstration laboratory in Saint-Petersburg where you are invited to. A contact for agreement of visit is: Maria Lukashova, mobile phone +7 (931) 202-09-89, e-mail LukashovaMV@tescan.ru.

# NUCLEATION OF THE GRAPHENE-LIKE $\text{Si}_3\text{N}_3$ LAYER ON THE Si (111) STUDIED BY STM

**Mansurov V.G., Galitsyn Yu.G., Malin T.V., Milakhin D.S., Teys S.A., Zhuravlev K.S.**

*Rzhanov Institute of Semiconductor Physics*

*mansurov@isp.nsc.ru*

Two-dimensional (2D) and graphene-like materials attract tremendous attention due to excellent electronic properties and compatibility with the well-developed Si-based semiconductor industry. It is usually assumed that nitridation of Si (111) (by ammonia or N - plasma source) results in a thin film of  $\beta\text{-Si}_3\text{N}_4$  with adsorbed nitrogen atoms. However, recently we have shown that the nitridation of Si(111) under ammonia flux results in a new graphene-like modification of silicon nitride  $g\text{-Si}_3\text{N}_3$  [1-3]. The  $g\text{-Si}_3\text{N}_3$  on the Si(111) consists of a graphene-like honeycomb structure and an adsorption phase of silicon on top of the honeycomb structure. In the present work, we study the kinetics and mechanism of the formation of  $g\text{-Si}_3\text{N}_3$  islands using the RHEED and STM methods.

In the previously proposed model for the (8x8) structure formation as  $\beta\text{-Si}_3\text{N}_4$  islands nucleation and growth [4] the authors wrote: “The decrease in number and increase in size of nucleation centers with increasing nitridation temperature can be explained in terms of thermal diffusion length”. For this mechanism of nucleation, a significant temperature dependence of the islands formation rate should be detected due to activation barriers for the components diffusion and also for incorporation of the atoms into lattice sites of  $\beta\text{-Si}_3\text{N}_4$ . In addition, in the work [4], it is believed that the silicon nitride islands are formed in pits of the Si(111) surface etched by active nitrogen. This interpretation arises because the silicon nitride islands in the STM images are shown up itself as darker areas. However, in our opinion, silicon nitride islands are formed on top of the silicon surface, and a dark contrast arises due to the low conductivity of silicon nitride (it is a good insulator).

Recently we have investigated the formation kinetics of  $g\text{-Si}_3\text{N}_3$  by RHEED and the barrier-free formation of the  $g\text{-Si}_3\text{N}_3$  phase have been demonstrated [1]. So, we consider the formation of  $g\text{-Si}_3\text{N}_3$  islands as a phase transition within the framework of the lattice gas model on the Si (111) surface. In this model, an important role is played by the, so-called, critical concentration of filled cells of the bonded silicon and nitrogen atoms (denoted as Si-N) on the surface, by the other words the Si-N lattice gas. When the critical Si-N concentration is reached, a phase transition from the lattice gas to the condensed phase of  $g\text{-Si}_3\text{N}_3$  occurs (i.e.  $g\text{-Si}_3\text{N}_3$  islands formation). The concentration of the filled Si-N cells is determined by the concentration of mobile silicon adatoms on the Si(111) surface. This concentration has a temperature dependence, as we showed earlier, with a heat of the mobile adatoms formation of 1.7 eV [1].

At relatively low temperatures ( $<800^\circ\text{C}$ ), and hence at low concentrations of mobile silicon adatoms, the critical concentration of the filled Si-N cells occurs in small regions only owing to fluctuations in the concentration of mobile silicon on the Si(111) surface. Therefore, small  $g\text{-Si}_3\text{N}_3$  islands appear. At high temperatures, i.e. with a high concentration of mobile silicon adatoms, the critical concentration is reached in large regions of the surface, and large two-dimensional  $g\text{-Si}_3\text{N}_3$  islands appear.

This work was supported by the Russian Foundation for Basic Research (grants 17-02-00947, 18-52-00008).

[1] V.G.Mansurov, T.V.Malin, Yu.G Galitsyn, et. al., J. Cryst. Growth, 441, 12 (2016).

[2] В.Г.Мансуров, Ю. Г.Галицын, Т.В.Малин, и др., ФТП, 52, 1407 (2018).

[3] V.G.Mansurov, Yu.G Galitsyn, T.V.Malin, et. al., in 2D Materials, IntechOpen, London (2018).

[4] S.Gangopadhyay, T. Schmidt, J. Falta, e-J. Surf. Sci. Nanotech., 4, 84 (2006).



# GaN NANOCRYSTALS FORMATION ON THE GRAPHENE-LIKE g-AlN AND g-Si<sub>3</sub>N<sub>3</sub> SURFACES

**Milakhin D.S.<sup>1</sup>, Malin T.V.<sup>1</sup>, Mansurov V.G.<sup>1</sup>, Galitsyn Yu.G.<sup>1</sup>, Zhuravlev K.S.<sup>1,2</sup>, Lebiadok Ya.V.<sup>3</sup>, Razumets A.A.<sup>3</sup>**

*1 - Rzhanov Institute of Semiconductor Physics*

*2 - Novosibirsk State University*

*3 - State Scientific and Production Association "Optics, Optoelectronics and Laser Technology"*

*dmilakhin@isp.nsc.ru*

After success in graphene synthesizing, the AlN and GaN binary compounds attracted great research interest due to the possibility of ultrathin layer formation with a graphene-like hexagonal structure having sp<sup>2</sup>-hybridized electronic states [1,2]. III-nitrides graphene-like layers are non-polar material with a non-zero band gap. Graphene-like AlN (g-AlN) can be used as a gate dielectric to isolate two-dimensional graphene or silicene-type conductors with zero bandgap in the synthesis of Van der Waals crystals, opening up new prospects in the nanoelectronics and spintronics development. The g-AlN / g-GaN layers synthesis and the quantum dots (QDs) formation with different sizes and densities on the III-nitrides graphene-like layers open up prospects for creating various light-emitting devices that require short radiative lifetimes, such as lasers, sources of single and entangled photons.

This work is devoted to the study of GaN nanocrystals formation on graphene-like (g-Si<sub>3</sub>N<sub>3</sub> and g-AlN) layers by the molecular beam epitaxy (MBE) technique. The samples were studied in situ by the reflection high-energy electron diffraction method. In diffraction patterns (DP), the appearance of disordered nanocrystals or 3D GaN islands with a characteristic distance 3.19 Å was observed, depending on the selected growth conditions and the nucleation surface (g-Si<sub>3</sub>N<sub>3</sub> or g-AlN).

GaN growth of on g-Si<sub>3</sub>N<sub>3</sub> in the temperature range of 600-850 °C using an ammonia flux 275 sccm had led to the polycrystalline GaN formation, while the GaN growth using the same growth conditions on w-AlN was characterized by the w-GaN layer formation with 3D-DP at substrate temperatures of 600-750 °C and 2D-DP at substrate temperatures of 750-850 °C. It can be assumed that the formation of GaN disordered crystals is associated with the absence of dangling bonds on the g-Si<sub>3</sub>N<sub>3</sub> surface. The components condensation (Ga and NH<sub>3</sub>) arriving on the surface in the absence of bonds that determine the orientation of the crystal being formed leads to the arbitrarily oriented GaN nanocrystals formation. With the GaN growth on g-Si<sub>3</sub>N<sub>3</sub> at a substrate temperature of 550 °C, a DP blanking was observed when ~ 2 nm layer thickness was reached, that is, the substrate surface was covered with Ga metal drops. A similar effect was observed with the w-GaN growth on w-AlN. This observation is associated with the absence of a chemical reaction between metallic gallium and ammonia. During the formation of thin (1-2 monolayers) GaN layers at temperatures of 550–650 °C by alternately feeding the components onto the substrate, a decrease in DP contrast was observed without new reflexes appearance on DP. However, an increase in the deposited metallic Ga concentration several times had led to the reflexes appearance on DP from GaN nanocrystals weakly oriented relative to each other. It should be noted that a similar method of GaN formation on the w-AlN surface leads to the formation of a two-dimensional w-GaN layer of small thickness. Thus, with both methods for the GaN synthesis on g-Si<sub>3</sub>N<sub>3</sub>, in such growth conditions, weakly oriented GaN nanocrystals are formed.

For epitaxial growth of GaN on g-AlN/Si (111), standard growth conditions for the w-GaN two-dimensional growth on w-AlN were used. Epitaxial growth of well oriented 3D GaN islands was observed. It is important to note that the characteristic feature on the observed DP was the presence of g-Si<sub>3</sub>N<sub>3</sub> reconstructed surfaces (8x8) and g-AlN (4x4), which indicates a substrate incomplete coating with newly synthesized GaN. The lattice parameter of three-dimensional GaN islands measured using the lattice parameter of silicon was 3.19 Å, which corresponds to the w-GaN lattice parameter.

We are grateful to RFBR (under grants no. 17-02-00947 and 18-52-00008) and Belarusian Republican Foundation for Fundamental Research grant no. Φ18P-234.

[1] Mansurov V, Malin T, Galitsyn Y, Zhuravlev K. Graphene-like AlN layer formation on (111)Si surface by ammonia molecular beam epitaxy. *Journal of Crystal Growth*. 2015; 428:93-97.

[2] Vladimir G. Mansurov, Yuriy G. Galitsyn, Timur V. Malin, Sergey A. Teys, Konstantin S. Zhuravlev, Ildiko Cora and Bela Pecz (November 12th 2018). Van der Waals and Graphene-Like Layers of Silicon Nitride and Aluminum Nitride [Online First], IntechOpen, DOI: 10.5772/intechopen.81775.

# CONTROL OF THE POLARITY OF GaN EPITAXIAL LAYERS GROWN ON SiC/Si TEMPLATES

**Mizerov A.<sup>1</sup>, Kukushkin S.<sup>2</sup>, Timoshnev S.<sup>1</sup>, Sharofidinov S.<sup>3</sup>, Bouravleuv A.<sup>1</sup>**

*1 - St Petersburg Academic University*

*2 - Institute of Problems of Mechanical Engineering RAS*

*3 - Ioffe Institute*

*andreyimizerov@rambler.ru*

Currently, the GaN-based wide bandgap semiconductors are under the deep study in order to apply them widely in various micro- and optoelectronic devices [1, 2]. However, GaN is usually grown on lattice mismatched substrates, such as sapphire and silicon. This fact results in respectively poor crystal quality of GaN-based heterostructures. Thus, the development of freestanding GaN substrate preparation technique is an important task, which should be solved for the further development of GaN-based technology.

Recently, different studies have been reported to separate GaN from substrates. In particular Ref. [3] reports on the approach for growing freestanding GaN films on Si substrates by integrating plasma assisted molecular beam epitaxy (PA MBE) and metal organic chemical vapor deposition (MOCVD) was demonstrated. In this paper the chemically active N-face self-organized GaN nano-rod structure, grown by PA MBE was employed as a buffer layer for subsequent growth of chemically more resistant Ga-face GaN by MOCVD.

The paper reports on a novel approach to get a 3  $\mu\text{m}$ -thick freestanding GaN film grown on SiC/Si(111) hybrid substrate by integrating PA MBE of N-face GaN and hydride vapor phase epitaxy (HVPE) of Ga-face GaN. In our experiments the hybrid SiC/Si(111) substrates were formed by substitution of atoms [4] on the Si(111) substrates. After that the N-face GaN interlayer with thickness of  $\sim 800\text{nm}$  was grown on SiC/Si(111) substrate by PA MBE [5]. The synthesized GaN/SiC/Si(111) structure was moved into the HVPE reactor for further overgrowth of N-face GaN layer with AlN layer which had inverted, Al-face surface. Finally, the upper detachable, crack-free, Ga-face GaN epilayer with thickness of 3  $\mu\text{m}$  was formed atop of AlN layer by HVPE. After growth, the sample was divided into several parts. Some parts of the sample were etched in KOH solution for different times - 5, 10 and 15 minutes. The scanning electron microscopy studies of the etched parts of the sample showed that increase of the etching time up to 15 minutes result in almost complete disappearance of the N-face GaN interlayer and separation of the upper Ga-face GaN epilayer from the SiC/Si(111) substrate. The PA MBE growth experiments were carried out within the framework of fulfilling the state task of the Ministry of Education and Science of the Russian Federation no. 16.9789.2017/BCh. Morphological studies of the samples were implemented in the framework of the general agreement about scientific research activity between Skoltech and St. Petersburg Academic University (no. 3663-MRA, project 4).

[1] R. Hentschel, J. Gärtner, A. Wachowiak, A. Großer, T. Mikolajick, S. Schmult, *Journal of Crystal Growth*, 500, 1–4 (2018).

[2] G.H. Chung, T.A. Vuong, H. Kim, *Results in Physics*, 12, 83–84 (2019).

[3] Tsung Hsi Yang et. al, *Journal of Crystal Growth* 311, 1997–2001 (2009).

[4] S.A. Kukushkin, A.V. Osipov, *Journal of Physics D: Applied Physics*, 47, 313001 (2014).

[5] S.A. Kukushkin, A.M. Mizerov, A.V. Osipov, A.V. Redkov, S.N. Timoshnev, *Thin Solid Films*, 646, 158-162 (2018).

# GROWTH OF AlN AND GaN BULK CRYSTALS BY SUBLIMATION SANDWICH-METHOD

**Mokhov E.N., Wolfson A.A., Kazarova O.P.**

*A. Ioffe Physical Technical Institute*

*mokhov@mail.ioffe.ru*

GaN and AlN - the most important wide-band semiconductor materials with high binding energy - are used to create a variety of optoelectronic devices, such as light sources with radiation in the visible and ultraviolet regions of light. These materials are also promising for the creation of devices in the field of power electronics, operating at elevated temperatures, high-power fields and penetrating radiation. To realize the potential of these materials, it is necessary to obtain bulk crystals of aluminum and gallium nitrides of high structural perfection with optimal geometric dimensions suitable for use as substrates for obtaining epitaxial structures.

The different methods of AlN and GaN bulk crystals growing are known. In this report emphasis is placed on the sublimation growth method by physical vapor transport (PVT) at optimal source to seed gap. It is shown that at small gaps between them, no more than 0.2 of the linear dimensions of the source, it is possible to obtain high quality bulk crystals of these materials with a diameter of up to two inches at high speeds (up to 0.5 mm/h). The method of sublimation growth at small gaps known as the sublimation sandwich method was proposed by Yu.Vodakov and E.Mokhov in 1970 for the growing of bulk crystals and epitaxial SiC layers, and later for the growth of GaN and AlN crystals.

This work considers the following specific features of sublimation growth of aluminum and gallium nitrides:

- equilibrium vapor over these materials contains practically no metal - nitrogen compounds, which could be transporters of the substance during mass transfer;
- there are kinetic limitations due to extremely low evaporation coefficients (about  $10^{-3} - 10^{-5}$ ) and N<sub>2</sub> sticking probability;
- high probability of formation of 3d-centers on the growing surface, which leads to deterioration of structural perfection of growing crystals;
- selective character of sublimation and condensation processes associated with the presence of the liquid phase on the crystal surface;
- lack of quality large diameter seeds for homoepitaxial growth, in consequence of which the crystals of nitrides has grown on a foreign seeds, for example on SiC wafers.

Our report presents data on the kinetics of sublimation growth of nitrides depending on the temperature, nitrogen pressure and the distance between the source and the seed and growth surface orientation. The mechanisms of sublimation and condensation, the role of the liquid phase formed on the evaporated and growth surface are analyzed. It is shown that selective sublimation on the growth surface causes the formation of pits and deep pores in the process of growth and cooling.

It is shown that at growing of AlN on SiC seeds cracks appear near the phase boundary due to mechanical stresses because of differences in the coefficients of thermal expansion of these materials, propagating along the direction of growth. The ways to eliminate the formation of cracks by evaporation of SiC substrates during growth at the stage preceding the cooling of bulk crystals are found. The two-stage method of growing ingots of nitrides is proposed. It includes obtaining of nitride seeds on substrates of SiC and further growth of the ingots on those seeds in a pure environment and with removed SiC substrate.

The suitability of the grown crystals for obtaining, in particular, ultraviolet LEDs is shown.

# GROWTH OF HIGH PURITY 3 INCH SiC CRYSTALS WITH HIGH STRUCTURAL PERFECTION

Nagalyuk S.<sup>1</sup>, Mokhov E.<sup>1</sup>, Ta Ching H.<sup>2</sup>

*1 - Ioffe Institute*

*2 - Industrial Technology Research Institute*

*snagalyuk@gmail.com*

Silicon Carbide (SiC) is a promising wide-band-gap semiconductor for applications in high-frequency, high-temperature and high-power electronic devices. For this purpose n- and p-type SiC is grown by incorporation of donor impurities, like N, or acceptor impurities, like B, Al and Ga. To further the development of such semiconductor devices a good understanding of the electronic and geometric properties of the created donor and acceptor centers is imperative. A complicating factor in such studies is that SiC can occur in different polytypes, with greatly different band structures, and also that the donor and acceptor impurities seem to occur at different sites in the SiC polytypes.

The SiC 6H 3" diameter crystals were grown by the sublimation (physical vapor transport, PVT) method in a resistively heated furnace with graphite felt thermal insulation. The felt for thermal insulation is Mersen GFA-22 and for rigid felt used a Calcarb CVI. The growth temperature was maintained within 2000–2150°C at the top of crucible and the gas pressure was controlled within 0.2–100 Torr. The main gas is Argon 99.9999% of purity flow rate about 20 sccm.

The axial gradient in the growth zone is about 1-2 ° C degrees per 1 mm. To ensure the stability of the grown 6H polytype, a convex crystallization front is maintained. For growth process was used SiC 6H wafer as seed. The growth face is Silicon face, orientation on axis (0001) +/- 0.5 deg. The Si-Face was optical polished, C-face rough lapped. The crystal growth by sublimation method in the resistive heated machine from specially prepared silicon carbide powder.

The crystal boule slicing to wafers by multi wire machine Takatori MWS. Lapping and polishing of wafers by single side lapping machines. Etching SiC wafer #17-1 was by molten KOH at temperature 450-500 °C, time 7 min. Before etching, wafer was heated to 200-250 °C to avoid cracking in the KOH molten. After etching crystal cleaning by water at 90-100 °C for remove KOH, time of cleaning 5-10 min. The average micropipe density (MPD) investigated by optical microscope. Measure micropipes in visual area and to calculate average micropipe density per cm<sup>2</sup>. The average MPD is about 2.5 per cm<sup>2</sup>. The EPD is about 3\*10E4 cm<sup>-2</sup>

# IMPURITY EFFECTS ON NUCLEATION AND GROWTH OF SiC CLUSTERS AND LAYERS ON Si(100) AND Si(111)

**Pezoldt J.<sup>1</sup>, Lubov M.N.<sup>2</sup>, Kharlamov V.S.<sup>3</sup>**

*1 - TU Ilmenau*

*2 - Saint-Petersburg Academic University*

*3 - Ioffe Physical Technical Institute*

*joerg.pezoldt@tu-ilmenau.de*

The growth of the silicon carbide (SiC) on silicon (Si) allows combining the benefits of SiC physical properties with the well-developed silicon technologies. The SiC/Si heterostructure could be used as substrate for graphene, III-nitrides epitaxy, diamond and gallium oxide and related materials. The main challenge in device processing with SiC/Si structure is the lattice and thermal mismatch between SiC and Si. As a result of a high mismatch SiC grows on Si substrate via Volmer-Weber mechanism (3D SiC clusters form on Si substrate). Pre-deposition of impurities on Si substrate before growth is one of the possibilities to control the nucleation process of SiC clusters and therefore control the quality of SiC/Si interface and the wafer bow. In this work a theoretical and experimental study of the SiC clusters and layers growth on Si substrate with the pre-deposited impurity is presented.

Nucleation and growth of the SiC clusters is simulated in the frames of Kinetic Monte Carlo (KMC) method. The kinetic model takes into account deposition of C atoms on the substrate, formation of Si adatoms on the substrate (and therefore a vacancies in substrate), diffusion of adatoms (Si, C, impurity) and SiC cluster nucleation. Two types of impurities interaction were studied: an attractive (growth of SiC clusters in a presence of surfactant) and repulsive (growth with antisurfactants, like Ge impurity during SiC/Si growth). A KMC simulation code was developed to study the growth of SiC clusters on Si with pre-deposited impurity within the proposed model. With the help of developed KMC code computer simulations of SiC cluster formation on Si surface with and without pre-deposited impurities were carried out. SiC cluster concentrations and lateral sizes for different surface concentrations of repulsive and attractive impurities (0 – 5%) were calculated. The attractive impurities decrease diffusivity of C adatoms nearby and therefore increase the number of nucleation sites, whereas repulsive impurities enhance diffusivity nearby and increase concentration of the C adatoms in the areas between the impurities. An experimental study of the effect of impurities on the growth of layers was carried out using the example of SiC/Ge/Si structure. The samples were grown by molecular beam epitaxy by the deposition of Ge layers (ranging from 0.5 to 8 ML) on the Si substrate followed by the deposition of carbon with the subsequent annealing. Annealing of such C/Ge/Si structures led to the formation of SiC layers on Si substrate. The thickness of the pre-deposited Ge layer significantly affected the characteristics of the resulting films: layer thicknesses, film grain size, roughness. To study the effect of impurities on the formation of SiC layers, it is necessary to know how the impurity is distributed in the structure during annealing. In-depth distributions of components were obtained by SIMS depth profiling measurements. The concentration profiles of the components were obtained from raw SIMS data by means of ballistic modeling of SiC/Ge/Si target sputtering using the dynamic Monte Carlo method. Ge presence before the carbonization procedure leads to: improvement of surface morphology of SiC layer; reduction of the internal strain; increase of the SiC nuclei density and improvement of film crystallinity. Optimum thickness of the pre-deposited Ge layer is 2 MLs. The obtained results showed that pre-deposition of impurities on the Si substrate can significantly influence nucleation and growth of SiC clusters and layers. Thus it is possible to control quality of the SiC/Si interface by implementing impurities.

## TWO DIMENSIONAL ELECTRON GAS FORMATION AT AlGaN/GaN INTERFACES

Caban P.<sup>1</sup>, Thorpe R.<sup>2</sup>, Feldman L.<sup>2</sup>, Michalowski P.<sup>1</sup>, Nielsen S.<sup>3</sup>, Julsgaard B.<sup>3</sup>, Pedersen K.<sup>4</sup>,  
Popok V.N.<sup>4</sup>

1 - Institute of Electronic Materials Technology, 01-919 Warsaw, Poland

2 - Department of Physics & Astronomy, Rutgers The State University of New Jersey, 08854  
Piscataway, USA

3 - Interdisciplinary Nanoscience Center (iNANO), Aarhus University, 8000 Aarhus C, Denmark

4 - Department of Materials and Production, Aalborg University, 9220 Aalborg, Denmark

vp@mp.aau.dk

Wide bandgap semiconductors, such as GaN and SiC, have a number of properties making them advantageous compared to Si in device production. For instance, formation of two dimensional electron gas (2DEG) at AlGaN/GaN interface makes it possible to fabricate high electron mobility transistors (HEMT). Critical AlGaN thickness is an important practical parameter which is under the study in this work.

Ultrathin layers of AlGaN (between 2-20 nm thick) are grown on top of GaN using the metal organic chemical vapour deposition. Composition and thickness of the AlGaN layers is studied using Rutherford backscattering, secondary ion mass spectroscopy (SIMS) and X-ray photoelectron spectroscopy (XPS) combined with ion sputtering. For selected samples, TEM analysis is performed revealing structure of the interfaces. Electron concentration and mobility are measured by Hall effect. Kelvin probe force microscopy is used to study surface potential distribution across the surfaces depending on AlGaN layer thickness.

GaN samples show homogeneous potential maps with a mean value of contact potential difference (CPD)  $0.72 \pm 0.03$  V. For the heterostructures, values of CPD rise with increase of AlGaN thickness reaching 1.21 V for the thickest layers that is in correlation with the band structure. Samples with thin (ca. 2, 4 and 6 nm) AlGaN layers show a mosaic-like potential distribution indicating significant fluctuations of electron density which is probably related to variations of film stoichiometry. Also, inhomogeneity of oxidation may play a role because SIMS show strong oxygen maximum at the surface. The Hall measurements for these samples do not show any reliable data suggesting that 2DEG is not formed yet. Homogeneity of the surface potential increases for layers thicker than 7-8 nm, which is in good correlation with XPS data showing nearly constant Al/Ga ratio of 0.26-0.28. Electron concentration and mobility become measurable. This allows us to conclude about critical thickness of AlGaN for the formation of 2DEG. Similar findings on critical thickness of a barrier layer for the formation of 2DEG were reported using KPFM for LaAlO<sub>3</sub>/SrTiO<sub>3</sub> heterostructures [1]. The obtained results are also in good correlation with earlier data reporting 2DEG observations for AlGaN layers thicker than 3.5 nm, in which the mobility and charge carrier concentration increase reaching maximal values for the layers at around 10 nm [2, 3]. Thus, the current work brings important insights into the formation of 2DEG at AlGaN/GaN interfaces.

[1] V.N. Popok, A. Kalabukhov, R. Gunnarsson, S. Lemeshko, T. Claeson, D. Winkler, *J. Adv. Microsc. Res.* **5**, 26-30 (2010).

[2] J.P. Ibbetson, P.T. Fini, K.D. Ness, S.P. DenBaars, J.S. Speck, U.K. Mishra, *Appl. Phys. Lett.* **77**, 250-252 (2000).

[3] S. Heikman, S. Keller, Y. Wu, J.S. Speck, S.P. DenBaars, U.K. Mishra, *J. Appl. Phys.* **93**, 10114-10118 (2006).

# MBE GROWTH AND PROPERTIES OF III-V AND NITRIDE NANOWIRES ON HYBRID SiC/Si SUBSTRATES. Si DIFFUSION INTO GaN NANOWIRES

**Reznik R.**<sup>1,2,3,4,5</sup>, **Kukushkin S.**<sup>6</sup>, **Osipov A.**<sup>6</sup>, **Talalaev V.**<sup>7</sup>, **Kotlyar K.**<sup>1</sup>, **Cirlin G.**<sup>1,4</sup>

1 - *St-Petersburg Academic University – Nanotechnology Research and Education Centre RAS, Khlopina 8/3, St-Petersburg, Russia*

2 - *Peter the Great St.Petersburg Polytechnic University, Polytechnicheskaya 29, St-Petersburg, Russia*

3 - *St Petersburg University, Universitetskaya Emb. 13B, St-Petersburg, Russia*

4 - *Institute for Analytical Instrumentation RAS, Rizhsky 26, St-Petersburg, Russia*

5 - *ITMO University, Kronverkskiy pr. 49, St-Petersburg, Russia*

6 - *Institute of Problems of Mechanical Engineering Russian Academy of Science, Bolshoj 6, St-Petersburg, Russia*

7 - *Martin-Luther-University Halle-Wittenberg, ZIK SiLi-nano, 06120 Halle, Germany*

*moment92@mail.ru*

The wide-gap nanoheterostructures based on GaN are of great interest for creating electronic and optoelectronic devices [1]. Works in growing GaN layers on silicon [2] have been very promising recently. However, the lattice misfit of such materials is 17%, which leads to the formation of defects of different nature. It is known that the optoelectronic GaN based devices can operate for a long time without degrading despite the high density linear defects. Nevertheless, to extend the lifetime of optoelectronic devices is necessary to increase the perfection of GaN structures.

In this work, in order to reduce the number of dislocations a nanometer (about 50 nm) buffer layer of SiC was used. It is grown on Si by solid-phase epitaxy, which provides extremely low values of the density of misfit dislocations. Since the difference in the lattice parameters between GaN and SiC is only 3%, and also, instead of a planar layer, growth GaN nanowires (NWs), we can count on a radical reduction of the density of structural defects in GaN.

Growth experiments were carried out using Riber Compact12 MBE setup equipped with the effusion Ga cell and the nitrogen source. Growth time of GaN NWs was 16 hours.

After the growth samples were studied by scanning electron microscopy (SEM) and low-temperature photoluminescence (PL) techniques.

Comparison of photoluminescence spectra of grown GaN on hybrid and the most successful GaN NWs structures on silicon shows that the intensity of radiation from grown on SiC buffer layer GaN NWs is more than two times higher than the intensity from the best GaN structures on silicon. This fact leads to the conclusion that grown structures have fewer defects compared with GaN NWs on silicon substrate. This is caused by a smaller lattice constant mismatch between GaN and SiC compared with GaN and Si.

Besides we have discovered a novel mechanism that allows Si to be incorporated into GaN NWs beyond the solubility limit. It is based on the use of vicinal SiC/Si hybrid substrates. The NWs grown on step bunces of vicinal become heavily Si doped. This is verified by the observation of high carrier concentrations in PL and high Si-concentrations by SIMS. Moreover, Raman spectroscopy in concert with quantum chemical modelling indicates the formation of Ga(Si)N solid solution. The microscopic mechanism responsible for heavy doping and even alloying beyond the solubility is diffusion driven by the mechano-chemical effect, which allows extremely efficient injection of Si atoms at the step bunces of vicinal SiC/Si substrates.

Moreover, a possibility of GaAs, AlGaAs and InAs nanowires growth on a silicon substrate with a nanoscale buffer layer of silicon carbide has been demonstrated for the first time. The diameter of these NWs is smaller than diameter of similar NWs which were grown on a silicon substrate, because of significant lattice mismatch. In particular, InAs NWs diameter was less than 10 nm. In addition, based on photoluminescence measurements, it was found that, in case of AlGaAs NWs growth on such substrates, complex structure forms.

1. S. J. Pearton, F. Ren, *Adv. Mater.* **11**, 1571 (2000).

2. I.G. Aksyanov, V. N. Bessolov, S.A. Kukushkin, *Techn. Phys. Lett.* **34**, 479 (2008).

## GaN SELECTIVE EPITAXY IN SUB-MICRON WINDOWS FORMED BY ION BEAM NANOLITHOGRAPHY

**Rodin S.N.<sup>1</sup>, Lundin W.V.<sup>1</sup>, Tsatsulnikov A.F.<sup>2</sup>, Sakharov A.V.<sup>1</sup>, Usov S.O.<sup>2</sup>, Mitrofanov M.I.<sup>1,2</sup>, Levitskii I.V.<sup>1,2</sup>, Evtikhiev V.P.<sup>1</sup>**

*1 - Ioffe Institute, 194021, Politechnicheskaya 26, Saint-Petersburg, Russian Federation*

*2 - Submicron Heterostructures for Microelectronics, Research & Engineering Center, RAS, 194021, Politechnicheskaya 26, Saint-Petersburg, Russian Federation*

*s\_rodin77@mail.ru*

The features of MOCVD epitaxial growth of GaN in submicron windows formed by a focused ion beam are investigated. Investigated structures contain 3 $\mu\text{m}$  thick GaN epitaxial layers on the surface of which ~5nm Si<sub>3</sub>N<sub>4</sub> layers were deposited in a single MOCVD process. Then windows of various shapes were formed using ion beam. The windows had a width of ~300 nm and a length of ~440  $\mu\text{m}$  and were located along the <10-20> GaN direction on 20  $\mu\text{m}$  from each other. The window array had a total size of 4.0 $\times$ 0.44 mm. The remaining surface of the substrate was covered with a layer of Si<sub>3</sub>N<sub>4</sub>. Thus, individual submicron elements or their arrays were obtained on the surface, while the entire surface of the structure between these objects remains a closed by mask.

GaN growth regimes optimized for selective epitaxy in windows with sizes (width) more than 1 $\mu\text{m}$ , formed by conventional lithographic methods, were used. The conventional growth temperature of 1030 $^{\circ}\text{C}$ , low concentration of ammonia, normal or increased, compared with the GaN planar growth, trimethylgallium flow were used for GaN growth. Under these conditions, the growth rate of planar GaN layers was ~5.5 $\mu\text{m}/\text{h}$ . In the case of conventional (non-submicron) selective epitaxy, these growth regimes led to a uniform start of growth in the windows and to a small lateral growth.

Investigations of the selective epitaxy in the stripe windows having submicron sizes showed that in the case of short process duration ( $t = 5\text{-}10\text{sec}$ ), the cross-sectional area of the strip ( $S$ ) increases with time approximately as  $S \sim t^{3/2}$ . At the same time, the number of material embedded in the strips is 2-3 times less than expected for a linear relationship. With increase of the duration of the epitaxial process, the dependence becomes linear. These results obtained differ from the results for selective epitaxy in wide windows ( $>1\mu\text{m}$ ), for which the cross-sectional area was linearly proportional to the deposition duration, the concentration of trimethylgallium and, accordingly, their product (exposure), which is explained by the fact that the growth of GaN is diffusional-limited process.

Thus, the following conclusions were made:

- GaN objects having submicron sizes are formed with a short duration of the MOCVD process of 5-10 seconds;
- The initial stages of the growth of micro- and nanostructures of GaN during selective epitaxy in submicron windows differ significantly from the growth of planar layers and selective epitaxy in windows with sizes  $>1\mu\text{m}$ .

This work was supported by RFBR project № 17-02-01099-a.



# SEMIPOLAR GaN ON A NANOSTRUCTURED Si(100) SUBSTRATE: THE TECHNOLOGY AND THE PROPERTIES

**Rodin S.N., Bessolov V.N., Kompan M.E., Konenkova E.V., Orlova T.A., Panteleev V.N., Seredova N.V., Scheglov M.P.**

*Ioffe Institute, 194021, Politechnicheskaya 26, Saint-Petersburg, Russian Federation*

*s\_rodin77@mail.ru*

**The purpose of work** is to find out the possibilities of synthesis of GaN(10-11) and GaN(10-12) layers depending on the conditions of nanostructuring of the NP-Si(100) substrate and to find the differences in the properties of polar and semipolar layers.

**Technology:** The GaN(0001), GaN(10-11) or GaN(10-12) were synthesized on Si(100) substrate with accuracy of surface orientation  $\pm 0.5^\circ$ . The surface of NP-Si(100) had "nanogrooves" with the value of the period between them  $\sim 100\text{nm}$ , and the height of the "grooves"  $\sim 50\text{nm}$ . The epitaxial growth of GaN layers was carried out by MOCVD and HVPE.

**Experimental results:** X-ray diffraction analysis showed that the GaN(0002) synthesized on NP-Si(100) has a full width at half maximum of the rocking curve  $\omega_\theta \sim 45\text{arcmin}$ , while the GaN(10-11) and GaN(10-12) layers with a thickness of  $1\mu\text{m}$  have  $\omega_\theta \sim 45\text{arcmin}$ , and  $\omega_\theta \sim 60\text{arcmin}$ , respectively, and GaN(10-11) layer grown by HVPE with a thickness of  $4\mu\text{m}$  has  $\omega_\theta \sim 22\text{arcmin}$ . The maximum energies of the photoluminescence spectrum GaN(0001) was  $h\nu = 3.46\text{eV}$ , the spectrum GaN(10-11) –  $h\nu = 3.39\text{eV}$  and  $h\nu = 3.33\text{eV}$ , and the spectrum GaN(10-12) –  $h\nu = 3.36\text{eV}$  and  $h\nu = 3.33\text{eV}$  at  $T = 80\text{K}$ .

The Raman scattering measured in the  $E_2(\text{high})$  region of the phonon mode showed that  $E_2(\text{high})$  had peaks of  $566.1\text{cm}^{-1}$ ,  $566.8\text{cm}^{-1}$  for the layers GaN(0001)/NP-Si(100), GaN(10-11)/NP-Si(100), respectively, and the peak of  $566.2\text{cm}^{-1}$  for the structure GaN(0001)/Si(111). For GaN(0001) and GaN(10-11) layers, the elastic stresses in the structures were  $-0.45\text{GPa}$  and  $-0.29\text{GPa}$ , respectively.

**Conclusions:** It is shown that the use of nanostructured substrate in MOCVD and HVPE are promising for the synthesis of GaN(0001), GaN(10-11) and GaN(10-12) layers, depending on the shape of the surface of the nanostructure.

# THE INFLUENCE OF SILICON SUBSTRATE ORIENTATION WITH A BUFFER SUBLAYER OF SILICON CARBIDE ON THE GROWTH AND POLAR PROPERTIES OF THIN ALUMINUM NITRIDE FILMS

**Sergeeva O.N.<sup>1,2</sup>, Solnyshkin A.V.<sup>1,2</sup>, Kiselev D.A.<sup>2,3</sup>, Kukushkin S.A.<sup>2,4</sup>, Sharofidinov S.<sup>2,5</sup>,  
Kaptelov E.Yu.<sup>2,5</sup>, Pronin I.P.<sup>2,5</sup>**

*1 - Tver State University, Tver, 170100, Russia*

*2 - Herzen State Pedagogical University of Russia, St. Petersburg, 191186, Russia*

*3 - National University of Science and Technology MISiS, Moscow, 119049, Russia*

*4 - Institute for Problems in Mechanical Engineering of the Russian Academy of Sciences (IPME  
RAS), St. Petersburg, 199178, Russia*

*5 - Ioffe Institute, St. Petersburg, 194021, Russia*

*o\_n\_sergeeva@mail.ru*

Thin films of aluminum nitride (AlN) are a promising material for the creation of devices for UV-optoelectronics [1]. The use of a buffer nanolayer of silicon carbide (SiC) allows epitaxially growing AlN layers and heterostructures based on Ga(In)N on a silicon substrate (Si). The presence of a spontaneously polarized state allows the use of these films also as piezo- and pyroelectric transducers [2]. To eliminate the effect of piezodeformation, which is undesirable for optoelectronics, in recent years a new direction of growth of semipolar nitrides has developed, in which the polar vector is at an angle to the surface [3].

In this work, we studied the dielectric, conductive, and polar properties of AlN films grown by the method of hydride-chloride vapor phase epitaxy (HVPE) on Si substrates oriented along crystalline directions of the  $\langle 100 \rangle$ ,  $\langle 110 \rangle$ , and  $\langle 111 \rangle$  types with a buffer SiC sublayer. The dielectric and conductive properties were studied using an E7-20 impedance meter, and the polar state was studied using the dynamic method for studying the pyroelectric effect, and the method of piezoatomic-force microscopy.

The results show that for the structures of AlN/SiC/Si(100) there is a dispersion of capacitance and dielectric losses in the frequency range of 10 Hz-1 MHz, as well as jumps in the volt-farad (C-V) and volt-ampere (I-V) characteristics indicating the presence of a potential barrier at the AlN/SiC and SiC/Si interfaces. Growing films on the (100)Si ( $4^\circ$ ) vicinal surface led to a sharp increase in conductivity and nonlinear I-V dependences caused by the appearance of conducting channels, which are clearly visible in AFM images of surface topography. The structures grown on the (110)Si substrate and the vicinal surface ( $6^\circ$ ) were characterized by the absence of capacitance dispersion, low values of dielectric loss ( $\sim 10^{-3}$ ), and the dielectric character of the I-V dependence. AlN films grown on (111)Si and on vicinal surfaces with small deflection angles had good dielectric properties. Growing on substrates with large angles ( $6-10^\circ$ ) led to a non-linear character of I-V, an increase in conductance by 3-4 orders of magnitude, a strong dispersion of capacity, and a non-linear C-V dependence.

Studies of the polar properties have shown that for the structures AlN/SiC/Si(100) and AlN/SiC/Si(110), piezoresponses at 8 V AC voltage have almost equal values, and the values of pyrocoefficients do not exceed  $1 \text{ nC/cm}^2$ . For AlN/SiC/Si(111) structures, the piezoelectric response is increased up to 8 times, and the pyroelectric coefficient almost doubles. However, as the angle of deviation from the (111) axis increases, the pyroelectric coefficient begins to decrease. The paper discusses the possible causes of changes in the dielectric, conductive, and polar properties of the structures under study.

The work was partly supported by the Ministry for Education and Science (Russian Federation) (Grant No 16.2811.2017/4.6).

1. Lia J. and Fan Z. Y. Appl. Phys. Lett., **89**, 213510 (2006).
2. Kukushkin S.A., Osipov A.V., Sergeeva O.N., et al. Phys. Solid State, **58**, 967 (2016).
3. Romanov A.E., Young E.C., Wu F., et al. J Appl Phys. **109**, 103522 (2011).

# BULK LAYERS OF POLAR AND SEMIPOLAR AlN, GaN AND AlGaN GROWN BY THE HVPE METHOD ON SI PLATES 2 'IN DIAMETER WITH A BUFFER LAYER OF NANO-SiC SYNTHESIZED BY THE ATOMIC SUBSTITUTION METHOD

**Sharofidinov Sh.Sh.<sup>1,2</sup>, Kukushkin S.A.<sup>2</sup>**

*1 - Ioffe Physical-Technical Institute RAS*

*2 - Institute of Problems of Mechanical Engineering of RAS (IPME RAS)*

*sergey.a.kukushkin@gmail.com*

The report describes a new approach to growing thick, about 20 mkm thick for AlN, about 150 mkm for GaN, and up to 400 microns for AlGaN layers on Si (111), (110) and (100) orientations without cracks followed by their possible lead from the silicon substrate. The basis of this approach is as follows. At the beginning, a nano-SiC layer is deposited on the Si surface of the (111), (110) or (100) orientation deviating from the base orientation by  $2^0-7^0$  using the method of chemical substitution of atoms [1,2]. The peculiarity of the properties and structure grown similarly nano-SiC layer is in two main differences between this substrate from other types of substrates with a SiC layer.

The first. In the process of converting Si to SiC under the layer of nano-SiC, specially formed pores are formed, which in the general case may contain SiO material remaining from the synthesis of SiC [1, 2]. At room temperature, SiO is solid, and at temperatures above  $800^0$  C, this substance becomes gaseous. As a result, during the deposition of AlN, GaN, AlGaN films on the surface of a substrate prepared in a similar way, it adjusts to the layer under condemnation and damps the resulting elastic stresses.

The second. Due to the special method of synthesis of the SiC layer, carbon-vacancy structures are formed on its surface [3], which have a positive effect on wetting and surface characteristics of nano-SiC and leads to 2D growth of III-nitride layers

X-ray diffraction, electron diffraction, ellipsometric, Raman, luminescent and other studies of AlN, GaN, AlGaN films have been carried out that prove the high perfection of the structure of the films obtained. The paper presents SEM images of the end cleavages of the grown heterostructures. Real samples of grown films will be presented.

## References

- [1] S.A. Kukushkin and A.V. Osipov. Topical Review. Theory and practice of SiC growth on Si and its applications to wide-gap semiconductor films. J. of Phys. D: Appl. Phys. (2014), **47**. 313001-313041.
- [2] S.A. Kukushkin, A. V. Osipov, and N. A. Feoktistov. Synthesis of Epitaxial Silicon Carbide Films through the Substitution of Atoms in the Silicon Crystal Lattice: A Review. Physics of the Solid State, (2014), **56**, No. 8, pp. 1507–1535.
- [3] S.A. Kukushkin and A.V. Osipov. Mechanism of Formation of Carbon–Vacancy Structures in Silicon Carbide during Its Growth by Atomic Substitution. Physics of the Solid State, (2018), **60**, No. 9, pp. 1891–1896.

## NUCLEATION AND GROWTH MECHANISM OF MOISSANITE - NATURAL SiC

**Shiryaev A.A.<sup>1</sup>, Pavlushin A.D.<sup>2</sup>**

*1 - Frumkin Institute of physical chemistry and electrochemistry RAS*

*2 - Institute of diamond geology SB RAS*

*a\_shiryaev@mail.ru*

Natural silicon carbide – moissanite – is a rare mineral observed in trace amounts in very different environments ranging from interstellar dust to various geological settings. Origin of extraterrestrial SiC grains (usually <10 µm in size) is relatively well understood and most likely they form by CVD mechanism. However, formation of SiC on Earth is much more difficult to explain, since thermodynamics of equilibrium SiC growth implies necessity of extremely reducing conditions, which are seldom encountered.

Earlier we have presented detailed investigation of polytypic composition, trace elements and structure of extensive collection of small (50-200 µm) SiC grains from several kimberlites and other sources and compared them with various types of synthetic SiC (Shiryaev et al., 2011). Concentration of elements like Al and Ti which readily enter SiC lattice is comparable for natural and synthetic samples, but overall concentrations of trace elements in moissanites is usually significantly higher, most likely due to numerous inclusions of native Si, various silicides and oxycarbides. Despite relatively extensive reports on SiC grains in nature, mechanisms of nucleation and growth remain debatable and are largely based on thermodynamic calculations (e.g. Shiryaev & Gaillard, 2014); experimental data are limited.

We present results of characterization of a uniquely large moissanite (~1 mm) crystal from a kimberlite pipe. It possess hexagonal morphology with only slight traces of mechanical damage. A second SiC crystal forms an ingrowth with the host crystal. Confocal light microscopy reveals several growth macrosteps with height ~100 nm, Aside from the macrosteps the surface is extremely flat. Raman spectroscopy show that the crystals belong to 6H polytype with occasional inclusions of 4H and 15R. The surface of the host crystal is covered by a few microns thick very rough film, which is easily detached mechanically. Raman spectra reveal that the film consists of 15R SiC polytype. The film is present both on the flat regions and on edges of the macrosteps.

The studied moissanite samples is small on industrial scale, but for physics of minerals explanation of its formation is a formidable challenge. Possible scenarios of SiC formation in natural environments will be discussed.

### **References:**

Shiryaev et al. (2011), *Lithos*, 122(3–4), 152-164; Shiryaev and Gaillard (2014), *Eur. J. Miner.*, 26, 53–59

# DISLOCATION REACTIONS IN SEMI-POLAR GaN EPITAXIAL LAYERS GROWN ON Si(001) OFFCUT SUBSTRATE USING AlN AND 3C-SiC BUFFER LAYERS

**Sorokin L.M.<sup>1</sup>, Gutkin M.Yu.<sup>2,3,4</sup>, Myasoedov A.V.<sup>1</sup>, Kalmykov A.E.<sup>1</sup>, Bessolov V.N.<sup>1</sup>,  
Osipov A.V.<sup>2</sup>, Kukushkin S.A.<sup>2</sup>**

*1 - Ioffe Institute, 26 Polytekhnicheskaya, St. Petersburg, 194021, Russia*

*2 - Institute of Problems of Mechanical Engineering, V.O., Bolshoj pr. 61, St. Petersburg, 199178, Russia*

*3 - ITMO University, St. Petersburg 197101, Russia*

*4 - Peter the Great St. Petersburg Polytechnic University, St. Petersburg 195251, Russia*

*lev.sorokin@mail.ioffe.ru*

In recent years, gallium nitride (GaN), as a direct wide-bandgap semiconductor (3.4 eV), has become the base material of optoelectronics in the short-wavelength region. High-efficiency UV and blue light-emitting diodes and laser diodes are fabricated on the basis of GaN and related (AlGaN and InGaN) alloys. The growth of GaN-based structures is carried out by heteroepitaxy on foreign substrates such as Al<sub>2</sub>O<sub>3</sub>(0001), SiC(0001) and Si(111). At the same time, the use of Si(001) substrates is attractive in view of the integration of GaN with silicon technology. The use of foreign substrates results in the generation of high density of threading dislocations (TDs) in heterostructures due to lattice mismatch and difference in thermal expansion coefficients of the film and the substrate. TDs can act as non-radiative centers, so the main research activities are focused on the reduction of TD density.

The presence of spontaneous and piezoelectric polarization along the [0001] axis, which considerably decreases the efficiency of light-emitting devices, is another issue of the III-nitride semiconductors with the polar orientation. The use of semipolar orientation can increase the external quantum efficiency.

We present the results of electron microscopy investigation of dislocation reactions in thick (up to 15 μm) semipolar GaN layer grown on the 3C-SiC/Si(001) template without any masking or etching. The growth of GaN and AlN buffer layers was realized by halide vapor phase epitaxy. The off-cut silicon (001) towards the [110] direction was used. The silicon carbide thin layer with the thickness about 100 nm was produced by topochemical substitution of atoms [1]. We show that the expansion of a dislocation half loop with Burgers vector  $\mathbf{b}_2 = \langle 1 \ -2 \ 1 \ 0 \rangle / 3$  in the semipolar GaN layer during cooling process can be blocked by its reaction with a TD with  $\mathbf{b}_1 = \langle -1 \ 2 \ -1 \ 3 \rangle / 3$  to form a dislocation segment with  $\mathbf{b}_3 = \langle 0001 \rangle$ . This dislocation reaction is revealed by the two beam analysis and discussed in terms of the energy relaxation. The first approximation estimate made within the linear tension approach [2] gives the total energy gain  $\sim 7.6 \text{ eV}/\text{\AA}$  (that is, in general,  $\sim 45.6 \text{ keV}$  for the dislocation segment of length 600 nm formed as a result of the reaction). Using the core energy calculations [3], we can also estimate the dislocation core contribution  $\sim 3.1 \text{ eV}/\text{\AA}$  (in general,  $\sim 18.6 \text{ keV}$ ) to this energy gain. Thus, roughly 59% of the energy gain is caused by relaxation of the strain energy of the dislocations, and 41% by decrease in their core energy.

1. S.A. Kukushkin, A.V. Osipov. // J. Appl. Phys. 113 (2013) 024909.

2. J.P. Hirth, J. Lothe. Theory of Dislocations. Wiley, New York, 1982.

3. R. Gröger, L. Leconte, A. Ostapovets. // Comp. Mater. Sci. 99 (2015) 195.

# SYNCHROTRON-BASED PHOTOEMISSION STUDY OF ELECTRONIC STRUCTURE OF GaN GROWN BY PLASMA ASSISTED MOLECULAR BEAM EPITAXY

**Timoshnev S.<sup>1</sup>, Mizerov A.<sup>1</sup>, Benemanskaya G.<sup>2</sup>, Kukushkin S.<sup>3</sup>, Bouravleuv A.<sup>1</sup>**

*1 - Saint-Petersburg National Research Academic University of the Russian Academy of Sciences*

*2 - Ioffe Institute of the Russian Academy of Sciences*

*3 - Institute of Problems of Mechanical Engineering of the Russian Academy of Sciences*

*timoshnev@mail.ru*

III-nitride semiconductor materials are of great interest due to their intensive use in optoelectronic devices operating in a wide spectral range from infrared to ultraviolet. GaN is also the most promising material for the development and creation of new electronic devices based on nanoheterostructures operating in aggressive media at high temperatures, frequencies and power.

The applications in micro- and nanoelectronics require comprehensive knowledge of structural and electronic properties. The most complete information about the electronic structure is given by the results of photoemission studies using photoelectron spectroscopy (PES). Recently the electronic and photoemission properties of Cs/GaN and Ba/GaN interfaces have been investigated [1, 2]. The electronic structure of the Li/GaN interface has not been studied enough.

In this study, we present detailed studies of a considerable variation of the electronic and photoemission properties due to effect of the Li adsorption on the GaN(0001) surface. The submonolayer Li coverage range was used. We demonstrate that the surface states spectrum and the Ga 3*d* and N 1*s* core levels spectra are essentially modified through the Li adsorption.

The epitaxial GaN layers were grown by plasma assisted molecular beam epitaxy on the Veeco's GEN200 MBE system. For activation of the nitrogen, we used high-frequency (13.56 MHz) plasma source Riber RFN 50/63. The substrate temperature was monitored *in situ* by infrared pyrometer. For the growth of undoped GaN layers, we used hybrid SiC substrates made by substitution of atoms on the Si(111) substrates [3]. The growth conditions were used as in paper [4]. The thickness of GaN sample was slightly less ~780 nm.

Photoemission investigations were carried out at the Russian-German beamline of BESSY II synchrotron (Berlin, Germany) by means of PES during synchrotron radiation with photon energies in the range of 75-850 eV. Photoemission studies were performed *in situ* in an ultrahigh vacuum of  $5 \times 10^{-10}$  Torr at room temperature. We recorded the normal photoemission spectra of electrons from the valence band and the spectra of the Ga 3*d*, N 1*s*, and Li 2*s* core levels. The overall energy resolution of the analyzer and monochromator was 50 meV.

Electronic structure of epitaxial layer GaN and Li/GaN interface has been investigated at different Li coverage. We perform first photoelectron spectroscopy study of electronic structure of the ultrathin Li/GaN interface. The evolution of both the surface states and core level spectra with increasing Li coverage demonstrates the adsorption activity of the N- and Ga-dangling bonds on the GaN surface. The intrinsic surface states S1 and S2 at binding energy of ~3 eV and ~7 eV are obtained for the clean GaN surface. The suppression of the S1 and S2 due to Li adsorption is revealed. The Li induced surface band IS1 is found to appear close to the  $E_{VBM}$ . The data can be explained by Li-induced saturation of Ga dangling bonds resulting in both the suppression of intrinsic surface states and semiconducting-like Li/GaN interface.

The growth experiments were carried out within the framework of fulfilling the state task of the Ministry of Education and Science of the Russian Federation no. 16.9789.2017/BCh. Photoemission investigations of the samples were implemented in the framework of the general agreement about scientific research activity between Skoltech and St. Petersburg National Research Academic University, Russian Academy of Sciences, (no. 3663-MRA, project 4). The authors thank Helmholtz-Zentrum Berlin and Russian-German beamline of Synchrotron BESSY II for providing the facilities to perform the experiments and for help during experiments.

## References

- [1] G.V. Benemanskaya, S.A. Kukushkin, P.A. Dementev, M.N. Lapushkin, S.N. Timoshnev, D.V. Smirnov. *Solid State Comm.* 271 (2018) 6.
- [2] G.V. Benemanskaya, S.N. Timoshnev, S.V. Ivanov, G.E. Frank-Kamenetskaya, D.E. Marchenko, G.N. Iluridze. *JETP* 118 (2014) 600.
- [3] S.A. Kukushkin, A.V. Osipov, *J. Appl. Phys.* 113 (2013) 0249091.
- [4] S.A. Kukushkin, A.M. Mizerov, A.V. Osipov, A.V. Redkov, S.N. Timoshnev. *Thin Solid Films* 646 (2018) 158.

## SESSION “Nonlinear and collective phenomena in the process of crystal growth”

### NON-LINEAR EFFECTS IN ELECTRODEPOSITION OF SEMICONDUCTOR NANOSTRUCTURES IN IONIC LIQUIDS

**Borisenko N., Lahiri A., Endres F.**

*Institute of Electrochemistry, Clausthal University of Technology, Arnold-Sommerferd-Strasse 6, 38678  
Clausthal-Zellerfeld, Germany*

*natalia.borissenko@tu-clausthal.de*

One-dimensional semiconductor nanostructures (nanowires, nanotubes, nanobelts) and two-dimensional and three-dimensional macroporous structures have recently attracted a great research interest due to their unique electronic and optical properties and potential applications in nanoscale devices. Semiconductor nanostructures are synthesized using vacuum techniques, which are usually cost-intensive and need vacuum conditions for preparation thus making the semiconductors quite expensive. Therefore, a simple technique to develop such nanostructures is of considerable interest. Electrochemical synthesis is an alternative way to produce these materials. However applying of a proper solvent is essential to produce semiconductors electrochemically. The electrodeposition from aqueous solutions is limited by a relatively low electrochemical stability of water. In the case of molten salts, high temperature is usually required for electrodeposition. Organic solvents are very volatile and many of them are quite toxic. The alternative to common electrolytes is to use ionic liquids (ILs) - materials that are solely composed of ions with melting points below 100-150 °C [1]. In general, ILs exhibit wide electrochemical windows (up to 6 V), good thermal stability, non-volatility, low toxicity and can be liquid even at room temperature that make ILs quite interesting as solvents for electrochemical applications.

In this lecture we will show that ILs are well suited for the electrodeposition of semiconductor macroporous structures and nanostructures (nanowires and nanotubes) with various architectures. Consequently, semiconductor (GaSb, InSb, Si<sub>x</sub>Ge<sub>1-x</sub>, etc.) nanowires, nanotubes and macroporous structures can be synthesized in ILs at room temperature by using template-assisted electrodeposition [1]. Some nanowires (e.g. ZnS and SnSi) can be obtained in ILs without any external template, which opens a new perspective for the synthesis of semiconductor nanostructures. Furthermore, the structure of the IL/electrode interface can significantly alter the deposition process that, in turn, may result in the deposits with various morphologies and properties.

In this lecture we will discuss recent findings on the influence of IL/electrode interface on electrochemical processes, the template assisted and template free electrodeposition of semiconductor nanostructures and non-linear effects in electrodeposition of semiconductor materials in ionic liquids.

#### References:

[1] F. Endres, A. Abbott, D. R. MacFarlane, *Electrodeposition from Ionic Liquids. 2<sup>nd</sup> Edition*. 2017, Weinheim: Wiley-VCH Verlag GmbH & Co. KGaA.

## CLUSTERING AND MELTING IN 2D CUPRATE-LIKE LAYERS

**Chetverikov A.<sup>1</sup>, Ebeling W.<sup>2</sup>, Velarde M.<sup>3</sup>**

*1 - Saratov National Research State University*

*2 - Humboldt University, Berlin*

*3 - University Complutense, Madrid*

*chetverikovap@info.sgu.ru*

Deformation of structure of a two-dimensional CuO<sub>2</sub> layer at different doping when temperature increases is studied by means of numerical simulation. As known the cuprate-like layer is a key element of cuprates which are layered materials most promising for realization of high temperature superconductivity (HTSC) [1]. Here the cuprate-like layer is considered as a combined lattice of two interconnected superposed quadratic sub-lattices, one consisting of rather motionless copper atoms and the other consisting of oxygen atoms free to oscillate near equilibrium positions in potential landscape formed due to mutual action of atoms of copper and oxygen. The density of particles in one layer is two times greater than the density of particles in another layer. Due to the fact the lattice axes in one layer are rotated by 45 degrees relative to the axes in other layer and if the characteristic bond length in one layer is exactly  $\sqrt{2}$  times larger than the bond length in the other layer particles of one layer are placed in the centers of square cells formed by particles of other layer. In this case, potential wells in which particles oscillate have one minimum. However, if the lengths of the bonds are slightly different, the formation of potential wells with two minima is possible. Both types of atoms are modeled as point particles such that O and Cu units interact via Morse potential forces [2]. The idea that nonlinear excitations may play a role for superconductivity [3] is supported by several experimental observations. More recently [4,5], experimental data have been obtained indicating the validity of such statements. Optimal conditions for ensuring the transport of charged particles in CuO<sub>2</sub> layers are achieved at certain levels of doping. In the limit of zero doping, the O-atoms are sitting at equilibrium on a quadratic lattice where they are located halfway between the Cu-atoms. Including temperature, hence heating the system, the O-atoms perform nonlinear oscillations. This effect provides electron transport, however oscillations become to be disordered with increasing temperature. It can be assumed [2] that doping reflects in a small change of the bond length of Cu–O (misfit of characteristic lengths of bonds Cu–Cu and O–O) and it leads to the possibility of bistable configurations. This brings specific effects - formation of stripes (clustering) of O units. We study changing of ordering of distribution of oxygen atoms with increasing temperature at different misfit of the nonlinear oscillations of the O-atoms to demonstrate that such oscillations are more ordered at optimal misfit due to formation of stripes. Also we define a temperature at which stripes begin to destroy and which is close to a melting temperature.

### References

1. A. Mourachkin. High-Temperature Superconductivity in Cuprates: The Nonlinear Mechanism and Tunneling Measurement. 2002 Kluwer Academic Publishers
2. M.G.Velarde. W.Ebeling, A.P.Chetverikov. Soliton-mediated compression density waves and charge density in 2d-layers of underdoped cuprate-like lattices. Comptes Rendus Mecanique (Comptes Rendues Acad. Sci, Paris) 340, 910-916, 2012
3. D.M. Newns, C.C. Tsuei, Fluctuating Cu–O–Cu bond model of high-temperature superconductivity, Nature Phys. 3 (2007) 184–191.
4. Theory of enhanced interlayer tunneling in optically driven high T<sub>c</sub> superconductors. Jun-ichi Okamoto, Andrea Cavalleri, Ludwig Mathey, Physical Review Letters, 117, 227001 (2016)
5. Charge-Stripe Crystal Phase in an Insulating Cuprate. He Zhao<sup>1</sup>, Zheng Ren<sup>1</sup>, Bryan Rachmilowitz<sup>1</sup>, John Schneeloch<sup>2</sup>, Ruidan Zhong<sup>2</sup>, Genda Gu<sup>2</sup>, Ziqiang Wang<sup>1</sup> and Ilija Zeljkovic<sup>1</sup>, arxiv.org/pdf/1812.07013 (2018)



# IN SITU RECONSTRUCTION OF CRYSTAL SHAPE GROWN IN AN AXISYMMETRIC KYROPOULOS SYSTEM

**Duffar T.<sup>1</sup>, Sen G.<sup>1</sup>, Braescu L.<sup>2</sup>**

*1 - Univ. Grenoble-Alpes, CNRS, Grenoble, France*

*2 - Institut National de la Recherche Scientifique - Centre Énergie, Matériaux et Télécommunications, Québec, Canada*

*thierry.duffar@grenoble-inp.fr*

The Kyropoulos growth system is used to grow large high quality sapphire crystals. But since they grow inside a sealed furnace, there is no established monitoring system to allow observing the growth. This makes it difficult to control the growth parameters ensuring a desired geometrical shape. In the present work a melt-height monitoring system is imagined in the growth system, which would allow the acquisition of the evolving melt level along with the pulling distance of seed and the measured weight of the growing crystal submerged in the melt. Based on all these parameters, it is demonstrated that it would be possible to trace in-situ and in real time the shape of the growing crystal. The needed accuracy for the measurement tools is studied.

GAUSSIAN BEAM SPHERE OPTICS IN CONDENSED MATTER RESEARCH

Bredikhin V.

*Institute of Applied Physics of the Russian Academy of Sciences (IAP RAS) 46 Ul'yanov Street, 603950,  
Nizhny Novgorod, Russia*

*bredikh@appl.sci-nnov.ru*

Spherical lenses underlie almost all present-day optical techniques. The theory of the sphere optics, however, is restricted primarily to “paraxial” consideration, when the radius  $r$  of the optical aperture (lens diameter) is much smaller than the radius  $R$  of the sphere. Numerous research studies are concerned with spherical aberrations (SA), when SA-induced distortions can be taken into consideration as a correction, with its role in object image distortions, and possible ways of their minimization. Transparent spheres with  $R \geq \lambda$  have currently become of particular interest for quite a number of problems of the physics of condensed media (2D colloidal crystal structures composed of transparent spheres, photonics crystals and meta-materials) and applications (laser lithography, fiber-optic systems, laser excitation by of high-frequency acoustic radiation waves in liquid systems, super resolution microscopy, biomedical applications, and others).

Optical properties of a “full” sphere, when  $r \approx R$ , i.e. when the sphere is a natural SA, have not been investigated in ample detail so far. Recently many publications appeared on the optics of micro-dimensional spheres having radii  $R$  commensurate with the wavelength of light  $\lambda$ . This is related primarily to the interest in using such spheres as focusing objects for focusing high-power laser radiation on a target in nanolithography applications. It is supposed that the diffraction limit can be overcome in such system, i.e., objects with size much smaller than  $\lambda$  can be created on the target. Strong spherical aberrations make the focusing nontrivial. Usually, the exact solution of sphere optics is obtained using the Mie theory, the generalized Lorenz–Mie theory (GLMT), DFT, DDFT codes, which does not give much of a physical insight as it requires summation of a large number of terms in a multipole expansion even for moderate sphere sizes. In some works it is suggested to use for the calculation of the main focusing properties of transparent dielectric spheres methods of geometrical optics based on spherical and cylindrical functions. All these methods are also rather complicated, labour consuming and require considerable computational power and time, the course of computations is unclear, which complicates physical interpretation of the results.

Among the most developed methods of calculating lens systems, the Gaussian beam approximation widely used in laser optics seems to be optimal for the solution of problems of the sphere optics. As compared to the mathematical apparatuses based on spherical and cylindrical functions, the Gaussian beam approach is well developed; the functions describing Gaussian beams belong to the class of solutions of the wave equation whose modes are self-similar (in other words, they preserve their structure, up to scale, in different sections  $z=\text{const}$ ). It is important that the self-similarity of the Gaussian beams is retained in lens systems. In this work we present an algorithm for describing focusing properties of a transparent sphere within the framework of the traditional geometrical optics using the Gaussian beam approximation that gives a good description of the field in the region of lens caustic. The algorithm developed for the spherical systems was used to create a code for calculating based on standard computation systems spheres with diameters ranging from  $\sim \lambda$  to thousands of  $\lambda$  over the time from a few minutes to a few hours. The results obtained were compared with the data of some authors obtained earlier by more sophisticated methods. Some computations for large spheres having diameters of tens and hundreds of micrometers in vacuum and in light absorbing media, which may be of interest for researchers, are also presented in the report. The proposed algorithm may be used for solution of other physic-technical problems some of which were mentioned above.

**Acknowledgements.** The research was performed with the financial support from the Russia Foundation for Basic Research (grant No. 18-02-00806 a).

# **TWO STEP ANNEALING NiO<sub>x</sub> PROMOTE THE GROWTH OF PEROVSKITE CRYSTAL TOWARD HIGH PERFORMANCE AMBIENT STABLE PEROVSKITE SOLAR CELL**

**Chen Ch.-P.**

*Ming Chi University of Technology*

*cpchen@mail.mcut.edu.tw*

In this study, two step annealing process is utilized to deposit the nickel oxide (NiO<sub>x</sub>) for perovskite solar cell (PSC) application. We compared the optoelectronic properties of the two-step NiO<sub>x</sub> and control NiO<sub>x</sub> (fabricated according to the literature) through X-ray photoelectron spectroscopy (XPS), UV-vis, photoluminescence (PL), conductivity (4-probe detector), transmission electron microscopy (TEM) and ultraviolet photoelectron spectroscopy (UPS). The modified annealing process allows the change in structure and chemical composition of NiO<sub>x</sub> led to the change in work function and the increase in the conductivity of NiO<sub>x</sub> coated ITO substrate. The modified NiO<sub>x</sub> serves as an efficient hole transporting layer promote the growth of perovskite crystal and provide better PL quenching behavior for efficient carrier extraction in the interface. The resulting increases in conductivity and carrier extraction of the PSC devices led to increases in the fill factor (FF) and power conversion efficiency (PCE) of the device. Our champion device displays a PCE of 19.04% which is comparable with the state-of-the-art NiO<sub>x</sub> based PSC. Furthermore, the devices showed excellent air-stability, retaining 97% of PCEs after storage in air for over 672 h (25 °C with a humidity of 40%).

# STRESS-ASSISTED PHASE AND CHEMICAL TRANSFORMATIONS IN SOLIDS VIA CHEMICAL AFFINITY TENSOR

**Freidin A.B.<sup>1,2,3</sup>, Morozov A.V.<sup>1,4</sup>, Muller W.H.<sup>4</sup>, Poluektov M.<sup>5</sup>, Figiel Ł.<sup>5</sup>, Sharipova L.L.<sup>1</sup>**

*1 - Institute for Problems in Mechanical Engineering of Russian Academy of Sciences*

*2 - Peter the Great St. Petersburg Polytechnic University*

*3 - St. Petersburg University*

*4 - Technische Universität Berlin*

*5 - International Institute for Nanocomposites Manufacturing, WMG, University of Warwick*

*alexander.freidin@gmail.com*

Stress-induced and stress-assisted phase transformations and chemical reactions between a deformable solid and diffusive constituents are modeled based on the expression of a chemical affinity tensor equal to the combination of the Eshelby energy-momentum tensors of solid constituents which act as chemical potential tensors with the addition of a chemical potential of the diffusive constituent in the case of a chemical reaction. The chemical potential tensor been introduced in the 70th-80th of XX century basing on the variational Gibbs principle and considerations of phase equilibrium and solid mixtures (see [1] and reference therein). The chemical affinity tensor was derived from fundamental laws and the entropy inequality written for an open system with chemical transformations (see, e.g., Appendix in [2]). Tensorial nature of the chemical potential and chemical affinity was also discussed in [3,4]. The normal component of the affinity tensor acts as a configurational force driving the transformation front. This allows to formulate a kinetic equation in a form of the dependence of the front velocity on the normal component of the affinity tensor. We present solutions of boundary value problems for solids undergoing phase and chemical transformations (see [5,6] and reference therein), including coupled mechanochemistry problems with nonlinear viscoelastic reaction product as it is in the cases of silicon lithiation in Li-ion batteries or silicon oxidation. We demonstrate how stresses induced by the transformation strain and external stresses accelerate or retard or even block the reaction front propagation. The latter corresponds to equilibrium. Then we focus on the blocking effects. We construct forbidden regions in strain space formed by strains at which the front cannot propagate [7] and then examine the stability of the transformation front in the vicinity of the equilibrium. With the use of numerical simulations, we study how instabilities grow during the front propagation. We note that the loss of the front stability may be the source of stress concentrations and further intensive inelastic deformations and damage.

**Acknowledgements.** The authors acknowledge the financial support from the joint project of Russian Foundation for Basic Research (RFBR, Grant No. 17-51-12055) and German Research Foundation (DFG, Grants MU 1752/47-1) and the EU Horizon 2020 funded project No. 685716.

## References

1. Grinfeld, M. (1991) *Thermodynamic Methods in the Theory of Heterogeneous Systems*. Longman, New York.
2. Freidin, A.B., Vilchevskaya, E.N., Korolev, I.K. (2014) *Int. J. of Engineering Sciences*, 83 57-75.
3. Rusanov, A.I. (2005) *Surface Science Reports*, 2005, 58 (5–8), 111–239.
4. Rusanov, A.I. (2006) *Thermodynamic foundations of mechanochemistry*. Nauka, St. Petersburg (In Russian).
5. Poluektov, M., Freidin, A.B., Figiel, Ł. (2018). *Int. J. of Engineering Sciences*, 128, 44-62.
6. Freidin, A.B., Korolev, I.K., Aleshchenko, S.P., Vilchevskaya, E.N. (2016) *International Journal of Fracture*. 202, 245–259.
7. Freidin, A.B., Sharipova, L.L. (2018) In: *Generalized Models and Non-classical Approaches in Complex Materials 1. Advanced Structured Materials*, Vol. 89, Springer, 335-348.

# INVESTIGATION OF ELASTIC PROPERTIES OF NANO SiC GROWN ON Si BY ATOMIC SUBSTITUTION

**Grashchenko A.S., Kukushkin S.A., Osipov A.V.**

*Institute for Problems in Mechanical Engineering RAS, Saint Petersburg, 199178, Russia*

*asgrashchenko@bk.ru*

In this work, we measured the Young's modulus of a nanoscale silicon carbide (SiC) film synthesized on a silicon (Si) substrate by a new method of atomic substitution [1]. Measurements of the Young's modulus were realized by the nanoindentation method, which was formerly used to study the deformation characteristics of SiC films [2]. In this study, two main methods for determining the Young's modulus of solids using nanoindentation data were used. In the first case, to measure the Young's modulus, nanoindentation experiments were done in a purely elastic region. The obtained data were described using the Hertz relation [3] between the reduced Young's modulus, the load and the size of the elastic deformation. As a result of comparison by the least squares method, the Young's modulus of the SiC film E<sub>SiC</sub> is equal 365 GPa. In the second case, the sample was subjected to a series of experiments on nanoindentation, in which the maximal penetration depth of the indenter into the material was varied: 5 nanoindentations for each maximum depth of penetration in the interval from 20 to 400 nm. The nanoindentation data were processed by the Oliver- Pharr method [4], after which the results were averaged over each maximum penetration depth and the dependence of the reduced Young's modulus on the contact depth was constructed. The value of the Young's modulus of the SiC film was determined by comparing the experimental dependence with the theoretical model of Doerner and Nix [5], which was tested in [6]. In this case the least-squares method yields E<sub>SiC</sub>=330 GPa. The experimental results were obtained using the unique scientific facility "Physics, chemistry and mechanics of crystals and thin films" (IPME RAS, St. Petersburg).

Kukushkin S.A. and Osipov A.V. Theory and practice of SiC growth on Si and its applications to wide-gap semiconductor films // J. of Phys. D: Appl. Phys. 2014, 47, 313001-313041.

Grashchenko A.S., Kukushkin S.A., Osipov A.V. Nanoindentation of GaN/SiC thin films on silicon substrate // J. of Phys. and Chem. of Sol. 2017, 102, 151-156.

Hertz H. On the contact of elastic solids // Z. Reine Angew. Mathematik. – 1881. – T. 92. – C. 156-171.

Oliver W. C., Pharr G. M. An improved technique for determining hardness and elastic modulus using load and displacement sensing indentation experiments // Journal of materials research. – 1992. – T. 7. – №. 6. – C. 1564-1583.

Doerner M. F., Nix W. D. A method for interpreting the data from depth-sensing indentation instruments // Journal of Materials research. – 1986. – T. 1. – №. 4. – C. 601-609.

Grashchenko A.S., Kukushkin S.A., Osipov A.V., Redkov A.V.. Nanoindentation of GaN/SiC thin films on silicon substrate // Journal of Physics and Chemistry of Solid, 2017, 102, p. 151-156.

# USING RECOVERED SILICON NANOPARTICLES FROM SILICON WIRE SAWING TO MODIFY THE SURFACE OF GRAPHENE NANOSHEETS FOR Li -ION BATTERIES ANODE APPLICATION

**Hecini M.<sup>1</sup>, Beddek S.<sup>1</sup>, Drouiche N.<sup>1</sup>, Aoudj S.<sup>2</sup>, Palahouane B.<sup>1</sup>**

*1 - The Research Center in Semiconductor Technology for Energetics, CRTSE*

*2 - Blida 1 University*

*mounasfn@yahoo.fr*

Polycrystalline silicon is one of the most important materials in the photovoltaic (PV) industry. The cost to produce Si wafers accounts for approximately 30-40% of the total solar cell fabrication cost. However, in the wire sawing process of silicon ingot into thin wafers only 60% of the ingot is processed into wafers, the rest being in the form of fine silicon particles mixed with used cutting fluid composed of a mixture of polyethylene glycol (PEG), abrasive in the form of silicon carbide microspheres (SiC) and iron (from the steel of the cable).

The silicon sludge contains valuable resources including high purity silicon, for this reason the recovery of nanometer-sized silicon (Si) particles from the sludge, particularly for Li-ion batteries applications, represents a very important step. Silicon has a much lighter and larger energy density and capacity than graphite and has been shown to have a high theoretical gravimetric capacity, approximately 4200 mA h/g, compared to only 372 mA h/g for graphite. Thereby, silicon anodes composed of silicon nanoparticles have demonstrated great potential as an anode material to replace the commonly used graphite.

The recycling consists of removal of the PEG by liquid-liquid extraction and distillation, magnetic separation was used to remove Metallic impurities, the Si nanoparticles were separated from SiC by phase transfer separation and by applying controlled ultrasonic waves and centrifugation in series. Si microparticles are purified by Rapid Thermal Process (RTP). The optimal results show that the Si-rich powder can reach 82% wt% Si and SiC-rich phase contains more than 91 wt% SiC.

A facile approach to fabricate the freestanding Si/graphene composite membrane for Si anode in a large scale was investigated by anchoring of Si nanoparticles onto the surface of graphene oxide sheets, allowing control over uniformly inserting Si nanoparticles into the pores between graphene sheets from nanoscale to macroscale.

## **References:**

1. M. Hecini, N. Drouiche, O. Bouchelaghem, *J Cryst Growth* 453, 143–150 (2016)
2. L. Yan, J. Yu, H. Luo, *Appl Mater Today* 8, 31–34 (2017)
3. F. Menglu, W. Zhao, C. Xiaojun, G. Shiyu, *Appl Surf Sci* 436, 345-353 (2018)

# CRYSTAL GROWTH OF LARGE ANISOTROPIC $\text{La}_2\text{NiO}_{4+\delta}$ PLATELETS VIA MOLTEN-FLUX

**Hinterding R.<sup>1</sup>, Zhao Z.<sup>1</sup>, Zhang C.<sup>2</sup>, Feldhoff A.<sup>1</sup>**

*1 - Leibniz University Hannover, Institute of Physical Chemistry and Electrochemistry*

*2 - Leibniz University Hannover, Institute for Mineralogy*

*richard.hinterding@pci.uni-hannover.de*

Anisotropic materials as  $\text{La}_2\text{NiO}_{4+\delta}$  make it difficult to utilize their full potential due to direction-dependent transport mechanisms. One possible way to overcome this problem is the crystal growth of large anisotropic sheets, which allow an easier arrangement in bulk materials than their nanoscaled counterparts. Therefore, the molten-flux synthesis was applied to the mixed ionic-electronic conducting oxide  $\text{La}_2\text{NiO}_{4+\delta}$ , which is known for its anisotropic transport properties in e.g. electrical conductivity or oxygen transport. To understand and control the crystal growth mechanism, synthesis parameters as water content, reagent homogeneity or heating duration were varied. Melt of NaOH was used to dissolve precursors, which were either coarse mixtures of the oxides  $\text{La}_2\text{O}_3$  and NiO from a classical solid state route or ultrafine mixtures of  $\text{La}_2\text{CO}_3$  and NiO from a sol-gel process. To estimate optimum synthesis temperature for the sol-gel process, reaction sequence was monitored by in-situ X-ray diffraction. The molten-flux synthesis in ambient air was conducted at 400 C for up to 14 hours with variation of additional water content and the precursor stoichiometry. Purity and composition of products were investigated by ex-situ X-ray diffraction and wavelength dispersive X-ray spectroscopy. Detailed information about the crystal structure was gained by scanning tunneling electron microscopy and electron diffraction patterns. A maximum length of platelets of ca. 30 microns was observed at a thickness of ca. 2 microns (i.e. aspect ratio of 15). By varying several parameters of the molten flux synthesis, both size and aspect ratio of  $\text{La}_2\text{NiO}_{4+\delta}$  platelets could be varied over a wide range. The experimental results allow better understanding of the crystal formation in molten-flux and the gained anisotropic platelets are promising regarding their application in bulk materials.

Reference: R. Hinterding, Z. Zhao, C. Zhang, A. Feldhoff, *Anisotropic growth of  $\text{La}_2\text{NiO}_{4+\delta}$ : Influential pre-treatment in molten-flux synthesis*, submitted to J. Cryst. Growth.

# **SURFACE OXIDATION EFFECT ON PHOTO-REACTIVITY OF TOPOLOGICAL INSULATOR $\text{Bi}_2\text{Se}_3$ THIN FILMS AS A FUNCTION OF AIR EXPOSURE TIME**

**Hong S.-B.<sup>1</sup>, Chae J.<sup>1</sup>, Kim D.-K.<sup>1</sup>, Jeong K.<sup>1</sup>, Kim H.<sup>2</sup>, Yoo B.<sup>3</sup>, Cho M.-H.<sup>1</sup>**

*1 - Department of Physics, Yonsei University, Seoul, 03722, Korea*

*2 - School of Advanced Materials Science and Engineering, Sungkyunkwan University, Suwon 16419, Korea*

*3 - Department of Materials Engineering, Hanyang University, Ansan-si, Gyeonggi-do, 426-791, Korea*

*mh.cho@yonsei.ac.kr*

Topological insulators are receiving attention in the field of optoelectronic device due to their broadband and high sensitive properties attributed from a narrow bandgap of a bulk state and high mobility of a Dirac surface state. The changes in the state of  $\text{Bi}_2\text{Se}_3$  by oxidation in aspects of the band structure and electrical characteristics have been actively studied, while the photo-reactivity of  $\text{Bi}_2\text{Se}_3$  depending on the oxidation has not been studied in detail. In this work, we investigated the change in optoelectronic properties of  $\text{Bi}_2\text{Se}_3$  as a function of air exposure time and verified the role of the oxidation effect on the  $\text{Bi}_2\text{Se}_3$ . For the preparation of the  $\text{Bi}_2\text{Se}_3$  5QL (1 Quintuple Layer = 0.954nm) thin films, Bi and Se were sequently deposited on the  $\text{SiO}_2/\text{Si}$  substrate by thermal evaporation in ultrahigh vacuum chamber (UHV) and annealed 230 °C 30 minutes. We exposed the  $\text{Bi}_2\text{Se}_3$  in ambient condition for oxidation and measured photocurrent and X-ray photoelectron spectroscopy (XPS) along with the oxidation time. We investigated the oxidation mechanism of the  $\text{Bi}_2\text{Se}_3$  by evolution of chemical bond using XPS results. We also verified the changes in the intensity of saturation photocurrent depending on the exposure time. From the results of XPS and photocurrent, the relationship between the oxidation process and photo-reactivity of  $\text{Bi}_2\text{Se}_3$  was confirmed. As a result, we clarified the relationship between surface oxidation effect and photo-reactivity of thin film topological insulator  $\text{Bi}_2\text{Se}_3$ , which suggests a meaningful result in the application of TI based optoelectronic device.



# HIGH RESOLUTION ANALYSIS ON Ni/Au/Ni/Au Ohmic CONTACT TO p-AlGaIn/GaN SEMICONDUCTOR

**Hu Z.-F.<sup>1</sup>, Li X.-Y.<sup>2</sup>, Zhang Y.<sup>2</sup>**

*1 - School of Materials Science and Engineering, Tongji University, Shanghai 201804, China*

*2 - Key Laboratory of Infrared Imaging Materials and Detectors, Shanghai Institute of Technical Physics, Chinese Academy of Sciences, Shanghai, 200083, China*

*huzhengf@tongji.edu.cn*

The low-resistance ohmic contact Ni/Au/ p-type AlGaIn/GaN was carefully investigated by high resolution electron microscope (HRTEM) and X-ray photoelectron spectroscopy (XPS) after two-step annealing at 550°C and 750°C. It is shown that complicated double-direction diffusion and reaction occurred in the metal layer and underlying GaN layer. The four metal stacks of Ni/Au/Ni/Au turned into almost one layer and an intimate relationship established at Ni/Au/GaN boundary which should play a primary role in ohmic contact to low the contact barrier. A great part of Ni atoms are oxidized and the oxide NiO is dispersive in metal layer which has an obvious effect to hinder Ga atoms emigrating upward. At the intimate interface, the metal layer close to the contact enriched with Ga and Au and the GaN upper layer metalized by Au and Ni. These characteristics may further low the contact barrier. Dislocations connected with the contact boundary absorbed interstitial atoms of Au or Ni may serve as channels for current carrier transportation as well.

# CHEMICAL CHARACTERISTICS OF STEAM-INDUCED HYDROXIDE COMPOSITE FILM SURFACE FORMED ON Mg ALLOYS

Miyashita T., Inamura M., Serizawa A., Ishizaki T.

*Shibaura Institute of Technology*

*ishizaki@shibaura-it.ac.jp*

Magnesium alloys have superior physicochemical properties such as high strength ratio and high damping capacity. However, they have a significant fault that is a low corrosion resistance. Various surface treatment methods have been developed to improve the corrosion resistance. Chemical conversion have been frequently utilized, however, they required treatment of liquid waste before disposal, leading to environmental load. Thus, it is essential to develop an environmentally-friendly surface treatment method to improve the corrosion resistance. We have developed a novel and environmentally-friendly coating technology, i.e., steam coating. In this study, we report on chemical characteristics of hydroxide composite film formed on Mg alloys by steam coating.

Mg alloys used as the substrate were ultrasonically cleaned in absolute ethanol for 10 min. The steam coating was performed using an autoclave made of stainless steel. 20 mL of ultrapure water was placed at the bottom of the autoclave to produce steam. The cleaned Mg alloy was set at substrate stage in the autoclave. The autoclave was maintained at a temperature of 433 K for 6 h.

XRD patterns of film-coated Mg alloy revealed that the film had some peaks of brucite-type  $\text{Mg}(\text{OH})_2$ . Two peaks at approximately  $2\theta = 11^\circ$  and  $23^\circ$  could be assigned to 003 and 006 diffraction peaks of  $\text{Mg}_{1-x}\text{Al}_x(\text{OH})_2(\text{CO}_3)_{x/2} \cdot n\text{H}_2\text{O}$  (Mg–Al LDH). These results show that the crystalline Mg–Al LDH was included in the  $\text{Mg}(\text{OH})_2$  film. Polarization curve measurements demonstrated that the corrosion resistance of the films coated magnesium alloy was greatly improved compared to the untreated one. Immersion tests in 5 wt.% NaCl aqueous solution were also performed to evaluate the corrosion rate of the film coated Mg Alloys.

## Acknowledgement:

This study was supported by Japan Science and Technology Agency (JST), Adaptable and Seamless Technology transfer Program through Target-driven R&D (A-STEP: AS2815047S), and Program on Open Innovation Platform with Enterprises, Research Institute and Academia (OPERA) (No. 18072116).

# HIGH-SPEED FORMATION OF SINTERED BOND-LINE BY ADDITION OF 350 nm Cu OR Cu@Ag PARTICLES BETWEEN MICRON Cu@Ag PARTICLES

**Jong-Hyun L., Sung Yoon K.**

*Seoul National University of Science and Technology*

*pljh@snut.ac.kr*

Soldering technique is with the history of mankind and solders have been used as an interconnection material for bonding and mounting of various electronic devices ever since the rapid expansion of semiconductor industry in the late 1900's. Although soldering enable many components to be simultaneously bonded at a time under relatively short time, following some problems are still restricting its application fields. As a representative drawback, low melting points of solders remains reliability issues such remelting or abrupt drop of mechanical properties in the application for the bonding material of high heat-generating devices. Without the suggestion of novel composition or technical progress regarding solder alloys of high melting points, high Pb-bearing composition is still used as a representative solder of high melting point. However, the enactment of ban regarding the prohibition of use of Pb and the pursuit of more reliable interconnection materials in high temperature are requiring researches for novel bonding methods and materials. Another notable drawback of solders is their low thermal conductivity. Under the miniaturization of electronic modules and products, solders cannot be considered any longer as a suitable interconnection material for heat dissipation.

The most representative process urgently needed to get away from the use of a traditional soldering method or a bonding material owing to above-mentioned problems about solders is the mounting of power devices on a direct bonded copper substrate in an electric motor vehicle industry. Although transient liquid phase (TLP) bonding, the modification of a soldering method, has been extensively studied, following problems continue to appear; the formation of stable intermetallic compound by TLP usually requires abnormal long bonding time approaching several hours.

With exchange of a bonding material, silver (Ag) particles has been considered as the first priority owing to both its extremely high thermal conductivity and good antioxidation. As the bonding using Ag particles proceeds by sintering, bonding time is inherently long compared with a soldering process. The time has been shortened using replacement or addition of Ag nanoparticles. However, the high cost of Ag is bigger problem. The use of nanoparticles additionally elevates the material cost.

As a next sinter-bonding material indicating high thermal conductivity in spite of low cost, copper (Cu) has been recently received lot of attention. Cu, which exhibits high electrical and thermal conductivities approaching those of Ag, is considered the best low-cost alternative material. However, the easy surface oxidation of Cu severely impairs its application as a bonding material. Hence, a die attachment technology has been suggested using Ag-coated Cu (Cu@Ag) with the oxidation suppression in the Cu core by the Ag shell. Moreover, the Ag shell was transformed into small nodules by the dewetting during heating and the formation of dense bond-line by sinter bonding between particles proceeded rapidly through fast Ag transfer from the top regions of the nodules, aided by the applied external pressure. In the mechanism, the adoption of cheaper micron Cu@Ag particles necessarily induces the formation of big voids between the particles, which is detrimental directly to bonding strength. Therefore, a more enhanced sinter-bonding process was suggested in this study by adding 350 nm Cu or Cu@Ag particles of optimum amount.

# ENERGY BAND DIAGRAM ANALYSIS OF TiO<sub>2</sub>/ELECTROLYTE INTERFACE IN PHOTOELECTROCHEMICAL CELL

Hien T.T., Quang N.D., Kim C., Kim D.

*Chungnam National University*

*dojin@cnu.ac.kr*

The solid-liquid interface in photoelectrochemical cell is revisited based on the energy diagram to elucidate the TiO<sub>2</sub> nanorod and various electrolytes of different pHs [1]. The photocurrents with the external bias are examined under the various electrolytes of H<sub>2</sub>SO<sub>4</sub>, NaCl, and NaOH. The energy diagrams of the whole PEC system as the water splitting device are constructed based on the current-voltage measurements in three-electrode configuration. Electrode potentials and photocurrents measured with the external bias in dark and under light are systematically correlated with the energy diagram of the PEC system. The pH dependent flat-band potential is explained by applying the pH dependent Helmholtz layer potential at the interface. In addition, the distribution of the applied potential in the PEC system during the water splitting process is understood by in-depth understanding of the energy band diagram.

## **A STUDY ON RECOVERY OF HIGH PURITY VALUABLE MATERIALS FROM END-OF - LIFE THIN FILM PHOTOVOLTAIC PANELS**

**Kim T.Y., Cho S.Y., Lee W.G.**

*Chonnam National University*

*tykim001@jnu.ac.kr*

End-of-life photovoltaic modules can be hazardous wastes if they contain hazardous materials. The main problem arising from this type of waste is the presence of environmentally toxic substances and the poor biodegradability. The present study deals with end-of-life polycrystalline silicon type photovoltaic modules. The photovoltaic modules are composed of silver, silicon and aluminum. The removal of Al from photovoltaic module was investigated in terms of concentration and temperature of phosphoric acid solution. After removal of Al from photovoltaic module, using nitric acid solution got rid of Ag from the module. The removal ratio of Al and Ag using phosphoric acid and nitric acid solution from the photovoltaic modules was 99.99%, respectively. The purity of valuable metals (Al, Ag) and silicon (Si) was analyzed by Energy Dispersive X-ray Spectroscopy(EDS) and Inductively Coupled Plasma (ICP).

# SIMULATION OF RADIATION-INDUCED SEGREGATION IN Fe–Cr–Ni ALLOYS

Skorokhod R.V., Koropov O.V.

*Institute of Applied Physics of NAS of Ukraine, 58, Petropavlivska St., 40000 Sumy, Ukraine*

*r.skorokhodqq@gmail.com*

Radiation-induced phenomena can lead to deterioration of the physical, chemical and mechanical properties of reactor structural materials [1]. One such phenomenon is the radiation-induced segregation (RIS), which consists in the spatial redistribution of components of a metal alloy under irradiation at elevated temperature. As a result, the enrichment or depletion of impurity and alloying components of the metal alloy can be observed in regions near surfaces, dislocations, voids, grain boundaries, and phase boundaries [2]. Such local changes in the concentration of components of the metal alloy, in particular, may lead to the formation of a supersaturated solid solution and to occurrence of precipitates of a new phase [3]. Of particular importance is the research of RIS in modern reactor materials that receive high doses of radiation damage (more than 40 displacements per atom) over a long service life and at the same time must retain the necessary mechanical and physical-chemical properties and stable dimensions [1].

In this work, the modified inverse Kirkendall model [2], which takes into account defect sinks inside the alloy for simulation of RIS in Fe–Cr–Ni alloys is used. Also, the grain boundary with low misorientation angle is considered as an array of dislocations [2, 4, 5]. The RIS in Fe–Cr–Ni alloys is described by a system of four coupled nonlinear partial differential equations, which describes the spatial and temporal dependence of the concentrations of alloy components and point defects (vacancies and interstitials) [6]. A computer code based on previously proposed [7] for numerical solution of this system is developed.

The present paper concerns calculation of the concentration profiles of components of a ternary Fe–Cr–Ni alloy and the concentration profiles of point defects in it under the irradiation for various initial temperatures, dose rates and doses. The process of achievement of steady state at dose rising is demonstrated. Grain boundary significance for alloy component concentration with respect to input parameters is evaluated. Similar to work [8], it is shown that under different dose rates, similar concentric profiles of the alloy components can be obtained using different irradiation temperatures to counteract the effect of the dose rate variation.

The work is performed within the framework of the scientific research program of the NAS of Ukraine "Support for the development of priority areas of scientific research".

## References

1. V.N. Voyevodin, I.M. Neklyudov. Evolution of the structure-phase state and radiation resistance of structural materials. Naukova Dumka, Kiev. (2006) 376 p. (in Russian)
2. G.S. Was. Fundamentals of Radiation Materials Science: Metals and Alloys. Springer-Verlag, Berlin (2007). 828 p.
3. O.V. Koropov, R.V. Skorokhod. East European Journal of Physics (1), 75 (2019). (in Ukrainian)
4. K.G. Field, L.M. Barnard, C.M. Parish, J.T. Busby, D. Morgan, T.R. Allen. J. Nucl. Mater. **435**, 172 (2013).
5. K. Vörtler, M. Mamivand, L. Barnard, I. Szlufarska, F.A. Garner, D. Morgan. J. Nucl. Mater. **479**, 23 (2016).
6. O.V. Koropov. Proc. of Eighteenth International Scientific Mykhailo Kravchuk Conference. NTUU "KPI", Kyiv. (2017). P. 86-90. (in Ukrainian)
7. R.V. Skorokhod, O.M. Buhay, V.M. Bilyk, V.L. Denysenko, O.V. Koropov. East European Journal of Physics **5**(1), 61 (2018). (in Ukrainian)
8. D. Xu, G. VanCoevering, B.D. Wirth. Comput. Mater. Sci. **114**, 47 (2016).

## WAVE HEAT PROCESSES IN LOW-DIMENSIONAL MATERIALS

**Krivtsov A.**

*Institute for Problems in Mechanical Engineering of the Russian Academy of Sciences (IPME RAS)*

*akrivtsov@bk.ru*

Methods and applications of mechanics of discrete media are presented. We consider problems where continuity of the media is broken either due to its discrete structure, or due the nature of the occurring processes. The anomalous thermal processes are considered in details: non-monotonic thermal relaxation, thermal superconductivity, and etc. Approaches allowing an analytical description of these processes are presented. It is shown that heat propagation in such systems is performed at a speed close to the speed of sound, which opens possibility for prespective practical applications.

# ADSORPTION INDUCED DEFORMATION AND PHASE TRANSFORMATIONS IN NANOPOROUS CRYSTALS

Neimark A.V.

*Department of Chemical and Biochemical Engineering, Rutgers University, Piscataway, NJ 08854*

*aneimark@rutgers.edu*

Nanoporous crystals represent a wide class of porous solids possessing crystallographic symmetry, such as zeolites, mesoporous molecular sieves (MMS), and metal-organic frameworks (MOF). Nowadays, MOF materials are of particular interest with thousands of structures synthesized within last 20 years. MOFs are 3D porous crystals built by metal atoms connected by organic linkers. Organic linkers may rotate, contract and expand, providing structure flexibility. When a fluid is adsorbed in pores, it exerts a stress that causes deformation of the solid matrix. Depending on the material structure, this deformation may be rather small (fractions of percent) or phenomenally large (hundreds of percent). In some cases, adsorption may induce sample contraction rather than swelling that seem to be counterintuitive. Moreover, adsorption-induced deformation may trigger phase transformations in MOFs, known as gate-opening and breathing transitions. The phenomenon of adsorption induced deformation is currently actively explored with respect to the design of novel flexible adsorbents and membranes for hydrocarbon separation, actuators, nanobumpers, energy storage devices; it plays an important role in oil and gas recovery from shales and carbon dioxide sequestration in coal mines.

I will present a unified theoretical approach that extends the Gibbs excess adsorption thermodynamics to poroelastic nanomaterials. The proposed theory is based on the notion of the adsorption stress tensor, which depends on the geometrical specifics of the material under consideration (pore size, shape, etc) and the potential of fluid-solid intermolecular interactions between fluid and solid. The adsorption stress can be calculated by using the density functional theory and/or Monte Carlo simulations, as well as empirical or classical thermodynamics theories.

Application of the adsorption stress approach allowed us to explain in a unified fashion distinct mechanisms of adsorption deformation, which will be demonstrated on examples of zeolites, micro- and mesoporous carbons and silicas, and MOFs. Special attention will be paid to the breathing transitions in MOFs of wine-rack morphology associated with transformations between narrow pore and large pore structures.

## Selected references

1. C. Balzer, A.M. Waag, S. Gehret, G. Reichenauer, R. Morak, L. Ludescher, F. Putz, N. Hüsing, O. Paris, N. Bernstein, G.Y. Gor, and A.V. Neimark, *Langmuir*, 2017, 33, 559.
2. H. S. Cho, H. Deng, K. Miyasaka, Z. Dong, M. Cho, A.V. Neimark, J. K. Kang, O.M. Yaghi, and O. Terasaki, *Nature*, 2015, 527, 503.
3. A.V. Neimark, F.X. Coudert, C. Triguero, A. Boutin, A. H. Fuchs, I. Beurroies, and R. Denoyel, *Langmuir*, 2011, 27, 4734.
4. G. Yu. Gor and A.V. Neimark, *Langmuir*, 2010, 26, 13021.
5. A.V. Neimark, F.X. Coudert, A. Boutin, and A. H. Fuchs, *J. Phys. Chem. Letters*, 2010, 1, 445.
6. P.I. Ravikovitch and A. V. Neimark, *Langmuir*, 2006, 22, 11171.



# THE TENSILE STRENGTH OF SiC FIBERS WITH THIN ZIRCONIA COATINGS DERIVED BY DIFFERENT METHODS

**Prokip V.E.<sup>1</sup>, Lozanov V.V<sup>1</sup>, Morozova N.B.<sup>2</sup>, Baklanova N.I.<sup>1</sup>**

1 - ISSC SB RAS

2 - NIIC SB RAS

*prokipvlad@gmail.com*

Silicon carbide composites reinforced by the silicon carbide fibers (SiC/SiC<sub>f</sub> composites) are of great interest in modern high-temperature applications. It is known that the mechanical behavior of the ceramic matrix composites (CMC's) directly depends on the properties of the interphase, an thin (usually, less than 1 micron) rintermediate layer(s) between a fiber and a matrix [1]. Zirconia has been also considered as a candidate for interphase material in SiC/SiC<sub>f</sub> composites due to its oxidation resistance, compatibility with SiC materials and simplicity of methods for fabrication as coatings and thin films [2]. The recent study of the sol-gel derived ZrO<sub>2</sub> coated fibers showed that the fiber/matrix decoupling in SiC/(ZrO<sub>2</sub>)<sub>n</sub>/SiC<sub>f</sub> composites can be regulated by designing of the multiple ZrO<sub>2</sub> interphase. However, in the process of the formation and exploitation of a composite, SiC reinforcing fibers undergo a multiple heat treatment procedure, which may cause changes in their strength characteristics. Since the fibers in the composite perform the reinforcing function, the degradation of their mechanical properties can lead to a drop in the strength of the composite as a whole. Most of the brands of reinforcing fibers SiC are characterized by high tensile strength properties. Therefore, it is importantly to conserve the level of these properties during interphase processing and further exploitation at high-temperatures.

The purpose of this work was to study the effect of the thin zirconia coatings derived by different methods on the tensile strength of the silicon carbide fibers.

As a substrate material, silicon carbide fibers of two brands Nicalon CG (Nippon Carbon Co, Japan) and Tyranno SAK (Ube Industry, Japan) were used. Zirconium dioxide coatings were applied using the sol-gel and MOCVD method. To apply coating according to the first method, a desized fiber tow was immersed in sol for 1 min. After drying in air, the tows were heat-treated in vacuum at 900 for 1 h. To produce multilayered zirconia coatings, the cycle was repeated 5 times. The microstructure of the coated fibers was investigated by high-resolution scanning electron microscopy combined with energy dispersive spectroscopy. The tensile strength of the as-prepared and zirconia-coated fibers was determined at room temperature on an Instron mechanical testing machine. At least one hundred individual tensile strength values for each type of sample were determined. The obtained values were processed using a bimodal two-parameter statistical Weibull distribution.

It was established that the tensile strength and Weibull moduli of the initial SiC fibers is effected by the thermal treatment. However, the Nicalon fiber degrades in greater extent than Tyranno SAK fiber that can be related to the composition and microstructure of fibers themselves. The application of the thin zirconia coatings, especially multilayered coatings also results in the decrease in tensile strength. The reasons of degradation of the mechanical properties of the uncoated and zirconia-coated SiC fibers are discussed in terms of microstructure of the coatings, methods for their application and the quantity of layers.

The obtained results are especially important for the development of CMC's reinforced with fibers, and prediction the performance of a composite material during exploitation.

[1] A.G. Evans, D.B. Marshall, General Atomics, San Diego, California (1990), pp. 1-39

[2] A.V. Utkin, A.A. Matvienko, A.T. Titov, N.I. Baklanova, Surface and Coatings Technology, 2011, V. 205, pp. 2724-2729

This work was supported by RFBR grant № 18-29-17013

# GROWTH OF A FACETED PORE IN CRYSTALLINE MEDIA VIA BURTON-CABRERA-FRANK MECHANISM

**Redkov A.V., Kukushkin S.A.**

*Institute for Problems in Mechanical Engineering*

*avredkov@gmail.com*

The work is devoted to the development of the crystal destruction theory for multicomponent systems. One of the approaches to describe the process of destruction is based on ideas about the formation of pore nuclei from a gas of vacancies and their growth under the influence of a tensile load, the detailed description of which is described in [1-4]. The main provisions of this concept are that the destruction of a crystal occurs in several stages. At the first stage, an excess of vacancies arises in the crystal under the influence of a tensile load, which, according to the nucleation theory, begin to form pore nuclei. After the nucleation process, the pores grow due to the inflow of vacancies from crystal bulk. After this, the stage of coalescence and coagulation begins - the pores become larger and after a while merge into single macropores, along which destruction occurs. Such kinetic approach allowed explaining the dependence of the strength of material on the loading time, and gave the results that were closest to the experimentally observed ones. In this regard, the further development of this direction of physics of destruction seems to be important and relevant. It should be noted that at low loads, growing pores may become faceted to minimize surface energy and their growth becomes similar to the growth of crystals of "void" from a gas of vacancies in the bulk of the crystal. The main goal of this work is to consider the growth of such faceted pore via terrace-step-kink mechanism, described in classical work of Burton, Cabrera and Frank. Here we suppose, that the role of moving adatoms is played by vacancies, which arrive from the crystal bulk onto terraces of void, diffuse along them and incorporate into existing steps and kink. This causes the movement of steps and growth of the faceted pore. The key difference of the proposed theory from classical BCF model is that here we consider the non-Kossel multicomponent crystal, which consists of a few different types of adatoms. Also the concentrations of vacancies depend on tensile load, which affects all components of the crystal in different way (due to different atomic volumes of the vacancies) whereas in classical BCF model concentrations of the different components are independent of each other. The expressions for the rate of advance of a single step on the pore surface, a group of parallel steps, and the step formed by screw dislocations are found. The growth rate of a pore is found. It is shown, that in certain range of tensile loads the pore growth rate may have the quadratic dependence on the tensile load.

- [1] Cheremskoy P.G., Slyozov V.V., Betekhtin V.I., Pores in solids, Moscow, Energoatomizdat, 1990. 376 p. (in Russian)
- [2] Vakulenko A. A., Kukushkin S. A. (2000). Phase transition kinetics in loaded solids. *Physics of the Solid State*, 42(1), 179-183.
- [3] Kukushkin S. A. (2005). Nucleation of pores in brittle solids under load. *Journal of applied physics*, 98(3), 033503.
- [4] Vakulenko A. A., Kukushkin S. A., Shapurko A. V. (2001). Kinetics of pore formation upon plastic deformation of crystals with a cesium chloride structure. *Physics of the Solid State*, 43(2), 270-273.

## DEPENDENCE OF PROPERTIES OF VARIABLE GRADIENT POROUS STRUCTURE OF SILICON ON THE METHOD OF FORMATION

**Rubtsova K., Silina M.**

*NUST "MISiS"*

*rubcova.karina@gmail.com*

Porous silicon is widely used in micro- and optoelectronics due its atoms arrangement from a single crystal substrate. In addition, the possibility of forming a variable gradient porous structure of silicon (GPS-var) by a single process of deep anodic etching process allows to use an external nanostructured layer (due to the "substrate" of macroporous silicon). It is characterized by high resistivity, low Young's modulus, high specific surface area and pore size from fractions to tens of nanometers. The combination of these physicochemical properties makes porous silicon a unique multifunctional material.

The modes of formation of GPS-var structures by anodic etching of p-type monocrystalline silicon wafers in anhydrous solution of hydrofluoric acid (HF) in isopropanol and ethanol are investigated in this research. The experimental dependence of the etching depth with the concentration of hydrofluoric acid in ethanol and isopropanol for the etching time of 60 minutes at a constant etching current density is presented. It was found that in the formation of membrane and electrode GPS-var layers with a depth of more than 200 microns, it is necessary to use solutions with hydrofluoric acid concentration exceeding 75%. At lower acid concentrations, cracking of the external nanostructured layer is observed. With a decrease in the concentration of hydrofluoric acid, the destruction is observed in the smaller depth layers. At the same time, more reproducible GPS-var structures are formed in solutions based on isopropanol, which can be explained by a relatively lower water content in isopropanol-containing solutions (alcohol concentration of 98%) compared to ethanol (alcohol concentration not higher than 96%). The change in the reflection coefficient of porous silicon structures in the wavelength ranging from 200 to 2400 nanometers was studied. As follows from the experimental data, the dependence of the reflection coefficient  $R$  on the wavelength is nonlinear and the lowest values of  $R$  correspond to higher wavelengths. At the same time, the angular dependence of the reflection coefficient is more typical for large wave lengths. To increase the stability of the external nanostructured layer of the GPS-var structure to the effects of water and reduce the specific resistance of the layer, it is proposed to passivate the nanoporous layer with graphene-like films (GLF).

For comparison, samples of GPS-var structures and passivated GPS-var structures were kept in water solution for 180 minutes. The dependences of the reflection coefficient on the wavelength of light for GPS-var structure and GPS-var/GLF after exposure in water solution were found. The reflection coefficient of GPS-var layers after keeping the samples in water solution has decreased significantly. At the same time, due to the contact with water, severe destruction of the GPS-var film is observed. It also has acquired a pronounced orange color, nanostructured and luminescent porous structures even in daylight. The coefficient  $R$  of the nanostructured layer has a minimum value and does not depend on the wavelength of light. At the same time, the layers of GPS-var/GLF after aging in water have not changed in appearance. The obtained experimental data suggest that the use of nanostructured structures based on GPS-var layers allows create a coating with an absorption coefficient of not less than 99% in the considered range of wavelengths.

## LINE AND POINT ENERGY OF GRAPHENE

**Rusanov A.I.**

*St Petersburg State University*

*airusanov@mail.ru*

Graphene is famous and seemingly studied far and wide, but few have had to look at it from the standpoint of colloid and surface science, and if it did, it was mainly empirical, without affecting the fundamental principles. Since graphene is a two-dimensional solid, the role of surface phenomena in it is played by linear phenomena. The main quantities, line tension and line energy, are essentially related to chemical bonds, and therefore the calculation of these linear characteristics (through the work of breaking bonds) is based on the data of quantum chemistry. In addition to the contribution of chemical bonds, there is also a contribution of van der Waals forces, but estimates made showed that it is small: after all, the unsurpassed strength of graphene is due precisely to the strength of its chemical bonds. Despite the high degree of symmetry of graphene, its cutting in different directions gives different values of line tension. The full characteristic of this dependence is given by the polar diagram, which is constructed on the same principle as the Wulff construction in the thermodynamics of single crystals. This diagram underlies the art of graphene sheet cutting, which has recently acquired exceptional practical value. The direction corresponding to the smallest line tension forms the natural zigzag linear boundary of graphene.

Line tension plays an important role in the behavior of the “holes” of graphene, i.e. clusters of vacancies that can freely migrate not only within one sheet, but also “jump over” from one sheet to another in graphite-type structures. The tendency of small holes to unite is nothing but the action of the Gibbs-Curie principle in two-dimensional thermodynamics of linear phenomena. Finally, it must be said that line tension is the driving force behind the spontaneous formation of nanotubes, and here we again come to the problem of cutting. Indeed, not only the magnitude of the line tension, but also the type of nanotube depends on the chosen direction. Billets along the zigzag and armchair directions in the hexagonal structure of graphene give achiral nanotubes, along other directions give chiral ones. The thermodynamics of the flat sheet-nanotube transition are also formulated in this presentation.

For two-dimensional structures, line energy and point energy are physical quantities of the same value as, respectively, surface energy and line energy for three-dimensional bodies. The presented theory calculates the contribution of dispersion forces to the local cohesive energy, the local line energy and the point energy of graphene from its microscopic parameters: lattice constant, two-dimensional atomic density and the pair interaction potential. The local values are calculated on the basis of the Irving-Kirkwood stress tensor inside a finitely long plane-parallel empty two-dimensional gap between two rectangular pieces of graphene lying in the same plane. The calculation is made for absolute zero of temperature (when energy is equivalent to free energy). The structure of graphene is assumed to be rigid, which means neglecting the relaxation effect during the separation of two pieces of graphene. The result of the calculation depends on the direction of the boundary line of graphene. For the calculations, we selected a line across the s-bonds corresponding to the natural boundary of graphene. The linear and point graphene energy was calculated for the hard ball model with dispersive forces and the Lennard-Jones model. It has been established that near the angle of a rectangular piece of graphene, the linear energy becomes variable within five distances between the atoms in the lattice, which makes it possible to estimate the contribution of dispersion forces to the point energy of graphene.

# GROWTH AND PROPERTIES OF NOVEL GRAPHENE-BASED MAGNETIC HETEROSTRUCTURES FOR SPINTRONIC DEVICE APPLICATIONS

Li S.<sup>1</sup>, Yamauchi Y.<sup>1,2</sup>, Sakai S.<sup>1,2</sup>

1 - National Institutes for Quantum and Radiological Science and Technology QST

2 - National Institute for Materials Science NIMS

sakai.seiji@qst.go.jp

Graphene is receiving great attention as one of the most promising materials for future spintronics due to their outstanding transport properties of spin-polarized charge carriers and two-dimensionality advantageous for nano-scale device applications. As a key research issue in developing graphene-based spintronic devices like magnetoresistance (MR) devices, spin transistors and spin logics, significant efforts have been made to improve the injection efficiency of spin-polarized carriers in graphene. However, the graphene-based devices consist of spin injection electrodes of ferromagnetic metals (FMs) (*e.g.*, Co and NiFe alloy) studied so far revealed the low spin injection efficiency, *i.e.*, the low spin polarization of injected carriers by direct contact *via* graphene/FM heterostructures and the high injection resistance by indirect contact *via* graphene/insulating barrier layer/FM heterostructures.

One of the most effective ways to solve the problem of the low spin injection efficiency in graphene-based spintronic devices is the application of half-metals (HMs) with completely-high spin polarization ( $P \sim 100\%$ ) at the Fermi level in place of conventional FMs with low spin polarization ( $P \sim 30\%$ ). Recently, we for the first time demonstrated the fabrication of novel heterostructures consisting of single layer graphene (SLG) and HMs, *i.e.*,  $\text{La}_{1/3}\text{Sr}_{2/3}\text{MnO}_3$  (LSMO) [1] and  $\text{Co}_2\text{FeGe}_{0.5}\text{Ga}_{0.5}$ (CFGG) [2]. We successfully revealed their spin-related properties at the interfaces of the heterostructures by utilizing cutting-edge spectroscopy techniques; outermost-surface sensitive spin-polarized metastable atom deexcitation spectroscopy (SPMDS) with a spin-polarized He beam and depth-resolved X-ray magnetic circularly dichroism (XMCD) spectroscopy [1-7]. In this talk, I will present the growth processes of the SLG/HM heterostructures and their promising electronic and magnetic properties revealed in our studies.

1. S. Sakai, S. Majumdar, Z. I. Popov, P. V. Avramov, Y. Hasagawa, Y. Yamada, H. Huhtinen, H. Naramoto, P. B. Sorokin, Y. Yamauchi, *ACS Nano* **10**, 7532 (2016).
2. S. Li, S. Sakai *et al.*, *to be published*.
3. S. Sakai, S. V. Erohin, Z. I. Popov, S. Haku, T. Watanabe, Y. Yamada, S. Entani, S. Li, P. V. Avramov, H. Naramoto, K. Ando, P. B. Sorokin, Y. Yamauchi, *Adv. Funct. Mater.* **28**, 1800462 (2018).
4. T. Watanabe, Y. Yamada, A. Koide, S. Entani, S. Li, Z. I. Popov, P. B. Sorokin, H. Naramoto, M. Sasaki, K. Amemiya, S. Sakai, *Appl. Phys. Lett.* **112**, 022407 (2018).
5. Y. Matsumoto, S. Entani, A. Koide, M. Ohtomo, P. V. Avramov, H. Naramoto, K. Amemiya, T. Fujikawa, S. Sakai, *J. Mater. Chem C* **1**, 5533 (2013).
6. S. Entani, M. Kurahashi, X. Sun, Y. Yamauchi, *Carbon* **61**, 134 (2013).
7. M. Ohtomo, Y. Yamauchi, X. Sun, A. A. Kuzubov, N. S. Mikhaleva, P. V. Avramov, S. Entani, Y. Matsumoto, H. Naramoto, S. Sakai, *Nanoscale* **9**, 2369 (2017).

# MECHANICAL PROPERTIES OF PVD DEPOSITED $\text{Al}_2\text{O}_3$ THIN FILM ON A SINGLE-CRYSTAL SUBSTRATE

**Shumilin A.I., Plotnikov M.V., Fomin A.A.**

*Yuri Gagarin State Technical University of Saratov*

*shumilinai@yandex.ru*

X-ray diffraction analysis (XRD) was used to study thin films of aluminum oxide ( $\text{Al}_2\text{O}_3$ ) obtained by the PVD method. The presence of the oxide orthorhombic k-phase was established. The nanoindentation method was used to study the elastic properties of the film-base system. The thickness of the considered films was 80, 160, 240 nm. The microhardness of the  $\text{Al}_2\text{O}_3$ - $\text{LiNbO}_3$  system with an indenter load of 5 mN was not lower than 30 GPa.

## 1. Introduction.

Currently, coatings of aluminum oxide ( $\text{Al}_2\text{O}_3$ ) are widely used in optics, microelectronics, and in solar energy [1]. There are many methods for producing thin films with the given properties of hardness, porosity, electrical conductivity, etc. In this study, thin  $\text{Al}_2\text{O}_3$  films as antireflection coatings for the optical surfaces of acousto-optic products were of particular interest. The wavelength of light was  $\lambda = 632.8$  nm. The lithium niobate single crystal ( $\text{LiNbO}_3$ ) used as the base has a low hardness [2] and the oxide film is also a mechanical protection and should have high adhesion and hardness values.

## 2. Methodology.

Parallelepipeds of single crystals ( $\text{LiNbO}_3$ ) with polished surfaces were the substrates for the aluminum oxide films. The films were deposited by DC-magnetron sputtering of an aluminum target in an Ar/ $\text{O}_2$  plasma with a ratio of the partial pressure of gases 1/1. The pressure in the vacuum chamber was  $P = 1.47$  Pa and the discharge current density was  $j = 49$  A/m<sup>2</sup>. The pre-heating temperature of the substrate equaled  $t = 80$  °C. For the studies, films with the thicknesses of 80, 160, 240 nm were obtained.

The hardness was determined using the Oliver–Pharr method (ISO 14577-1:2015).

X-ray diffraction analysis (XRD) was performed using  $\text{CuK}\alpha$  radiation ( $\text{CuK}\alpha$ ,  $\lambda = 0.15412$  nm) in the angle range of  $2\Theta = 5$ – $60$  °. For the analysis of XRD patterns, the international electronic database of diffraction standards "Powder Diffraction File – 2" was used.

3. Results. As a result of the XRD performed in  $\text{Al}_2\text{O}_3$  films, an orthorhombic structure was found, which was a k-phase. The presence of a crystalline modification provided the microhardness of thin films of about 32.5 and 35 GPa, with the film thicknesses of 160 and 80 nm, respectively (Berkovich prism, load 5 mN). This microhardness value is comparable to the  $\alpha$ -modification of  $\text{Al}_2\text{O}_3$  [3]. Microhardness reached the values above 100 GPa with a film thickness of 240 nm (load 5 mN). With a load of 20 mN on the indenter, the microhardness decreased to 20–30 GPa that was due to the effect of the  $\text{LiNbO}_3$  substrate, the hardness of which did not exceed 12 GPa [2].

## 4. Conclusions.

Thin  $\text{Al}_2\text{O}_3$  films deposited on a  $\text{LiNbO}_3$  single crystal by PVD magnetron sputtering had a crystalline structure. The microhardness of the layered  $\text{LiNbO}_3$  –  $\text{Al}_2\text{O}_3$  system exceeded 30 GPa. The resulting oxide films can be used for anti-reflective and protective coatings on monocrystals with lower hardness, which are the basis of modern microelectronic devices of solar electronics and acousto-optics.

## Acknowledgments.

The authors express their gratitude to Dr. Gorshkov N.V. and Dr. Nikishin E.L. for the conducted XRD analysis and discussion of the results. This work was supported by a grant from the Russian Foundation of Basic Research, project No. 18-07-00687.

## References

1. Swatowska B 2018 *Microelectron. Int.* 35 177. doi:10.1108/MI-04-2018-0020
2. Wang H, Zhang Y, Xiang D and Xu J 2018 *Optik* 164 385. doi: 10.1016/j.ijleo.2018.03.011
3. Chou T, Nieh T, McAdams S and Pharr G 1991 *Scripta Metall Mater* 25 10 2203 doi: 10.1016/0956-716X(91)90001-H

# OPPORTUNITIES OF ATOMIC FORCE MICROSCOPY TO STUDY THE NUCLEATION OF THIN COATING FORMED IN THE MOLECULAR LAYERING PROCESS

Sosnov E.A.

*Saint-Petersburg State Institute of Technology*

*sosnov@lti-gti.ru*

The report considers the application of atomic force microscopy to the study of the formation processes by the Molecular Layering method (ML) (also called as Atomic Layer Deposition) (due to the chemical interaction of active functional groups (FG) of the matrix surface with low molecular weight reagents) of nanoscale coatings with different from the matrix chemical nature and, accordingly, the phase composition.

At the initial stage of the synthesis, the future new phase acts as grafted FGs that form "island" structures on the matrix surface. Due to the geometric non-uniformity of the distribution of highly active FGs, which interact with low molecular weight reagents first, the lateral dimensions of the "islands" can vary within fairly wide limits.

It should be noted that the formation of "island" structures is not accompanied by the appearance of objects on the AFM reconstruction of surface topography and is manifested only in the study of materials in "contrasting" techniques. That is, the "islands" are monolayer two-dimensional formation, the forming of which results in the rearrangement of the surface region of the matrix, accompanied by a change in its optical [1] and adhesive [2] characteristics.

Since already during the formation by ML of a monolayer coating, an increase in the coordination state of the modifier atom to the values characteristic of it in the corresponding chemical compound is observed due to the formation of coordination bonds with both the screened FGs of surface and the newly formed FGs [3], the surface "island" structures are two-dimensional nuclei (chemically bound to the matrix) for the further formation of a coating.

The boundaries between the islands, which are still manifested at the stage of chemisorption of the first monolayer of the modifier element, apparently separate the regions of the subsequent nucleation of crystallites. These boundaries are preserved in the course of further synthesis, when complete overlapping of the surface by the modifying layer is achieved. When the critical thickness of the "island" is reached, which is determined by the parameters of the crystal cell of the forming phase, the surface layer is compacted [4] to form a polycrystalline coating.

This work was supported by the Ministry of Science and Higher Education of the Russian Federation (project 16.1798.2017/4.6)

[1] Kol'tsov S.I., Gromov V.K., Aleskovskii V.B. in: *Ellipsometry - the Method of Surface Studying* / Ed. by A.V.Rzhanov. Novosibirsk: Nauka, 1983, P.73-76. [in russian]

[2] Dorofeev V.P., Sosnov E.A., Malygin A.A. // *J Surface Investigation: X-Ray, Synchrotron and Neutron Techniques*. 2006. N 2. P.55-60. [in russian]

[3] Sosnov E.A., Malkov A.A., Malygin A.A // *Rus. J Appl. Chem.* 2007. V.80. N 12. P.2057-2062.

[4] Dorofeev V.P., Malygin A.A., Kol'tsov S.I. // *Rus. J Appl. Chem.* 2004. V.77. N 7. P.1061-1065.

## SYNTHESIS AND ASSEMBLY OF COLLOIDAL NANOCRYSTALS TOWARDS ADVANCED FUNCTIONALITIES

**Striccoli M.<sup>1</sup>, Fanizza E.<sup>1,2</sup>, Panniello A.<sup>1</sup>, Depalo N.<sup>1</sup>, Ingrosso C.<sup>1</sup>, Comparelli R.<sup>1</sup>, Petronella F.<sup>1</sup>, Dibenedetto C.N.<sup>2</sup>, Triggiani L.<sup>1</sup>, Vischio F.<sup>1</sup>, Rizzi F.<sup>1</sup>, Agostiano A.<sup>1,2</sup>, Curri M.L.<sup>1,2</sup>**

*1 - CNR-IPCF Division of Bari*

*2 - Chemistry Dept., University of Bari, Italy*

*m.striccoli@ba.ipcf.cnr.it*

In recent years, the term “nanomaterials” has almost monopolized the scientific language. At the nanoscale, materials present new and original properties. In this regime, the electronic structures can be tuned by varying the physical size of the crystal, leading to new phenomena, as superparamagnetism of magnetic nanocrystals (NCs), surface plasmon resonance in metal nanoparticles (NPs) and size-dependent optical transitions in semiconductor quantum dots, opening interesting opportunities for device applications. NCs synthesized by solution processes represent potential building blocks for inexpensive manufacturing of low cost and large area devices. The synthesis, carried out by decomposition of precursors at high-temperature in the presence of surfactants as stabilizers, allows to control in a reproducible manner size, shape and crystalline phase of the nano-objects. Accordingly, the choice of the organic ligands depends on their capability to coordinate the surface of the nanoparticles in growth. Procedures of cation exchange allow the modification of composition after synthesis, while the fabrication of heterostructures with exotic shape and conformations can be driven by a proper choice of precursors and surfactants. In addition, such solution based synthetic strategy allows to obtain NCs functionalized with organic molecules which can be manipulated as macromolecules and modified at room temperature to tune the surface chemistry of NCs. Such approach is widely exploited for the ordered assembly of NPs in thin films and in advanced applications where the NPs can be integrated in conventional functional systems or used to manufacture micro/nano devices. Here a summary of the synthetic strategies and the peculiar properties of the colloidal nanomaterials will be overviewed, in order to give a panorama of the potentialities of such interesting materials in the field of nanocrystal based energy devices.



**THEORETICAL MODELLING OF OXYGEN VACANCY CHARACTERISTICS IN LEAD ZIRCONATE TITANATE  $\text{PbZr}_{1-x}\text{Ti}_x\text{O}_3$  (PZT). EFFECTS ON STRUCTURAL AND FERROELECTRIC PROPERTIES**

**Bogdanov A.<sup>1,2</sup>, Kimmel A.<sup>3</sup>**

1 - Irkutsk National Research Technical University, 83 Lermontov str., Irkutsk, 664074, Russia

2 - Vinogradov Institute of Geochemistry SB RAS, 1A Favorsky str., Irkutsk, 664033, Russia

3 - University College London, London, UK

*alex.bogdanov2012@gmail.com*

The lead zirconate titanate  $\text{PbZr}_{1-x}\text{Ti}_x\text{O}_3$  (PZT) piezoelectric ceramics possesses a great variety of local structures, which is connected to the absence of any long range order in the B-cation sublattice. Therefore, at a local scale the *true* symmetry of the PZT structure deviates from its *average* symmetry almost throughout the PZT's phase diagram in “composition”-“temperature” coordinates. This multiphase picture – especially close to the so-called *morphotropic phase boundary* at  $x \approx 0.48$  – is accepted worldwide [1-3].

The oxygen vacancy  $\text{V}_\text{O}$  appears to be the most abundant defect in oxide materials, and affects greatly physics of oxides. In the present work we studied quantum chemically effects, the  $\text{V}_\text{O}$  has on the structural and ferroelectric properties of PZT. We modelled possible local structures using a structure search approach [4], and studied systematically the characteristics of  $\text{V}_\text{O}$ . The summarized results are: i) the  $\text{V}_\text{O}$  in PZT arises in chemically different environment, and no specific arrangement of B-cations (like Ti-O-Ti-, Ti-O-Zr- chains etc.) was found that would be energetically more favorable than others for formation and accumulation of  $\text{V}_\text{O}$ ; ii) the presence of  $\text{V}_\text{O}$  causes strong structural relaxation that can change the direction of spontaneous polarization  $\bar{P}$  at local scale, while the change of the  $\bar{P}$  vector magnitude reaches up to 15 %, depending on local structure, thus  $\text{V}_\text{O}$  affects greatly the ferroelectric properties of PZT.

This work was supported by National Research Irkutsk State Technical University (NR ISTU) Scientific Council grant 05-FPK-19.

1. H. Yokota, N. Zhang, A.E. Taylor, P.A. Thomas, A.M. Glazer. “Crystal structure of the rhombohedral phase of  $\text{PbZr}_{1-x}\text{Ti}_x\text{O}_3$  ceramics at room temperature”. Phys. Rev. B, V. 80, p. 104109, 2009.
2. N. Zhang, H. Yokota, A. M. Glazer, Z. Ren, D. Keen, D. S. A. Keeble, P. A. Thomas и Z.-G. Ye, “The missing boundary in the phase diagram of  $\text{PbZr}_{1-x}\text{Ti}_x\text{O}_3$ ”. Nat. Commun., V. 5, p. 5231, 2014.
3. N. Zhang, H. Yokota, A.M. Glazer, D.A. Keen, S. Gorfman, P.A. Thomas, W. Ren, Z-G. Ye. “Local-scale structures across the morphotropic phase boundary in  $\text{PbZr}_{1-x}\text{Ti}_x\text{O}_3$ ”. IUCr J, V. 5, P. 73-81.
4. A. Bogdanov, A. Mysovsky, C.J. Pickard, A.V. Kimmel. “Modelling the structure of Zr-rich  $\text{Pb}(\text{Zr}_{1-x}\text{Ti}_x)\text{O}_3$ ,  $x = 0.4$  by a multiphase approach”. Phys. Chem. Chem. Phys., V. 18, p. 28316-28324, 2016.

# THE CORRELATION STUDY OF THE CRYSTAL STRUCTURE WITH OPTICAL PROPERTIES OF AMMONIUM HYDROGEN PHOSPHATE SINGLE CRYSTALS DOPED BY CHROMIUM AND TITANIUM

**Bolshakova N.<sup>1</sup>, Efimov N.<sup>1</sup>, Bushinsky M.<sup>2</sup>, Mudryi A.<sup>2</sup>, Turchenko V.<sup>3</sup>, Efimov V.<sup>3</sup>**

*1 - Middle School of General education №9 Dubna, Moscow region, Russia*

*2 - Scientific and Practical Materials Research Centre, National Academy of Sciences of Belarus, Minsk, Belarus*

*3 - Joint Institute for Nuclear Research, Dubna, Moscow region, Russia*

*bolshakova@9sch.ru*

In the present work, the correlations of the crystal structure parameters with the optical properties of ammonium hydrogen phosphate (NH<sub>4</sub>)(H<sub>2</sub>PO<sub>4</sub>) single crystals at different doped by chromium and titanium have been studied by the high-resolution X-ray diffraction and optical microscopy as well as fluorescence methods.

The method preparation of these single crystals at “home conditions” makes it possible to obtain enough large crystals (approximately 50x20x10 mm<sup>3</sup>) having defects due to the temperature stress arising during the growth of crystals. Such method of preparing single crystals could be used as a model for the study, for example, of aluminum oxide crystals doped by chromium and titanium that is working element of an optical quantum generator in the red region of the spectrum.

A high-resolution X-ray single crystal diffraction experiments (Fig. 1\*) reveal an increase of the lattice volume (shifting of the peaks located in far  $2\theta$  region) as well as atomic disorder (Fig. 1\*, inset) and stress states (decrease in the peak amplitude) due to the incommensurate average atomic radii of matrix (0.53 Å) and chromium (0.61 Å).

Optical microscopy results show the elongated defects in the region of highest chromium concentration and their absence in an undoped (the transparent central part) single crystal characterized by large single-domain crystallites.

In a single crystal doped with titanium, the optical microscopy displays of the stepped, plastic-deformed formations and large single-domain crystallites in a transparent part of the single crystal with a lower concentration.

Photoluminescence, as a structural-sensitive method, reflects the presence of anionic vacancies in the form of F-centers (charged and neutral vacancies) that can be generated by radiation of various nature as well as a heat treatment in active media and also mechanical processing. The photoluminescence spectrum of the F centers is characterized by bands of 450–550 nm (Fig. 2\*). These bands could be attributed to the intrinsic structural defects of the type of oxygen vacancies (F centers).

At points with an increased concentration of chromium ions in the lattice, an R-band with a maximum of 658 nm appears. A decrease in the chromium concentration at the central point of the single crystal leads to a suppression of the luminescence intensity of the F centers (Fig. 2\*). This may be due to a decrease in the number of vacancies, stress states and the more perfect crystal structure formation. In addition, the effect of shifting the luminescence spectrum towards the blue glow is observed with prolonged illumination of the crystal in a chromium-saturated region. This effect indicates the existence of relaxation processes at the interface between chromium and the matrix.

The correlation complex analysis in the crystal structure and the optical properties on the obtained results has been performed.

This work was supported by the RFBR-BRFFR grant No. 18-52-00020.

Fig. 1\*. Room temperature Rietveld refinement of the X-ray diffraction pattern. The red circles correspond to experimental data and the solid line represents the calculated pattern. The ticks indicate the calculated nuclear (lower row) reflection positions. The residual curve is shown at the bottom. Inset shows the pikes measured at min and max chromium concentration.

Fig. 2\*. Luminescence spectra of the (NH<sub>4</sub>)(H<sub>2</sub>PO<sub>4</sub>) single crystal with different chromium concentration points.

\*The abstract with figures is available at <http://2019.mgctf.ru/01000036ba.doc>

# TRANSFORMATION OF LATTICE POINT DEFECTS UNDER INFLUENCE OF LIGHT PULSES IN IRRADIATED LiF CRYSTALS

**Bryukvina L.I.**

*Irkutsk Branch of the Institute of Laser Physics of the SB RAS*

*baikal@ilph.irk.ru*

Lithium fluoride (LiF) crystals are ideal objects for studying fundamental phenomena at the level of point defects, and are also widely used in dosimetry and laser physics. To create luminescent color centers (CCs), which underlie the use of crystals, special conditions are created for growing crystals and subsequent radiation processing. In order to avoid laser losses caused by light-scattering nanoparticles, and to obtain the maximum concentration of working CCs, the crystals are irradiated with ionizing radiation at low temperature. The impurities of divalent metals ( $\text{Me}^{2+}$ ) and hydroxyl ions ( $\text{OH}^-$ ) are introduced into the melt for creating of the required CCs.

To study the change of the crystal lattice and the effect of light-scattering nanoparticles,  $\gamma$ -irradiated crystals LiF:OH,  $\text{Mg}^{2+}$  were exposed to integral light pulses with an energy of 625 J and a duration of  $10^{-3}$  s.

Irradiation of crystals with ionizing radiation creates color centers F,  $\text{F}_2$  and  $\text{F}_2^+$  and molecular defects with a hydrogen bond, which have an absorption in the region of IR vibrations  $1800\text{--}3600\text{ cm}^{-1}$  (Fig. 1\*, curve 1).

Fig. 1\*. IR transmittance spectra of  $\gamma$ -irradiated LiF:OH,  $\text{Mg}^{2+}$  crystals: initial (curve 1), after impact of 290 (curve 2) and 615 light pulses (curve 3).

From the spectrum in the region of  $3570\text{--}3800\text{ cm}^{-1}$  (curve 1), it can be seen that in the initial  $\gamma$ -irradiated crystal, the ions of the “free” and “magnesium-perturbed” hydroxyl have been remained non decomposition by radiation. After exposure to 290 light pulses of the IFP-800 xenon lamp, the absorption bands of  $\text{OH}^-$  ions disappeared (curve 2). However, in our opinion, the  $\text{OH}^-$  ions did not decompose into hydrogen and oxygen defects under the action of radiation, but the formation of complexes with a hydrogen bond occurred (a wide band in the region of  $\sim 2000\text{ cm}^{-1}$ ) [1, 2]. The impact of 615 pulses led to a significant reduction in all absorption bands (curve 3). Along with the transformation of molecular impurity defects in the crystal, the integration of electronic CCs with the formation of light-scattering nanoparticles of lithium and magnesium and the alternative process of formation of fluorine bubbles from hole centers are occur. The sizes of metal areas and gas bubbles reached 1000 nm and more. Due to the integration of point defects, the number of centers involved in hydrogen bonding has decreased so much that their absorption bands almost did not display in the IR spectrum (curve 3). Thus, the LiF crystal lattice has undergone significant changes. However, during thermal annealing at a temperature close to the melting point, the lattice of the LiF crystal was restored.

## Literature

1. Lyubov I. Bryukvina, Nikolay A. Ivanov, J. of Fluor. Chem., 2016, Vol. 192 Part A, P. 124–130.
2. L. Bryukvina, N. Ivanov, S. Nebogin, J. of Phys. Chem. Sol., 2018, Vol. 120, P. 133-139.

\*The abstract with figures is available at <http://2019.mgctf.ru/0100003141.doc>

# INFLUENCE OF DISLOCATIONS AND TOPOLOGICAL DEFECTS IN THIN SMECTIC FILMS ON STRUCTURE AND POLAR CHARACTERISTICS

**Dolganov P.V.<sup>1</sup>, Shuravin N.S.<sup>1</sup>, Dolganov V.K.<sup>1</sup>, Fukuda A.<sup>2</sup>**

*1 - Institute of Solid State Physics, Russian Academy of Sciences, Moscow Region, 142432  
Chernogolovka, Russia*

*2 - Department of Electronic and Electrical Engineering, University of Dublin, Dublin 2, Ireland*

*pauldol@issp.ac.ru*

Dislocations and point topological defects cardinaly influence the structure, polar and optical characteristics of thin liquid crystal films. This influence is the topic of our report.

Smectic liquid crystals have layered structure. In polar phases the molecular long axes are tilted with respect to the layer normal. Each molecular layer bears electric polarization directed in the layer plane. Smectic liquid crystals can form free-standing (substrate-free) smectic films with thickness several molecular layers. Smectic layers in the films are parallel to the free surfaces. Such films can have an extremely large ratio of lateral size to thickness and in many aspects act as two-dimensional systems. Edge dislocations can form in the film during film preparation or can be created applying stress on the film. The dislocations influence various properties of the films.

We investigate the effect of edge dislocations on the orientation of molecules in the film [1]. In films formed by the ferroelectric liquid crystal near the dislocation the molecular tilt plane orients parallel to the dislocation. In antiferroelectric films the situation is more complex. We found that the relative orientation of the molecular tilt plane on the two sides of the dislocation depends on the parity of the number of layers in the dislocation. Dislocations with the Burgers vector equal to an even number of layers orient the molecular tilt planes on the two sides of the dislocation parallel to the dislocation. Dislocations with the Burgers vector equal to an odd number of layers orient the molecular tilt plane parallel to the dislocation on the one side from the dislocation and perpendicular to the dislocation on the other side. Molecular reorientation in the vicinity of dislocations influences the optical characteristics of the films. The effect of external electric field on the molecular orientation near dislocations is studied.

We describe properties of topological defects located near the dislocations or trapped on the dislocation. Special attention is given to structure of topological defects located inside closed dislocation loops (regions of larger or smaller thickness than the surrounding film). We found that the combination of the orientational action of dislocations and topological restrictions lead to unusual structures formed by topological defects [2]. Configuration of the field of molecular ordering around the topological defects in ferroelectric and antiferroelectric films is described. We discuss the origin of the influence of dislocations on the orientation of molecules and propose a model which explains the observed effects.

This work was supported by the Russian Science Foundation under grant 18-12-00108.

[1] P.V. Dolganov, N.S. Shuravin, V.K. Dolganov, and Atsuo Fukuda, *Phys. Rev. E* 95, 012711 (2017).

[2] P.V. Dolganov, N.S. Shuravin, V.K. Dolganov, E.I. Kats, and Atsuo Fukuda, *Surface Innovations*, accepted for publication.

# ATOMIC SCALE TUNING OF QUANTUM DOT NUCLEATION AND EPITAXIAL GROWTH WITH STRAIN INDUCED TECHNIQUES

**Dvurechenskii A.**<sup>1,2</sup>, **Smagina Zh.V.**<sup>1</sup>, **Zinoviev V.A.**<sup>1</sup>, **Rudin S.A.**<sup>1</sup>, **Nenashev F.V.**<sup>1,2</sup>,  
**Novikov P.L.**<sup>1,2</sup>, **Rodyakina E.E.**<sup>1,2</sup>, **Fomin B.I.**<sup>1</sup>

*1 - Rzhanov Institute of Semiconductor Physics Siberian Branch of Russian Academy of Science*

*2 - Novosibirsk State University*

*dvurech@isp.nsc.ru*

Quantum dots (QDs) nanostructures are promising candidates to be implemented in next generation CMOS-compatible optoelectronic and nanoelectronic devices if they can be formed in regular and uniform arrays with controlled size, shape, chemical composition, and the properties of their surrounding like choice of matrix material. For realistic integration of QD into Si-technology devices, the QDs have to be site-controlled to ensure their large scale addressability. Besides, ordered QDs provide several more benefits as compared to their randomly nucleated counterparts: a more homogeneous chemical composition and energy spectrum. In this report, we will focus on self-assembled, group-IV, Ge-on-Si epitaxial QDs, formed during with dislocation-free growth [1].

We have studied nucleation sites of Ge nanoislands grown on pit-patterned Si(001) substrate prepared by electron-beam lithography followed by plasma chemical etching. The geometry of the pits was controlled by varying the etching conditions and the electron-beam exposure duration. It was shown that the site location of three-dimensional epitaxial grown (3D) Ge nanoislands subsequently grown on the pit-patterned Si substrates depends on the cross-section shape of the pits. In the case of the V-shaped pits, 3D Ge islands nucleate inside the pits. For U-shaped pits the 3D Ge island nucleation takes place around the pit periphery. This effect is attributed to the strain relaxation depending not only on the initial pit shape, but also on its evolution during the Ge wetting layer deposition. It was shown by Monte Carlo simulations that in the case of a V-shaped pits with a pointed bottom, the strain relaxation is most effective inside the pit, while for a U-shaped pits with a wide bottom, the most relaxed area migrates during Ge deposition from the pit bottom to its edges, where 3D Ge islands nucleate. The interpretation of the results given in the present study is consistent with the general approach, considering the strain as a driving force for the island positioning. In addition, a specific mechanism, associated with a shift of the relaxed area from a pit bottom to its top during Ge deposition, was identified.

The linear ordered chains of quantum dots were formed on Si groove patterned Si(001) substrate formed by using combination of nanoimprint lithography and ion irradiation through mask. Ordered structures with grooves and ridges were prepared by the selective etching of regions amorphized by ion irradiation. Laterally ordered chains of Ge nanoislands were grown by MBE of Ge on the prepatterned Si substrates. It was shown that temperature during ion irradiation affects the location of subsequently grown Ge nanoislands at MBE: inside grooves or on ridges. The effect is interpreted in terms of additional surface tensile strain formed inside grooves by residual irradiation-induced defects with concentration depending on substrate temperature during irradiation. It was shown also, that the location of subsequently grown Ge nanoislands depends upon the sidewall inclination in grooves. The effect is ascribed to strain induced by Ge implanted interstitials under the groove's bottom. The molecular dynamics calculations allowed the determination of strain in grooves as dependent on the groove's shape.

It was shown also, that the location of subsequently grown Ge nanoislands depends upon the sidewall inclination in grooves. The effect is ascribed to strain induced by Ge implanted interstitials under the groove's bottom. The molecular dynamics calculations allowed the determination of strain in grooves as dependent on the groove's shape.

The size homogeneity and density of the arrays of quantum dots was found to be tuned with low-energy ion-beam actions during molecular - beam epitaxy (MBE). Nucleation of QDs due to a pulsed low-energy (100 eV) beam action of intrinsic ions (Ge<sup>+</sup>) resulted in the increasing of QDs density and improving of homogeneity in QDs sizes.

[1] A.V.Dvurechenskii, A.I.Yakimov. Silicon-Based Nanoheterostructures with Quantum Dots. In: *Advances in Semiconductor Nanostructures: Growth, Characterization, Properties and Applications*, Ed. by A.V.Latyshev, A.V.Dvurechenskii, A.L.Aseev. Elsevier, Amsterdam, Boston, Heidelberg, London NewElseviear, Amsterdam, Boston, Heidelberg, London Nework, Paris, 2017, p.p. 59 – 99.

The work was supported by RFBR grant No. 18-52-00014.

# STRAIN-DRIVEN SELF-ASSEMBLY OF PLASMONIC NANO-VOIDS AND DOTS IN SiGeSn/Si MULTILAYERS

**Gaiduk P.**

*Department of Physical Electronics and Nanotechnology, Belarusian State University, Minsk, Belarus*

*gaiduk@bsu.by*

We will briefly review the effect of strain-driven nano-void formation in pseudomorphic Si/SiGeSn/Si structures, gettering and segregation of impurities with formation of buried nano-shells, dots or platelets in the Si layers. The structures of Si/SiGeSn are prepared by MBE growth followed by implantation of a number of ions at various fluence-temperature regimes.

The following points will be presented and discussed in a systematic way:

- Spatial separation of interstitials and vacancies by strain fields of pseudomorphic Si/SiGeSn layer and formation of a 2D *I-V* defect layer (2D dilatation layer).
- Strain-driven self-assembly of nano-voids and evolution of secondary defects in the Si/SiGeSn layers.
- Monitoring of interstitials and vacancies in strained multilayer structures.
- Segregation of C, Ge, Sn or Au atoms at the walls of the voids and formation of plasmonically active nano-shells, dots and platelets.
- Enhancement of the PL emission from the layers of self-assembled nano-voids and dots

The concept of strain-driven self-assembly of nano-voids will be discussed which utilize the ability of compressively strained layers to collect small-sized atoms (H, He, C) or vacancies. It will be discussed in the talk that metallic nano-shells possess tuneable optical absorption with a possibility to tune the plasmon resonance in the near-infrared region. The plasmonic excitations might then be transferred to a semiconductor to generate electron-hole pairs if the strained Si/SiGeSn heterostructures are grown in the close vicinity to p-n-junction.

# GROWTH OF $\text{Ho}_{0,9}\text{Er}_{0,1}\text{Fe}_3(\text{BO}_3)_4$ FROM SOLUTIONS BASED ON $\text{Bi}_2\text{Mo}_3\text{O}_{12}$ AND $\text{Li}_2\text{WO}_4$

**Gudim I.<sup>1</sup>, Demidov A.<sup>2</sup>, Eremin E.<sup>1</sup>, Shukla D.K.<sup>3</sup>**

*1 - Kirensky Institute of Physics, SB RAS, 660038 Krasnoyarsk, Russia*

*2 - Bryansk State Technical University, 241035 Bryansk, Russia*

*3 - UGC DAE Consortium for Scientific Research, Indore, India*

*irinagudim@mail.ru*

In recent years, considerable attention has been paid to the study of multiferroic crystals, in particular, crystals of rare-earth ferrobates  $\text{RFe}_3(\text{BO}_3)_4$  ( $\text{R} = \text{Y}, \text{La-Lu}$ ) [1,2], have a noncentrosymmetric trigonal structure (isometric to a natural material, huntite  $\text{CaMg}_3(\text{CO}_3)_4$ ).

A specific feature of the structure of these crystals is the helicoidal chains of octahedra  $\text{FeO}_6$ . Chains can be present in the crystal, twisted both to the left and to the right. The ratio of the number of right and left enantiotropes significantly affects the properties of the grown crystals [3].

This work is devoted to the growth of crystals of the family  $\text{Ho}_{1-x}\text{Er}_x\text{Fe}_3(\text{BO}_3)_4$  from different melt-solutions. We propose two systems for the growth of such crystals:  $\text{Bi}_2\text{Mo}_3\text{O}_{12} + \text{B}_2\text{O}_3$  and  $\text{Li}_2\text{WO}_4 + \text{B}_2\text{O}_3$  [4-5].

First, we proposed a melt-solvent based on bismuth molybdate, from which a number of qualitative crystals of the family of rare-earth alumina-, gallium- and ferrobates with a huntite structure were produced.

However, researches have shown that part of the bismuth replaces ions of rare earth in the crystal [6]. In order to evaluate the influence of bismuth ions on crystal formation and the properties of grown crystals, we used a solution-melt based on lithium tungstate, which does not contain bismuth.

Next, we are going to add a controlled amount of bismuth oxide and will study its effect on the properties of the grown crystals.

1. Yutaro Kitagawa, Yuji Hiraoka, Takashi Honda, et al. NATURE, MATERIALS, VOL 9, 2010, 797-802.
2. Yu.F. Popov, G.P. Vorob'ev, A.K. Zvezdij, et al. Ferroelectrics, v. 169, 1995. p. 85-95
3. I.A. Gudim, E.V. Eremin, V.L. Temerov, Journal of Crystal Growth 312 (2010) 2427–2430.
4. R. P. Chaudhury, B. Lorenz, Y. Y. Sun, et al. Phys. Rev. B 81, 220402 (2010).
5. N.V. Volkov, I.A. Gudim, E.V. Eremin, et al. PvZETP 2014, 99, No. 2, pp. 72–80.
6. Ekaterina S. Smirnova, Olga A. Alekseeva, Alexander P. Dudka, et al. Acta Cryst. (2018). B74, 226–238.

The study was supported by the Russian Foundation for Basic Research, projects no. 17-02-00826, 17-52-45091 and 18-02-00696.

# NUCLEATION AND EQUILIBRIUM DENSITY OF MISFIT DISLOCATION LOOPS IN CORE-SHELL NANOWIRES

Kolesnikova A.L.<sup>1,2</sup>, Chernakov A.P.<sup>1,3</sup>, Gutkin M.Yu.<sup>1,2,4</sup>, Romanov A.E.<sup>1</sup>

1 - ITMO University, Kronverkskiy pr. 49, St. Petersburg, 197101, Russia

2 - Institute of Problems of Mechanical Engineering, Russian Academy of Sciences, Bolshoj 61, Vasil. Ostrov, St. Petersburg, 199178, Russia

3 - Ioffe Physical Technical Institute, Russian Academy of Sciences, Polytekhnicheskaya 26, St. Petersburg, 194021, Russia

4 - Department of Mechanics and Control Processes, Peter the Great St. Petersburg Polytechnic University, Polytekhnicheskaya 29, St. Petersburg, 195251, Russia

*m.y.gutkin@gmail.com*

Fabrication of crystalline core-shell nanowires (CSNWs) is accompanied by formation of misfit strains, caused by the lattice mismatch of core and shell materials, and misfit defects which are generated in CSNWs and partly relax these misfit strains. Both the misfit strains and defects can strongly affect upon the unique functional properties of CSNWs which are considered as promising materials for optoelectronics [1-4], energy storage devices [5], heat conversion [6], solar cells [7], etc. That is why the problem of misfit strains and defects in CSNWs has been in the focus of many researchers during the last two decades. Experimental observations revealed that two kinds of misfit defects are common for CSNWs, which are straight misfit dislocations (MDs) parallel to the CSNW axes and prismatic loops of MDs surrounding the CSNW cores [8]. The first ones provide strain/stress relaxation in the cross sections of CSNWs, while the second ones provide axial relaxation in CSNWs. The principal questions to answer in this respect are (i) what is the critical condition for the onset of MD generation, and (ii) what is the equilibrium density of MDs at the core-shell interface? Until now, only the first question has been studied in a number of theoretical works [9-12].

In the present work, we revisit the problem of circular prismatic loops of MDs in CSNWs to answer both the questions. First, we solve the boundary-value problem in the classical theory of elasticity for a circular prismatic dislocation loop in an elastically isotropic cylinder by the Lurie method [13] different from those [10, 11] used before for solving this problem. Based on this solution, we find both the self strain energy of the loop and the interaction energy for a pair of such loops. Then we apply these results to calculating the critical conditions for nucleation of a circular prismatic MD loop in a CSNW. Finally, we calculate the change in the total energy of the CSNW in a partly relaxed state, with an infinite row of MD loops periodically distributed at the core-shell interface along the CSNW axis, per unit period of this row. Minimizing this energy change by the row period, we find the equilibrium distance between the MD loops and compare it with results of direct experimental observations of MDs in InAs-GaAs CSNWs [8]. Our theoretical results (8.35–9.05 nm) well correspond to the experimental data (7.0–8.5 nm).

*This work is supported by the Russian Science Foundation (project No. 19-72-30004, Basic research and innovative design of optoelectronic heterostructures based on III-V nanowires).*

## References

- [1] Zhang Y., Wu J., Aagesen M., Liu H., J. Phys. D: Appl. Phys. 48 (2015) 463001.
- [2] Ghosh R., Giri P.K., Nanotechnology 28 (2017) 012001.
- [3] Koblmüller G., Mayer B., Stettner T., et al., Semicond. Sci. Technol. 32 (2017) 053001.
- [4] Royo M., De Luca M., Rurali R., Zardo I., J. Phys. D: Appl. Phys. 50 (2017) 143001.
- [5] Yu K., Pan X., Zhang G., et al., Adv. Energy Mater. 8 (2018) 1802369.
- [6] Swinkels M.Y., Zardo I., J. Phys. D: Appl. Phys. 51 (2018) 353001.
- [7] Li Z., Tan H.H., Jagadish C., Fu L., Adv. Mater. Technol. 3 (2018) 1800005.
- [8] Popovitz-Biro R., Kretinin A., Von Huth P., Shtrikman H., Cryst. Growth Des. 11 (2011) 3858.
- [9] Gutkin M.Yu., Ovid'ko I.A., Sheinerman A.G., J. Phys.: Condens. Matter 12 (2000) 5391.
- [10] Ovid'ko I.A., Sheinerman A.G., Phil. Mag. 84 (2004) 2103.
- [11] Aifantis K.E., Kolesnikova A.L., Romanov A.E., Phil. Mag. 87 (2007) 4731.
- [12] Enzevaev C., Gutkin M.Yu., Shodja H.M., Phil. Mag. 94 (2014) 492.
- [13] Lurie A.I., The spatial problem of elasticity theory. M., State publishing house of technical- theoretical literature, 1955 (in Russian).



## PARTITIONING AND SEGREGATION IN 12Cr Fe-BASE OXIDE DISPERSION STRENGTHENED STEEL

**Jang J.<sup>1</sup>, Mao X.<sup>2</sup>, Oh K.H.<sup>3</sup>, Rogozhkin S.V.<sup>4</sup>, Han C.H.<sup>1</sup>, Kim T.K.<sup>1</sup>**

*1 - Korea Atomic Energy Research Institute, Daejeon, Korea*

*2 - Institute of Nuclear Energy Safety Technology, Hefei, China*

*3 - Seoul National University, Seoul, Korea*

*4 - Institute for Theoretical and Experimental Physics of National Research Center "Kurchatov Institute", Moscow, Russia*

*jjang@kaeri.re.kr*

Oxide dispersion strengthened (ODS) steel is one of the strong candidate materials for in core components of next generation nuclear systems. Its good macroscopic behavior such as excellent radiation resistance and superior high temperature creep rupture properties are usually attributed to the evenly dispersed nano-scale oxide particles within the steel matrix. The crystallographic characteristics and the chemistry as well as the size distribution of the dispersed particles shall be critical to the macroscopic beneficial effects to the ODS steels.

In this study 12Cr Fe-base ODS steel samples were prepared by mechanical alloying (MA) in argon atmosphere, hot isostatic pressing (HIP) under 104 MPa at 1050 degree C, and hot rolling at 1150 degree C with 70 per cent of thickness reduction. Several ODS steel samples containing boron up to 100 ppm in addition to the same ODS steel sample without boron were prepared, in which boron isotope of <sup>11</sup>B was utilized for the sample preparation to preemptively avoid neutron reaction or absorption issue with boron atoms.

The effect of boron addition to grain structure was investigated by using SEM / EBSD (electron backscattered diffraction). By addition of boron in ODS steel bimodal grain structure seemed to be suppressed, and the number density of nano-scale oxide particles appeared to increase. Behavior of boron atoms such as the partitioning into the nano-scale oxide particles and the segregation at the interfaces were examined by using STEM (scanning transmission electron microscope) / HAADF (high angle annular dark field) / EELS (electron energy loss spectroscopy), and boron atoms were found to segregate along the boundary through EELS map.

Partitioning behavior of the other alloying elements like vanadium, titanium as well as yttrium and oxygen in a 12Cr Fe-base ODS steel sample was also investigated by using STEM and APT (atom probe tomography). Size distribution of the dispersed particles in ODS steel was also estimated by using TEM and SANS (small angle neutron scattering).

Comprehensive analyses have allowed to better understand the details about the nano-scale oxide particles formation in 12Cr Fe-base ODS steel.

# SYNTHESIS, GROWTH AND STRUCTURAL FEATURES OF NEW RARE EARTH BORATE $\text{KCaNd}(\text{BO}_3)_2$

**Kononova N.G.<sup>1</sup>, Kuznetsov A.B.<sup>1</sup>, Shevchenko V.S.<sup>1</sup>, Uralbekov B.M.<sup>2</sup>, Bolatov A.K.<sup>2</sup>,  
Kokh A.E.<sup>1</sup>, Simonova E.A.<sup>1</sup>**

*1 - Sobolev Institute of Geology and Mineralogy SB RAS, Novosibirsk 630090, Russia  
2 - Al-Farabi Kazakh National University, Almaty 050040, Kazakhstan*

*n.g.kononova@gmail.com*

In recent years, numerous studies of new three cations orthoborates  $\text{ABR}(\text{BO}_3)_2$  containing alkaline metals (A), alkaline earth (B) and rare earth (R) have been investigated as a promising materials for use in a wide spectral range from UV to IR. For example, complex rare earth borates  $\text{NaBaSc}(\text{BO}_3)_2$  and  $\text{NaBaY}(\text{BO}_3)_2$  have been discovered in  $\text{R}_2\text{O}_3\text{-BaO-Na}_2\text{O-B}_2\text{O}_3$  system [1]. The consequent substitution of  $\text{Na}\rightarrow\text{K}$  and of  $\text{Ba}\rightarrow\text{Sr}$  has resulted in obtaining new compounds of  $\text{KBaR}(\text{BO}_3)_2$  and  $\text{KSrR}(\text{BO}_3)_2$  [2,3]. Obtained compounds are characterized by double-layered structures, where the first layer is formed by  $\text{RO}_6$  octahedra and the second is formed by polyhedral of alkaline and alkaline earth metals. Typically, these layers are perpendicular to the *c* axis and are connected by isolated  $\text{BO}_3$  triangles. The second layer in the structure of compounds  $\text{KBaR}(\text{BO}_3)_2$  is formed by Ba and K atoms having a common nine coordinated position, while atoms K and Sr occupy different position for  $\text{KSrR}(\text{BO}_3)_2$  compounds.

New  $\text{KCaNd}(\text{BO}_3)_2$  compound have been successfully obtained as results cationic position replacing of alkaline earth metal in  $\text{KSrNd}(\text{BO}_3)_2$  ( $\text{Sr}\rightarrow\text{Ca}$ ). A polycrystalline sample of  $\text{KCaNd}(\text{BO}_3)_2$  was prepared by the method of two stage solid state synthesis in a Pt crucible. The stoichiometric mixtures of pure raw  $\text{K}_2\text{CO}_3$ ,  $\text{CaCO}_3$ ,  $\text{H}_3\text{BO}_3$  and  $\text{Nd}_2\text{O}_3$  reactants were heated at 650 C to remove  $\text{H}_2\text{O}$  and  $\text{CO}_2$ . At the second stage, the mixtures were grinded in agate mortar, pressed into pills and heated again at 850°C for 12h until the powder X-ray method showed no peaks of initial compounds. Spontaneous crystals were grown from  $\text{KF-B}_2\text{O}_3$  flux on Pt loop.  $\text{KCaNd}(\text{BO}_3)_2$  belong to orthorhombic system, *Pbca* space group with cell parameters of  $a=10.2069(5)\text{\AA}$ ,  $b=9.0293(4)\text{\AA}$ ,  $c=13.1634(5)\text{\AA}$  and  $Z=8$ .

The crystals exhibit high transparency in the range 300-1100 nm. It shows an emitting band transition of  $\text{Nd}^{3+}$  ion in the range from 850 to 1080 nm.

Acknowledgements: This work is supporting by RFBR project #18-32-20001, state contract of IGM SB RAS and partially by Project GF MES RK IRN AP05130794.

## References:

1. Y.V. Seryotkin, V.V. Bakakin, A.E. Kokh, N.G. Kononova, T.N. Svetlyakova, K.A. Kokh, T.N. Drebuschak, Synthesis and crystal structure of new layered  $\text{BaNaSc}(\text{BO}_3)_2$  and  $\text{BaNaY}(\text{BO}_3)_2$  orthoborates, *J. Solid State Chem.* 183 (5) (2010) 1200–1204.
2. L. Han, Y. Wang, Y. Wang, J. Zhang, Y. Tao, Observation of efficient energy transfer from host to rare-earth ions in  $\text{KBaY}(\text{BO}_3)_2:\text{Tb}^{3+}$  phosphor for plasma display panel, *J. Alloys Compd.* 551 (2013) 485-489.
3. A.E. Kokh, N.G. Kononova, V.S. Shevchenko, Y.V. Seryotkin, A.K. Bolatov, K.A. Abdullin, B.M. Uralbekov, M. Burkitbayev, Syntheses, crystal structure and luminescence properties of the novel isostructural  $\text{KSrR}(\text{BO}_3)_2$  with  $\text{R}=\text{Y}$ , Yb, Tb, *Journal of Alloys and Compounds* 711 (2017) 440-445.

# EFFECT OF DOPING WITH RARE-EARTH OXIDES ON THE STRUCTURAL AND MECHANICAL CHARACTERISTICS OF ZIRCONIA CRYSTALS PARTIALLY STABILIZED BY YTTRIA

**Kulebyakin A.V.<sup>1</sup>, Alisin V.V.<sup>2</sup>, Borik M.A.<sup>1</sup>, Lomonova E.E.<sup>1</sup>, Milovich F.O.<sup>3</sup>, Myzina V.A.<sup>1</sup>, Osiko V.V.<sup>1</sup>, Ryabochkina P.A.<sup>4</sup>, Sidorova N.V.<sup>4</sup>, Tabachkova N.Yu.<sup>3</sup>**

*1 - Prokhorov General Physics Institute of the Russian Academy of Sciences*

*2 - Mechanical Engineering Research Institute of the Russian Academy of Sciences*

*3 - National University of Science and Technology «MISIS»*

*4 - Ogarev Mordovia State University*

*kulebyakin@lst.gpi.ru*

The partially stabilized zirconia (PSZ) crystals have a high mechanical characteristics, stable properties over a wide range of temperatures, as well as chemical and biological inertness. These crystals are very promising construction materials for the manufacture of components operating in aggressive conditions.

PSZ crystals are a solid solution of  $ZrO_2$  with the addition of impurities of rare earth elements at a concentration sufficient to stabilize the tetragonal modification of zirconia. Depending on the type of impurity, the structure of the crystals may undergo significant changes: the parameters of the unit cell, the number of defects (oxygen vacancies) and the positions of atoms in the crystal lattice. It is possible to obtain materials with a given combination of physicochemical properties necessary for a particular practical application by controlling the introduction of impurities into the crystals during their synthesis.

The aim of this work is to study the effect of the type and concentration of the impurity on the phase composition, structure and properties of  $ZrO_2 - Y_2O_3$  solid solution crystals. PSZ crystals were grown by directional melt crystallization in a cold crucible at a 10 mm/h crystallization rate. Yttrium oxide at a concentration of 1-2.5 mol. % was used as a stabilizer.  $CeO_2$ ,  $Nd_2O_3$ ,  $Er_2O_3$  and  $Yb_2O_3$  at a concentration of 0.3-1.8 mol. % were used as dopants.

The studies of PSZ crystals by the transmission electron microscopy showed that all samples have a developed domain twin structure with the size of the elementary domains of 5-10 nm.

Studies of the phase composition showed that two tetragonal phases are simultaneously present in the most grown PSZ crystals: an untransformable  $t'$ -phase with a degree of tetragonality close to the cubic phase ( $c/a = 1.006$ ) and a transformable  $t$ -phase ( $c/a = 1.016$ ), which under the application of a mechanical load can be transformed into a monoclinic phase.

Mechanical characteristics were measured by Vickers indentation technique. In the area of the indenter imprint on PSZ crystals, the phase composition was studied using local Raman spectroscopy. It is shown that the maximum values of crack resistance are crystals containing a larger amount of the  $t$ -phase ( $ZrO_2 - 2.0$  mol. %  $Y_2O_3 - 0.8$  mol. %  $Ce_2O_3$ ), since in this case the transformation mechanism of hardening, which is derived from the tetragonal-monoclinic transition, is more intensive. In addition, not only trivalent but also tetravalent cerium ions are present in the  $t$ -phase of 0.8Ce2YSZ crystal, which have a smaller ionic radius and do not require charge compensation due to the formation of oxygen vacancies. Due to this  $t$ - $m$  phase transition is easier and this leads to an increase in crack resistance.

The work was supported by research grants № 18-13-00397 of the Russian Science Foundation.

# GROWTH AND STRUCTURAL STUDY OF THE NEW LITHIUM BARIUM BORATE $\text{Li}_3\text{Ba}_4\text{Sc}_3\text{B}_8\text{O}_{22}$

**Kuznetsov A.<sup>1</sup>, Ezhov D.<sup>2</sup>, Kononova N.<sup>1</sup>, Kokh A.<sup>1</sup>, Uralbekov B.<sup>3</sup>**

*1 - Sobolev Institute of Geology and Mineralogy SB RAS, Novosibirsk 630090, Russia*

*2 - Tomsk State University, Tomsk 634050, Russia*

*3 - Al-Farabi Kazakh National University, Almaty 050040, Kazakhstan*

*ku.artemy@igm.nsc.ru*

Tremendous attentions have been attracted to materials for light-emitting diodes in order to improve their advantages such as high intensity, long operation lifetime, small size and environmental friendliness. One of these functional materials are borates being used as a perspective luminophores and nonlinear crystals. For example, most popular acentric alkali and alkali earth borates as  $\text{LiB}_3\text{O}_5$  (LBO),  $\text{BaB}_2\text{O}_4$  (BBO),  $\text{CsLiB}_6\text{O}_{10}$  (CLBO) are mainly used in nonlinear optics. In addition to acentric borates, there are many centrosymmetric borates doped or contained REE like  $\text{YAl}_3(\text{BO}_3)_4$  (YAB),  $\text{YCa}_4\text{O}(\text{BO}_3)_3$  (YCOB) used as laser host materials. The ability of the boron atom to form different anion  $[\text{BO}_3]$ ,  $[\text{BO}_4]$  and polyanions  $[\text{B}_5\text{O}_{10}]$ ,  $[\text{B}_9\text{O}_{15}]$  leads to the diversity of chemical compositions and crystal structures of borates. Thus, the understanding of the interrelation between the crystal structure and the properties is of high importance for the improvement and development of new functional materials. Among many synthetic borates the alkali and alkali earth borates are of practical interest as effective host lattice for luminescent materials. In the ternary  $\text{Li}_2\text{O}$ - $\text{BaO}$ - $\text{B}_2\text{O}_3$  system three phases  $\text{LiBaBO}_3$ ,  $\text{LiBa}_2\text{B}_5\text{O}_{10}$  and  $\text{LiBaB}_9\text{O}_{15}$  have been found.  $\text{LiBaB}_9\text{O}_{15}$  exists in two different phases  $R\bar{3}c$  and  $R\bar{3}c$ . These structures are reported to have 3D networks built from  $[\text{B}_3\text{O}_7]^{5-}$  groups. The other anionic groups  $[\text{B}_5\text{O}_{10}]^{5-}$  and  $[\text{BO}_3]^{3-}$  are main building units in  $\text{LiBa}_2\text{B}_5\text{O}_{10}$  and  $\text{LiBaBO}_3$ , respectively. However, undoped  $\text{LiBaBO}_3$ ,  $\text{LiBa}_2\text{B}_5\text{O}_{10}$  and  $\text{LiBaB}_9\text{O}_{15}$  crystals do not have own luminescent properties and their use as phosphors is associated with doping. But rare earth cations in these compounds do not have suitable position ( $\text{III}^+$ ) that limit the range of their concentrations at the level of the first percents. According to [1] there is a family of lithium barium rare earth borates  $\text{LiBaR}_2(\text{BO}_3)_3$  (where  $R = \text{Pr, Nd, Sm-Tm}$ ), which crystallize in  $P\bar{3}m_1$ . These crystals have layered structure where  $\text{RO}_8$  polyhedral form hexagonal block  $[\text{R}_6\text{O}_{33}]$  along the  $c$ -axis. In the  $[\text{R}_6\text{O}_{33}]_n$  layer there are three sorts of tunnels - trigonal, hexagonal, and rhombic. The trigonal and hexagonal tunnels are occupied by triangle and pyramid  $\text{BO}_3$  groups, respectively. The rhombic tunnels accommodate distorted  $\text{LiO}_6$  octahedra. Meanwhile, Ba atoms, situated in the interstices between these polyhedral layers, are surrounded by ten oxygen atoms.

In this work, the  $\text{Li}_3\text{Ba}_4\text{Sc}_3\text{B}_8\text{O}_{22}$  compound has been found as derivative from  $\text{LiBaR}_2(\text{BO}_3)_3$ .  $\text{Li}_3\text{Ba}_4\text{Sc}_3\text{B}_8\text{O}_{22}$  was synthesized by solid state reaction and successfully grown by TSSG method. Powder and single X-ray diffraction, thermal behaviour as well as optical properties including infrared spectra, UV-NIR diffuse reflectance spectra of the crystal were studied.

Acknowledgements: This work is supported by RFBR project #18-32-20001 and 18-48-543012, state contract of IGM SB RAS and partially by Project GF MES RK IRN AP05130794.

References:

[1] Chen, P., Xia, M., Li, R. A terbium rich orthoborate  $\text{LiSrTb}_2(\text{BO}_3)_3$  and its analogues new Journal of Chemistry, 39(12), (2015), 9389–9395.

## OPTICAL PROPERTIES OF DEFECTIVE CdMnSe EPITAXIAL FILMS

**Mehrabova M.<sup>1</sup>, Nuriyev H.<sup>2</sup>, Hasanov N.<sup>3</sup>, Kazimova A.<sup>4</sup>, Safarov N.<sup>5</sup>, Sadigov R.<sup>2</sup>**

*1 - Institute of Radiation Problems of Azerbaijan National Academy of Sciences*

*2 - Institute of Physics of Azerbaijan National Academy of Sciences*

*3 - Baku State University*

*4 - Ganja State University*

*5 - Khazar University*

*m.mehrabova@mail.ru*

Cd<sub>1-x</sub>Mn<sub>x</sub>Se semimagnetic semiconductors are quite interesting and important because of their major contribution in the solar cells, photodetectors, light amplifiers, light emitting diodes, lasers, photoelectrochemical cells and electronic elements. Most of the research done so far has focused extensively on determination the major features such as structural, optical and electrical properties of Cd<sub>1-x</sub>Mn<sub>x</sub>Se crystals and thin films on their base. However, the study of influence of defects on structural and optoelectronic characteristics of Cd<sub>1-x</sub>Mn<sub>x</sub>Se epitaxial films is rare in the literature.

In the present paper it has been calculated the electronic band structure, density of states, band gap, and total energy of the ideal and defective Cd<sub>1-x</sub>Mn<sub>x</sub>Se (0.01≤x≤0.06) by ab-initio method using the Functional Density Theory. It has been established that, with an increase in the concentration of Mn atoms, the band gap decreases. Vacancy type defects lead to an increase in the band gap, a change in the total energy, and the formation of local levels in the band gap. It has been defined, that besides of Mn atoms defects form magnetic moments, and the ferromagnetic state is more stable. Obtained results were confirmed experimentally.

Cd<sub>1-x</sub>Mn<sub>x</sub>Se (x=0.03, 0.06) epitaxial films were obtained on glass substrates in a vacuum of 10<sup>-4</sup>Pa by Molecular Beams Condensation method. It is defined the optimal conditions for creation of epitaxial films with perfect structure and clean, smooth surface. The substrate temperature was 673K, source temperature was 1100K. Dark aggregates, observed at the film surface, were removed using a source of compensating Se vapors in the growth process. The crystal structure and surface morphology were studied by XRD method on Bruker D8 Advance XRD and SEM method on Carl Zeiss Sigma VP respectively.

Absorption and transmission spectra of Cd<sub>1-x</sub>Mn<sub>x</sub>Se (x=0.03, 0.06) epitaxial films were investigated on double-beam spectrophotometer UV/Vis SPECORD 210 PLUS. The transmission spectra of the Cd<sub>1-x</sub>Mn<sub>x</sub>Se epitaxial film have peaks and valleys caused by interference phenomena, which indicates a high structural perfection of the films. We use envelope method to determine the optical constants and thickness of films. Thus, the refractive index, the absorption coefficient, the band gap and the film thickness were determined from the transmission spectra using the envelope method.

It was defined, that band gap of Cd<sub>1-x</sub>Mn<sub>x</sub>Se epitaxial films for x=0.03 was E<sub>g</sub>=1.72eV, for x=0.06 was E<sub>g</sub>=1.7eV whereas for CdSe band gap is E<sub>g</sub>=1.74eV. This means that with an increase in Mn concentration in the Cd<sub>1-x</sub>Mn<sub>x</sub>Se, there is a decrease in the band gap. Results correspond to our theoretical calculations as well as to literature data.

In this paper it was studied effect of γ-irradiation on optical parameters of Cd<sub>1-x</sub>Mn<sub>x</sub>Se epitaxial films. Samples were irradiated by γ-quanta at doses Dγ≤350Gy. It is defined, that at low doses, there is no change in the band gap, but optical transmittance decreases.

## EFFECT OF GAMMA IRRADIATION ON CONDUCTIVITY OF CdFeTe

**Mehrabova M.<sup>1</sup>, Nuriyev H.<sup>2</sup>, Orujov H.<sup>2,3</sup>, Kerimova T.<sup>1</sup>, Abdullayeva A.<sup>3</sup>, Hasanov N.<sup>4</sup>,  
Nazarov A.<sup>2</sup>**

*1 - Institute of Radiation Problems of Azerbaijan National Academy of Sciences*

*2 - Institute of Physics of Azerbaijan National Academy of Sciences*

*3 - Azerbaijan Technical University*

*4 - Baku State University*

*m.mehrabova@science.az*

Cd<sub>1-x</sub>Fe<sub>x</sub>Te are semimagnetic semiconductors, iron atoms introduce deep levels into the forbidden band. Such properties are conditions for the emergence of additional polarization due to hopping charge exchange.

In this paper we have investigated temperature dependences of dielectric constant and conductivity of Cd<sub>1-x</sub>Fe<sub>x</sub>Te semimagnetic semiconductors ( $x=0.03$ ) at frequencies of 25Hz-1MHz, at temperatures of 294-550K.

Cd<sub>1-x</sub>Fe<sub>x</sub>Te semimagnetic semiconductors were synthesized and crystal structure has been studied by X-ray diffraction method on the BRUKER D8 ADVANCE X-ray diffractometer.

Dielectric constant  $\varepsilon'$  was carried out by using a digital E7-20 immittance meter at frequencies of 25 Hz-1 MHz in the temperature range of  $T = 294-550K$ . The amplitude of the measuring field did not exceed  $1V\text{ cm}^{-1}$ . The sizes of sample were  $0.2 \times 0.4 \times 0.6$  mm.

The temperature dependences of conductivity  $\sigma(T)$  of Cd<sub>1-x</sub>Fe<sub>x</sub>Te ( $x=0.03$ ) defined on the base of measurements of dielectric constant. The boundaries of the temperature range for each frequency were determined.

It was found that with increasing of temperature, an increase in  $\varepsilon'$  and  $\sigma$  is observed, the slope of the curves remains constant. It have been defined that in the dependence of  $\varepsilon'(T)$ , the higher the frequency of the measuring field, the later begins the growth of  $\varepsilon'$ , but in dependence of  $\sigma(T)$ , the lower the frequency of the measuring field, the later begins the growth of  $\sigma$ . The dielectric constant remains almost unchanged up to temperature of  $\approx 400K$  and the conductivity remains unchanged up to temperature of  $\approx 480K$  over the entire studied frequency range. A maximum are observed in the temperature dependences both  $\sigma(T)$  and  $\varepsilon'(T)$  at a temperature of 550K. The conductivity at temperature of 500K at low frequencies is  $10^{-2}$  S/cm. With an increase in frequency of the measuring field, the features on the curves of  $\sigma(T)$  shift to lower temperatures, but on the curves of  $\varepsilon'(T)$  to higher temperatures.

The effect of  $\gamma$ -irradiation ( $E=1.27$  MeV,  $E=1.33$  MeV) at the dose  $D_\gamma=605.6kGy$  on the temperature dependences of conductivity and dielectric constant of Cd<sub>1-x</sub>Fe<sub>x</sub>Te ( $x=0.03$ ) were investigated. It have been found that in the dependences of  $\varepsilon'(T)$  of the irradiated Cd<sub>1-x</sub>Fe<sub>x</sub>Te, the nature of the dependence changes, there is a decline in the curves in the temperature range of  $300 \div 400K$  in all frequencies of the measuring field, and the values of  $\varepsilon'$  increase for 20 times. In the dependences of  $\sigma(T)$  of the irradiated Cd<sub>1-x</sub>Fe<sub>x</sub>Te, a pronounced maximum appears at a temperature of  $\approx 400K$  at a frequency of 25Hz-1MHz, and the value of conductivity decreases by  $\approx 40$  times in all frequencies of the measuring field.

Such increasing of dielectric constant and conductivity is caused by structural defects as well as radiation defects, since the hopping electron exchange between the defects in the crystal involve to the appearance of dipoles, and consequently, to increasing of dielectric constant.

# EFFECT OF LOCAL CRYSTAL STRUCTURE AND PHASE COMPOSITION ON TRANSPORT PROPERTIES OF SOLID SOLUTIONS $ZrO_2$ - $Y_2O_3$ AND $ZrO_2$ - $Gd_2O_3$

**Milovich E.<sup>1</sup>, Volkova T.<sup>2</sup>, Agarkova E.<sup>3</sup>**

1 - National University of Science and Technology (MISIS), Leninskiy prospekt 4, 119049 Moscow, Russia

2 - Ogarev Mordovia State University, 68 Bolshevistskaya Str., Saransk 430005, Republic of Mordovia, Russia

3 - Institute of Solid State Physics, RAS, Academician Osip'yan str. 2, Chernogolovka 142432, Russia

*filippmilovich@mail.ru*

Currently, the use of materials based on zirconia as a solid electrolyte for solid oxide fuel cells (SOFC) is associated with the need to solve a number of scientific and technological problems. The production of materials with high conductivity in the range of average temperatures (500-700 °C) and the increase in the stability of the electrophysical characteristics of solid electrolyte at operating temperatures for a long time are some of these issues. In accordance with this, the identifying of various factors, such as phase composition and local crystal structure, affecting the magnitude of oxygen-ionic conductivity of zirconia-based solid solutions, is a relevant research topic.

Comprehensive studies of the phase composition and local structure of zirconium dioxide crystals stabilized by yttrium and gadolinium oxides in a wide range of compositions from 2.7 to 38 mol.%  $R_2O_3$  (where R is Y, Gd) are performed by TEM, Raman spectroscopy, X-ray and optical spectroscopy. The influence of the phase composition and local structure on the transport characteristics of the crystals of these solid solutions was established.

The presence of transformable  $t$  and untransformable  $t'$  tetragonal phases is established in oriented crystals of zirconium dioxide, partially stabilized by gadolinium oxide, with a concentration of 2.7 and 3.6 mol.%  $Gd_2O_3$ . The presence of the twin structure formed during the transition of the high-temperature cubic phase to the tetragonal phase in  $ZrO_2$  crystals with a content of 8 mol%  $Gd_2O_3$  is shown. The twin structure is absent at the same content of yttrium oxide in  $ZrO_2$ -8 mol%  $Y_2O_3$  crystals, and the crystal structure corresponds to the structure of the  $t''$ -phase.

The local structure of the solid solutions  $ZrO_2$ - $R_2O_3$  (R - Y, Gd) is determined mainly by the concentration of stabilizing oxides  $Y_2O_3$  or  $Gd_2O_3$  and practically does not depend on the type of stabilizing oxide. It is shown that the decrease in the ionic conductivity in the concentration range of stabilizing oxides above 12 mol.%  $Y_2O_3$  ( $Gd_2O_3$ ) is due to the increase in the relative share of the positions of  $Y^{3+}$  ( $Gd^{3+}$ ) cations with oxygen vacancy in the nearest crystalline surrounding, and the reduction of ionic conductivity in the concentration range above 20 mol.%  $Y_2O_3$  ( $Gd_2O_3$ ) is due to by the formation of two anion vacancies in the nearest crystal surrounding of  $Y^{3+}$  ions ( $Gd^{3+}$ ). The difference in the values of ionic conductivity for  $ZrO_2$  crystals containing 8 mol.%  $Y_2O_3$  ( $Gd_2O_3$ ) is due to the peculiarities of their phase composition.

The work was carried out with financial support in part from the RSF (№ 18-79-00323).

# LOW-TEMPERATURE THERMOCYCLING AS A NEW METHOD OF EXPULSION OF QUENCHING DEFECTS FROM THE PEIERLS CONDUCTOR ORTHORHOMBIC TANTALUM TRISULFIDE

Minakova V.E., Nikitina A.M., Zaitsev-Zotov S.V.

*Kotelnikov IRE RAS*

*mina\_cplire@mail.ru*

In this work, samples of orthorhombic  $\text{TaS}_3$  (*o*- $\text{TaS}_3$ ) with growth defects intentionally created in the crystals by quenching were subjected to multiple thermocyclings to temperatures below the Peierls transition temperature,  $T_P$ , and back. The process of evolution of transport properties of these samples caused by the thermocyclings has been studied.

The existence of two different types of the crystals is revealed. Most of the crystals have ordinary properties and show no change both in  $T_P$  and  $E_T(T)$  with the number of thermocycling,  $N$ , where  $E_T(T)$  is the threshold field value of nonlinear conduction characterizing the force of pinning, which prevents the movement of the charge density wave (CDW) in electric field. The crystals of another group have unusual properties, the quality of these crystals improves with an increase in  $N$ . Namely, initially extremely low value of  $T_P(N)$  can be significantly (up to 15 K) increased by means of numerous thermocyclings. Moreover, the process is accompanied by a substantial (up to 2.5 times) decrease in  $E_T(T, N)$ , directly indicating an improvement in the crystal quality. The dependences of  $T_P(N)$  and  $E_T(N)$  with increasing  $N$  reach saturation up to values characteristic of crystals without quenching defects. As a result, in a sample subjected to a sufficiently large number of thermocyclings, a non-uniform distribution of quenching defects is established along the crystal with their lower concentration near its ends. With decreasing sample length, the process of the crystal quality evolution appreciably accelerates.

Such a behavior is opposite to the expected effect of deteriorating crystal quality due to thermocyclings [1, 2] and is presumably associated with forced diffusion of quenching defects due to the intrinsic for the Peierls conductors strong interaction of the CDW with the pinning centers. So this unusual effect is presumably a feature of the Peierls conductors.

The dependences of  $E_T(T_P)$  are linear with a slope dependent on  $T$ . Such a relationship is contrary to the case of both strong [3] and weak [4, 5] pinning carried out by local pinning centers, and is presumably characteristic of extended (nonlocal) pinning sources, for example, dislocations.

- [1] P. Monceau, *Adv. Phys.*, **61**, 325 (2012); G. Grüner. *Rev. Mod. Phys.* **60**, 1129 (1988).
- [2] F.Ya. Nad', M.E. Itkis, *ZhETP Lett.* **63**, 262 (1996).
- [3] H. Mutka, S. Bouffard, G. Mihály, L. Mihály, *J. Physique Lett.*, **45**, L1-13 (1984).
- [4] Pei-Ling Hsieh, F. de Czitto, A. Janossy, J. W. Savage, *J. Physique* **44** (1983) C3-1753.
- [5] V.F. Nasretdinova, E.B. Yakimov, S.V. Zaitsev-Zotov, *Physica B: Condensed Matter*, **460**, (2015) 180.



# STRUCTURE, THERMOPHYSICAL AND ELECTROPHYSICAL PROPERTIES OF SINGLE CRYSTALS OF SOLID SOLUTIONS BASED ON ZIRCONIUM DIOXIDE, CO-DOPED WITH SCANDIUM, YTTRIUM AND CERIUM

**Popov P.A.<sup>1</sup>, Borik M.A.<sup>2</sup>, Kulebyakin A.V.<sup>2</sup>, Lomonova E.E.<sup>2</sup>, Kuritsyna I.E.<sup>3</sup>, Milovich F.O.<sup>4</sup>, Myzina V.A.<sup>2</sup>, Tabachkova N.Yu.<sup>2</sup>**

*1 - Federal State-Funded Educational Institution of Higher Education «Bryansk State Academician I.G. Petrovski University»*

*2 - Prokhorov General Physics Institute of the Russian Academy of Sciences*

*3 - Institute of Solid State Physics of the Russian Academy of Sciences*

*4 - National University of Science and Technology «MISIS»*

*tfbgubry@mail.ru*

For practical applications of materials based on zirconia as heat barrier coatings, structural materials, solid electrolytes, optical materials of photonics, information about their thermal characteristics, in particular, thermal conductivity is very important. The data in the literature on these characteristics are limited to a small amount of materials studied in a narrow range of compositions, mainly on ceramic samples.

The aim of this work was to study the effect of doping impurities of yttrium, cerium and scandium on the heat and electrical conductivity of solid solutions of  $ZrO_2 - R'_2O_3 - R''_2O_3 - R'''_2O_3$  compositions (where  $R'$  - Sc,  $R''$  - Y,  $R'''$  - Ce).

The study was conducted on single crystals of solid solutions based on zirconium dioxide in a wide range of compositions grown by directional crystallization of the melt in a cold container. The distribution of oxides of scandium, yttrium and cerium in crystals was investigated. The phase composition, crystal structure, thermal conductivity and specific electrical conductivity were investigated depending on the chemical composition of the crystals.

The dependence of the specific conductivity on the composition is correlated with the data obtained in the measurement of thermal conductivity. With an increase in the total concentration of stabilizing oxides, due to the larger number of oxygen vacancies arising according to the electroneutral requirement in the heterovalent replacement of four valence zirconium cations with trivalent impurity cations, the amount of thermal conductivity decreases. With a total concentration of salt-forming oxides of 10 mol.%, crystals with higher conductivity have a lower thermal conductivity, which is associated with greater mobility of oxygen vacancies in them. The mobility of oxygen vacancies depends on the local structure of solid solutions, that is, the location of the vacancy in the first coordinate sphere of the trivalent cation or in more distant spheres. With a further increase in the concentration of impurities and the number of vacancies, the local structure of the solid solution changes. There is an increase in the number of "related" vacancies that are close to the trivalent impurity. Such vacancies have a lower mobility than those located near zirconium cations and actively participate in the conductivity of solid electrolytes. At the same time heat conductivity increases. Thus, it has been shown that the local structure of the solid solution has a great influence on the thermal conductivity and electrical conductivity. Thermal conductivity is lower in materials with a large number of free oxygen vacancies, but an increase in the concentration of "bonded vacancies" can lead to an increase in thermal conductivity and a decrease in electrical conductivity.

The work was supported by research grants № 18-02-00566 of RFBR

# PERSPECTIVE MATERIALS FOR PHOTONICS BASED ON $\text{LiBa}_{12}(\text{BO}_3)_7\text{F}_4$ FLUORIDE BORATES CRYSTALS GROWN IN THE Li, Ba, B // O, F QUATERNARY RECIPROCAL SYSTEM

**Simonova E.<sup>1</sup>, Kokh A.<sup>1</sup>, Kononova N.<sup>1</sup>, Kuznetsov A.<sup>1</sup>, Schevchenko V.<sup>1</sup>, Svetlichny V.<sup>2</sup>**

*1 - Sobolev Institute of Geology and Mineralogy SB RAS, Novosibirsk 630090, Russia*

*2 - Siberian Physical–Technical Institute of Tomsk State University, 634050, Tomsk, Russia*

*simonovakatherine1986@gmail.com*

At the present time borate systems are regarded as the most challenging for the creation of the new functional optical materials. The  $\text{LiBa}_{12}(\text{BO}_3)_7\text{F}_4$  fluoride borates crystals suitable for fabrication of polarization filters were grown on platinum loop in quaternary reciprocal system Li, Ba, B // O, F [1]. Crystals grown from melt composition  $\text{BaCO}_3:\text{BaF}_2:\text{H}_3\text{BO}_3:\text{Li}_2\text{CO}_3 = 3:3:3:1$  were found to possess a linear dichroism effect, which is due to the redistribution of positions of Li, Ba, B polyhedral in layers and wells. It should be noted that this effect was not described in the previous research on this compound [2]. The  $\text{LiBa}_{12}(\text{BO}_3)_7\text{F}_4$  crystals grown from composition  $\text{BaCO}_3:\text{BaF}_2:\text{H}_3\text{BO}_3:\text{Li}_2\text{CO}_3 = 2.5:2.5:3.5:1.5$  has a uniform pinkish color.

Due to the fact that fluoride borates with complex cationic composition, rare earth elements activated can be used as new phosphors, surpassing in their functional properties currently used by us have carried out experiments on the doping of fluoride borate crystals. Samples of  $\text{LiBa}_{12}(\text{BO}_3)_7\text{F}_4$  fluoride borate compounds were obtained by the method of solid-phase synthesis at 720-740 °C. As a result of the experiments, methods of growing crystals were worked out, optimal growth parameters were selected. The method of spontaneous crystallization on a platinum loop of growing crystals of fluoride borates of alkali and alkaline earth metals doped rare earth elements. The chemical composition of the grown samples was determined, the inclusion of rare earth elements in the structure of crystals was confirmed.

As a result of this work, crystals with composition  $\text{LiBa}_{12}(\text{BO}_3)_7\text{F}_4$  pure and doped Pr, Nd, Sm, Tb, which can be used as dichroic polarizers and luminescent materials were obtained. The structure parameters were refined by means of Rietveld method. Chemical compositions by SEM EDX and microprobe were evaluated and correlated with the unit cell parameters. Transparency and luminescence spectra of  $\text{LiBa}_{12}(\text{BO}_3)_7\text{F}_4$  have been measured in range 250-1100 nm. Spectral-luminescent properties in powders, influence of synthesis conditions and type of alloying element on optical properties were investigated.

Acknowledgements: This work is supporting by RFBR project #18-32-20001 and 18-48-543012.

References:

[1] Kokh A., Simonova E., Maillard A., Maillard R., Svetlichnyi V., Andreev Yu., Kragzhda A., Kuznetsov A., Kokh K. Linear dichroism effect in  $\text{LiBa}_{12}(\text{BO}_3)_7\text{F}_4$  crystal // *J. Cryst. Res. Technol.* 2016. V. 51. No. 9. P. 530-533.

[2] Zhao J. and Li R.K. Two new barium borate fluorides  $\text{ABa}_{12}(\text{BO}_3)_7\text{F}_4$  (A= Li and Na) // *Inorganic Chemistry*. 2014. V. 53. P. 2501-2505.

# EFFECTIVE CHARGE IN LiNbO<sub>3</sub> FILMS FABRICATED BY RADIO-FREQUENCY MAGNETRON SPUTTERING METHOD

Dybov V.<sup>1</sup>, Serikov D.<sup>1</sup>, Belonogov E.<sup>1</sup>, Sumets M.<sup>2</sup>

1 - Voronezh State Technical University

2 - Voronezh State University

*maxsumets@gmail.com*

Lithium niobate (LiNbO<sub>3</sub>) is a ferroelectric with unique properties such as the high Curie temperature ( $T_c=1210^\circ\text{C}$ ), the wide bandgap ( $E_g=3.7\text{eV}$ ) and relatively high electro-optical coefficients. Thin LiNbO<sub>3</sub> films are especially attractive due to the possible integration with the existing silicon technology. Si-LiNbO<sub>3</sub> heterostructures is the elemental basis of ferroelectric memory units, optoelectronic devices. Radio-frequency magnetron sputtering method is one of the most effective deposition techniques suitable for complex oxides. However, the successful application of these heterostructures is limited by some issues [1]. Specifically, the positive oxide charge influences negatively ferroelectric domain switching and memory effects. In our works we have demonstrated that the effective positive charge formed in LiNbO<sub>3</sub> films depends neither on the substrate orientation nor on reactive gas pressure used in the RFMS process [2,3]. Besides, the presence of oxygen in the reactive chamber reduces the positive oxide charge [4]. In this work we investigate the evolution of electric properties of amorphous films fabricated by thermal annealing of Li-Nb-O onto Si substrates with the formation of Si-LiNbO<sub>3</sub> heterostructures. At the first time, we demonstrate that this charge is located in LiNbO<sub>3</sub> films rather than at the Si/LiNbO<sub>3</sub> interface. Moreover, our analysis of C-V and I-V characteristics of Si-LiNbO<sub>3</sub> heterostructures demonstrates, that the effective oxide charge depends on the films thickness and even it changes its sign from positive to negative when the thickness becomes less than 200nm. Also, our study demonstrates that the electric characteristics of Si-LiNbO<sub>3</sub> heterostructures are affected by electronic traps existing in LiNbO<sub>3</sub> films. Thermal annealing of as-grown amorphous films changes the trap distribution from exponential to nearly uniform.

## References

- [1] M. Sumets, Lithium Niobate-Based Heterostructures: Synthesis, properties and electron phenomena, IOP Publishing Ltd, Bristol, UK, 2018. doi:10.1088/978-0-7503-1729-0.
- [2] M. Sumets, V. Ievlev, A. Kostyuchenko, V. Kuz'mina, V. Kuzmina, Influence Sputtering Conditions on Electrical Characteristics of Si-LiNbO<sub>3</sub> Heterostructures Formed by Radio-Frequency Magnetron Sputtering, *Mol. Cryst. Liq. Cryst.* 603 (2014) 202–215. doi:10.1080/15421406.2014.967607.
- [3] M. Sumets, A. Kostyuchenko, V. Ievlev, V. Dybov, Electrical properties of phase formation in LiNbO<sub>3</sub> films grown by radio-frequency magnetron sputtering method, *J. Mater. Sci. Mater. Electron.* 27 (2016) 7979–7986. doi:10.1007/s10854-016-4792-y.
- [4] M. Sumets, V. Ievlev, A. Kostyuchenko, V. Vakhtel, S. Kannykin, A. Kobzev, Electrical properties of Si-LiNbO<sub>3</sub> heterostructures grown by radio-frequency magnetron sputtering in an Ar + O<sub>2</sub> environment, *Thin Solid Films.* 552 (2014) 32–38. doi:10.1016/j.tsf.2013.12.005.

# STRUCTURAL AND OPTICAL RESEARCH OF A GaAs LAYER GROWN ON A Si/Al<sub>2</sub>O<sub>3</sub> SUBSTRATE

**Sushkov A.A., Pavlov D.A., Shengurov V.G., Denisov S.A., Chalkov V.Yu., Baidus N.V., Rykov A.V., Kryukov R.N.**

*Lobachevsky University, 23/3 Gagarin avenue, Nizhny Novgorod, 603950, Russia*

*sushkovartem@gmail.com*

Radiation-resistant substrates are used as the basis for integrated circuits (IC) in electronic control systems for the nuclear power engineering, in the aerospace and military industries. Silicon on sapphire (SOS) is well-known implementation of this structure. Enhancement of efficiency of IC on SOS is the key task of present. A way to solve is to develop new optical interconnects. The approach is to fabricate hybrid A<sup>3</sup>B<sup>5</sup> heterolasers, where light-emitting semiconductors are grown on radiation-resistant substrates. As far as particular features of the SOS substrates, they have upper Si layer. Taking into account that A<sup>3</sup>B<sup>5</sup> growth on exactly (001)-oriented Si substrates, using buffer layers [1], seems to have been well-studied, it looks logical to transfer the technology to SOS substrates. This paper presents the results of research of the optical and structural properties of GaAs layer 1200 nm, which was grown both on set of AlAs/GaAs/AlAs/Ge buffer layers with thicknesses of 10/50/10/1700 nm and on Si/Al<sub>2</sub>O<sub>3</sub> (1 $\bar{1}$ 02) substrate.

The dislocation density in the upper layer of GaAs, detected using selective etching, was estimated by the method of counting etching pits on an image obtained using atomic force microscopy. The optical quality of the epitaxial layers was investigated using photoluminescence spectroscopy (PL). Structural and analytical investigations were provided by high-resolution transmission electron microscopy (HRTEM) and X-ray energy dispersive spectroscopy (EDS), respectively. The PL maps demonstrate the uniformity of the grown GaAs top layer over the substrate area: the average value of the wavelength maxima is (862.3 ± 0.7) nm, and the peak width at half-height is (26.7 ± 1.1) nm. The shift of the maximum of the PL spectrum in the direction of short wavelengths is typical of GaAs grown on Ge and Ge/Si substrates. HRTEM studies have shown that the GaAs layer has a monocrystalline structure. Defects formed near the AlAs/Ge heterointerface and propagating to the surface have been trapped partly between the layers of AlAs and did not pass further. The EDS studies confirm that the AlAs layer prevents the mutual diffusion of Ge, Ga, and As atoms between GaAs and Ge, which is consistent with the results in other papers [1]. Etch pit density is 9·10<sup>7</sup> cm<sup>-2</sup>, which is comparable with the results for samples grown on Si substrates [2]. The results of this work indicate the possibility of growth of strained InGaAs/GaAs quantum wells on a SOS substrate using AlAs/GaAs/AlAs/Ge buffer layers to create light-emitting structures on radiation-resistant substrates.

This study was supported by the Russian Foundation for Basic Research (project no. 18-32-00636 – metallorganic chemical vapour deposition and PL spectroscopy) and the Ministry of Education and Science of the Russian Federation (projects no. 16.7443.2017/BCh).

[1] N. Baidus, V. Aleshkin, A. Dubinov et al. *Crystals*, **8**(8), 311 (2018).

[2] A. V. Rykov, M. V. Dorokhin et al. *J. Phys.: Conf. Ser.*, **1124**, 022037 (2018).

## CROSS-SECTIONAL STUDIES OF HEXAGONAL Ge INCLUSIONS IN THE Ge/Si (001) STRUCTURE

**Sushkov A.A., Pavlov D.A., Krivulin N.O., Kochugova E.S., Murtazin R.I.**

*Lobachevsky University, 23/3 Gagarin avenue, Nizhny Novgorod, 603950, Russia*

*sushkovartem@gmail.com*

Fabricate effective light-emitting structures on a silicon substrate to create optoelectronic integrated circuits of the new generation is an actual problem. Recently predicted increase in the probability of interband electron-hole transitions in 9R-Si and 9R-Ge semiconductors in comparison with their 3C (diamond) modifications has led to rigorous research of these materials [1]. Thus, for example, theoretical calculations indicate that the 9R-Ge polytype, the proportion of hexagonality is 2/3, has a direct-gap energy structure [1]. In this connection, the problem of synthesizing of the 9R-Ge phase on a Si substrate and investigating its optical properties arises.

The crystal structure of Ge layer on the Si (001) substrate was investigated. The structure was obtained by molecular beam epitaxy in a single growth chamber in two stages. Thermal cleaning of the Si substrate was carried out before beginning of growth at 1000°C within 10 minutes. At the first stage, Si interlayer was grown at 400°C within 5 minutes. At the second stage, Ge layer were grown at 300°C within 10 minutes. Structural and analytical investigations were provided by high-resolution transmission electron microscopy (HRTEM) and X-ray energy dispersive spectroscopy (EDS), respectively. Regions with a high concentration of stacking faults were detected in the HRTEM images in the phase contrast mode of the cross section of the Ge/Si (001) heterostructure in the Ge layer. The calculation of the interplane distance ( $d(hkl)$ ) in these areas in the direction of the [111] type gives the value  $d(111)=(0.97\pm 0.04)$  nm, which is three times higher (to within the error of measurement) than  $d(111)$  for Ge with a diamond (3C-Ge) structure type. In the diffraction pattern of these areas, in addition to reflections of the type (111), characteristic of 3C-Ge, there are reflexes that are located at 1/3 and 2/3 distance from the central spot to the distance (111). This diffraction pattern is a characteristic of the 9R-Ge polytype, for which the reflex (009) should almost coincide with the (111) 3C-Ge reflex ( $d(111)=0.33$  nm), and the other two has indices (003) and (006). The phase contrast modeled using the 9R-Ge primitive unit cell is the same as that obtained at the HRTEM. It confirms the correctness of the hexagonal polytype decoding. The EDS results show that these 9R-Ge inclusions are consisted of Ge atoms. The cause of the formation of 9R-Ge inclusions is assumed to be a significant mechanical stress arising in the process of Ge growth on Si due to the lattice mismatch of these materials, which is 4%.

The hexagonal phase formation of the diamond-like semiconductors in the process of heteroepitaxy is a new and almost unexplored approach to solve the problem of integrating light-emitting structures within standard silicon technology. The conditions of the formation of the phase are unclear yet. We are on the way to find out how the substrate orientation, growth temperature, and other parameters of heteroepitaxial processes affect it. Now obtaining only 9R-Ge inclusions on a Si (001) substrate by molecular beam epitaxy seems to be possible.

The work is supported by the Russian Foundation for Basic Research (Grant No. 18-32-20168-mol\_a\_ved).

[1] A. A. Nikolskaya, D. S. Korolev et al. Appl. Phys. Lett., **113**, 182103 (2018).

# INFLUENCE MECHANISM OF TEMPERATURE ON THE LATTICE MISFIT AND ELASTIC MODULE IN Mo-RICHEN Ni<sub>3</sub>Al BASED SINGLE CRYSTAL SUPERALLOY

**Zeng X.**

*Beihang University*

*mayue@buaa.edu.cn*

The variation of the lattice parameter of a Mo-richen Ni<sub>3</sub>Al based single crystal superalloy IC32 with temperature was observed with the use of high-temperature X-ray diffraction (HT-XRD) technique at temperatures between 25°C and 1200°C. The influence of temperature, especially by the redistribution of element, on lattice misfit, elastic modulus misfit and volume fraction of  $\gamma'$  phase were investigated in this study. The results have shown that absolute value of misfit increased with elevating temperature within 1100°C, reaching the maximum -0.54% at 1100°C, then being the tendency of decrease above 1100°C. The  $\gamma'$  precipitation was dissolved and the concentration of Re and Mo decreased gradually in  $\gamma$  phase above 1100°C according to analyzing the microstructure and composition. The interfacial dislocation network appeared under thermal exposure at 1200°C for 10h and it was in unstressed state caused by the Mo-richen Ni<sub>3</sub>Al based superalloy which has a large and negative lattice misfit at high temperature. And the elastic modulus for  $\langle 001 \rangle$  orientations maintains higher level, 108GPa at 1100°C. The elastic modulus misfit increase with the elevation of temperature, which was attributed to the concentration of Re and Mo in  $\gamma$  phase decreased gradually above 1100°C, and the effect of Re was even more visible.

# CHARACTERISTICS OF THE COMPOSITION, PURITY AND HOMOGENEITY OF SUBSTANCES IN THE MATERIAL SCIENCE

**Zlomanov V.P., Gaskov A.M.**

*Faculty of Chemistry, Moscow State University*

*zlomanov1@mail.ru*

The study of the relationship of the composition, structure and properties of matter is the main task of chemistry and materials science. A substance is a set of interacting particles, which is characterized by: composition, structure, type of chemical bond and particle size.

It is necessary to include in the characteristics of the composition of complex substances not only the concentration of the major components (stoichiometry) and the content of impurities, but also the concentrations of intrinsic and impurity defects associated with them. In connection with this the classification of defects, the processes of their formation, the methods of managing the defective composition are discussed in the report.

The concept of purity is relative and is associated with the comparison (measurement) of the composition of the substance with a certain standard, which is difficult to choose. A comparison of the actual composition of the substance with the one that ensures its functional application can be chosen as a criterion of purity.

The properties of semiconductors are determined by the concentration of charge carriers-electrons, holes. The criterion of purity in this case is the ratio between the required functional concentration of charge carriers ( $N_{\text{FUNCT.}}$ ) and that ( $N_{\text{intrinsic}}$ ), which is due to the properties of the substance. For example, in IR detectors for the occurrences of the necessary functional response (signal) to external influence value  $N_{\text{intrinsic}}$  must be less than the  $N_{\text{FUNCT.}} = 10^{16} \text{ cm}^{-3}$ , i.e., a substance in which the total concentration of carriers due to the properties of the substance is less than  $10^{-4} \%$  at can be considered pure.

An important problem of materials science is the question of uniform distribution of particles forming the composition and structure. Their distribution is random.<sup>[1]</sup> In this regard, the statistical criteria of homogeneity of the composition are considered. If  $\delta$  is the value of the confidence interval, and  $c_i$  is the concentration of particles in the  $i$ -th micro volume, then under the condition  $|(c_i - 1)/N \sum_{i=1}^N c_i| \leq \delta$  the substance can be called homogeneous. If at least one value of  $i$  does not fulfill this inequality, the substance should be considered as heterogeneous. For the practical use of the material, it is important that the deviation of the property value in this object from the weighted average value in the whole system, which goes beyond the confidence interval. In this sense, heterogeneity can be called a set of values of the measured property that go beyond the mentioned boundaries and taken over all micro volumes.

[1] Nikitina V. G., Orlov A. G., Romanenko V. N. The problem of nonuniform distribution of atoms and defects in the study of the perfection of semiconductor crystals. Growth processes of semiconductor crystals and films. Novosibirsk: Science, 1981. Vol.6. P. 204.

LOW DIMENSIONAL NANOSTRUCTURE GROWTH ON ANISOTROPIC SILICON (110)  
RECONSTRUCTION SURFACE

Asaoka H.A.

*Advanced Science Research Center, Japan Atomic Energy Agency*

*asaoka.hidehito@jaea.go.jp*

Control of low dimensional nanostructures on semiconductor surfaces is one of the most attractive studies. Among the semiconductor surfaces, a reconstructed Si(110)-“16×2” is a promising template for nanostructure, because of its one dimensional up-and-down terrace of 2.5 nm width. We succeeded in preparation of ordered Si, Ge(110)-“16×2” single-domain surfaces [1-4]. One-dimensional structures with C<sub>60</sub> molecules [5-6] and Si, Ge nanodot [7-9] formed on the surfaces. Furthermore, we determined the initial oxidation [10-11] and the oxide layer decomposition [12-13] process on reconstructed Si(110)-“16×2” surface.

1. Y. Yamada, A. Girard, H. Asaoka, H. Yamamoto, S. Shamoto, Phys. Rev. B **76** (2007) 153309.
2. Y. Yamada, A. Girard, H. Asaoka, H. Yamamoto, S. Shamoto, Phys. Rev. B **77** (2008) 153305.
3. Y. Yokoyama, Y. Yamada, H. Asaoka, M. Sasaki, e-J. Surf. Sci. Nanotech. **10** (2012) 509.
4. Y. Yokoyama, A. Sinsarp, Y. Yamada, H. Asaoka, M. Sasaki, Appl. Phys. Express **5** (2012) 025203.
5. Y. Yamada, S. Yamada, T. Nakayama, M. Sasaki, T. Tsuru, Jpn. J. Appl. Phys. **50** (2011) 08LB06.
6. Y. Yokoyama, Y. Yamada, H. Asaoka, M. Sasaki, J. Phys.: Conf. Ser. **417** (2013) 012036.
7. M. Yano, Y. Uozumi, S. Yasuda, H. Asaoka, Jpn. J. Appl. Phys. **57** (2018) 06HD04.
8. Y. Yokoyama, T. Yamazaki, H. Asaoka, J. Cryst. Growth **378** (2013) 230.
9. Y. Yokoyama, Y. Uozumi, H. Asaoka, J. Cryst. Growth **405** (2014) 35.
10. H. Togashi, Y. Takahashi, A. Kato, H. Asaoka, A. Konno, M. Suemitsu, Jpn. J. Appl. Phys. **46** (2007) 3239.
11. Y. Yamamoto, H. Togashi, A. Kato, Y. Takahashi, A. Konno, Y. Teraoka, A. Yoshigoe, H. Asaoka, M. Suemitsu, Appl. Surf. Sci. **254** (2008) 6232.
12. M. Yano, Y. Uozumi, S. Yasuda, C. Tsukada, H. Yoshida, A. Yoshigoe, H. Asaoka, Jpn. J. Appl. Phys. **57** (2018) 08NB13.
13. M. Yano, Y. Uozumi, S. Yasuda, H. Asaoka, C. Tsukada, H. Yoshida, A. Yoshigoe, e-J. Surf. Sci. Nanotech. **16** (2018) 370.



# IDEAL AND ULTIMATE TENSILE STRENGTH OF SOLIDS: MOLECULAR DYNAMICS MODELING

**Baidakov V.G.**

*Institute of Thermal Physics, Ural Branch of the Russian Academy of Sciences, Amundsen street 107a, Ekaterinburg, 620016, Russia*

*baidakov@itp.uran.ru*

A stretched solid is in a metastable state and is characterized by a finite time until the destruction. To an overall stretching corresponds a negative external pressure.

A study has been made of the mechanical stability of an ideally elastic solid with respect to infinitesimal and finite changes in state parameters. Elastic properties have been determined and the process of nucleation in a stretched Lennard-Jones crystal with a face-centered cubic (FCC) lattice has been investigated in molecular dynamics experiments. It is shown that, as distinct from a liquid phase, the boundary of the crystal stability against infinitesimal deformations (ideal strength boundary) depends not only on thermodynamic state parameters but also on the type of deformation (homogeneous or inhomogeneous). At homogeneous deformations and temperatures above that of the endpoint of the melting line  $T_k$  the crystal ideal strength boundary is determined by the shear moduli  $\mu$ ,  $\mu'$ , and at lower temperatures by the bulk modulus  $K$ . The crystal reaction to inhomogeneous deformation depends on the moduli of unilateral compression. At temperatures below  $T_k$ , the moduli of unilateral compression of an FCC crystal have finite values on the line where the bulk modulus  $K$  takes a zero value. Thus in a solid at  $K = 0$ , when  $\mu > 0$  and  $\mu' > 0$ , spatially inhomogeneous deformations, as long-wave as is wished, will be finite. This makes it possible to realize states with  $K < 0$  in a crystal, which are unstable (labile) in a liquid phase.

The process of crystal destruction at high tensile stresses has been investigated. It has been established that at temperatures both above the endpoint of the melting line and below it the destruction proceeds by the mechanism of spontaneous formation and growth of new-phase nuclei. Spontaneous nucleation determines the boundary of resistance of a solid to destruction, i.e. the limiting strength. As distinct from an ideal strength, the notion of a limiting strength is connected with the spatial (the body volume  $V$ ) and the temporal (the expectation time for destruction, longevity  $\tau$ ) factor. The limiting strength may be determined by specifying the nucleation rate or the mean expectation time for a nucleus in the system unit of volume. A solids spontaneous nucleation of voids (cracks), whose development leads to continuity violation, is observed both in states where  $K > 0$  and in states with  $K < 0$ . The latter is observed at  $T < T_k$ . The method of the mean lifetime of a metastable system  $\bar{\tau}$  has been used to determine the nucleation rate, which is comparable to calculations by classical nucleation theory.

Data of molecular dynamics simulation on the mean longevity  $\bar{\tau}$  of a stretched Lennard-Jones crystal are also analyzed in the context of the Zhurkov thermofluctuation concept of strength. It is shown that classical nucleation theory leads to a steeper dependence of longevity on the tensile stress than the Zhurkov theory and this parameter agrees well with the results of molecular dynamics simulation. Some discrepancy between classical nucleation theory and simulation in the value of the limiting stretching may be connected with the neglect of the size effect in the nucleus-parent phase interfacial free energy.

The molecular dynamics simulation conducted testifies that at low temperatures and high negative pressures in a quasi-static process it is possible to achieve not only states where  $K = 0$ , but also states with  $K < 0$ , which, as distinct from a liquid phase, in a solid will be metastable.

The work has been performed with a financial support of the Russian Science Foundation (project N 18-19-00276).

# ATOMISTIC MODELING OF SOLID-STATE PHASE TRANSITIONS IN POLY(3-ALKYLTHIOPHENES): FROM FORM II TO FORM I POLYMORPHS

**Casalegno M.<sup>1</sup>, Nicolini T.<sup>1</sup>, Famulari A.<sup>1</sup>, Raos G.<sup>1</sup>, Po R.<sup>2</sup>, Meille S.V.<sup>1</sup>**

*1 - Department of Chemistry, Materials, Chemical Engineering "G. Natta", Politecnico di Milano*

*2 - Research Center for Renewable Energies and Environment,  
Istituto Guido Donegani, Eni S.p.A.*

*mose.casalegno@polimi.it*

Poly(3-alkylthiophenes) (P3ATs) represent an important class of p-type semiconductors in organic electronics, thanks to their processability and favorable charge transport properties. Polymorphism and solid-state phase transitions in these materials have a deep impact on their electronic properties, yet the relationship between different polymorphs is not-so-well understood. Computational methods offer a powerful tool to investigate these processes on a molecular scale, but they have rarely proven successful for crystalline polymers.

In the present work, we report a successful attempt to explore the experimentally observed transition from form II to the more common form I type polymorphs, via molecular dynamics (MD) simulations. The transition is followed continuously for poly(3-hexylthiophene) (P3HT) and poly(3-butylthiophene) (P3BT) evidencing three main steps: i) loss of side chain interdigitation ii) partial disruption of the original stacking order and, iii) reorganization of polymer chains into new, tighter, main-chain stacks, and new layers with characteristic form I periodicities, substantially larger than those in the original form II. Our findings are rationalized in the context of organic electronics and phase transition modeling.

# MICRO-CANONICAL DESCRIPTION OF GROWTH AND THERMAL DECOMPOSITION OF ALUMINA CLUSTERS

**Chemin A.<sup>1</sup>, Allouche A.-R.<sup>1</sup>, Melinon P.<sup>1</sup>, Miyajima K.<sup>2</sup>, Mafuné F.<sup>2</sup>, Amans D.<sup>1</sup>**

*1 - Univ Lyon, Univ Claude Bernard Lyon 1, CNRS, Institut Lumiere Matiere, F-69622, Villeurbanne, France*

*2 - Department of Basic Science, Graduate School of Arts and Sciences, The University of Tokyo, Komaba, Meguro-ku, Tokyo 153-8902, Japan*

*arsene.chemin@univ-lyon1.fr*

Clusters have been greatly studied for chemical catalysis purposes and are of first interest for laser generation of nanoparticles, including Laser Ablation in Liquide [Amendola PCCP 2012], being the first step of the growing process. Yet, no simple theory enables general description of cluster behaviour. While Classical nucleation theory fails to explain it [Merikanto PRL 2007], models based on thermodynamics are still developed to draw out general considerations [Davari & Mukherjee AIChE 2017, Gross AIP 1997]. In this work, we explore a micro-conical approach to describe growth and thermal decomposition of alumina clusters considering Weisskopf model which was first developed for nuclear reactions [Weisskopf PR 1937], and later adapted for gas aggregate [Engelking JCP 1986, Franklin Science 1976] and unimolecular evaporation [Hermite EPL 2012].

We then confront it with experimental measurements on alumina clusters obtained by ablation of an aluminium rod in an oxygen rich environment. The obtained clusters population was then heated at different temperatures and the size distribution evolution measured. Experimental observations can be very well predicted by Weisskopf model on the condition that dissociation energy decreases with the cluster size. Such a decrease is confronted with *ab initio* calculations and experimental measurements of activation energies underlining the fundamental molecular aspect of this problem.

# **A FLOW EFFECT ON DISTRIBUTION OF SUPERCRITICAL NUCLEATION CENTERS DURING THE CRYSTALLIZATION PROCESS ILLUSTRATED BY THE EXAMPLE OF BORON CARBIDE-REINFORCED ALUMINUM**

**Eydelman E.D.<sup>1,2</sup>, Durnev M.A.<sup>1</sup>**

*1 - St. Petersburg Chemical-Pharmaceutical University. St. Petersburg, Russia*

*2 - Ioffe Institute. St. Petersburg, Russia*

*mad5245mail@gmail.com*

In the first-order phase transition, e.g., crystallization, two steps are identified. The first one is the formation of critically sized nucleation centers in the metastable system, i.e. the size of nucleation centers is such that the system does not return to the initial one-phase state. The second step is the evolution of post-critical big nucleation centers of a new phase. It is such quickly growing nucleation centers that accumulate, integrate, and absorb the metastable phase with small-sized nucleation centers.

This work focuses on the second step, using the example of crystallization.

The actual structure of a solid state is formed precisely at the supercritical stage of crystallization. This stage (and the possibility of producing a given distribution of the main and additional materials under centrifugal casting) remains unstudied.

In connection with the use of centrifugal casting technologies with a high rotary speed of lingots, a problem arose when predicting the influence of the flow, first of all, rotation, will have on crystallization and, in a broader sense, on first-order phase transitions.

The investigation of rotations influence is important for developing technologies for gradient spatially-inhomogeneous composite material production. Due to spatial inhomogeneity, for example, surface hardening, such materials could potentially be used for manufacturing structures operating under extremely difficult conditions.

In present work, the effect of flow that created specifically by centripetal forces, the force of buoyancy, and the force of viscous friction of boron carbide particles at the final stage of crystallization, the coalescence stage, in which growth of large nuclei is determined by absorption of small ones, is considered in the case of a liquid-solid first-order phase transition.

We also present the characteristic results of microscopic investigations. The hardness of samples was studied using an MET-U1 ultrasonic hardness tester (TS 4271-001- 18606393-00). We established that additional material B<sub>4</sub>C can increase the surface layer hardness compared to reference alloy AK12. We estimated here the value of phase transition time. As expected, the presence of reinforcing particles, which are the primary critical nucleation centers, accelerates the phase transition.

The distribution of supercritical nucleation centers in the presence of flow effect, which was obtained here theoretically, is confirmed experimentally using the example of a composite produced by centrifugal casting from the aluminum alloy AK12 and boron carbide particles.

A specific distribution of supercritical nuclei, taking into account the presence of the macroscopic motion, i.e., rotation, has been found for the first time. This allows one to hope that melt motion will be a tool for constructing materials with new properties.

# THE EVOLUTION OF POST-CRITICAL NUCLEATION CENTERS OF THE CRYSTALLIZATION PROCESS AT THE CENTRIFUGAL-CASTING METHOD FOR DESIGN OF GRADIENT COMPOSITES OF ALUMINUM AND GRAPHITE

**Eydelman E.D.<sup>1,2</sup>, Durnev M.A.<sup>1</sup>**

*1 - St. Petersburg Chemical-Pharmaceutical University. St. Petersburg, Russia*

*2 - Ioffe Institute. St. Petersburg, Russia*

*eugeny.eidelman@pharminnotech.com*

The consideration of processes occurring during centrifugal casting must be based on the theory of first-order phase transitions and, in particular, on the theory of crystallization. This theory has a wide variety of applications. In all studies of the theory of first-order phase transitions, the most relevant task is to construct the nucleation centers size distribution immediately before the transition's end at the supercritical stage. When the transition takes place from the liquid phase during crystallization, e.g., during centrifugal casting, we need to allow for the macroscopic motion of small nuclei in the metastable condition, i.e., the presence of flows. As a rather rough approximation, we may restrict ourselves to the motion-flows caused by viscous forces and buoyant force if we have, for instance, large rotation velocities.

Gradient composite materials (GCMs) may serve to solve problems arising in the design of structures intended to operate in extreme conditions. Centrifugal casting is an advanced method to produce GCMs especially for aluminum-based materials [1]. GCMs differ from conventional isotropic composites because of the presence of spatially inhomogeneous structures due to which these materials take on novel properties and novel functions. The search for and development of new technological processes for GCM synthesis and modeling of their production process, determined by loading parameters, are urgent tasks.

In the present work, the general problems of GCM production will be solved in the context of aluminum-based materials. The main material is AK12 aluminum alloy. The admixtures are aluminum oxide ( $\text{Al}_2\text{O}_3$ ) and graphite particles (C). The general result is distribution of supercritical nuclei for two components of the admixture.

We present the characteristic results of microscopic investigations. The hardness of samples was studied using an MET-U1 ultrasonic hardness tester (TS 4271-001- 18606393-00). We established that graphite particles do not increase the GCM hardness compared to reference alloy AK12. Introduction of  $\text{Al}_2\text{O}_3$  particles increases the surface layer hardness. We performed the conversion into the reinforcing phase fraction. We discovered that the gradient layer width and particle distribution vary with variation of particle volume weight and along the cylinders height

Crystallization occurs mainly on the nucleation centers forming around admixture particles. At the supercritical, the distribution of nucleation centers by size is determined. During the phase transition, nucleation centers grow, and their growth is limited only by the size of the melt. With a strong rotation, centrifugal forces promote growth mainly in the direction of rotation to the ingot. It is important that the calculated distribution of large nuclei of reinforcing materials,

is in good agreement with the experimental results obtained as a result of the processing of direct microscopic observations.

We showed that choosing reinforcing admixtures having densities larger and smaller than the density of the main material allows creating GCMs with the prescribed hardness by the centrifugal casting process.

## **References**

[1] Eydelman E.D., Durnev M.A. Tech. Phys.Let.2018, 44(7), P. 23-29.

## THE CRYSTALLIZATION PROCESS IN THE PRESENCE OF A FLOW

**Eydelman E.D.<sup>1,2</sup>, Durnev M.A.<sup>1</sup>**

1 - St. Petersburg Chemical-Pharmaceutical University. St. Petersburg, Russia

2 - Ioffe Institute. St. Petersburg, Russia

*eugeny.eidelman@pharminnotech.com*

The evolution of post-critical “big” nucleation centers of a new phase is identified. Such quickly growing nucleation centers accumulate, integrate, and absorb the metastable phase with small-sized nucleation centers.

This presentation focuses on this step, using the example of crystallization. The theory of this step of the nucleation process without the macroscopic flow effect in the metastable material is well known, but this theory is constructed using the example of vapor condensation (see, for example, review [1]). In the recent years, the size distribution of supercritical nucleation centers and its time evolution were obtained within the frame of this theory [2, 3].

In connection with the use of centrifugal casting technologies with a high rotary speed of lingots, a problem arose when predicting the influence of the flow, first of all, rotation, will have on crystallization and, in a broader sense, on the first order phase transitions. Certainly, flow effects of different kinds occur during the material treatment. However, it is the influence of rotation that to be of special interest.

The investigation of rotation influence is important for developing technologies for gradient spatial-inhomogeneous composite material production.

In this work, the distribution of supercritical embryos in the presence of flow effect, which was obtained theoretically, will be confirmed experimentally using the example of a composite produced by centrifugal casting from the aluminum alloy AK12 [4] and 1) Boron carbide particles [5]; 2) Graphite [6]; 3) Basalt fibers [7].

A specific distribution of supercritical nuclei, taking into account the presence of the macroscopic motion, i.e., rotation, has been found for the first time. This allows one to hope that melt motion will be a tool for constructing materials with new properties.

### References

- [1] Kuni F.M., Shchekin A.K., Grinin A.P. *Phys. Usp.*, 2001, **44**, P. 331–370.
- [2] Kurasov V.B. *Advances in the first order phase transitions. II*. VVM Publishing Ltd., St. Petersburg, 2013.
- [3] Kurasov V.B. *Tech. Phys. Lett.*, 2015, **41**, P. 348–351.
- [4] Kevorkijan V. *American Ceramic Society Bulletin*, 2003, 82 (2), P. 60–64.
- [5] Durnev M.A., Eydelman E.D. *Nanosystems: physics, chemistry, mathematics*, 2017, **8**(3), P. 360-364.
- [6], Eydelman E.D., Durnev M.A. *Tech. Phys.* 2018, **63**(11), P. 1615-1619.
- [5] Eydelman E.D., Durnev M.A. *Tech. Phys.Let.*2018, **44**(7), P. 23-29.

# STRIATION IN MELT-GROWN CRYSTALS AS A SELF-OSCILLATING PROCESS

**Fedorov P.P., Kuznetsov S.V., Konyushkin V.A., Nakladov A.N., Chernova E.V.**

*Prokhorov General Physics Institute of the Russian Academy of Sciences*

*ppfedorov@yandex.ru*

Striation is a characteristic growth defect of crystals, deteriorating their optical quality. Thermodynamic--topologic analysis of crystallization processes [1] showed that congruent-melting points, whose concentration vicinities are used for single-crystal growth, frequently correspond to unstable nodes in phase portraits that image the crystallization of phases of variable composition. The instability of the chemical composition of melt during crystallization is manifested as striation in growing crystals. For the provision of steady-state crystallization in the vicinity of peaks and saddles on liquidus surfaces, a bifurcation cascade is evidently required. The primary bifurcation is the limiting cycle generation bifurcation in the concentration space. For peak points, this is Hopf bifurcation discovered by Andronov [1]. For saddles, the simplest cycle generation bifurcation is a nonlocal cosymmetric bifurcation 1 (the saddle separatrix loop), as described in [2].

Vertical directional solidification in a fluorinating atmosphere was used to grow a series of single crystals of fluorite solid solutions in  $\text{SrF}_2\text{-BaF}_2\text{-RF}_3$  ( $R = \text{Pr, Er, Tm, Ho}$ ) ternary systems, these crystals corresponding to the vicinities of saddle-type congruent-melting points. The existence of this type of node was predicted in [3]. Thus-grown crystals have no cellular superstructure, which proves the stability of growth to constitutional undercooling, but have striate. Concentration distribution along the length of crystals was analyzed.

The authors acknowledge the support from Presidium RAS Program No.5: Photonic technologies in probing inhomogeneous media and biological objects.

## References

1. P.P.Fedorov. Russian Journal Inorganic Chemistry, **50** (12) (2005), 1933.
2. E. Leontovich. Dokl. Akad. Nauk SSSR, **78** (1951), 641 (in Russian).
3. P.P. Fedorov. Growth of Crystals. **20**. Ed.E.I. Consultants Bureau. N.Y.-London 1996, 103-116.

## NON-CLASSICAL CRYSTAL GROWTH OF FLUORIDES AND OXIDES

**Fedorov P.P.<sup>1</sup>, Kuznetsov S.V.<sup>1</sup>, Mayakova M.N.<sup>1</sup>, Maslov V.A.<sup>1</sup>, Baranchikov A.E.<sup>2</sup>,  
Gaynutdinov R.V.<sup>3</sup>, Ivanov V.K.<sup>2</sup>, Osiko V.V.<sup>1</sup>**

*1 - Prokhorov General Physics Institute of the Russian Academy of Sciences*

*2 - Kurnakov Institute of General and Inorganic Chemistry*

*3 - Crystallography and Photonics Federal Research Center*

*ppfedorov@yandex.ru*

The review of own experimental results on research of processes of crystal formation on the non-classical crystal growth (NCCG) mechanism, namely - by the oriented attachment growth is made [1-4]. A set of experimental research methods (SEM, TEM, AFM, X-ray diffraction) was used. The processes of crystal formation during the growth of crystals from nitrate and chloride fluxes, coprecipitation from aqueous solutions (including geological processes) were investigated. The main regularities and general scenarios of NCCG processes are formulated.

Fig. 1\*. SrF<sub>2</sub> microcrystal, consisting of nanocubic particles, which was synthesized by the reaction of SrCl<sub>2</sub> + KF = SrF<sub>2</sub>↓ + KCl at 1000 °C.

### References

1. V.K. Ivanov, P.P. Fedorov, A.Y. Baranchikov, V.V. Osiko. Oriented aggregation of particles: 100 years of investigations of non-classical crystal growth // Russ. Chem. Rev., 2014, **83** (12), 1204–1222
2. P. Fedorov, V.V. Osiko, S.V. Kuznetsov, O.V. Uvarov, M.N. Mayakova, D.S. Yasirkina, A.A. Ovsyannikova, V.V. Voronov, V.K. Ivanov. Nucleation and growth of fluoride crystals by agglomeration of the nanoparticles // J. Crystal Growth, 401 (2014) 63-66.  
DOI: 10.1016/j.jcrysgro.2013.12.069
3. P.P. Fedorov, V.K. Ivanov, V.V. Osiko. Basic Features and Crystal\_Growth Scenarios Based on the Mechanism of Oriented Attachment Growth of Nanoparticles // Doklady Physics, 2015, V. 60, No. 11, pp. 483–485.  
DOI: 10.1134/S1028335815110105
4. P.P. Fedorov, M.N. Mayakova, A.A. Alexandrov, V.V. Voronov, S.V. Kuznetsov, A.E. Baranchikov, V.K. Ivanov. The melt of sodium nitrate as a new medium for synthesis of fluorides. // Inorganics. Special Issue “Inorganic Fluorides” 2018, V. 6. 38; DOI:10.3390/inorganics6020038,

*The study was funded by Russian Foundation for Basic Research №2018-18-29-12050-MK*

\*The abstract with figures is available at <http://2019.mgctf.ru/0100003501.doc>



# A MODEL OF SHAPES OF LIQUID CYLINDRICAL INCLUSIONS MIGRATING THROUGH A CRYSTAL, AND ITS APPLICATIONS FOR STUDYING KINETICS OF CRYSTALLIZATION (DISSOLUTION)

**Garmashov S.**

*Southern Federal University*

*garmashov@sfedu.ru*

One of the methods for studying the properties of crystals is based on the analysis of the behavior of liquid inclusions in these crystals under external influence, for example, upon their non-uniform heating. As is known [1], a liquid inclusion can move through the crystal under the action of a temperature gradient due to the processes of dissolution and crystallization at its boundary and diffusion in the liquid phase. The velocity and shape of the migrating inclusion depend on various factors: the mechanism and degree of difficulty of interfacial processes, the volume of the liquid phase, the applied temperature gradient, the interfacial energy and its anisotropy. This makes it possible to draw conclusions about the mechanism and kinetics of crystallization (dissolution) by analysis of experimental data with using the corresponding mathematical model of inclusions migrating in a crystal.

One of such models was proposed in [2–4] and applied [5, 6] to interpreting the cross sectional shapes of cylindrical inclusions that migrated in a crystal under stationary thermal conditions. The model is based on the balance of fluxes in the liquid and at solid-liquid interfaces, and takes into account capillary effects, anisotropy of both interfacial energy and interfacial kinetics. The analysis of the influence of various parameters of the migration process on the velocity and cross-sectional shape of the inclusion, and the processing of experimental data can be performed with using the model. For each of the cases of applying the model, computer programs have been developed with appropriate interfaces for displaying the calculation results. In the case of processing experimental data, the program provides the ability to download a digital micrograph of the cross section of the inclusion migrated in a crystal, and to fit a model shape directly against the microphoto of the experimentally obtained one.

From the results of the calculations, it follows that the dependence of the inclusion velocity on the cross-sectional area can be non-monotonic (to have a maximum) provided that the degree of anisotropy of the specific interfacial energy is sufficiently small and the difficulty of the interfacial processes is sufficiently large. In addition, with increasing the cross-sectional area of the inclusion, its shape becomes more flattened in the direction of motion (the ratio of the inclusion width to its thickness increases), and the velocity tends to some value lower than the diffusion velocity (i.e., the inclusion velocity without account of interfacial kinetics) that determined mainly by the specific interfacial energy of the singular parts of the inclusion boundary and the degree of difficulty of the dissolution process. On the basis of the developed model, techniques have been proposed for determining the degree of anisotropy of interfacial energy and the degree of difficulty of interfacial processes over data on several (at least three) cross-sectional shapes of inclusions (with different areas) migrated in a crystal under the same thermal conditions.

1. G.G. Lemmlein, Reports of the USSR Academy of Sciences, 1952, 85, 325-328.
2. S.I. Garmashov, V.Yu. Gershanov, J. Cryst. Growth, 2009, 311, 413–419.
3. V.Yu. Gershanov, S.I. Garmashov, Technical Physics, 2015, 60, 61–65.
4. S.I. Garmashov, Y.V. Prikhodko Abstracts of Lecturers and Young Scientists of Fourth China-Russia Conference on Numerical Algebra with Applications (CRC-NAA'15, 26-29 June 2015, Rostov-on-Don), 2015, 99–103.
5. S.I. Garmashov, Crystallography Reports, 2018, 63, 844-848.
6. S.I. Garmashov, V.V. Protsenko, Communication on Applied Mathematics and Computation, 2018, 32, 190 – 201.

# KINETIC MODEL FOR CONDENSATION-INDUCED RESTRUCTURING OF ATMOSPHERIC SOOT AGGREGATES

**Gor G., Enekwizu O., Khalizov A.**

*New Jersey Institute of Technology*

*gor@njit.edu*

Soot is major pollutant and climate forcer [1]. The optical properties of soot nanoparticles that determine its impact on the climate strongly depend on the particle morphology [2]. When initially generated, soot nanoparticles are branched fractal agglomerates consisting of spherical primary carbon particles. However, during its aging in the atmosphere, the morphology of soot nanoparticles is often changed: condensation of vapors on the agglomerates induces their collapse into globules. Although there have been several studies of this effect [3-5], a model which could predict whether the agglomerates will collapse or not is still lacking.

Analysis of the recent laboratory experiments suggested that the spacial distribution of condensate on the soot agglomerates may determine its fate with respect to restructuring [6]. When a vapor condenses in the junction between the spheres, the capillary and disjoining forces are likely to generate mechanical stresses sufficient for plastic deformation of an agglomerate. Therefore, the agglomerate restructuring is directly related to the domination of one of the scenarios of vapor condensation: if condensation on the surface of primary carbon particles dominates, the agglomerate will unlikely restructure; if condensation in the junction between the primary particles (“capillary condensation”) dominates, the agglomerate will likely collapse.

This presentation will focus on our recent results, reported in [7]: laboratory study of condensation-induced restructuring supported by the condensation model. We introduced a dimensionless parameter,  $\chi$ , which includes the size of the soot primary particles, vapor supersaturation, surface tension and density of the condensate. We showed that when  $\chi \ll 1$ , the surface condensation dominates and aggregates do not restructure, while at  $\chi \sim 1$ , the capillary condensation dominates, and the aggregates restructure. We showed that this simple model is consistent with our and others experimental data.

1. Bond, T. C., Doherty, S. J., Fahey, D., Forster, P., Berntsen, T., DeAngelo, B. J., Flanner, M. G., Ghan, S., Karcher, B., Koch, D., et al. (2013). *J. Geophys. Res. Atmos.*, 118(11):5380–5552
2. Xue, H., Khalizov, A. F., Wang, L., Zheng, J., and Zhang, R. (2009). *Phys. Chem. Chem. Phys.*, 11(36):7869–7875
3. Weingartner, E., Baltensperger, U., and Burtscher, H. (1995). *Environ. Sci. Technol.*, 29(12):2982–2986.
4. Miljevic, B.; Surawski, N. C.; Bostrom, T. and Ristovski, Z. D., (2012) *J. Aerosol Sci.*, 47:48-57.
5. Schnitzler, E. G.; Gac, J. M. and Jäger, W. (2017) *J. Aerosol Sci.*, 106:43-55
6. Chen, C., Fan, X., Shaltout, T., Qiu, C., Ma, Y., Goldman, A., and Khalizov, A. F. (2016). *Geophys. Res. Lett.*, 43(20).
7. Chen, C., Enekwizu, O. Y., Fan, X., Dobrzanski, C. D., Ivanova, E. V., Ma, Y., Gor, G. Y. and Khalizov, A. F. (2018). *Environ. Sci. Technol.*, 52(24), 14169-14179.

# NUCLEATION EFFECTS IN RECEPTORS CLUSTERING ON A T-CELL'S SURFACE

**Prikhodko I.V.<sup>1,2</sup>, Guria G.Th.<sup>1,2</sup>**

*1 - National Research Center for Hematology, Moscow, Russia, 125167*

*2 - Moscow Institute of Physics and Technology, Dolgoprudny, Russia, 141701*

*guria@blood.ru*

The presence of viruses in the cell is determined by the change in the composition of short fragments of all the proteins present in it — epitopes exposed on the cell surface. Virus-infected cells are recognized by T-cell. When T-cell receptors come in contact with viral epitopes it activates. In some cases, just one viral epitope is enough to activate T-cell [1].

At the same time, the presence one receptor on T-cell's surface is not enough for T-cell activation. Signal transmission through the membrane of the T-cell is carried out only through clusters of several hundred receptors [2]. The developed approach implies that the receptors on the T-cell membrane are clustered in a threshold manner. In this case, viral epitopes act as exogenous nuclei for the transition of receptors from chaotic to the cluster phase. In other words, the task of virus recognition is reduced to the problem of finding the conditions for heterogeneous nucleation [3].

In droplet models of nucleation theory, the critical parameter is the size of the “droplet” [4]. The T-cell receptor's system allows the formation of clusters that have complex (non-cylindrical) shape. Thus the search for critical parameter is an independent task. It was shown that the transition from a sub- to a supercritical cluster is associated with a sharp increase in the entropy of the receptor's coupling graph. Various options for the introduction of corresponding entropy were analyzed. As a result, the probability of a signaling cluster formation was calculated as a function on the type and number of viral epitopes. The possibility of transferring the results to the analysis of other blood cell's activation is discussed.

This work was supported by Russian Science Foundation, grant 19-11-00260.

## Literature

1. Huang, J., Brameshuber, M., Zeng, X., Xie, J., Li, Q. J., Chien, Y. H., ... & Davis, M. M. (2013). A single peptide-major histocompatibility complex ligand triggers digital cytokine secretion in CD4+ T cells. *Immunity*, 39(5), 846-857.
2. Pigeon, S. V., Tabarin, T., Yamamoto, Y., Ma, Y., Nicovich, P. R., Bridgeman, J. S., ... & Tungatt, K. (2016). Functional role of T-cell receptor nanoclusters in signal initiation and antigen discrimination. *Proceedings of the National Academy of Sciences*, 113(37), E5454-E5463.
3. Becker, R., & Döring, W. (1935). The kinetic treatment of nuclear formation in supersaturated vapors. *Ann. Phys*, 24(719), 752.
4. Frolov, V. A. J., Chizmadzhev, Y. A., Cohen, F. S., & Zimmerberg, J. (2006). “Entropic traps” in the kinetics of phase separation in multicomponent membranes stabilize nanodomains. *Biophysical journal*, 91(1), 189-205.

## THE FASTEST CRYSTAL FORMATION MECHANISM

**Kashchenko M.<sup>1,2</sup>, Kashchenko N.<sup>1</sup>, Chashchina V.<sup>1,2</sup>**

*1 - Ural Federal University*

*2 - Ural State Forestry University*

*mpk46@mail.ru*

Using the example of the fcc-bcc ( $\gamma$ - $\alpha$ ) martensitic transformation (MT) occurring during cooling in iron-based alloys, the principal features of the formation of  $\alpha$ -phase crystals (martensite) are discussed. Namely: the rapid (supersonic) growth of martensite crystals is due to the controlling wave process (CWP), directly related to the initial excited state (IES) [1].

IES (oscillatory type) occurs at temperatures  $M_s$  below the equilibrium temperature  $T_0$  of the  $\gamma$  and  $\alpha$  phases due to the release of energy of supercooled austenite in certain local regions of the initial  $\gamma$ -phase (austenite) with reduced interfacial barriers due to elastic fields of dislocations that violate the initial crystal symmetry. Thus, the concept of IES as applied to MT reveals the essence of the initial stage of the formation of a martensite crystal that differs significantly from the traditional idea of heterogeneous nucleation suggesting the existence of quasi-equilibrium nuclei of a new phase [2].

CWP is a mechanism for the transfer of threshold strain that violates the stability of the initial phase. Information about the wave structure of the CWP is crucial for understanding the features of the course of all MT stages, including details of the formation of morphological characters, in particular, the fine structure of transformation twins [3-6].

A review of recent advances in the dynamic theory of MTs is given, including an analysis of the spectral composition of the vibrational modes of the IES.

### References

1. Kashchenko M. P., Chashchina V. G. *Physics-Uspehi*. 2011. V.54. №4. 331-349.
2. Kashchenko M. P., Chashchina V. G. *Materials Science Forum*. 2013. V. 738-739. 3-9.
3. Kashchenko M. P., Chashchina V. G. *Phys. Met. Metallog.* 2013. V. 114. №10. 821-825.
4. Kashchenko M. P., Kashchenko N.M., Chashchina V. G. *Phys. Met. Metallog.* 2018. V.119. №1. 3-8.
5. Kashchenko M., Chashchina V., Kashchenko N. *Materials Today: Proceedings*. 2017. 4605-4610.
6. Kashchenko M. P., Kashchenko N.M., Chashchina V. G. *Letters on materials*. 2018. V. 8, №4. 424–429.

# NUCLEATION AND GROWTH OF NEW PHASE NUCLEI IN HETEROGENEOUS REACTIONS

**Kortsenshteyn N.M.**

*G.M. Krzhizhanovsky Power Engineering Institute*

*naumkor@yandex.ru*

From the standpoint of chemical thermodynamics, the process of phase transition from the vapor to the condensed state in simple systems (for example, water vapor – water) can be viewed as a heterogeneous reaction of the form  $C \rightarrow C^*$  (1) (the condensed state of the substance is marked with an asterisk). In a two-component system, several possible paths of phase transformation arise, one of which is the process according to scheme  $A + B \rightarrow C^*$  (2). Case (2) corresponds to the heterogeneous reaction of gas phase molecules on the surface of nuclei with the formation of condensed phase molecules. This situation is realized, apparently, in the Al – O system, where the condensed phase is represented by  $Al_2O_3$  oxide, and the gas phase is represented by  $Al_2O$ ,  $AlO$ ,  $AlO_2$  molecules and Al atoms. A process similar to (2) is implemented with solid-phase heteroepitaxy of silicon carbide on a silicon substrate (Kukushkin, SA and Osipov, AV, Physics of the Solid State, 2008). The process of phase transition according to scheme (2) was the subject of consideration in this paper. Using the formalism of the classical nucleation theory, a general form of the expression for the rate of stationary nucleation in a heterogeneous reaction of type (2) was given. Based on the assumption about the mechanism of the reaction through the formation of intermediate complexes, the relationship between the rate constant of a heterogeneous reaction and the rate constants of intermediate processes was determined. The found equilibrium distributions of nuclei and intermediate complexes by size were used to obtain expressions for the rate of stationary nucleation and the rate of growth of condensate particles formed in a heterogeneous reaction of the form (2). The results of this work are expressions that give a closed description of the kinetics of the phase transition in some complex systems. The difference between the results obtained and the expressions describing the kinetics of the phase transition in simple systems is as follows. First, the using of a generalized condensation coefficient with a constant characterizing a heterogeneous chemical reaction. Second, the using of a generalized supersaturation ratio for calculation the size, work of formation, and the equilibrium concentration of critical nuclei.

# DYNAMICS OF NON-STATIONARY GROWTH OF BUBBLES AT DEGASSING OF LIQUID SOLUTION WITH CAPILLARY AND VISCOUS EFFECTS

**Kuchma A.E., Shchekin A.K.**

*St. Petersburg State University, St. Petersburg, 199034 Russia*

*an.kuchma@gmail.com*

Nucleation formation and subsequent growth of bubbles play an important role in many physical phenomena, such as cavitation in one-component liquid and degassing in binary and multi-component solutions. The study of the growth of gas bubbles in supersaturated liquid solutions has a long history, but does not lose its relevance still now [1]. One of the actual tasks is the construction of a detailed theory of swelling and decomposition of a supersaturated-with-gas solution during its rapid decompression. The growth dynamics of supercritical gas bubbles at the nucleation stage and, accordingly, their size distribution to the end of this stage substantially depend on the degree of gas supersaturation and the Laplace pressure inside the bubbles and viscous forces acting on the bubbles. In the case of low gas solubility and supersaturation in the solution, diffusion of gas molecules to the growing bubble is quasi-stationary. Corresponding dynamics of supercritical bubble growth and analytical kinetics of the nucleation stage with allowance for the excess Laplace pressure in the bubbles are considered in detail in [2]. Similarly to the Laplace pressure, it is possible simultaneously to describe analytically the effect of viscous forces on the bubbles for a fairly wide range of viscosity values.

In the case of large gas supersaturations and solubilities, the situation becomes much more complicated. Diffusion of gas molecules to the bubble (while it grows from a slightly supercritical size) gradually becomes substantially non-stationary. Accordingly, to find the diffusion gas flux, it is necessary to solve the non-stationary equation of diffusion in the solution surrounding the bubble with taking into account the mobility of the bubble boundary. The exact analytical solution of the bubble growth problem in this case can only be obtained with neglecting the influence of the Laplace forces and viscosity. Such a solution corresponds to the self-similar growth mode. As a consequence, the use of the self-similar solution in describing the nucleation stage of degassing [3] is justified under condition that the sizes of the bubbles formed to the end of this stage are sufficiently large. To obtain a closed equation describing bubble growth in the region of significant influence of Laplace forces and viscosity, we use in this report an approximate expression for the current profile of the concentration of the dissolved gas in a non-stationary diffusion shell around the bubble. The proposed approximate expression corresponds to the quasi-stationary diffusion flow of gas molecules to a near-critical bubble and provides a gradual transition to the self-similar growth mode as the bubble size increases. It is significant that in this approximation, in contrast to the one used in [4] with taking into account the influence of viscosity, the condition of the balance of the number of molecules of the dissolved gas is strictly satisfied.

**Acknowledgments** This work was supported by the Russian Foundation for Basic Research (grant 19-03-00997)

- [1] A.E. Kuchma, A.K. Shchekin, D.S. Martyukova, *J. Chem. Phys.*, 2018, 148, 234103.
- [2] A.E. Kuchma, A.K. Shchekin, D.S. Martyukova, A.V. Savin, *Fluid Phase Equil.*, 2018, 455, 63.
- [3] A.E. Kuchma, A.K. Shchekin, M. Yu Bulgakov, *Physica A*, 2017, 468, 228.
- [4] A.A. Chernov, A.A. Pil'nik, M.N. Davydov, E.V. Ermanyuk, M.A. Pakhomov, *Int. J. Heat Mass Transf.*, 2018, 123, 1101.

# METHOD OF CHEMICAL SUBSTITUTION OF ATOMS IS A NEW METHOD OF GROWING LOW-DEFECTIVE EPITAXIAL FILMS. NANOSCALED SILICON CARBIDE ON SILICON: A NEW BANDGAP MATERIAL FOR MICRO- AND OPTOELECTRONICS

**Kukushkin S.A., Osipov A.V.**

*Institute of Problems of Mechanical Engineering of RAS (IPME RAS)*

*sergey.a.kukushkin@gmail.com*

A mechanism of a wide class of heterogeneous chemical reactions between a gas phase and a solid has been discovered on the example of the chemical interaction of gaseous carbon monoxide (CO) with a single-crystal silicon (Si) lattice, and a theory of first-order phase transitions has been developed for systems, where the direct formation of nuclei of a new phase is difficult by some reason, for example, because of the enormous elastic energy [1,2]. It has been shown that in this case the phase transition is realized through a certain intermediate state, which greatly facilitates the formation of new phase nuclei. For the silicon – silicon carbide (SiC) phase transition, such an intermediate state is a "pre-carbide" state of silicon saturated with dilatation dipoles, i.e. with pairs of carbon atom – silicon vacancy that are strongly attracted to each other [1,2].

It has been theoretically described a new kind of phase transitions, during which one of the phases stimulates the appearance of another phase. In this particular case, the formation of a SiC nucleus stimulates the formation of contraction pores [1]. The formation of contraction pores is associated with a change in the density of the initial solid phase of silicon during its chemical treatment with CO gas and its subsequent chemical transformation into silicon carbide. The formation energy and all the basic thermodynamic and kinetic characteristics of two-phase phase transitions have been calculated taking into account the occurring chemical reactions. More specifically, a generalized expression of the formation energy of the silicon carbide nucleus and the pore has been derived taking into account the interaction energy of vacancies and carbon atoms in the silicon substrate; an expression of the joint nucleation rate of the silicon carbide nuclei and the contraction pores has been obtained; the generalized diffusion coefficient in the space of sizes of the SiC nuclei and contraction pores has been calculated. It has been calculated the critical thickness of a silicon layer with the dilatation dipoles, above which a process of the irreversible transformation of the silicon layer into the silicon carbide layer takes place. This theory has a general character, since an equation describing the simultaneous nucleation of two joint phases has been derived. This equation essentially generalizes the well-known Zel'dovich equation in the kinetics of first-order phase transitions [1]. It has been shown that a key role in such phase transitions is played by an intermediate state realized at one of the stages of the chemical interaction [1]. In the case of the transformation of silicon into silicon carbide, such an intermediate metastable state is silicon saturated with dilatation dipoles. It has been carried out direct experiments, where the processes of phase transitions, formation of pores and processes of their "healing" have been observed in-situ.

The growth of films by the classical mechanism is realized by placing atoms on the surface of a substrate. The new method consists in replacing a portion of the atoms of the silicon lattice by the carbon atoms, thus forming silicon carbide molecules. The new growth method allows to solve one of the main problems of heteroepitaxy, namely, to synthesize low-defect and stress-free epitaxial films despite a large difference between the lattice parameters of the film and substrate. Experimental results on the growth of low-defect epitaxial SiC layers on Si and on their structural and electrophysical properties have been presented. On the SiC/Si template obtained by the solid-phase epitaxy method, we managed to grow on silicon a number of heteroepitaxial films of wide-bandgap semiconductors, such as SiC, AlN, GaN, AlGaIn. The grown films do not contain cracks and have a quality sufficient for manufacturing a wide class of micro- and optoelectronic devices [1,2].

## **References**

- [1] S.A. Kukushkin and A.V. Osipov. Topical Review. Theory and practice of SiC growth on Si and its applications to wide-gap semiconductor films. *J. of Phys. D: Appl. Phys.* (2014), **47**, 313001-313041.
- [2] S.A. Kukushkin, A. V. Osipov, and N. A. Feoktistov. Synthesis of Epitaxial Silicon Carbide Films through the Substitution of Atoms in the Silicon Crystal Lattice: A Review. *Physics of the Solid State*, (2014), **56**, No. 8, pp. 1507–1535.

# PROFESSOR V.V. SLEZOV IS ONE OF THE FOUNDERS OF THE KINETIC THEORY OF FIRST-ORDER PHASE TRANSITIONS

**Kukushkin S.A.**

*Institute of Problems of Mechanical Engineering of RAS (IPME RAS)*

*sergey.a.kukushkin@gmail.com*

In 2018, 60 years have passed since the publication of the famous paper by I.M. Lifshits and V.V. Slezov [1], in which the theory of the late stage of first-order phase transitions was developed. In this work, one of the fundamental laws of the evolution of ensembles of new nuclei was discovered at the late stage of first-order phase transitions — the Lifshitz – Slezov law. Prior to the publication of this work, the researchers did not guess that at a late stage of phase transitions in any systems a universal distribution of the nuclei of a new phase in size was formed. Another surprising feature of the open law was that with the diffusion mechanism of mass transfer between the nuclei and the medium, the average size of the nuclei obeys not the usual law  $\bar{R} \sim t^{1/2}$ , as everyone believed, but the law  $\bar{R} \sim t^{1/3}$ . Later this law was subjected to a thorough theoretical and experimental verification. hundreds of the finest experimental studies have been carried out, fully confirmed the discovery made by I.M. Lifshits and V.V. Slezov.

I was lucky. I have had the fortune to communicate with V.V. Slezov for many years. We work together with him. We wrote the book [2] together with V.V. Slezov. The report will tell you about the history of the Lifshits-Slezov theory, which I had the opportunity to hear firsthand.

Will be told about Professor V.V. Tears as about one of the founders of the Petersburg school of phase transitions and about unforgettable moments of human communication with one of the outstanding physicists of the 20th century.

## **References**

- [1] I. M. Lifshits and V. V. Slezov. On the Kinetics of Diffusion Decomposition of Supersaturated Solid Solutions. Zh. Eksp. Teor. Fiz. 35 (2(8)), 479–492 (1958).
- [2] S. A. Kukushkin and V. V. Slezov. Disperse Systems on Solid Surfaces (Nauka, St. Petersburg, 1996).



# CRYSTAL STRUCTURES AND PHASE TRANSITIONS OF ALUMINA AT NANOSCALE: A THEORETICAL STUDY BASED ON A BENCHMARKING OF EMPIRICAL POTENTIALS

**Laurens G., Amans D., Allouche A.-R.**

*Institut Lumière Matière, UMR5306 Université Lyon 1-CNRS, Université de Lyon, F-69622  
Villeurbanne cedex, France*

*gaetan.laurens@univ-lyon1.fr*

During the growth of nanocrystals, the surface energy is predominant over the free energy of the bulk due to a large surface-to-volume ratio. Polymorphs with low surface energy may thus be stabilized at the nanoscale even though they are metastable in the bulk. Therefore, several phase transitions may occur during the nanoparticle growth until reach the bulk equilibrium. Such crossover in polymorph stability was reported for several materials including TiO<sub>2</sub>, ZrO<sub>2</sub>, Fe<sub>2</sub>O<sub>3</sub> or Al<sub>2</sub>O<sub>3</sub> [1,2]. This latter is under the scope of this study where two phase transitions were experimentally reported [3,4]. A first transition from corundum alumina ( $\alpha$ -Al<sub>2</sub>O<sub>3</sub>) to cubic alumina ( $\gamma$ -Al<sub>2</sub>O<sub>3</sub>) has been measured at around 12 nm while amorphous alumina ( $a$ -Al<sub>2</sub>O<sub>3</sub>) becomes the stable polymorph below 4 nm.

Clusters of few atoms to nanoparticles as large as 12 nm were calculated by implementing four empirical potentials which were developed for the alumina description [5-8]. At small sizes, a conformation research of random geometries was performed to find the most stable structures. The results were compared to DFT-calculated isomers. At larger scale, geometry optimisations were performed and structures were analysed by classical molecular dynamics statistics. The calculations reproduce the atomic relaxation due to the surface stress. Within the first atomic layers, a surface shell with a constant thickness independent of the particles' size appears as an amorphous-like structure. Particles larger than the amorphous shell have a bulk-like core whereas the smaller ones are deformed by the surface as a whole. At the end, the phase transition between the amorphous phase and the crystal structure is predicted at 3 nm by the best potentials, based on experiments comparison. However, the potentials differ in the prediction of the phase stability domains.

- [1] Navrotsky, *Geochem. Trans.* **4**, 34 (2003)
- [2] Li *et al.*, *Mater. Res. Bull.* **43**, 3149 (2008)
- [3] J. McHale *et al.*, *Science* **277**, 788 (1997)
- [4] Tavakoli *et al.*, *J. Phys. Chem. C* **117**, 17123 (2013)
- [5] Alvarez *et al.*, *J. Phys. Chem.* **99**, 17872 (1995)
- [6] Streitz and Mintmire, *Phys. Rev. B* **50**, 11996 (1994)
- [7] Vashishta *et al.*, *J. Appl. Phys.* **103**, 083504 (2008)
- [8] Woodley, *Proc. R. Soc. A* **467**, 2020 (2011)

# CRYSTAL NUCLEATION- AND CRYSTAL GROWTH-CONTROLLED FORMATION OF BULK METALLIC GLASSES

Louzguine-Luzgin D.V.<sup>1,2</sup>

1 - *Mathematics for Advanced Materials-OIL, National Institute of Advanced Industrial Science and Technology (AIST), Sendai 980-8577, Japan*

2 - *WPI Advanced Institute for Materials Research, Tohoku University, Sendai 980-8577, Japan*

*dml@wpi-aimr.tohoku.ac.jp*

Two general types of bulk (massive, volumetric) metallic glasses/amorphous alloys are formed by suppressing either nucleation or growth process of a competing crystalline phase(s). Nanocrystallization of a  $\text{Ti}_{50}\text{Ni}_{23}\text{Cu}_{22}\text{Sn}_5$  bulk metallic glass, a representative of the former glass family, which formation is crystal nucleation-controlled was studied within the supercooled liquid region by using a state-of-the-art experimental technique with elemental mapping at near-atomic resolution<sup>1</sup>. An especial focus was made on the nature of incubation period at constant temperature and pressure which is still poorly understood from both theoretical and experimental viewpoints. Molecular dynamics simulation was also performed. Both experimental and simulation data indicate nanometer-range chemical rearrangements which are supposed to reduce the energy barrier in the complex energy landscape on heating. This process leads to a high density of homogeneously nucleating crystallites after the completion of a macroscopically observed incubation period. Phase separation preceding crystallization was observed in a  $\text{Zr}_{63}\text{Cu}_{22}\text{Fe}_5\text{Al}_{10}$  bulk metallic glass<sup>2</sup> which however, crystallized by a eutectic reaction. Two Fe-based alloys with good glass-forming ability (GFA):  $\text{Fe}_{48}\text{Cr}_{15}\text{Mo}_{14}\text{C}_{15}\text{B}_6\text{Ti}_2$  and  $\text{Fe}_{48}\text{Cr}_{15}\text{Mo}_{14}\text{C}_{15}\text{B}_6\text{Y}_2$  represent the latter glass family<sup>3</sup>. The reasons for significantly enhanced GFA of these alloys are connected with low growth rate of the pre-existing nuclei of the  $\chi$ - $\text{Fe}_{36}\text{Cr}_{12}\text{Mo}_{10}$  phase. The low growth rate is connected with large inhomogeneous strain in the growing nanoparticles, while nucleation of the eutectic colonies is hampered by slow diffusion of a rare-earth alloying element.

## References:

1. Z. Wang, C.L. Chen, S. V. Ketov, K. Akagi, A. A. Tsarkov, Y. Ikuhara and D. V. Louzguine-Luzgin, *Materials & Design*, 156, (2018), 504-513.
2. D.V. Louzguine-Luzgin, J. Jiang, A.I. Bazlov, V.S. Zolotarevzky, H. Mao, Yu P. Ivanov, A.L. Greer, *Scripta Materialia*, 167, (2019) 31-36.
3. D.V. Louzguine-Luzgin, A.I. Bazlov, S.V. Ketov and A. Inoue, *Materials Chemistry and Physics*, 162, (2015), 197-206.

## **SIMULATION OF NUCLEATION BY FREE ENERGY DENSITY FUNCTIONAL METHOD**

**L'vov P.E.<sup>1,2</sup>, Svetukhin V.V.<sup>3</sup>, Bulyarskii S.V.<sup>3</sup>**

*1 - Ulyanovsk State University, Ulyanovsk, Russia*

*2 - Institute of Nanotechnology of Microelectronics of the Russian Academy of Science, Moscow, Russia*

*3 - Research and Manufacturing Complex Technology Center MIET, Moscow, Zelenograd, Russia*

*LvovPE@sv.uven.ru*

Non-classical nucleation theory is a well-known approach employing free energy density functional method that can be applied to describe characteristics of critical nuclei and dynamics of the first order phase transitions both at early and later stages.

In this study, we investigate the process of nucleation in binary alloys by the Cahn-Hilliard (CH) equation with constant and degenerative mobility. By the direct simulation, we have demonstrated changes in stages of nucleation, diffusion growth and coalescence. For the case of constant mobility, the growth law for these stages correlates with conclusions of diffusion growth theory and Lifshitz-Slezov (LS) theory of coalescence. For the case of degenerative mobility, the growth law has subdiffusional character at all stages. The calculated "detectable" nucleation rate can be approximated satisfactorily by the linear or power-law dependence on supersaturation. We analyze the evolution of distribution function that agrees satisfactorily with LS theory at the stage of coalescence.

Also, non-classical nucleation theory can be realized in terms of kinetic equations describing the walking of nuclei in size space. This formulation can be effectively employed for nucleation in dilute solutions. For this purpose, we apply the CH equation to describe dissolution and growth of the solitary nucleus that is characterized by the spherical symmetry. Solution of the problem allows to define kinetic coefficients for master equation that is employed for supercritical nuclei. Characteristics of critical nucleus and time-dependant nucleation rate are extracted directly from the simulation by stochastic CH equation. At the early stage, solution of the approximate equations gives kinetics of average radius and concentration of nuclei that agrees well with simulation by the stochastic CH equation. At the later stage, the growth rate obtained by the kinetic equations agrees well with LS theory.

Free energy density functional method can be also employed for description of cluster formation in thin films (~10nm). This type of phase transitions (wetting transitions) is usually described in terms of thin film hydrodynamics leading to CH equation, where film thickness is considered as an order parameter. Basing on this approach, we have simulated thin film rupture and evolution of clusters formed on the film surface. The kinetics of concentration, average size and height of clusters as well as distribution function are studied both for early and later stage of wetting transition.

The work is supported by Ministry of Science and High Education of the Russian Federation (grant №0004-2019-0001) and Russian foundation for basic research (№18-42-732002).

# CRYSTALLINE NUCLEATION IN AMORPHOUS MATERIALS UNDER SHEAR DEFORMATION

**Mokshin A.V., Galimzyanov B.N.**

*Kazan Federal University*

*anatolii.mokshin@mail.ru*

Formation of nuclei of a new phase and their subsequent growth represent a general scenario of a first-order phase transition initiation outside the spinodal regime. In accordance with the classical nucleation theory, it is expected that with an increase of metastability level the spatial scale characterizing the nucleus critical size decreases until the nucleus reaches a size equal to several tens of particles (atoms, molecules). Under such the conditions, the use of traditional experimental methods to study the initial stages of phase transitions, associated with nucleation and growth processes, is not efficient. On the other hand, due to small characteristic spatial scales of the nucleation and growth processes, the molecular dynamics simulations provide useful tools to study these processes.

In this study, we demonstrate the theoretical method to evaluate quantitatively the nucleation and growth process characteristics. This method can be applied to molecular dynamics simulation results of a phase transition to determine values of the stationary and non-stationary nucleation rates, the nucleus growth rate, the phase transition rate, the average times expectation of nuclei of a certain size, the induction time, the critical size of nucleus, the nucleation free energy, the Zeldovich factor [1-6]. We demonstrate efficiency of the method as applied to the case of crystal nucleation in amorphous solids under stationary homogeneous shear.

This work was supported by the Russian Science Foundation (project No. 19-12-00022).

- [1] A.V. Mokshin, B.N. Galimzyanov, *J. Chem. Phys.* **142**, 104502 (2015).
- [2] A.V. Mokshin, B.N. Galimzyanov, *J. Chem. Phys.* **140**, 024104 (2014).
- [3] A.V. Mokshin, B.N. Galimzyanov, J.-L. Barrat, *Phys. Rev. E* **87**, 062307 (2013).
- [4] A.V. Mokshin, B.N. Galimzyanov, *J. Phys. Chem. B* **116**, 11959 (2012).
- [5] A.V. Mokshin, J.-L. Barrat, *Phys. Rev. E* **82**, 021505 (2010).
- [6] B.N. Galimzyanov, D.T. Yarullin, A.V. Mokshin, *Acta Materialia* **169**, 184 (2019).

# AB INITIO METHODS IN THE DESCRIPTION OF PHASE TRANSITIONS AND INTERMEDIATE AND TRANSITION STATES

**Kukushkin S.A., Osipov A.V.**

*Institute of Problems of Mechanical Engineering (IPME), RAS, St Petersburg, 199178 Russia*

*andrey.v.osipov@gmail.com*

This work focuses on study of transformation of a silicon crystal into matched to it crystal of silicon carbide via substitution reaction with carbon monoxide gas. As an example, the Si (100) surface is considered. The cross section of the potential energy surface of the first stage of transformation along the reaction pathway is calculated by the method of nudged elastic bands. It is found that in addition to intermediate states associated with adsorption of CO and SiO molecules on the surface, there is also an intermediate state in which all the atoms are strongly bonded to each other. This intermediate state significantly reduces the activation barrier of transformation down to 2.6 eV. The single imaginary frequencies corresponding to the two transition states of this transformation are calculated, one of which is reactant-like, whereas the other is product-like. By methods of quantum chemistry, the second stage of this transformation is described, namely, the "collapse" of precarbide silicon into silicon carbide. Energy reduction per one cell is calculated for this "collapse" process, and bond breaking energy is also found. Hence, it is concluded that the smallest size of the collapsing islet is 30 nm. It is shown that the chemical bonds of the initial silicon crystal are coordinately replaced by the bonds between Si and C in silicon carbide, which leads to a high quality of epitaxy and a record low concentration of misfit dislocations.

The mechanism of displacement of one close-packed SiC layer from one minimum position to another on the example of SiC polytype transition  $2H \rightarrow 4H$  has been studied by ab initio methods. It has been shown that the intermediate state with monoclinic symmetry  $C_m$  greatly facilitates this displacement breaking it into two stages. Initially, the Si atom chiefly moves, only then—mainly the C atom. In this case, the Si–C bond is significantly tilted in comparison with the initial position, which allows the reducing of the compression of the SiC bonds in the (11-20) plane. Two transition states of this process, which also possess the  $C_m$  symmetry, is computed. It is found that the height of the activation barrier of the process of moving the close-packed layer of SiC from one position to another is equal to 1.8 eV. The energy profile of this transformation is calculated.

# DYNAMICS OF CRYSTAL NUCLEATION IN DEEPLY SUPERCOOLED METALLIC MELT

**Pisarev V.V.<sup>1,2</sup>, Kirova E.M.<sup>1,2,3</sup>**

*1 - National Research University Higher School of Economics, 20 Myasnitskaya str., 101000  
Moscow, Russia*

*2 - Joint Institute for High Temperatures of RAS, 13/2 Izhorskaya str., 125412 Moscow, Russia*

*3 - Moscow Institute of Physics and Technology, 9 Institutskiy per., 141700 Dolgoprudnyy, Russia*

*vpisarev@hse.ru*

We investigate the nucleation and growth of crystal phase in a supercooled molybdenum melt using the molecular dynamics method. The nucleation is characterized by the probability density maps for the crystalline clusters in coordinates of the cluster size and the asphericity parameter. The changes is studied for the cooling rates  $5 \cdot 10^{13}$ ,  $6 \cdot 10^{13}$  and  $7 \cdot 10^{13}$  K/s. The simulations show the following features of the dynamics:

1. Regions are found on the probability density maps that characterize long-lived crystalline clusters. Trajectories that have clusters in those regions show reduced tendency to crystallization. We demonstrate that this region corresponds to high asphericity values at the lowest cooling rate and as the cooling rate increases, the span and the probability of finding clusters in those regions increase.
2. There are two mutually exclusive nucleation mechanisms. The first one is through low asphericity values: attachment of separated atoms to a crystalline nucleus one by one, as in the classical theory of nucleation. The second one is through high values of asphericity due to the coalescence of small-sized crystals to the largest one.
3. The cooling rate significantly effect the crystallization mechanism. Attachment mechanism is dominant in the melt cooled down at a slower rate, and the mechanism gradually shifts to the coalescence as cooling rate increases.

Thus, we argue that the crystallization process in metallic melt is multi-dimensional process and should be described using two variables — the crystal size and the parameter characterizing the shape of the cluster.

The abstract was prepared within the framework of the Basic Research Program at the National Research University Higher School of Economics (HSE) and supported within the framework of a subsidy by the Russian Academic Excellence Project '5-100'.

# AMENDING CRYSTALLISATION DRIVING FORCE TO ASSESS THE GLASS FORMING ABILITY OF MELTED METALLIC GLASSES

**Roula A., Ikhlef E.**

*Fac. Sci. & Technol., M S Benyahia Univ. Jijel; LIME; BP 98; Ouled Aissa; 18000 ; Algeria*

*amkroula@mail.ru*

Glass scientists always consider the Glass Formation with a lot of thermal criteria [1-26]; among them, the Global Relative Glass Forming Ability for oxides :  $GRGFA = [(E_d/I.T_m).1/C_p].[(v/(r_c+1.26)^2).(V/(r_c+1.26))]$  (1) where  $E_d$ ,  $I$ ,  $T_m$ ,  $C_p$ ,  $v$ ,  $r_c$  and  $V$  are the dissociation energy, the crystal coordination number, the melting temperature, the isobaric thermal capacity, the valence, the cationic radius and the cell volume of the studied oxide (while  $1.26 \text{ \AA}$  is the oxygen anionic radius).

Considering that “both the stability of the liquid phase and the resistance of the glass against crystallization should be considered together to improve the GFA of alloys” [19, 20, 21], the Crystallisation Driving Force criterion is the most used criteria for materials  $CDF = (\Delta G_m/R.\Delta T)$  (2) where  $\Delta G_m$ ,  $T$  and  $R$  are the Gibbs free energy change for solidification, temperature and the universal gas constant, respectively. Aiming to describing the opposite phenomena (the glass formation), the mathematical nondimensional analysis rules suggest to amended CDF criterion using the isobaric thermal capacity of the studied alloy  $C_p$  instead of the universal gas constant  $R$  in one hand and the undercooled liquid range  $\Delta T_{xg} = (T_x - T_g)$  instead of any other chosen temperature or temperature range (not  $T_l$ ,  $T_x$ ,  $T_g$  nor  $(T_l - T_x)$  neither  $(T_l - T_g)$  in the other hand ( $\Delta T_{xg}$  is the temperature interval where the competition Vitrification Vs Crystallisation is occurring (not before and nor after).

Thus, authors propose the following formulation:

$$RGFA^{BMG} = \frac{1}{(CDF \cdot \frac{R}{C_p})} = \frac{1}{(\frac{\Delta G_m}{R \cdot \Delta T_x} \cdot \frac{R}{C_p})} = \frac{1}{(\frac{\Delta G_m}{C_p \cdot \Delta T_x})} = \frac{C_p \cdot (T_x - T_g)}{\Delta G_m} \quad (3) \text{ to assess the Relative GFA}$$

of any BMG (considering it as the inverse value of its own Crystallisation Driving Force and expressed without measurement units). The application of this model for Cu–Zr binary systems revealed a strong correlation with  $C_p$  and therefore has proven its suitability to quantify the GFA of melted solid materials.

# CRYSTALLIZATION OF GLASS-FORMING MELTS: NEW ANSWERS TO OLD QUESTIONS

**Schmelzer J.W.P.**

*Institute of Physics, University of Rostock, Germany*

*juern-w.schmelzer@uni-rostock.de*

Classical nucleation theory (CNT) is the major tool utilized commonly for the interpretation of experimental data on nucleation processes in a variety of different systems. In some cases, it allows one not only a qualitative treatment of nucleation data but even a quantitatively correct description, in other cases, it may fail even dramatically. Consequently, the question arises how these problems can be explained and overcome, what the origin is for the high success of CNT in some and its failure in other cases. The answer to this question can be searched for in different directions as will be discussed in detail in the talk.

One of the basic ingredients of classical nucleation theory consists in the appropriate specification of the work of critical cluster formation in nucleation. It determines widely the probability of formation of a supercritical cluster of the newly evolving phase capable to a further deterministic growth. In line with Gibbs' [1] classical method of description of heterogeneous systems it is supposed in CNT that the bulk properties of the critical clusters are widely identical to the properties of the newly evolving macroscopic phases [2]. Following this basic assumption of CNT, in the first part of the talk general equations and analytical estimates for the dependence of the thermodynamic driving force of crystallization and the specific interfacial energy melt-crystal of critical crystal clusters on temperature and pressure are derived directly applicable in the analysis of experimental data on crystal nucleation and growth. In particular, it is shown that at the Kauzmann temperature, corresponding to states where the specific entropies of glass-forming melt and crystal coincide, the thermodynamic driving force has a maximum in dependence on temperature. In addition, similarly to the mentioned well-known notation of a Kauzmann temperature, the concept of a Kauzmann pressure is introduced for crystallization induced by variations of pressure. It is shown that the thermodynamic driving force of crystal nucleation has similarly maxima also at the Kauzmann pressure [3].

One serious problem in the application of CNT to melt crystallization consists in the limitations due to the fact that the specific surface energy melt-crystal cannot be determined with the desired accuracy. By this reason, in applications of CNT frequently the Stefan-Skapski-Turnbull relation is employed for its determination. In its standard so far application, it involves the assumption of the capillarity approximation i.e. that the surface tension of critical clusters is equal to the respective value of equilibrium coexistence of both phases at a planar interface. However, the application of the capillarity approximation leads to serious problems in CNT [4]. They can be overcome by introducing a curvature dependence of the surface tension as suggested already by J. W. Gibbs [1] and widely employed in CNT. Based on a generalization of the Stefan-Skapski-Turnbull equation, a relation for the dependence of the surface tension on pressure and temperature has been derived by us [3, 5]. It can be employed, in particular, to specify the values of the Tolman parameter in the Tolman equation for the curvature dependence of the surface tension. Such estimates can be given both for crystal nucleation caused by temperature and pressure variations. Utilizing such approach, the application of the Tolman equation supplies us with a sufficiently accurate tool in the interpretation of crystal nucleation rates. The physical origin of such finding will be discussed showing that in such approach the Tolman equation has to be treated in a more general way as initially derived by Tolman.

Mentioned basic assumption of CNT supported by Gibbs' theory – the assumed independence of the properties of critical clusters on the degree of deviation from equilibrium - is in a variety of cases in conflict with alternative theoretical approaches like density functional computations, computer simulations, and experimental data. It has been questioned immediately after the formulation of CNT and attempted to be overcome inside the framework of Gibbs theory (Scheil, Hobstetter). This critique finally led then to the rediscovery of density functional methods of determination of the properties of critical clusters by methods originally developed by van der Waals. As it turned out, the properties of critical clusters and the size of the critical clusters as determined via density functional computations



first by Hillert, Cahn and Hilliard [6] are quite different as compared to the results obtained via the classical Gibbs method. Consequently, the problem arises which of the theories is correct and which one has to be abandoned.

This problem in the theoretical description can be overcome by generalizing the classical Gibbs' approach as performed by us in the last two decades. This method has been employed widely so far to the interpretation of nucleation and growth processes in condensation and boiling and of segregation in multi-components solutions. As shown the results obtained via the generalized Gibbs approach are in agreement with predictions of density functional computations. In particular, it is shown that nucleation for segregation in solutions does not proceed via the classical scenario but via a scenario resembling widely spinodal decomposition processes. In addition, it has been shown that the classical Gibbs method involving the capillarity approximation overestimates the work of critical cluster formation and underestimates the values of the steady-state nucleation rate. In the talk it will be demonstrated further how the generalized Gibbs approach can be applied to the description of crystallization and some principal consequences will be analyzed in detail. In addition, some other new approaches will be briefly described allowing one to arrive at a satisfactory description of experimental data which cannot be achieved in terms of standard CNT.

#### References

1. J. W. Gibbs, *Collected Works*, vol. 1, *Thermodynamics* (Longmans & Green, New York - London - Toronto, 1928).
2. J. W. P. Schmelzer and A. S. Abyzov, *Crystallization of glass-forming liquids: Thermodynamic driving force*, *J. Non-Crystalline Solids* **449**, 41-49 (2016).
3. J. W. P. Schmelzer, A. S. Abyzov, and V. M. Fokin, *Thermodynamic Aspects of Pressure Induced Nucleation: Kauzmann Pressure*, *International Journal Applied Glass Science* **7**, 474-485 (2016).
4. A. S. Abyzov, V. M. Fokin, A. M. Rodrigues, E. D. Zanotto, and J. W. P. Schmelzer, The effect of elastic stresses on the thermodynamic barrier for crystal nucleation, *J. Non-Crystalline Solids* **432**, 325-333 (2016).
5. J. W. P. Schmelzer and A. S. Abyzov, *Crystallization of glass-forming liquids: Specific surface energy*, *J. Chem. Phys.* **145**, 064512/1-11 (2016).
6. J. W. Cahn, *Reflections on Diffusive Interfaces and Spinodal Decomposition*. In: *The Selected Works of J. W. Cahn*, Eds. W. C. Carter and W. C. Johnson (The Minerals, Metals, and Materials Society, 1998, pages 1-8).

## NUCLEATION OF $\text{Sb}_2\text{S}_3$ IN THIN FILM Ge-Sb-S

Martinková S., Shánelová J., Málek J.

*Department of Physical Chemistry, University of Pardubice, Studentská 573, Pardubice 532 10, Czech Republic*

*jana.shanelova@upce.cz*

The nucleation in thin chalcogenide film  $(\text{GeS}_2)_{0,1}(\text{Sb}_2\text{S}_3)_{0,9}$  was studied using optical microscopy. Given the fact that temperature ranges of nucleation and crystal growth overlap, a single-stage heat treatment method was used to observe a formation of crystals in situ. The transient character of nucleation was detected and described by the Shneidman equation. The applicability of classical nucleation theory was verified on the basis of determined steady state nucleation rate, induction period and time lag of nucleation. The weak dependence of surface tension on temperature was found. The thermodynamic barrier calculated from experimental data was monotonically increasing and no deviation from a theoretical course was found. Approximations of classical nucleation theory were fulfilled in the measured range.

# MOLECULAR COMPONENT OF THE DISJOINING PRESSURE IN DROPLETS AT HETEROGENEOUS NUCLEATION

**Shchekin A.<sup>1</sup>, Lebedeva T.<sup>1</sup>, Suh D.<sup>2</sup>**

*1 - St. Petersburg State University*

*2 - University of Tokyo*

*akshch@list.ru*

Modern computational methods of molecular and statistical physics allow one to explicitly find the nanoscale structure in nonuniform molecular systems. The thermodynamic effects of internal inhomogeneity in small droplets at homogeneous and heterogeneous nucleation must be taken into account when comparing theory with experiment because these effects can be very significant [1]. In the case of homogeneous nucleation, these thermodynamic effects manifest through the dependence of the surface tension of the critical droplet on its radius [2-11]. In the case of heterogeneous nucleation on wettable solid particles, these effects can be taken into account through the dependence of the disjoining pressure on the thickness of the liquid condensate film [12-21]. For a flat liquid thin film between a solid substrate and undersaturated vapor, the disjoining pressure was first defined by Derjaguin [22] as the difference between external pressure and the bulk pressure in the film mother phase, provided it has the same values of temperature and chemical potentials as in the film. A modified definition was suggested by Rusanov and Kuni [23] as the difference in the normal component of the pressure tensor in the film and the bulk pressure in the liquid phase for a given chemical potential and temperature. However, because the normal component of the pressure tensor in the liquid film with curved interfaces depends on the location inside the film, even for a spherical droplet around a solid spherical core, there are some difficulties in defining the disjoining pressure for such films [13,14,16]. The disjoining pressure in spherical films was typically taken to be the same as in flat films of the same thickness. This pressure was considered as a counterpart to the Laplace pressure in the spherical film and to the corresponding contribution to the molecular chemical potential in the film [13-18]. A rigorous analysis of the mechanical equilibrium condition of a curved wetting liquid film on a solid substrate [24-26] established a relationship between the normal component of the pressure tensor inside the curved film in the vicinity of the solid substrate, the Laplace pressure of the film, and the difference in bulk pressures in the liquid and gas phases for a given molecular chemical potential. This relation was successfully used to describe the deliquescence phenomena [27,28]. It should also be noted that there were attempts in the literature [4,29] to extend the concept of the disjoining pressure for a small droplet formed in homogeneous nucleation considering the central inhomogeneity of such droplet as a result of self-overlapping of the internal part of surface layer.

In this report, all the aforementioned problems are directly analyzed within a consistent molecular approach with the help of the density functional theory (DFT) for a Lennard-Jones fluid with the Carnahan-Starling hard-sphere contribution in small droplets and thin liquid films. Our aim was to examine the inhomogeneity in the central part of a small droplet (and of the flat film on a solid substrate) due to overlapping surface layers, and to clarify its relation to the disjoining pressure in thermodynamics of heterogeneous nucleation on wettable spherical nanosized particles. This study has been performed by the square-gradient variant of the DFT. We use this simplest variant of DFT because it is possible to extend its application for polar molecules with non-central interactions and to multicomponent systems without changing the basic methodology. We have found a condensate density peak in the vicinity of the solid substrate, which exceeds the bulk value for the liquid phase density and weakly depends on the value of the condensate chemical potential. In such case, the substrate is completely wettable by the condensate which means that the liquid films formed in heterogeneous nucleation should be continuous and uniform in thickness. Our analysis on the nonuniformity of the density in the central part of the droplet with a solid core demonstrates overlapping of surface layers of solid-liquid and liquid-vapor interfaces. We have shown that the disjoining pressure for a flat thin liquid film on a solid substrate in the undersaturated vapor can be related to the disjoining pressure in small spherical droplets on completely wettable solid cores found through the thermodynamic and mechanical routes. The disjoining pressure of the spherical liquid

films depends on the internal and external radii of the film. For a fixed radius of the core, the disjoining pressure depends on the thickness of the spherical film.

A special study on the density and pressure inhomogeneity has been conducted for a homogeneously nucleated droplet without a solid core. As it follows from the results, the normal component of the pressure tensor inside the droplet is smaller everywhere than the bulk liquid pressure at the same value of the chemical potential. Thus the loss of the bulk properties at the center of this nanosized droplet is not due to the disjoining pressure but is an effect of a reduction in the surface tension.

**Acknowledgments.** This work was supported by the Russian Foundation for Basic Research (grant 18-53-50015 ЯФ\_a).

## References

1. S. Ayuba, D. Suh, K. Nomura, T. Ebisuzaki, and K. Yasuoka, Kinetic analysis of homogeneous droplet nucleation using large-scale molecular dynamics simulations, *J. Chem. Phys.* 149, (2018) 044504.
2. V.G. Baidakov and G.Sh. Boltachev, Curvature dependence of the surface tension of liquid and vapor nuclei, *Phys. Rev. E* 59 (1999) 469.
3. K. Koga, X.C. Zeng, A.K. Shchekin, Validity of Tolman's equation: How large should a droplet be?, *J. Chem. Phys.* 109 (1998) 4063.
4. T.V. Bykov, A.K. Shchekin, Thermodynamic characteristics of small droplet in terms of the density functional method, *Colloid J.* 61 (1999) 144.
5. T.V. Bykov, A.K. Shchekin, Surface tension, Tolman length, and effective rigidity constant in the surface layer of a drop with a large radius of curvature, *Inorganic Materials* 35 (1999) 641.
6. V.G. Baidakov, G.Sh. Boltachev, Curvature dependence of the surface tension of liquid and vapor nuclei, *Phys. Rev. E* 59 (1999) 469.
7. H.M. Lu, Q. Jiang, Size-dependent surface tension and Tolman's length of droplets. *Langmuir* 21 (2005) 779.
8. J. Julin, I. Napari, J. Merikanto, and H.A. Vehkamäki, Thermodynamically consistent determination of surface tension of small Lennard-Jones clusters from simulation and theory, *J. Chem. Phys.* 133 (2010) 044704.
9. E.M. Blokhuis, A.E. van Giessen, Density functional theory of a curved liquid-vapour interface: evaluation of the rigidity constants, *J. Phys. Condens. Matter* 25 (2013) 225003.
10. Ø. Wilhelmsen, D. Bedeaux, D. Reguera, Tolman length and rigidity constants of the Lennard-Jones fluid, *J. Chem. Phys.* 142 (2015) 064706.
11. A. Aasen, E.M. Blokhuis, Ø. Wilhelmsen, Tolman lengths and rigidity constants of multicomponent fluids: Fundamental theory and numerical examples, *J. Chem. Phys.* 148 (2018) 204702.
12. N.V. Alekseechkin, Surface effects in droplet nucleation, *Journal of Aerosol Science* 116 (2018) 1.
13. F.M. Kuni, A.K. Shchekin, A.I. Rusanov, B. Widom, Role of surface forces in heterogeneous nucleation on wettable nuclei, *Adv. Colloid Interface Sci.* 65 (1996) 71.
14. F.M. Kuni, A.K. Shchekin, A.P. Grinin, Theory of heterogeneous nucleation for vapor undergoing a gradual metastable state formation, *Phys. Usp.* 44 (2001) 331.
15. I. Napari, A. Laaksonen, Disjoining pressure of thin films on spherical core particles, *J. Chem. Phys.* 119 (2003) 10363.
16. T.V. Bykov, X.C. Zeng, Heterogeneous nucleation on mesoscopic wettable particles: a hybrid thermodynamic/density-functional theory, *J. Chem. Phys.* 117 (2002) 1851.
17. T.V. Bykov, X.C. Zeng, Homogeneous nucleation at high supersaturation and heterogeneous nucleation on microscopic wettable particles: a hybrid thermodynamic/density-functional theory, *J. Chem. Phys.* 125 (2006) 144515.
18. J. Mitrovic, Phase equilibrium of a liquid droplet formed on a solid particle. *Chem. Eng. Sci.* 61 (2006) 5925.
19. A.K. Shchekin, T.S. Podguzova, The modified Thomson equation in the theory of heterogeneous nucleation on charged solid particles, *Atmos. Res.* 101 (2011) 493.
20. A.K. Shchekin, T.S. Lebedeva, Density functional description of size-dependent effects at nucleation on neutral and charged nanoparticle, *J. Chem. Phys.* v.146 (2017) 094702.
21. Z. Wang, F. Qin, and X. Luo, Numerical investigation of effects of curvature and wettability of particles on heterogeneous condensation, *J. Chem. Phys.* 149 (2018) 134306.
22. B.V. Derjaguin, N.V. Churaev, V.M. Muller, *Surface Forces*, Consultants Bureau, New York (1987).
23. A.I. Rusanov, F.M. Kuni. *Research in Surface Forces*, Vol.3, p. 111, Consultants Bureau, New York (1971).
24. A.I. Rusanov, A.K. Shchekin, Local mechanical equilibrium conditions for interfaces and thin films of arbitrary shape, *Molecular Physics* 103, n.21-23 (2005) 2911.
25. A.I. Rusanov and A.K. Shchekin, The Condition of Mechanical Equilibrium on the Surface of a Nonuniform Thin Film, *Colloid Journal* 67 (2005) 205.
26. A.K. Shchekin, A.I. Rusanov, Generalization of the Gibbs–Kelvin–Köhler and Ostwald–Freundlich equations for a liquid film on a soluble nanoparticle, *J. Chem. Phys.* 129 (2008), 154116.
27. A.K. Shchekin, I.V. Shabaev, A.I. Rusanov, Thermodynamics of droplet formation around a soluble condensation nucleus in the atmosphere of a solvent vapor, *J. Chem. Phys.* 129 (2008) 214111.
28. A.K. Shchekin, I.V. Shabaev, O. Hellmuth, Thermodynamic and kinetic theory of nucleation, deliquescence and efflorescence transitions in the ensemble of droplets on soluble particles, *J. Chem. Phys.*, 138 (2013) 054704.
29. R. Tsekov, K.W. Stoeckelhuber, and B. V. Toshev, Disjoining Pressure and Surface Tension of a Small Drop, *Langmuir* 16 (2000) 3502.

# SUPERFAST DOMAIN WALL MOTION AND GROWTH OF DENDRITE DOMAINS IN FERROELECTRICS. ANALOGY WITH CRYSTAL GROWTH

Shur V.Ya., Akhmatkhanov A.R., Esin A.A., Chuvakova M.A.

*School of Natural Sciences and Mathematics, Ural Federal University, Ekaterinburg, Russia*

*vladimir.shur@urfu.ru*

The experimental study of the formation and growth of dendrite domains and superfast shape transformation of the concave polygonal domain appeared after merging to the convex one in uniaxial ferroelectric will be presented and described. The obtained effects will be considered using kinetic approach based on the analogy between kinetics of ferroelectric domains and crystal growth.

The evolution of the isolated ferroelectric domains during polarization reversal in uniform electric field was studied in congruent lithium niobate  $\text{LiNbO}_3$  (CLN) single crystals by *in situ* optical imaging with high temporal resolution. The static domain patterns were imaged at the surface by scanning electron microscopy and in the bulk by confocal Raman microscopy and Cherenkov-type second harmonic generation.

The variety of the domain shapes including regular convex polygons, stars and dendrites has been obtained for switching in wide temperature range and in the samples with artificial dielectric layer.

It was demonstrated that the stochastic nucleation dominating in CLN at the elevated temperatures leads to topological instability and appearance of the dendrite domain shapes [1,2]. The growth of dendrite domains (snowflakes) has been studied at the temperatures above 220°C in the plates covered by artificial dielectric layer [3]. The field dependence of the dendrite envelope was revealed.

The kinetic approach to domain growth based on step (pairs of kinks) generation and kink motion along the wall has been used for shapes explanation [4]. The nucleation probabilities are determined by the excess of the local value of the sum of the external field and partially screened (residual) depolarization field over the threshold value.

The domain shape change due to ineffective screening and formation of the trail of residual charges was demonstrated experimentally and by computer simulation [4]. It was shown that the determined step nucleation at the vertices and anisotropic kink motion dominated at low temperatures (< 200°C), whereas the stochastic nucleation with equiprobable nucleation sites is observed at the elevated temperatures (> 200°C). The convex hexagon domain shapes determined by symmetry have been observed for effective screening of depolarization field. Screening retardation leads to the irregular polygons and stars.

The first experimental study of the transformation of the concave polygonal domain appeared after merging to the convex (shape stability effect) [5] one has been realized. The convex growth of isolated hexagonal domains was governed by the slowest domain walls, while the concave growth after domain merging – by superfast walls with three orders of magnitude higher velocity. We reconstructed experimentally the  $v$ -plot (kinetic Wulff plot) for domain wall motion by analysis of both convex and concave domain growth [6].

Acknowledgements: The research was made possible by Russian Science Foundation (Project № 19-12-00210). The equipment of the Ural Center for Shared Use “Modern nanotechnology” Ural Federal University was used.

[1] V.Ya. Shur, D.S. Chezganov, M.S. Nebogatikov, I.S. Baturin, M.M. Neradovskiy, *J. Appl. Phys.*, **112**, 104113 (2012).

[2] V.Ya. Shur, M.S. Kosobokov, E.A. Mingaliev, D.K. Kuznetsov, P.S. Zelenovskiy, *J. Appl. Phys.*, **119**, 144101 (2016).

[3] V.Ya. Shur, A.R. Akhmatkhanov, *Phil. Trans. R. Soc. A*, **376**, 20170204 (2018).

[4] V.Ya. Shur, *J. Mater. Sci.*, **41**, 199 (2006).

[5] V.Ya. Shur, A.I. Lobov, A.G. Shur, E.L. Rumyantsev, K. Gallo, *Ferroelectrics*, **360**, 111 (2007).

[6] A.A. Esin, A.R. Akhmatkhanov, V.Ya. Shur, *Appl. Phys. Lett.*, **114** (2019) (in press).

## MODEL OF NUCLEATION LIMITED BY ANOMALOUS GRAIN-BOUNDARY DIFFUSION

**Sibatov R.<sup>1</sup>, Svetukhin V.<sup>2</sup>**

1 - Ulyanovsk State University

2 - Scientific Manufacturing Complex "Technological Centre", Moscow

ren\_sib@bk.ru

Grain boundary (GB) diffusion in engineering materials at elevated temperatures often determines the evolution of microstructure, phase transformations, and certain regimes of plastic deformation and fracture. Interpreting experimental data with the use of the classical Fisher model sometimes encounters contradictions that can be related to violation of Fick's law. We generalize [1] the Fisher model to the case of non-Fickian (anomalous) diffusion ubiquitous in disordered materials. The process is formulated in terms of the subdiffusion equations with time-fractional derivatives of order 'alpha' and 'beta' for grain volume and GB, respectively. It is shown that propagation along GB for the case of a localized instantaneous source and weak localization in GB is approximately described by distributed-order subdiffusion with exponents 'alpha/2' and 'beta'. Further, we consider the kinetics of subdiffusion-limited growth and dissolution of new phase particles in solid solutions within the approach [2] based on the tempered fractional diffusion equation and corresponding Monte Carlo algorithm. The known models of precipitation (Ham, Aaron-Kotler, Lifshitz–Slyozov) are generalized to the case of transient subdiffusion. The growth kinetics for various precipitate shapes is considered (spherical, disk-like, cylindrical, rod-like and some others). In the generalized Aaron-Kotler model, analytical results are obtained mainly for the stationary interface approximation. Solute particle profiles in the infinite matrix are expressed in terms of stable distributions, which are generalizations of the Gaussian distribution. Excluding the Gibbs-Thomson effect, the subdiffusive models gives the power law growth of spherical precipitates with exponent  $\alpha/2$ . Taking the Gibbs-Thomson effect into account leads to the time dependence steeper at early stages, but asymptotically approaching the indicated power law. Fractional model of subdiffusion limited Ostwald ripening is proposed and analyzed.

1. Sibatov R.T. Anomalous grain boundary diffusion: Fractional calculus approach. *Advances in Mathematical Physics*, 2019, 8017363, 1-9.
2. Sibatov, R. T., & Svetukhin, V. V. (2015). Fractional kinetics of subdiffusion-limited decomposition of a supersaturated solid solution. *Chaos, Solitons & Fractals*, 81, 519-526.

# DOPING LIMIT IN GaAs:Te AS A DISORDER TO (PARTIAL LOCAL) CHEMICAL SHORT-RANGE ORDER TRANSITION IN CRYSTALLINE ALLOY - ELECTRICAL AND DIFFUSE X-RAY SCATTERING STUDIES USING ANNEALING

Slupinski T.

*Institute of Electron Technology, Lukasiewicz Research Network, Warsaw, Poland*

*tslupinski@ite.waw.pl*

Technological experiments in n-GaAs studying maximum concentration of free carriers (doping limit) show that at ultra-high doping (high  $10^{18}$  cm<sup>-3</sup> range) the concentration of active electrical donors (and free carriers) is lower than the concentration of impurity atoms built in the crystal lattice. Part of impurities may exist in electrically deactivated state. In n-GaAs in such doping range, quite old experiments [1-3] showed that high temperature annealing (~ 600-1100 °C) of crystalline samples can reversibly deactivate or reactivate donors depending on the annealing temperature. Annealing can have direct impact on the deactivation state of donor atoms at ultra-high doping. Results [1-3] seem to be never clarified in a physically satisfactory way. In author's paper [4], some of many experimental arguments from literature were mentioned, which give arguments against dominantly considered in literature models of universal electrical compensation by native acceptors. E.g. in n-GaAs at doping limits, charged vacancies  $V_{Ga}$  are considered, originally from Baraff and Schluter calculations [5], assuming Kruger and Vink chemical formalism of point defects statistics (of type of ideal gas of defects). In [4], in double-doped GaAs:Te,Ge we studied concentrations of  $Ge_{Ga}$  and  $Te_{As}$  deactivated donors and their changes caused by reactivating annealing using Hall effect measurements under 0-15 kbar pressure and utilizing properties of DX states of  $Ge_{Ga}$  donor. Studies [4] indicate for a formation of  $Ge-Te_n$  molecules ( $n=3-4$ ) in GaAs:Te,Ge when donor atoms are deactivated. Impurity-impurity molecules which trap free electrons were originally hypothetically proposed by Fuller and Wolfstirn [1] to describe electron concentration changes in annealed n-GaAs. I will present X-ray diffuse scattering (DXS) results (reciprocal space maps) measured in annealed GaAs:Te, showing that the electrical deactivation of donors is accompanied by a strong increase of DXS intensity close to fundamental  $hkl$  Bragg reflections. This is a continuation of author's studies [6] for other  $hkl$  reflections. I will discuss that measured features of DXS in reciprocal space maps (symmetry, fluctuations length) can be well described using Krivoglaz model of DXS due to *spatial fluctuations of impurity-impurity pair correlation function* in a crystalline alloy [7]. Krivoglaz model uses lattice gas language and a very intuitive analysis of alloy's crystal lattice in the harmonic approximation. This model shows an existence of partial local (or fluctuating in space) chemical short-range order in GaAs:Te crystalline alloy. Similar shape reciprocal space maps of DXS were reported for ultra-highly doped GaAs:Si [8], but no atomistic interpretation was proposed. Model of short-range order is consistent with Fuller and Wolfstirn hypothesis of impurity molecules [1] or with impurity polytypism [9].

- [1] C.S. Fuller, K.B. Wolfstirn, *J. Appl. Phys.* **34**, 2287 (1963)
- [2] M.G. Milvidskii, W.B. Osvenskii, W.I. Fistul, E.M. Omeljanovskii, S.P. Grishina, *Fiz. Tekh. Poluprov.* **1**, 969 (1967)
- [3] J.K. Kung, W.G. Spitzer, *J. Appl. Phys.* **44**, 912 (1973); *J. Appl. Phys.* **45**, 4477 (1974)
- [4] T. Slupinski, D. Wasik, J. Przybytek, *J. Cryst. Growth* **468**, 433 (2017)
- [5] G.A. Baraff, M. Schluter, *Phys. Rev. Lett.* **55**, 1327 (1985)
- [6] T. Slupinski, E. Zielinska-Rohozinska, *Thin Solid Films*, **367**, 227 (2000); MRS Symp. Proc. Vol. **583** (2000), p. 261
- [7] M.A. Krivoglaz, "Diffuse scattering of X-rays and neutrons by fluctuations", Springer-Verlag, 1996 (Chap. 3)
- [8] P.A. Filatov, V.T. Bublik, A.V. Markov, K.D. Shcherbachev, M.I. Voronova, *Crystallogr. Reports*, **52**, 292 (2007)
- [9] V.I. Fistul, "Impurities in semiconductors, solubility, migration and interactions", CRC Press, 2004 (Chap. 6)

# UNUSUAL TEMPERATURE INDUCED SHORTENING OF C(sp<sup>3</sup>)-C(sp<sup>3</sup>) BOND LENGTH IN BIBENZYL COMPOUNDS IN CRYSTAL STATE: OBSERVATION AND EXPLANATION

**Smirnov A., Odintsova O., Shirin O., Starova G., Solovyeva E.**

*Chemistry Institute, Saint-Petersburg State University, 26 Universitetsky pr., 198504, Peterhof, Saint-Petersburg, Russian Federation*

*alexnicksmirnow@gmail.com*

This report is dedicated to the description and analysis of recently obtained high-quality crystallographic and vibrational data of two stilbene derivatives. The work is based on the combined results of X-Ray diffraction, IR, Raman investigations supported by the quantum-chemical simulations at a high level of theory.

We focused on a comparative study of 4,4'-diaminobibenzyl (DABB) and 4,4'-dichlorobibenzyl (DCBB). The first, for example, has a wide range of applications: it serves as an intermediate for hybrid membranes, metal-organic frameworks and nanostructures (Manna *et al.*, 2013.), synthesis of photochemically active materials and biologically active agents, some of which are able to fight Alzheimer's disease (de Aquino *et al.*, 2013.). There is a discussable fundamental problem belonging to the bibenzyl class: Anomalous temperature-induced shortening of C(sp<sup>3</sup>)-C(sp<sup>3</sup>) bond length in ethane fragment of a molecule in a crystalline form which has been studied by several research groups over the past two decades (Harada and Ogawa, 2001.). Despite the great interest of researchers, there was no structural and vibrational analysis of selected molecules presented in the literature in general.

X-Ray analysis at 122 K revealed four independent structures with C<sub>2h</sub> point group of symmetry for DCBB and four independent structures with C<sub>1</sub> point group of symmetry. Only one C<sub>2h</sub> structure was determined in case of DABB. Such variety of structures of DCBB agrees well with the known freedom of rotation around the central bond, which is typical for bibenzyls, whereas in the case of DABB it is probably stabilized by hydrogen bridges between the amino groups and the water molecules found in its crystalline structure. When analyzing the structure, we noted, that the length of the central C-C bond for DCBB structures lies in the interval from 1.523 to 1.538 Å, which is less than the average length of the single C-C bond, equal to 1.541 Å.

To verify these results, an X-Ray study was reproduced at four different temperatures: 122, 200, 250 and 300 K. The distinct linear decrease in the length of the central bond was detected when the temperature increased from 122 to 300 K: from 1.528-1.533 to 1.509-1.512 Å. This is despite the fact that calculations for single molecule in vacuum showed 1.55 Å for DCBB. This deviation is much larger than the mean instrumental error. This finding agrees with behavior observed for other bibenzyl derivatives and can be explained as follows. The torsional vibrations of carbon atoms around the central bond are not sufficiently compensated for in the case of crystalline form (Harada and Ogawa, 2001.). In other words, the observed shortening of this bond can be explained by intermolecular interactions that stabilize the energy of bond vibrations in the crystal structure. We also analyzed the potential energy distribution of simulated normal modes for the most complete assignment. Thus, we present comprehensive data of characteristic modes of the fingerprint area for DABB and DCBB for the first time.

In short, we obtained the geometry of molecules, the parameters of a crystal cell and vibrational modes using a comprehensive study, including experiment, calculations and PED analysis. This integrated approach allowed us to identify and explain some unusual structural relationships. These results will help researchers discover new opportunities for application and help explain the behavior of these other related compounds in more complex systems of interest.

The work was supported by the Russian Science Foundation (grant № 17-73-10209) and performed in the Research Center for X-ray Diffraction Studies and the Computing Centre.



## WATER CONDENSATION AND ATMOSPHERIC PHENOMENA

**Smirnov B.M.**

*Joint Institute for High Temperatures, Izhorskaya 13/19, Moscow 127412, Russia*

*bmsmirnov@gmail.com*

The analysis of nucleation processes in the Earth's atmosphere allows us to understand deeper both growth of water microdrops in the atmosphere and to understand deeper some atmospheric problems which include the atmospheric electricity and greenhouse effect. Indeed, atmospheric electricity starts from collision water particles located in different phase state and leads to formation of clouds consisting of weakly charged microdrops. Next, water microdrops are responsible for approximately 30% of infrared radiative flux which is created at frequencies above  $750\text{ cm}^{-1}$  and is directed toward the Earth.

There are four processes of formation and growth of microparticles in the atmosphere which include attachment of free water molecules to a drop, coagulation, i.e. joining of two microdrops as a result of their contact, coalescence or Ostwald ripening, i.e. growth of large microdrops and evaporation of small ones as result of their interaction with a water vapor through processes of attachment and evaporation, and the gravitation growth of microdrops. The later takes place in the course of rain formation, where large microdrops fall faster than small ones that leads to their joining. As a result, water microdrops are transformed into millimeter ones during falling to the Earth.

Each of indicated mechanisms of growth of a condensed phase dominate under appropriate conditions. In particular, the classical mechanism of nucleation through formation of an embryo of a critical size is not working in the real atmosphere, and penetration of a supersaturated water vapor in a region with a microdrops which work subsequently as nuclei of condensation. For this reason, the distribution of clouds in the atmosphere is non-uniform. On contrary, near the Earth's surface in regions where winds are absent and nuclei of condensation are present, a mist is formed at nighttime, if the temperature changes sharply, as it takes place at autumn.

Thus, we analyze individual mechanisms of formation and growth of water microparticles in a real atmosphere. Usage of parameters of atmospheric phenomena where these processes are of importance allows us to understand the conditions under which this phenomenon is realized.

# PREPARATION AND FORMATION MECHANISM OF NANO-Mg MATERIALS PREPARED BY PHYSICAL VAPOR DEPOSITION

**Song X., Su H., Liu J., Zhang B.**

*University of Science and Technology Beijing*

*xpsong@skl.ustb.edu.cn*

Nanowires, nanoparticles as well as nanoporous materials are three kinds of nanomaterials. In this paper, the Mg nanowires, Mg nanoparticles as well as nanoporous Mg materials are prepared by a physical vapor deposition method and the formation mechanisms of these nanomaterials are discussed based on the oriented growth of metal atoms.

A [11-20]-oriented Mg nanowires is prepared at 703K by a physical vapor deposition method, with the length of about 1.25 $\mu$ m and diameter of about 75nm. It is found that the evaporation/deposition temperature, vacuum level, Mg vapor concentration as well as deposition time all have an effect on the formation of Mg nanowires. And a high vacuum level(vapor flow rate) and a high concentration of magnesium vapor play decisive roles in the formation of magnesium nanowires. With the increase of evaporation temperature or Mg vapor concentration or deposition position, Mg nanowires become thicker and longer and finally convert into magnesium nanoparticles.

During the formation of Mg nanoparticles, two kinds of surface morphology of these nanoparticles are found: one is smooth and the other is porous. Note that the smooth surface are usually on the windward side, which has a higher concentration, and the porous surfaces are usually on the leeward side, which has a lower concentration, it is reasonable to conclude that the high concentration leads to the formation of smooth surfaces, while the low concentration leads to the formation of porous surfaces.

With the further increase of Mg vapors concentration and a high deposition temperature, cellular nanoporous Mg are produced, with the nano pores diameter varying from 110 nm to 280 nm.

For the formation mechanism of Mg nanowires, a growth mechanism that magnesium atoms prefer to grow in the closest packed direction, which has the largest binding strength, is proposed to explain the oriented growth of the magnesium nanowires. When the initial growth direction is close to the closest packed direction, then Mg nanowires will growth in priority, otherwise Mg nanoparticles will take place. For the formation of nanoporous Mg, it is suggested that as the Mg atom growth in a crystal plane, they prefer to grow along the three equivalent packed direction of Mg crystal. When the Mg atom supply is not enough, then the vacancy will appear in their grow direction. As a result, the nanoporous Mg will be produced, with a regular distribution of nanopores in their growth plane.

## EFFECT OF DIFFUSION ON NUCLEATION OF DISLOCATION LOOPS

**Sorokin M.**

*National Research Centre “Kurchatov Institute”*

*m40@lab2.ru*

The nucleation of vacancy loops is considered taking into account diffusion profiles of point defects in the loop vicinities [1-3]. Since the vacancy profile is formed by the vacancies both incoming from the bulk and recently evaporated from the loop edge, their attachment and detachment rates should be redefined to consider the loop size evolution as a Markovian process [4]. Then, if the defect profiles quickly adjust themselves to the actual loop sizes (adiabatic principle), the master [2] or the Fokker-Planck equation [3] can be employed for the nucleation description. However the adiabatic assumption case can be fulfilled only for sufficiently high concentration of the forming loops or other sinks of both kinds of the point defects.

The simple model of the intermediate layer [4] is employed to analyze the applicability domain of the Fokker-Planck equation and the diffusion effect beyond it. Stochastic process, accounting attachment and detachment of vacancies and incoming of interstitials, is evaluated by Monte-Carlo simulation, giving the distribution of the nucleation time, required to a critical loop formation. Effect of diffusional parameters of point defects is discussed.

1. G.S. Was, *Fundamentals of Radiation Materials Science: Metals and Alloys*. 2<sup>nd</sup> ed. (Springer, NY, 2017)
2. K.C. Russell, R.W. Powell, *Acta Metallurgica* **21** (1973) 187
3. A.A. Semenov, C.H. Woo, *Phil. Mag.* **83** (2003) 3765
4. M.V. Sorokin, V.I. Dubinko, V.A. Borodin, *Phys. Rev.* **E 95** (2017) 012801

# VAPORIZATION AND THERMODYNAMIC PROPERTIES OF OXIDE SYSTEMS AND MATERIALS: FROM BORATE TO HAFNATE

Stolyarova V.

*Saint Petersburg State University*

*v.stolyarova@spbu.ru*

During synthesis of oxide materials at high temperatures especially thin films and coatings the question on the vaporization features and thermodynamic description of oxide systems has the great importance. From this point of view the unique information that may be obtained by Knudsen effusion mass spectrometric method up to the temperatures 3000 K on vaporization processes and thermodynamic properties of oxide systems may be extremely useful for obtaining oxide materials with the required properties. Review on high temperature behavior of binary and multicomponent borate, phosphate, germanate, silicate, zirconate and hafnate systems containing oxides from first till fifth groups of the D.I. Mendeleev Periodic Table including lanthanides is presented. Various types of vapor species were found over oxide systems studied such as the associated, dissociated and polymerized products of vaporization. The regularities of the vaporization of the binary and multicomponent oxide systems were illustrated and discussed from the point of view of the acid-base concept.

The vapor composition over the binary borate, phosphate, germanate, silicate, zirconate and hafnate systems identified by high temperature mass spectrometric method was summarized and grouped according to the number of outer valence electrons of an oxide modifier. More complex associated vapour species over oxide systems were observed as a result of increasing atomic mass numbers of oxide-modifiers in lower rows of the Periodic Table. One of the reason for that may be the participation of d- and f- electrons in the chemical bonds and the penetration of 6s-electrons under the cover of 3d-, 4d-, 4f- and 5d- electrons. For understanding the features of vaporization behaviour of the binary oxide systems from the point of view of the acid-base concept the following parameters may be analysed:

- values of the differences of electron potentials (electronegativities), forming oxides;
- enthalpies of formation of oxide modifier;
- the lattice energy of oxide modifier calculated per mole of  $O^{2-}$  at 298 K;
- the energies of the M-O-X bond when second coordination sphere was taken into consideration.

The main factors for the prediction of the relative volatility of the binary and multicomponent oxide systems were considered on the basis of the data on the composition of vapor and thermodynamic properties obtained by Knudsen effusion mass spectrometric method. Among them it is necessary to underline the following.

If oxide modifier was the same one could observe the increase of volatility of components in the order from hafnate and to borate systems, as a consequence of the increase of acidity of the melts in the order indicated;

predominant species in the vapor over germanate, silicate, zirconate and hafnate systems were the forms characteristic of dissociative vaporization of the oxides forming the systems;

in the vapor over borate systems containing oxides of alkali metals and of beryllium, lead, bismuth or barium, the formation of gaseous borates was most probable, their polymerization was also possible.

Advantages of semi-empirical and statistical thermodynamic approaches such as Kohler and Barker methods were also illustrated for the prediction of thermodynamic properties of oxide systems as well as partial pressures of vapor species at high temperatures required for obtaining of oxide materials with the reliable physicochemical properties.

Present study was supported by the Russian Fund for Basic Research according to Project N 19-03-00721.

## STRUCTURAL CHANGE OF AGGREGATES OF MAGNETIC NANOPARTICLES IN ROTATING MAGNETIC FIELD

**Storozhenko A.<sup>1</sup>, Stannarius R.<sup>2</sup>, Shabanova I.<sup>1</sup>, Arefyev I.<sup>3</sup>**

*1 - Southwest State University, Kursk, Russia*

*2 - Otto-von-Guericke University Magdeburg, Germany*

*3 - Ivanovo State Power University, Russia*

*storogenko\_s@mail.ru*

As a smart material, magnetic suspension is able to change some properties under the influence of external conditions (mainly, magnetic fields). We study the behavior of suspensions of magnetic nanoparticles and non-magnetic anisotropic pigment microparticles in a spherical container under the action of a rotating magnetic field.

The experimental functions of torque on magnetic field frequency are non-monotonic and strongly depend on the concentration of magnetic phase. This problem has a long history. In some papers, a magnetic fluid is considered as an ideal multi-component gas, so associations of particles and their possible agglomeration in chains in the magnetic field are investigated. With increasing concentration of the solid phase, the average number of particles in aggregates increases. Other authors provided evidence that the aggregates start with small formations from larger particles that exist even in absence of a magnetic field. In magnetic fields, interactions between aggregates lead to their association. It was noted that in order to understand such processes it is necessary to investigate characteristic aggregation times and the impact of shear forces on aggregates experimentally. Research results in this area could also be useful from the point of view of creating seals where a magnetic fluid is exposed alternatively to strong magnetic fields or shear.

The process of particle aggregation was discussed in detail many times. Two types of aggregates are possible: liquid drop-like, which can change their shape in a magnetic field, and quasi-solid ones, which can stay magnetized even without magnetic field. Our experimental data can be explained assuming aggregation of magnetic nanoparticles. When the concentration of the magnetic phase is high and the field rotation frequency is low, a few large aggregates are formed. Their relaxation time is much longer than that of single particles, so these aggregates are unstable and they are rapidly destroyed when the rotation frequency of the magnetic field is increased. Indeed, the experimental dependence of the torque has a sharp decline after reaching a peak at low rotation frequencies, which we explain by the above mentioned decomposition process. Thereafter, the signal increases again, which indicates the orientation of individual particles and small clusters following the field with increasing phase lag. With the dilution of the material, two effects come into play. The first one is the reduced viscosity, the second one is that the cluster size at low rotation rates is much smaller than in the non-diluted suspensions. The decomposition of these clusters occurs at higher frequencies since they can follow the field more efficiently. Moreover, their contribution to the rotational effect is smaller compared to the non-diluted ferrofluid. In the high-diluted samples, aggregates are practically absent, thus there is a monotonous growth of the signal with frequency.

In addition to the aggregation phenomenon, the rotational effect is also influenced by the decreasing viscosity and changes of magnetic properties of the system as a consequence of the dilution with low-viscosity non-magnetic solvent.

This study was funded by Grant of the President of Russia, contract № 075-02-2018-844.

# SELF-ASSEMBLY PROCESSES OF ARRAYS OF CdS NANOCRYSTALS SYNTHESIZED USING THE LANGMUIR-BLODGETT METHOD

**Svit K.<sup>1</sup>, Duda T.<sup>1</sup>, Kozhuhov A.<sup>1</sup>, Zhuravlev K.<sup>1,2</sup>**

*1 - Rzhanov Institute of Semiconductor Physics of the Siberian Branch of the RAS, 13, Ac. Lavrentieva ave., Novosibirsk, Russia, 630090*

*2 - Novosibirsk State University, 1, Pirogova str., Novosibirsk, Russia, 63090*

*svit@nanotech.nsk.ru*

Semiconductor nanocrystals (NC) are very promising materials for novel optical and electron devices due to their unusual properties different from the bulk material. In particular II-IV compounds NC are promising in the field of creation different optoelectronic devices such as lasers, sensors and solar cells [1-2]. The most common way for preparing semiconductor NC is colloidal synthesis. This method is quite simple and low-cost but allows making high quality NC from a wide range of materials. However colloidal NC have feature such as ligand shell that creates a number of problems for these NC application. The main problem is limited and quite large separation distance between neighboring colloidal NC within the array which is bad for charge transport between the NC and suppress different collective properties that are very interesting from a fundamental, research point of view. NC synthesis technique within organic layers based on Langmuir-Blodgett (LB) method is alternative lacking abovementioned disadvantage [3]. LB technique doesn't require using organic ligands and use passivation gas such as ammonia to eliminate surface states influence. In that case NC separation distance limited only by the gas molecule size that is several times smaller in comparison with organic ligands. Despite such advantages NC synthesized using LB technique are poorly investigated. The process of NC formation in the LB matrix has been previously described in the framework of the Lifshitz-Slezov diffusion model for two-dimensional case. However, further process of NC arrays self-assembling after the LB matrix removal which is a key for NC array formation and further investigation of any collective properties or practical application has not been studied yet.

In the present work processes of CdS NC self-assembly on substrates with different wettability induced by thermal desorption of the LB matrix are studied. It was found that the NC self-assembly mainly determined by the LB matrix wetting properties. In the case of high wettability and homogeneous matrix evaporation NC tend to self-organize into predominantly two-dimensional arrays. At the small thickness of the initial LB matrix NC form rare round-shaped arrays due to its low concentration in the initial matrix. Increase in the LB matrix thickness leads to increase of the NC density that in their turn results in formation of fractal-like NC arrays going into transient gel with further NC density increase. Almost complete monolayer is formed at higher NC density. Self-assembly on non-wettable substrate is determined by the matrix dewetting process. Two types of the NC arrays are formed in this case. The first one is large round-shaped NC arrays formed during the LB matrix breakup into drops and the second one is finger-like arrays formed during dewetting, namely the holes growth and coarsening within liquid matrix layer.

This work was supported by the Russian Scientific Foundation (grant No. 18-72-00027).

[1] P. Weinmann, C. Zimmermann, T. W. Schlereth, C. Schneider, S. Höfling, M. Kamp, and A. Forchel, *J. Sel. Top. Quantum Electron.* 15, 780 (2009).

[2] N. Singh, M. R. Mehra, A. Kapoor, and T. Soga, *J. Renew. Sustain. Energy* 4, 013110 (2012).

[3] A. G. Milekhin et al., *Phys. Solid State* 44, 1976 (2002).

# THERMODYNAMICS OF NANOSIZED SESSILE DROPLETS ON SOLID SUBSTRATE: CONTACT ANGLE, ADSORPTIONS AND LINE TENSION

**Tatyanenko D.V., Shchekin A.K.**

*St. Petersburg State University, 7–9 Universitetskaya nab., St. Petersburg, 199034, Russia*

*d.tatyanenko@spbu.ru*

We consider a multicomponent liquid sessile droplet with curvature radius  $R$  forming a contact angle  $\theta$  with surface of a rigid solid substrate. Thus, the contact line radius equals  $r = R \sin \theta$ . To find equilibrium conditions, we consider the grand thermodynamic potential of the system

$$\Omega = -p^\alpha V^\alpha - p^\beta V^\beta + \omega^\gamma V^\gamma + \sigma^{\alpha\beta} A^{\alpha\beta} + \sigma^{\alpha\gamma} A^{\alpha\gamma} + \sigma^{\beta\gamma} A^{\beta\gamma} + \kappa L$$

with  $V$  the volumes of the corresponding phase,  $A$  the areas of the interfacial dividing surfaces,  $L$  the length of the three-phase contact line,  $p$  the bulk pressures (in the fluid phases),  $\omega^\gamma$  the bulk density of the grand potential in the solid phase,  $\sigma$  the thermodynamic surface tensions ('surface energies'),  $\kappa$  the thermodynamic line tension ('line energy'). Greek superscripts  $\alpha$  refer to the liquid phase,  $\beta$  to the surrounding vapor/gas phase,  $\gamma$  to the solid phase of the substrate; double Greek superscripts refer to the corresponding interfaces.

At thermodynamic equilibrium,  $\partial\Omega/\partial R = 0$  and  $\partial\Omega/\partial r = 0$ . This gives the Laplace formula

$$p^\alpha - p^\beta = 2\sigma^{\alpha\beta}/R$$

and the generalized Young equation

$$\sigma^{\alpha\beta} \cos \theta = \sigma^{\beta\gamma} - \sigma^{\alpha\gamma} - \kappa/r - \partial\kappa/\partial r. \quad (1)$$

To characterize the size dependence of the contact angle  $\theta$ , Eq. (1) is usually compared with the 'classical' Young equation for the macroscopic contact angle  $\theta_0$

$$\sigma_0^{\alpha\beta} \cos \theta_0 = \sigma_0^{\beta\gamma} - \sigma_0^{\alpha\gamma}.$$

The '0' subscripts mark values of quantities in the thermodynamic state at the binodal the "macroscopic" contact angle  $\theta_0$  correspond to. This leads to the equation for the contact-angle-cosine correction:

$$\sigma_0^{\alpha\beta} (\cos \theta_0 - \cos \theta) = \delta\Delta\sigma^\gamma + \delta\sigma^{\alpha\beta} \cos \theta + \kappa/r + \partial\kappa/\partial r \approx \delta\Delta\sigma^\gamma + \delta\sigma^{\alpha\beta} \cos \theta_0 + \kappa/r + \partial\kappa/\partial r \quad (2)$$

with  $\delta\Delta\sigma^\gamma \equiv \Delta\sigma^\gamma - \Delta\sigma_0^\gamma$ ,  $\Delta\sigma^\gamma \equiv \sigma^{\alpha\gamma} - \sigma^{\beta\gamma}$ ,  $\Delta\sigma_0^\gamma \equiv \sigma_0^{\alpha\gamma} - \sigma_0^{\beta\gamma}$ ,  $\delta\sigma^{\alpha\beta} \equiv \sigma^{\alpha\beta} - \sigma_0^{\alpha\beta}$ .

Usually, only the line-tension term  $k/r \simeq k_0/r$  is taken into account in Eq. (2). This, particularly, is widely used to measure the line tension [1] and has crucial implications for thermodynamics of nucleation [2,3]. However, all the correction terms are generally non-zero and should be estimated, at least, by order in the contact line curvature  $1/r$ . To examine the size (contact-line-curvature) dependence of the contact angle, we employ

1) the Gibbs–Duhem relations for the bulk fluid phases giving us the estimation

$$\tilde{\mu} \equiv (p^\alpha - p^\beta)/\sigma^{\alpha\beta} = 2/R \approx \sum_i n_{i0}^\alpha \delta\mu_i / \sigma_0^{\alpha\beta} \quad (3)$$

with  $\delta\mu_i \equiv \mu_i - \mu_{i0}$  the deviations of the chemical potentials from their values in the reference state at the binodal,  $n_i^\alpha$  the number density of the  $i$ -th component in the liquid phase;

2) the Gibbs adsorption equations for the interfaces giving

$$\delta\Delta\sigma^\gamma \approx \sum_i (\Gamma_{i0}^{\beta\gamma} - \Gamma_{i0}^{\alpha\gamma}) \delta\mu_i = O(\tilde{\mu}) = O(1/r), \quad \delta\sigma^{\alpha\beta} \equiv \sigma^{\alpha\beta} - \sigma_0^{\alpha\beta} \approx -\sum_i \Gamma_{i0}^{\alpha\beta} \delta\mu_i = O(\tilde{\mu}) = O(1/r) \quad (4)$$

with  $\Gamma$  the values of adsorptions (surface excess of matter per unit area) at the interfaces;

3) the line adsorption equation, which gives

$$\frac{\partial\kappa}{\partial r} = \frac{d\kappa}{dr} - \sum_i \Lambda_i \left( \frac{dr}{d\mu_i} \right)^{-1} = O(\tilde{\mu}^2) = O(1/r^2) \quad (5)$$

with  $\Lambda$  the value of the line adsorption (line excess of matter per unit length) at the contact line.

Combining estimations (3)–(5), we see that the adsorption-related corrections  $\delta\Delta\sigma^\gamma$  and  $\delta\sigma^{\alpha\beta} \cos\theta$  as well as the line-tension-related correction  $\kappa/r$  are of the first order in  $\tilde{\mu}$  (or, in the contact line curvature  $1/r$ ). It means that the slope of the graph  $\cos\theta$  vs  $1/r$  equals [4]

$$-\frac{\kappa_0}{\sigma_0^{\alpha\beta}} - 2 \sin\theta_0 \sum_i \left( \Gamma_{i0}^{\beta\gamma} - \Gamma_{i0}^{\alpha\gamma} - \Gamma_{i0}^{\alpha\beta} \cos\theta_0 \right) \left( \sum_k n_{k0}^\alpha \frac{d\mu_k}{d\mu_i} \right)^{-1}$$

at  $1/r \rightarrow 0$ , in contrast to widely used  $-\kappa_0/\sigma_0^{\alpha\beta}$  [1]. The second, adsorption-related, term depends, in systems with multicomponent fluids, on the “path” in the space of the chemical potentials  $\{\mu_i\}$  to the reference thermodynamic state  $\{\mu_{i0}\}$  at the binodal (with the contact angle  $\theta_0$ ).

For smaller droplets (i.e., critical droplets in nucleation on partially wettable substrates), *all* the corrections on the right-hand side of Eq. (2) become significant, including the term  $\partial\kappa/\partial r$  related to an intrinsic size-dependence of the line tension [5].

The work was supported by the Russian Foundation for Basic Research (grant 18-53-50015 ЯФ\_a).

## References

1. Law B.M et al. *Progr. Surf. Sci.* 2017. V. 92. No. 1. P. 1.
2. Gretz R.D. *Surf. Sci.* 1966. V. 5. No. 2. P. 239.
3. Navascués G, Tarazona P. *J. Chem. Phys.* 1981. V. 75. No. 5. P. 997.
4. Tatyshenko D.V., Shchekin A.K. To appear in *Colloid J.* 2019. V. 81. No. 3.
5. Tatyshenko D.V., Shchekin A.K. *Interfac. Phenom. Heat Transfer.* 2017. V. 5. No. 2. P. 113.



# ANISOTROPY IN THE ELASTICITY OF CRYSTALS: FUNDAMENTAL SOLUTION, DEFECTS, NONLINEARITIES, HARDNESS, HETEROSTRUCTURES – APPROXIMATIONS, AB INITIO AND FINITE-ELEMENT STUDIES

**Telyatnik R.S.**

*Institute for Problems in Mechanical Engineering of Russian Academy of Sciences*

*statphys@ya.ru*

Theory of anisotropic elasticity is discussed in general and exemplified by single-crystals of different symmetries up to the most general triclinic case with 21 independent elastic constants. Fundamental solution (Green's tensor function) of elastostatics, i.e. displacement field caused by a point force in an infinite continuous medium, can be resolved analytically only for isotropic and transversely-isotropic (hexagonal) symmetries, while for the cubic case there are expansions derived with mistakes in proximity to isotropic relation of elastic constants [1, 2]. Symbolic computations in MATLAB software allowed us to correct and get high-order expansions not only for a cubic crystal, but also for trigonal (such as sapphire  $\text{Al}_2\text{O}_3$ ), tetragonal and orthorhombic cases in proximity to the hexagonal solution. Approximation of a numerical solution of the Green's function by a series of spherical harmonics [3] allowed to determine zero and symmetric terms of the series for every elastic case. Such analytic expressions may improve computational Boundary Element Method [4] relying on the evaluation of the Green's function.

Theory of crystal defects in the continual limit exploits the apparatus of the fundamental solution as well [5]. As a demonstrative scalar characteristic, the energy of elastic interaction of two point defects [6] as a function of their relative orientation is presented for every elastic symmetry. The distance limit of applicability of the continuous fundamental solution is shown by its deviation from the corresponding lattice solution calculated *ab initio* by ABINIT software of computational quantum chemistry that has been used as well for computation of dopant atoms.

Nonlinear elasticity for the cubic diamond-like semiconductors Ge, Si, SiC [7], as well as AlN, GaN and their hexagonal 2H and 4H polytypes, was also calculated *ab initio* for large uniaxial and shear strains up to fracture or structural transformation (e.g. diamond has metastable tetragonal phase under uniaxial compression, while other similar crystals for such transition require biaxial strains as in film-substrate heterostructures). Linear proportionality limits and strength limits exhibit strong anisotropy, which also may implicitly estimate the anisotropic plasticity driven by crystal slip planes. Finite-element computation (ANSYS software) of indentation [8], accounting also creep deformation in a quasi-static approach, has proved that hardness anisotropy for surfaces (111), (011), (001) of diamond-like crystals is explained by the predicted parameter  $h > 1$  of Hill's orthotropic plasticity between compression and shear.

Anisotropic aspects in the elasticity and curvature of laminated composites with a mismatch between thermal expansions and lattice parameters of the constituent layers [9] will be briefly discussed together with energetically preferable directions for cracking, delamination, twinning and diffusion [10] to fulfill the subject of the conference.

1. I.M. Lifshitz, L.N. Rozentsveig. *ZhETF* **17**, 783 (1947) – in Russian.
2. P.H. Dederichs, G. Leibfried. *Physical Review* **188**, 1175 (1969).
3. R.S. Telyatnik. *Materials Physics and Mechanics* **27**, 98 (2016).
4. L. Gaul et al., “Boundary element methods for engineers and scientists” (Springer, 2003).
5. T. Mura, “Micromechanics of defects in solids” (Martinus Nijhoff Publishers, 1987, 2<sup>nd</sup> ed.).
6. S.A. Kukushkin, A.V. Osipov, R.S. Telyatnik. *Physics of the Solid State* **58**, 971 (2016).
7. R.S. Telyatnik, A.V. Osipov, S.A. Kukushkin. *Materials Physics and Mechanics* **29**, 1 (2016).
8. R.S. Telyatnik. *IOP Conf. Series: Materials Science and Engineering* **387**, 012078 (2018).
9. L.B. Freund et al, “Thin film materials: stress, defect formation and surface evolution” (2003).
10. R.S. Telyatnik, A.V. Osipov, S.A. Kukushkin. *Physics of the Solid State*, **57**, 162 (2015).

# METHOD OF MATCHED ASYMPTOTIC EXPANSIONS TO CALCULATE THE RADIUS OF A DISPERSED PARTICLE IN THE PROCESS OF ITS HOMOGENEOUS GROWTH

**Tropp E.A.<sup>1</sup>, Galaktionova N.E.<sup>2</sup>, Galaktionov E.V.<sup>1</sup>**

*1 - Ioffe Institute*

*2 - Peter the Great St. Petersburg Polytechnic University*

*tropp@mail.ioffe.ru*

In recent decades, research into physical processes in dispersed systems has been actively developed. They are of great practical importance, representing an important stage in the process of growth of films and coatings. In the monograph [1], the theory of coalescence of the final stage of first-order phase transitions — the phenomenon underlying high technologies for creating quantum-dimensional structures and devices based on them, is described in detail.

This paper is caused by the desire of the authors to give a mathematically correct description of the growth of an embryo formed on a solid wall. The case of homogeneous nucleation in the volume of the metastable phase is considered. Following [1], we will investigate the evolution of the embryo for a sufficiently long period of time. Analysis of the formulation of the problem given in [1] shows that this is possible in the case when the thermal conductivity of the solid phase is much greater than the thermal conductivity of the liquid. An asymptotic method, namely the method of two-scale asymptotic expansions [2, 3], is an adequate method for solving the arising problem.

Due to the fact that the problem is centrally symmetric, its solution is constructed in spherical coordinates. The ratio of the thermal conductivity of the particle and the melt is used as a small parameter. The solution of the problem is in the form of series in powers of the root of a small parameter. The internal problem is solved in “slow” time, while the external problem is solved in “fast” time.

It is established that the temperature field in the liquid matrix changes in “fast” time. The hypothesis adopted in [1] that the thermal field in both a liquid and a solid embryo evolves in a “slow” time is not true.

Built zero approximation. A nonlinear ordinary differential equation is obtained, the general integral of which gives a transcendental equation for finding the particle radius. In the first and next approximations, we obtain linear equations with the same operator, but with different right-hand sides. As a result, we managed to find a transcendental equation that determines the magnitude of the particle radius in the main approximation, as well as the problem for finding the following approximations.

1. Kukushkin S.A., Slezov V.V. Disperse systems on the surface of respiratory bodies (evolutionary approach): mechanisms for the formation of thin films. SPb.: "Nauka", 1996. 309 p.
2. Van Dyke M. Perturbation Methods in Fluid Mechanics. Acad.Press., New York-London, 1964. 271 p.
3. Zino I.E., Tropp E.A. Asymptotic Methods in Problems of the Theory of Heat Conduction and Thermoelasticity. Leningrad: Izd. Leningrad Univ., 1978. 224 p.

## BIFURCATION THEORY OF PLASTICITY, DAMAGE AND FAILURE

Umantsev A.R.<sup>1,2</sup>

1 - Department of Chemistry and Physics, Fayetteville State University, Fayetteville, NC 28301

2 - Center of Hierarchical Material Design, Northwestern University, Evanston, IL 60208

*aumantsev@uncfsu.edu*

Two important trends are taking place simultaneously in the community of materials scientists. On one hand, after accumulating substantial knowledge of phase transformations, researchers began paying more attention to the problem of damage and reliability of the materials in service. On the other hand, mechanicians realized the critical importance of microstructure in the problem of material failure. All this makes us, theoretically inclined materials scientists, think about theoretical approaches that would combine both trends and allow us to model realistic multiscale and multiphase material behavior from cradle to grave.

In this presentation I will introduce a novel approach to plasticity, damage and failure which includes all major components of the mechanical behavior of ductile materials and covers all regimes of viscoplastic tensile/compressive loading and unloading. The approach is based on the concepts of an internal damage parameter and internal energy and has the attributes of both rate-dependent and rate-independent plasticity. The ultimate failure of a specimen is defined as a point of critical value of the damage parameter. I will analyze the phenomenon of fatigue (see Figure) and identify various regimes of this processes—low-cycle and high-cycle fatigue. The approach allowed me to derive a Paris-type equation for the rate of degradation of the specimen as a function of the cyclic plastic work and to find a Coffin-Manson-type power-law relation between the plastic strain amplitude and the number of load reversals to failure. The approach also allowed me to analyze the frequency effect in fatigue. In the end, I will look at the experiments on the rotary bulk-forming of high strength steel and see how the simulation results can be used for the design of new products.

Figure\*. Quasi-static fatigue simulations. (a) Rotational ratcheting of the stress-strain loops. (b) Woehler's S-N curves for the specimens with different yield strains (shown on the diagram).

\*The abstract with figures is available at <http://2019.mgctf.ru/01000037a5.doc>

## DIFFUSE $\alpha$ - $\beta$ PHASE TRANSITION IN THE SURFACE LAYERS OF QUARTZ

**Vettegren V.I.**<sup>1,2</sup>, Mamalimov R.I.<sup>1,2</sup>, Sobolev G.A.<sup>1</sup>, Ponomarev V.A.<sup>1</sup>, Kulik V.B.<sup>2</sup>

*1 - Schmidt Institute of Physics of the Earth of the Russian Academy of Sciences, Moscow*

*2 - Ioffe Institute of the Russian Academy of Sciences, St. Petersburg*

*Victor.Vettegren@mail.ioffe.ru*

The temperature dependence of the  $\alpha$ -phase concentration in surface layers of solution-grown and nature quartz single crystals has been studied in the range 290–820 K using IR and Raman spectroscopy. It has been found that, in the surface layer  $\sim 0.15$   $\mu\text{m}$  thick and in the volume of crystals, the concentration of the  $\alpha$ -phase behaves with increasing temperature as expected for a first-order phase transition, namely, before 800 K, it remains constant, and it tends to zero at  $T \rightarrow 846$  K. At a distance from  $\sim 1$  to 20  $\mu\text{m}$  from the surface, however, the concentration of the  $\alpha$ -phase starts to decrease already at  $\sim 350$  K, while at 812 K it decreases to one-fifth of the original value. This is paralleled by the increase of the concentration of the  $\beta$ -phase. The diffusive of the  $\alpha$ - $\beta$  phase transition is initiated by distortion of the quartz crystal lattice around growth dislocations. The volume of  $\beta$ -phase is the greater than  $\alpha$ -phase. That is why appearing of  $\beta$ -phase leads to internal stresses. It has been established that at distances up to  $\sim 1$   $\mu\text{m}$  from the surface, tensile stresses appear at 400 K reaching  $\sim 300$ – $400$  MPa. At the same time, compressive stresses develop in a layer  $\sim 1$  to 20  $\mu\text{m}$  thick at a temperature above 500 K, and reach a maximum at  $\sim 650$  K. This effect caused by “unfreezing” transverse vibrations of growth dislocations. Because of this the single crystal is split into nanocrystals with linear sizes from  $\sim 8$  to  $\sim 28$  nm in this layer. The nanocrystals are again transformed into a single crystal at a temperature above 650 K and compressive stresses begin decreases.

The temperature dependence of the concentration of  $\alpha$ -phase is changed in the surface layer of a natural crystal under influence of water. Concentration of the  $\alpha$ -phase decreases by about one half in the layer at a depth of  $\sim 6$   $\mu\text{m}$  at  $\sim 370$  and  $\sim 570$  K. The revealed behavior of the  $\alpha$ -phase concentration with the increase in the temperature has been assigned to the influence of water on crystal lattice distortions near growth dislocations. It has been found that tensile stresses generated with increasing temperature in a near surface quartz layer to  $\sim 0.8$   $\mu\text{m}$  thick can reach  $\sim 170$  MPa at 780 K. The onset of such stresses brings about destruction of surface layers of quartz.

# DETERMINATION OF THE CRITICAL NUCLEI SIZE OF POLYMER FOLDED CHAIN CRYSTALS VIA A MICROSCOPIC KINETICS MODEL

Zhang S.J., Guo B.H., Xu J.

*Department of Chemical Engineering, Tsinghua University, 100084, Beijing, China*

*jun-xu@tsinghua.edu.cn*

Nucleation is a fundamental step of crystallization and its mechanism still remains unclear. Classical nucleation theory based on the capillary approximation has achieved success; however, there are still some open questions remained. To understand what happens in the nucleation stage, we propose a microscopic kinetics model, which considers nucleation process from amorphous state as a series of reversible attaching and detaching steps. Different from the previous models, we adopt correlation factors describing the multi-body interaction between the units and the variation of the rate constant for a cluster to attach and detach a unit with the cluster size. The model describes nucleation of small molecules and polymer chains in a unified view, which we believe can be applied to crystallization far from equilibrium. Furthermore, we propose a method to determine the size of the critical secondary nuclei on the lateral growth front of polymer folded chain crystals. For the secondary nucleation, the slope of the log-log plot of the spherulitic radial growth rate versus the content of crystallizable units in the random copolymers gives the number of units in the critical secondary nuclei. This method is based on the stochastic feature of nucleation of random copolymers during crystallization and is independent of the detailed nucleation pathway. Our results on the poly(butylene succinate-co-butylene methylsuccinate) random copolymers show that a critical secondary nucleus consists of 15 to 27 butylene succinate units, corresponding to 6 to 9 chain stems when the polymers were isothermally crystallized from quiescent melt at the temperatures ranging from 70 to 95 °C. The results contradict the classical Lauritzen-Hoffman theory, which predicted that the critical secondary nucleus should be a single chain stem. Our method can be generally applied to other flexible polymers and would be beneficial for understanding the nucleation mechanism of polymer folded chain crystals.

# UNIFIED TEMPERATURE SCALE FOR DESCRIPTION OF CRYSTALLIZATION KINETICS IN SUPERCOOLED LIQUIDS AND GLASSES

Yarullin D.T., Galimzyanov B.N., Mokshin A.V.

*Kazan Federal University*

*yarullindt@gmail.com*

At the present time, the study of nucleation processes is one of the actual tasks in condensed matter physics. Here, the one of the main tasks is detection of universal laws in the temperature dependencies of the crystal nucleation and growth characteristics. One of the main barrier in resolving of this issue is that the temperature range, ( is the melting temperature), may change significantly with changing the type of systems. Therefore, the reduced temperature scales are necessary to investigate the temperature dependencies of the characteristics of systems of various types. The most common are temperature scales of the form: and , ( is the glass transition temperature). However, such scales do not allow to cover a wide temperature range, which complicates the construction of universal temperature dependences.

In the present work, an original temperature scale is presented. This temperature scale allows to compare the kinetic characteristics of crystallization of the systems with different types on the basis of experimental data and simulation results [1, 2]. Universal scaling relations are obtained, which reproduce the temperature dependencies of crystal nucleation and growth characteristics in supercooled liquids and glassy materials.

This work is supported by the Russian Science Foundation (project 19-12-00022).

- A.V. Mokshin, B.N. Galimzyanov, *J. Chem. Phys.* **142**, 104502 (2015).
- A.V. Mokshin, B.N. Galimzyanov, *PCCP*. **19**, 11340 (2017).

# ON THE PROBABILITY-FREE MECHANISM OF MACROSCOPIC IRREVERSIBILITY AND MICROSCOPIC FOUNDATION OF THERMODYNAMICS

Zakharov A.Yu.

*Yaroslav-the-Wise Novgorod State University, Veliky Novgorod, 173003, Russia*

*anatoly.zakharov@novsu.ru*

At present, there is no real alternative to statistical mechanics, which is the basis of theoretical study of many-particle systems, including the theory of non-ideal gases, plasma, condensed matter physics, etc. It is considered that the problem of calculating of the thermodynamic properties of a substance is reduced to purely mathematical problems such as finding of partition functions or uncoupling BBGKY hierarchies.

However, there are very significant actual problems of statistical mechanics, which are related not to the computational part, but to the problem of its substantiation. The most significant of these problems is the problem of the existence of thermodynamic equilibrium. In thermodynamics, the existence of thermodynamic equilibrium is postulated as a zeroth law. This postulate is in obvious contradiction with the principles of classical mechanics. Using the probabilistic concept by Maxwell, Boltzmann and Gibbs does not eliminate this contradiction. Moreover, the thermodynamic behavior of systems cannot in principle be derived within the framework of classical mechanics.

Probably for the first time the hypothesis that retarded potentials are one of the sources of the second law of thermodynamics was formulated by Walter Ritz shortly before his early death in 1909 [1]. In this regard, attention should be paid to the work of Synge “The electromagnetic two-body problem” [2]. In this work, it is shown that the retardation in the interaction of these bodies, even without taking into account radiation friction, leads to an irreversible collapse of the system. Of course, taking into account the delay in the interaction between particles can be performed within the framework of the field theory. However, owing to the works of Wheeler and Feynman [3], who established the equivalence of the field theory of electromagnetic interaction between particles and the theory of direct (not instantaneous) interaction, instead of field theory, the theory of direct (not instantaneous) interaction between particles can be used. This approach has been implemented in our work [4–6].

The main new results in this direction are as follows.

1. The irreversible behavior of closed classical systems of interacting particles is their common property regardless of the number of the particles. This property due to the unavoidable retardation of the interactions between the particles. The retarded part of interatomic interactions plays the role of an unavoidable thermostat.
2. Classical systems are irreversible by themselves. There is no need to use any probabilistic or other uncontrollable hypotheses to explain the phenomenon of irreversibility in a system of interacting particles.

**Acknowledgment:** The work was carried out with financial support of the Ministry of Education and Science of Russian Federation within the framework of the project part of the state order (project No.3.3572.2017)

## References

- [1] W. Ritz, A. Einstein. *Physikalische Zeitschrift*, **10**(9) (1909) 323-324.
- [2] J. L. Synge. *Proc. Roy. Soc. A.*, **177** (968) (1940) 118-139.
- [3] J. Wheeler, R. Feynman. *Rev. Mod. Phys.*, **21** (3) (1949) 425-433.
- [4] A.Yu. Zakharov. *Intern. J. Quant. Chem.* **116** (3) (2016), 247--251.
- [5] A.Yu. Zakharov, M.A. Zakharov. *Phys. Lett. A*, **380** (3) (2016) 365–369.
- [6] A.Yu. Zakharov. *Physica A: Statistical Mechanics and its Applications*, **473** (2017) 72–76.

## PHASE DIAGRAM CALCULATION IN THE GENERALIZED LATTICE MODEL

**Zakharov M.A.**

*Novgorod State University*

*ma\_zakharov@list.ru*

A brief review of the methods for calculating the basic types of binary phase diagrams is done in the framework of generalized lattice model [1-3]. The short-range parts of the interatomic interactions are taken into account by introducing atomic self-volumes. The long-range parts of the potentials are taken into account in the effective-field approximation. The construction of binary phase diagrams with unlimited solubility of the components in the solid state, the phase diagrams of eutectic and peritectic types, as well as diagrams with intermediate phases is considered. The results of the calculations performed are compared with phase diagrams of real binary solutions.

**Acknowledgment:** The work was carried out with financial support of the Ministry of Education and Science of Russian Federation within the framework of the project part of the state order (project No.3.3572.2017).

### References

- [1] Zakharov A.Yu., Zakharov M.A. and Loginova O.V. *Int. J. Quant. Chem.* (2004) Vol. 100. P. 435-441.
- [2] Korzun E.L., Terekhov S.V. *Zh. Phys & Chem.* (1987) Vol. 61 P.1186-1189.
- [3] Zakharov M.A. *Phys. Solid State* (2007) Vol. 49. P. 2312-2317.



# PHASE FIELD SIMULATION OF LITHIUM DIFFUSION AND DIFFUSION-INDUCED STRESSES IN BATTERY ELECTRODES WITH CONSIDERATION OF PHASE SEPARATION

**Song Y., Zhang J.**

*Shanghai University*

*jqzhang2@shu.edu.cn*

Phase separation in an electrode of a lithium ion battery, which is a phenomenon where an active electrode material is separated into Li-rich and Li-poor phases, exists widely in many active materials and has significant impacts on the diffusion of lithium ions and diffusion-induced stresses. A phase field model is developed to study the phase separation. Firstly, the influences of various energies, such as the free energy of uniform Li-ion concentration, gradient energy and elastic energy, on phase separation are discussed. Secondly, the impacts of charge operation, e.g. galvanostatic and potentiostatic, on Li-ion diffusion and diffusion-induced stresses in a planar phase separating electrode are investigated. Calculations are also made for single phase electrodes based on Fick's law for comparison. The obtained simulation results show that the Li-ion diffusion in a phase separating electrode depends significantly on the phase separating profile and movement of phase boundary, but it is not sensitive to charge operation. The diffusion-induced stresses also separate into high and low stress regions. Finally, based on the diffusion process and diffusion-induced stress, it is suggested that phase separation should be avoided for the sake of fast charging and mechanical reliability.

# THE FLUCTUATION STAGE OF PHASE TRANSITION: NON - EQUILIBRIUM KINETICS

Zmievskaia G.I.

*Keldysh Institute of Applied Mathematics Russian Academy of Sciences, Moscow*

*zmig@mail.ru*

The kinetic theory of phase transitions at the initial non - equilibrium stage are related with names of V.V.Slyozov and Ya.B. Zel'dovich. Basing on their ideas and new numerical methods for solving quasi-linear equations of mathematical physics [1-4] it appears ability to study mechanisms of a fluctuational stage phase transition (condensation vapors in the discharge plasma and the formation of vacancy-gas pores in the crystal lattice during the implantation of ions into the surface). The solution of the kinetic equations: Kolmogorov - Feller, Smoluchowski or Fokker – Planck with nonlinear coefficients for effects associated with clustering of germs, gives the evolution of non-equilibrium probability density in the phase space [3]. Clustering is represented by the Markov diffusion process given by the stochastic differential equation / SDEs / in the sense of Stratonovich, the Rosenbrock method of SDEs solution has a second - order standard convergence. Algorithms probabilistic measures are used for the generalized stochastic molecular dynamics method [3], continuous trajectories of random processes models (with number  $\sim 10^6$ ) were added by random jumps for accounting clusters dispergation. During vapors condensation in plasma we take into account the criterion Rayleigh instability which is limiting growth charged drops that leads to fragmentation of clusters. Obtaining condensate drops of a given size is an important process prior to solidification of the melt in the preparation of powders. Charged clusters deposition model [4] has been extended by the accounting of the criterion instability of drop sizes in plasma discharge and their non-equilibrium probability density distribution during the fluctuation stage of the phase transition had been received. The distribution silicon carbide melt drops is of interest for the production of reinforcing grains of diamond-like material for composite materials.

Computer simulation the porosity formation (or “blistering”) into crystal lattice during inert gases flux interaction with surface and Xe ions implantation with the creation of gaseous pores (“brownian particles” /BPs/) into thin layers of surface of solid sample. Model is presented by lattice defects clustering and their brownian motion /BM/. The coordinates BPs center of masses changes under the action of the total potential of the indirect elastic interaction between BPs, each with other, external and internal surfaces of the layers. Such potential has been obtained by quantum – empirical method for weakly anisotropic lattice and point wise defects of lattice. Different characteristic time of blisters clustering ( $\sim 10^{-8}$ s) and BM( $\sim 10^{-7}$ s) allowed us to divide the problem into physical processes. Strains in lattice due to porosity depends on the energy and dose implanted ions and temperature surface. BM under action self-consistent potential of pores interaction leads to the occurrence of "structures" of self-organization, or long - living space - time structures of voids in phase spaces of random dynamical variables[5].

1. G.I. Zmievskaia, T.A. Averina, A.L. Bondareva // Applied Numerical Mathematics. Intern. Conference “Difference Schemes and Applications” in Honor of the 90-th Birthday of Professor V.S. Ryaben’kii. V. 93. July 2015 : 15–29. –2015.
2. G.I. Zmievskaia, A.L. Bondareva // Journal of Surface Investigation. X-ray, Synchrotron and Neutron Techniques, Volume 10, Issue 4, 802–808. –2016.
3. G. I. Zmievskaia, A. L. Bondareva, V. D. Levchenko, and T. V. Levchenko // J. Phys. D : Appl.Phys., 40: 4842–4849, –2007.
4. G. I. Zmievskaia and A. L. Bondareva. Plasma Phys. Reports, 37(1) : 87–95,– 2011.
5. L.Arnold. Random dynamical system. Springer Monographs in Mathematics,1998,586p.

# **SHEAR INDUCED MARTENSITIC TRANSFORMATIONS IN CRYSTALLINE POLYETHYLENE: DIRECT MD SIMULATION**

**Strelnikov I.A., Zubova E.A.**

*N.N. Semenov Institute of Chemical Physics*

*zubova@chph.ras.ru*

For the first time, we carry out molecular dynamics (MD) simulation of shear-induced martensitic phase transitions between the orthorhombic and non-orthorhombic (triclinic and monoclinic) phases of crystalline polyethylene (PE) in the framework of a realistic all atom model of the polymer. We show that the variation of the shear rate allows observing on a nano-sample both a strongly nonequilibrium phase transition occurring by random nucleation and irregular growth of a new phase ('civilian' way, for rapid deformations) and the coherent, or 'military', kinetics (generally considered as usual for martensitic transformations). We induce transitions from the orthorhombic to the triclinic phase according to two transformation modes observed in experiment on PE single crystals. Rapid deformation favors the transition directly to the triclinic phase, slow deformation - first to the intermediate monoclinic, and only then - to the triclinic phase. The second way corresponds to the experiment on extended chain PE. We explain this result and analyze the competition between different transformation and plastic deformation modes. Rotations of PE chains around their axes necessary for the transition between the orthorhombic and non-orthorhombic phases are executed by short twist defects diffusing along the chains. The transition between the monoclinic and triclinic phases occurs through half-chain-period translations of the chains along their axes, mostly collectively, as crystallographic slips. The part of the work regarding the kinetics of the transitions was supported by the Russian Science Foundation (Award No. 16-13-10302). The study of the formation of twist defects and their energies was supported by the Program of Fundamental Researches of the Russian Academy of Sciences (Project No. 0082-2014-0013, state Registration No. AAAA544 A17-117042510268-5). The simulations were carried out in the Joint Supercomputer Center of the Russian Academy of Sciences.

# ON THE THEORY OF NUCLEATION AND GROWTH IN HIGH-TEMPERATURE SYNTHESIS OF COLLOIDAL QUANTUM DOTS

Razumov V.F.<sup>1,2,3</sup>, Tovstun S.A.<sup>1,2</sup>

1. *Institute of Problems of Chemical Physics of the Russian Academy of Sciences, Moscow region, Chernogolovka, Prospekt Akad. Semenova, 1*
2. *Moscow Institute of Physics and Technology, Dolgoprudny, Moscow region, Institute lane, 9*
3. *Moscow state University. M. V. Lomonosov, 119991, Moscow, Lenin's hills*

*tovstun@icp.ac.ru*

One of the most popular methods for producing nanoparticles is the precipitation from supersaturated solution. To optimize this method requires a detailed description of the evolution of the particle size distribution during all stages of the synthesis. Therefore, we have performed the numerical simulation of nanoparticle nucleation and growth from the supersaturated solution. The simulation was based on the Fokker-Planck equation for the particle size distribution function:  $\partial_t f = \partial_r (B \partial_r f - A f)$ , where  $t$  is time,  $f = f(r, t)$  is the distribution function of the particle radius  $r$ ,  $A$  is the particle growth rate,  $B$  is the diffusion coefficient in the particle size space. In the simulation, it was assumed that the particle growth rate is diffusion controlled and that the solubility depends on the size in accordance with the Kelvin equation. Simulation was performed for the case of instantaneous creation of supersaturation and for the case of continuous feed of reagents to the solution. For the case of instantaneous creation of supersaturation the following stages of the distribution function evolution were revealed: the attainment of stationary nucleation, stationary nucleation, narrowing of the distribution, broadening of the distribution, Ostwald ripening. From the analysis of these stages we have derived the conditions under which the stage of narrowing of the distribution is long-continued and leads to nanoparticles with low polydispersity. For the case of continuous reagents feed to the solution, all stages of the distribution function evolution were also revealed and it has been shown that at the end of the nucleation stage the polydispersity is almost independent of the reagents feed rate and equal to 20%. This work was performed under the State Assignment (no. 0089-2019-0003) and was made possible by Government of the Russian Federation (Agreement № 074-02-2018-286).

## TRAVELLING WAVE SOLUTIONS FOR THE PENROSE-FIFE PHASE FIELD MODEL

**P. O. Mchedlov-Petrosyan<sup>1</sup>, L. N. Davydov<sup>2</sup>**

NSC “Kharkov Institute of Physics and Technology”

<sup>1</sup> *E-mail:* [peter.mchedlov@free.fr](mailto:peter.mchedlov@free.fr)

<sup>2</sup> *E-mail:* [ldavydov@kipt.kharkov.ua](mailto:ldavydov@kipt.kharkov.ua)

The concept of the phase field is currently widely used in the theory of phase transitions and material science. The Penrose-Fife phase field model is now a well-established model proposed within this concept. In the course of study of this model both the rigorous mathematical results and approximate solutions were obtained. However, until now, no exact solutions were given in the literature. In this talk exact travelling wave solutions for this system are presented. While the functional form of the solutions is rather simple, the dependence of solutions on the parameters of the model is quite complicated. Also, an interesting link between this model and the convective-viscous Cahn-Hilliard equation is discussed.

# CONTROLLED NUCLEATION OF NANOPORES IN GLASS OPTICAL FIBERS UNDER POWERFUL LIGHT ILLUMINATION AND TENSILE STRESS

**Shlyagin M.<sup>1</sup>, Kukushkin S.A<sup>2</sup>**

<sup>1</sup>*CICESE (Mexico)*

<sup>2</sup>*IPME RAS (Russia)*

*mish@cicese.mx*

Silicate glass is a very important material in optics, including fiber optics and integrated optics. It was found, that a powerful laser light is able to modify the structure of glass not only at the glass sample surface, but also in its volume, introducing local changes of the refractive index of material. This phenomenon is the basis for direct recording of planar waveguides and Bragg reflectors in optical fibers. In optical fibers, using side irradiation with a light beam having a periodical power distribution along the fiber axis, reflective filter can be formed in the fiber core, so-called fiber Bragg gratings (FBGs). FBGs found very broad applications in optoelectronics, in fiber-optic communication systems and sensors.

Depending on the laser power, many different effects were observed in optical glasses, from the formation of color centers to plasma excitation in a small volume in the lens focusing point. During FBGs inscription in optical fibers with intermediate and high light intensity, non-monotonic behavior of grating reflectivity was observed. An appearance of an initial fiber grating was attributed mainly to glass densification mechanism. Then, with continuation of irradiation, formation of second so called negative FBG can be observed, which possess very similar optical properties, however has much higher temperature resistance. Also, second type of high temperature gratings (so-called regenerated gratings) can be obtained with smaller light exposure but with post-exposure thermal treatment of the seed grating.

In this talk we will present a possible mechanism responsible for such a non-monotonic behavior during fiber Bragg grating inscription in optical fiber. The proposed mechanism is based on controlled nucleation of nano-pores in the glass fiber core area in accordance with a spatial distribution of light intensity along the fiber. Using the theory of phase transitions (considering pores, or voids as a emerging new phase) it was possible to estimate the basic parameters of the pores, such as the critical radius of a stable pore, rate and time of nucleation, dependence on tensile stress and temperature, etc. Proposed mechanism and theoretical estimates correspond well to some effects and parameters observed and measured at experiments.

## CONTENTS

<b>SESSION “Mechanisms of crystal formation and growth in single- and multi-component systems: theoretical description of the process, numerical modeling, experimental results” .....</b>	<b>5</b>
PHOTOPOLYMERIZATION PRODUCTS OF NEW DIACETYLENE ALCOHOL DERIVATIVES <u>Alekseev A.S.</u> , Domnin I.N., Ivanov A.B. ....	5
CRYSTALLISATION OF LAYERS IN PZT/LNO/Si HETEROSTRUCTURES <u>Atanova A.V.</u> , Zhigalina O.M., Khmelenin D.N., Seregin D.S., Vorotilov K.A., Sigov A.S. ....	6
THEORETICAL STUDIES OF THE STRUCTURAL PECULIARITIES IN III/V SEMICONDUCTORS <u>Baranovskii S.D.</u> .....	7
THE MODEL FOR IN-PLANE AND OUT-OF-PLANE GROWTH REGIMES OF III-V NANOWIRES <u>Berdnikov Y.</u> , Sibirev N. ....	8
STRUCTURE AND PROPERTIES OF SiO <sub>x</sub> FILMS PREPARED BY CHEMICAL ETCHING OF AMORPHOUS METALLIC GLASS Fedorov V., <u>Berezner A.</u> , Beskrovnyi A., Fursova T., Pavlikov A. ....	9
THE ORIGIN OF PHASE TRANSITION AND THE USUAL EVOLUTIONS OF THE UNIT-CELL CONSTANTS OF THE NASICON STRUCTURES OF THE SOLID SOLUTION LiTi <sub>2-x</sub> Ge <sub>x</sub> (PO <sub>4</sub> ) <sub>3</sub> <u>Boumar N.</u> .....	10
FORMATION OF WIDE-BANDGAP SEMICONDUCTORS ON Al <sub>2</sub> O <sub>3</sub> <u>Bouravleuv A.</u> , Sobolev M., Ilkiv I., Pirogov E., Ubyivovk E., Sharofidinov S., Kukushkin S. ....	11
2D MESOSCALE COLLOIDAL CRYSTAL PATTERNS COMPOSED BY MICROSPHERES ON SUBSTRATES <u>Bredikhin V.</u> , Bityurin N. ....	12
QUANTITATIVE STRAIN DISTRIBUTION IN ELECTROMECHANICALLY COUPLED IV-IV AND III-V SEMICONDUCTOR QUANTUM DOTS <u>Cherkashin N.</u> , Nevedomskiy V., Sakharov A., Tsatsulnikov A., Nikolaev A., Ledentsov N., Shchukin V. ....	13
THE PROCESSES OF CRYSTALLIZATION AND DEGASSING OF METAL MELTS, QUENCHING FROM THE LIQUID STATE <u>Chernov A.A.</u> , Pil'nik A.A. ....	14
EFFECT OF GROWTH CONDITIONS ON SURFACE MORPHOLOGY AND CONCENTRATION OF GROWTH DEFECTS OF CdTe/GaAs (100) EPITAXIAL LAYERS IN THE MOCVD PROCESS <u>Chilyasov A.V.</u> , Evstigneev V.S., Moiseev A.N. ....	15
MECHANISMS OF SILICON ALLOTROPES' CRYSTALLIZATION IN CONDENSED MEDIA BY IN SITU DIFFRACTION OF SYNCHROTRON RADIATION <u>Courac A.</u> .....	16
ROLE OF NUCLEATION IN THE VAPOR-LIQUID-SOLID GROWTH OF III-V SEMICONDUCTOR NANOWIRES <u>Dubrovskii V.G.</u> .....	17
INFLUENCE OF INDIUM ADDITION ON NUCLEATION AND GROWTH OF WHISKERS FROM TIN FILMS IN ELECTRONICS <u>Dutta I.</u> , Das Mahapatra S. ....	18
ION BEAM AND X-RAY METHODS OF THIN FILM COATING DIAGNOSTICS <u>Egorov V.</u> , Egorov E., Afanas'ev M. ....	19

NONSTATIONARY NUCLEATION IN LAYERS OF GAS-SATURATED AMORPHOUS ICE IN THE PRESENCE OF ARTIFICIALLY INTRODUCED CRYSTAL CENTERS <u>Faizullin M.Z.</u> , Vinogradov A.V., Tomin A.S., Koverda V.P.....	20
GROWTH OF CRYSTALS FROM THE GASEOUS PHASE ON THE SURFACES OF CLEAVAGE OF IONIC CRYSTALS UNDER CONDITIONS OF THERMO-ELECTRICAL SYNERGETIC INFLUENCE <u>Fedorov V.A.</u> , Karyev L.G.....	21
EFFECT OF DOUBLE SOLID-PHASE EPITAXIAL RECRYSTALLIZATION ON THE DEFECT DENSITY IN ULTRATHIN SILICON-ON-SAPPHIRE LAYERS <u>Fedotov S.D.</u> , Statsenko V.N., Golubkov S.A., Egorov N.N. ....	22
CELLULAR NANO-STRUCTURING IN SiGe(Sn) ALLOY AFTER FAST CRYSTALLIZATION: A PLATFORM FOR HETEROEPITAXY <u>Gaiduk P.</u> .....	23
CALCULATION OF THE SHAPE OF A MELT DROP LEAVING THE SHAPER WHEN GROWING A CRYSTAL BY THE STEPANOV METHOD <u>Galaktionova N.E.</u> , Galaktionov E.V., Tropp E.A. ....	24
VERTICAL LIQUID BRIDGES AND CRYSTAL GROWTH BY THE STEPANOV METHOD <u>Galaktionov E.V.</u> , Galaktionova N.E., Tropp E.A. ....	25
ON GROWTH OF SbSI FILMS BY THE QUASI-CLOSED VOLUME TECHNIQUE AND THEIR PROPERTIES <u>Garmashov S.</u> .....	26
NUCLEATION STATISTICS AND LENGTH DISTRIBUTIONS FOR WURTZITE AND ZINC BLENDE III-V NANOWIRES GROWING FROM LIQUID NANODROPLETS WITH VERY LOW GROUP V CONTENT <u>Glas F.</u> .....	27
TWO APPROACHES TO FORMATION OF THIN Mg <sub>2</sub> Si FILMS ON Si SURFACE: ULTRA-FAST DEPOSITION AT 400 C AND ROOM TEMPERATURE DEPOSITION ON AMORPHOUS Si <u>Gouralnik A.S.</u> , Shevlyagin A.V., Chernev I.M., Gerasimenko A.V., Gutakovskii A.K.....	28
FORMATION AND COMPOSITION FEATURES OF SELF-SCROLLING HYDROSILICATE CRYSTALS Krasilin A.A., Khrapova E.K., <u>Gusarov V.V.</u> .....	29
DYNAMICS OF ATOMIC STEPS AND SHAPE TRANSFORMATIONS OF NANOWIRES Filimonov S.N., <u>Hervieu Yu.Yu.</u> .....	30
RELAXED STRUCTURE OF INTERPHASE BOUNDARIES IN TWO-LAYER METAL FILMS: MOLECULAR DYNAMICS <u>Ievlev V.M.</u> , Prizhimov A.S. ....	31
DETERMINATION OF CRYSTALLISATION TEMPERATURE OF MULLITE BY LUMINESCENCE SPECTRA OF EUROPIUM AND CHROMIUM IONS <u>Igo A.V.</u> .....	32
SILICON NANO-CRYSTALLITES FOR ADVANCED APPLICATION <u>Ivanda M.</u> , Gebavi H., Mikac L., Đerek V., Baran N., Ristić D., Životkov D.....	33
MATHEMATICAL MODELING OF DENDRITIC CRYSTAL GROWTH IN MUSHY ZONE OF METALLIC ALLOYS <u>Ivanova A.</u> .....	34
THE SCALING OF SUBNANOMETER EOT GATE DIELECTRICS FOR ULTIMATE NANO CMOS TECHNOLOGY <u>Iwai H.I.</u> .....	35



THE INFLUENCE OF ARGON GAS FLUX AND DEPOSITION RATE ON OPTICAL AND PHYSICAL PROPERTIES OF DC MAGNETRON SPUTTERED ITO THIN FILM <u>Kadivar E.</u> , Moshabaki A. ....	36
CRYSTAL GROWTH AT SPONTANEOUS CRYSTALLIZATION IN NON-INERTIAL SYSTEMS IN SPACE STATION AND EARTH CONDITIONS BY THE EXAMPLE OF SYNTHESIS AND GROWTH OF CRYSTALS FROM SOLUTION-MELT <u>Kalashnikov E.V.</u> , Gurin V.N., Nikanorov S.P., Derkatchenko L.I., Yagovkina M.A. ....	37
OPTICAL PROPERTIES OF SPATIALLY INDIRECT EXCITONS IN ZINC BLENDE GaSb/GaAs QD STRUCTURE <u>Kang H.-K.</u> , Kim J.-H., Lee E.-H., Baik M., Song J.-D., Cho M.-H. ....	38
THREE-CATION SCANDOBORATES: SYNTHESIS, STRUCTURE, PROPERTIES AND CRYSTAL GROWTH <u>Kokh A.</u> , Kononova N., Kuznetsov A., Kokh K., Shevchenko V., Uralbekov B., Bolatov A., Svetlichnyi V. ....	39
PHASE COMPOSITION AND ELECTRICAL TRANSPORT IN THIN FILMS SYNTHESIZED BY EVAPORATION OF Bi <sub>2</sub> Se <sub>3</sub> ON MICA <u>Kokh K.A.</u> , Nebogatikova N.A., Tereshchenko O.E., Kustov D.A., Antonova I.V. ....	40
QUARTZ GLASS OBTAINED ON THE PLASMATRON OF JSC "DINUR" FROM RAMENSKOYE SAND. FEATURES OF CRYSTALLIZATION ON A POLISHED SURFACE <u>Kolobov A.Yu.</u> , Sycheva G.A. ....	41
STUDY OF PHASE EQUILIBRIA IN THE C <sub>5</sub> H <sub>5</sub> SO <sub>4</sub> -C <sub>5</sub> H <sub>2</sub> PO <sub>4</sub> -NH <sub>4</sub> H <sub>2</sub> PO <sub>4</sub> -H <sub>2</sub> O SYSTEM <u>Komornikov V.A.</u> , Timakov I.S., Grebenev V.V., Zajnullin O.B., Makarova I.P., Selezneva E.V. ....	42
PROTON-CONDUCTING COMPOSITE MATERIALS BASED ON SUPERPROTONIC CRYSTALS <u>Komornikov V.A.</u> , Grebenev V.A., Timakov I.S., Zajnullin O.B. ....	43
REVERSIBLE 2D-3D TRANSITION IN THIN GAN LAYER FORMED ON THE AlN (0001) SURFACE Mansurov V.G., Galitsyn Yu.G., Malin T.V., Milakhin D.S., <u>Konfederatova K.A.</u> , Zhuravlev K.S. ....	44
FORMATION OF AgInS <sub>2</sub> /ZnS COLLOIDAL NANOCRYSTALS AND THEIR PHOTOLUMINESCENCE PROPERTIES <u>Korepanov O.A.</u> , Mazing D.S., Aleksandrova O.A., Moshnikov V.A. ....	45
VAPOR-SOLID-SOLID MECHANISM OF Au-CATALYZED III-V NANOWIRE GROWTH <u>Koryakin A.A.</u> , Kukushkin S.A., Kotlyar K.P., Ubyivovk E.D., Reznik R.R., Cirlin G.E. ....	46
ON THE FORMATION OF AXIAL HETEROSTRUCTURES IN CATALYTIC TERNARY III-V NANOWIRES <u>Koryakin A.A.</u> , Leshchenko E.D., Kotlyar K.P. ....	47
THE GROWTH AND PROPERTIES OF GUANYLUREA(1+) HYDROGEN PHOSPHATE (GUHP) CRYSTAL Kaminskii A.A., Manomenova V.L., Rudneva E.B., Sorokina N.I., Grebenev V.V., <u>Kozlova N.N.</u> , Angeluts A.A., Ozheredov I.A., Solyankin P.M., Denisyuk I.Yu., Fokina M.I., Zulina N.A., Shkurinov A.P., Voloshin A.E. ....	48
THE FINGERPRINTS OF HOMOGENEOUS NUCLEATION AND CRYSTALLIZATION IN POLYAMID-66 AS STUDIED BY COMBINED INFRARED (IR) SPECTROSCOPY AND FAST SCANNING CHIP CALORIMETRY Anton A.M., Zhuravlev E., Kossack W., Andrianov R., Schick C., <u>Kremer F.</u> ....	49

HIGHLY-LUMINESCENT CRYSTALS OF A NOVEL LINEAR PI-CONJUGATED THIOPHENE-PHENYLENE CO-OLIGOMER WITH BENZOTHIADIAZOLE FRAGMENT Postnikov V.A., <u>Kulishov A.A.</u> , Lyasnikova M.S., Sorokina N.I., Voloshin A.E., Borshchev O.V., Surin N.M., Svidchenko E.A., Ponomarenko S.A. ....	50
INVESTIGATION OF THERMOELECTRIC PROPERTIES OF THIN-FILM NANOSTRUCTURES MnSi <u>Kuznetsov Y.</u> , Dorokhin M., Erofeeva I., Demina P., Lesnikov V. ....	51
GROWTH FROM SOLUTIONS, STRUCTURE AND PROPERTIES OF CRYSTALLINE FILMS OF LINEAR OLIGOPHENYLS AND THEIR DERIVATIVES WITH END SUBSTITUENTS <u>Lyasnikova M.S.</u> , Postnikov V.A., Kulishov A.A., Grebenev V.V., Sorokina N.I., Lebedev-Stepanov P.V., Stepko A.S., Borshchev O.V., Surin N.M., Svidchenko E.A., Ponomarenko S.A., Voloshin A.E. ....	52
IN SITU INVESTIGATIONS OF THE GROWTH KINETICS OF THE PRISM AND PYRAMID FACES OF KDP CRYSTAL AT ULTRAHIGH SUPERSATURATIONS <u>Lyasnikova M.S.</u> , Kovalyov S.I., Grebenev V.V., Rudneva E.B., Voloshin A.E., Manomenova V.L. ....	53
THIN FILMS OF BISMUTH: PREPARATION METHODS AND STRUCTURAL CHANGES UNDER THE INFLUENCE OF LASER RADIATION <u>Makarova E.S.</u> , Kablukova N.S., Novotelnova A.V., Tukmakova A.S., Khodzitsky M.K., Demchenko P.S. ....	54
FEATURES OF KDP CRYSTAL GROWTH AT ULTRAHIGH SUPERSATURATION <u>Manomenova V.L.</u> , Rudneva E.B., Kovalyov S.I., Voloshin A.E. ....	55
CRYSTALLIZATION OF HYDROXYAPATITE ON WATER-SOLUBLE POLYMER. A BIOMIMETIC APPROACH TO HYBRID MATERIALS <u>Mizutani T.</u> , Okuda K. ....	56
NANOSCALE ELECTROLESS SILVER PLATING WITH CONTROLLED NUCLEATION AND GROWTH CHARACTERISTICS <u>Muench F.</u> , Vaskevich A., Ensinger W. ....	57
POROUS CARBON NANOMATERIALS PRODUCED AS INVERSE OR DIRECT REPLICA OF ION-TRACK ETCHED POLYMER MEMBRANES <u>Muench F.</u> , Ensinger W. ....	58
SYNTHESIS OF TiN, Ti AND TiSi <sub>2</sub> THIN FILMS FOR THE CONTACT SYSTEM OF SOLAR CELLS <u>Nussupov K.Kh.</u> , Beisenkhanov N.B., Bakranova D.I., Keiinbay S., Turakhun A.A., Sultan A.A. ....	59
EFFECTS OF AMORPHOUS STRUCTURES ON EXPLOSIVE CRYSTALLIZATION OF SPUTTER-DEPOSITED AMORPHOUS GERMANIUM THIN FILMS <u>Okugawa M.</u> , Nakamura R., Numakura H., Heya A., Matsuo N., Yasuda H. ....	60
2D ISLAND NUCLEATION CONTROLLED BY NANOCUSTER DIFFUSION DURING Si AND Ge EPITAXY ON Si(111)-(7×7) SURFACE AT ELEVATED TEMPERATURES <u>Petrov A.</u> , Rogilo D., Sheglov D., Latyshev A. ....	61
PHENOMENOLOGICAL MODELS OF NUCLEATION AND GROWTH OF METAL ON A SEMICONDUCTOR <u>Plusnin N.I.</u> ....	62
CRYSTALS OF PI-CONJUGATED LINEAR CO-OLIGOMERS: NUCLEATION AND GROWTH FROM SOLUTIONS <u>Postnikov V.A.</u> , Kulishov A.A., Lyasnikova M.S., Sorokina N.I., Ostrovskaya A.A., Borshchev O.V., Ponomarenko S.A. ....	63

SURFACE MORPHOLOGY, MICROSTRUCTURE AND PIEZOELECTRIC RESPONSE OF PEROVSKITE ISLANDS DURING THE PYROCHLORE TO PEROVSKITE PHASE TRANSFORMATION IN THIN PZT FILMS <u>Pronin I.P., Kaptelov E.Y., Senkevich S.V., Kiselev D.A., Osipov V.V., Pronin V.P.</u> .....	64
PECULIARITIES OF GROWTH OF A NON-KOSSEL CRYSTAL VIA CHERNOV'S MECHANISM <u>Redkov A.V., Kukushkin S.A., Gangrskaya E.S.</u> .....	65
ANOMALIES OF PROPERTIES IN KCNSH MIXED CRYSTALS <u>Rudneva E.B., Manomenova V.L., Koldaeva M.V., Sorokina N.I., Voloshin A.E., Grebenev V.V., Verin I.A., Lyasnikova M.S., Vasilyeva N.A., Masalov V.M., Zhokhov A.A., Emelchenko G.A.</u> .....	66
FILIFORM POLYCRYSTALLINE PHOSPHOR Cd <sub>0,1</sub> Zn <sub>0,9</sub> S: Cu, Ag ON THE SURFACE OF THE NEW MATERIAL Si/(NANO-SIC) <u>Sergeeva N.M., Bogdanov S.P.</u> .....	67
CRYSTAL GROWTH AND UNIQUE MORPHOLOGY OF HETEROSTRUCTURED ALUMINUM HYDROXIDE FILM FORMED ON ALUMINUM ALLOYS USING STEAM <u>Serizawa A., Kanasugi K., Tanabe M.</u> .....	68
GROWTH AND CHARACTERIZATION OF ALKALI-EARTH HALIDE SCINTILLATOR CRYSTALS <u>Shalaev A., Shendrik R., Rusakov A., Rupasov A., Myasnikova A.</u> .....	69
MORPHOLOGY EVOLUTION DURING EARLY STAGE OF SINGLE CRYSTAL DIAMOND HOMOEPITAXIAL GROWTH BY MICROWAVE PLASMA CHEMICAL VAPOR DEPOSITION <u>Shu G., Ralchenko V., Bolshakov A., Komlenok M., Khomich A., Ashkinazi E., Dai B., Zhu J.</u> .....	70
MICROSTRUCTURE OF BARIUM-STRONTIUM TITANATE BASED GLASS CERAMICS <u>Turygin A.P., Abramov A.S., Alikin D.O., Chezganov D.S., Baturin I.S., Song X., Zhang T., Zhang Y., Hu K., Zhao Z., <u>Shur V.Ya.</u></u> .....	71
INFLUENCE OF ELASTIC STRESS ON CRYSTAL PHASE OF GaP NANOWIRES <u>Sibirev N.V., Berdnikov Y.S., Sibirev V.N.</u> .....	72
DIAMOND NUCLEATION FROM ACTIVATED VAPOR PHASE <u>Spitsyn B.V.</u> .....	73
FORMATION OF STEPS AT THE THREE-PHASE LINE OF CONTACT UNDER THE GROWTH VAPOR-LIQUID-SOLID NANOWIRES <u>Nebol'sin V.A., <u>Swaikat N.</u></u> .....	74
GLASS FORMATION AND NUCLEATION KINETICS IN THE MeO-B <sub>2</sub> O <sub>3</sub> -P <sub>2</sub> O <sub>5</sub> SYSTEM, WHERE Me=Ca, Sr, Ba <u>Sycheva G.A.</u> .....	75
SURFACE ENERGY AT THE CRYSTAL NUCLEUS-GLASS INTERFACE, THE SIZE OF THE CRITICAL NUCLEUS OF CRYSTALS AND THE ENERGY BARRIER FOR THE FORMATION OF A STABLE CRYSTALLINE NUCLEUS IN ALKALI SILICATE GLASSES <u>Sycheva G.A.</u> .....	76
CRYSTAL GROWTH OF LARGE CZTS SINGLE CRYSTAL BY VERTICAL GRADIENT FREEZE <u>Tablaoui M., Khelfane A., Ziane M.-I.</u> .....	77
THE CALCIUM CARBONATE CASE STUDY. FROM IONS TO THE AMORPHOUS PHASE. CLASSICAL OR NON-CLASSICAL NUCLEATION? <u>Testino A., Carino A., Mohammed A.S.A., Cervellino A.</u> .....	78
SYNTHESIS OF COMPLEX HYDROSULPHATES OF SINGLY CHARGED CATIONS <u>Timakov I.S., Grebenev V.V., Komornikov V.A., Zainullin O.B., Selezneva E.V.</u> .....	79

DIFFERENT MORPHOLOGIES OF SILICOALUMINOPHOSPHATE SAPO-11: EXPERIMENT AND THEORY <u>Tiuliukova I.A., Parkhomchuk E.V.</u> .....	80
ORIENTED GROWTH OF BaSrTiO <sub>3</sub> THIN FILMS ON SEMI-INSULATING SILICON CARBIDE <u>Tumarkin A., Odinets A., Zlygostov M.</u> .....	81
GLYCINE-NITRATE SYNTHESIS OF CRYSTAL SOLID SOLUTIONS OF BARIUM-STRONTIUM TITANATE Belysheva D.N., Sviridov S.I., Sinelshchikova O.Y., <u>Tumarkin A.V.</u> , Tyurnina N.G., Tyurnina Z.G.....	82
GROWTH OF HIGH-PERFECT MIXED COBALT NICKEL POTASSIUM SULFATE HEXAHYDRATE CRYSTALS BY THE TEMPERATURE DIFFERENCE TECHNIQUE WITH CONTINUOUS SOLUTION FEEDING <u>Vasilyeva N.A., Rudneva E.B., Manomenova V.L., Masalov V.M., Zhokhov A.A., Emelchenko G.A., Voloshin A.E.</u> .....	83
THE PROBLEM OF GROWING MIXED CRYSTALS AND HIGH-EFFICIENCY K <sub>2</sub> (Co, Ni)(SO <sub>4</sub> ) <sub>2</sub> · 6H <sub>2</sub> O OPTICAL FILTERS <u>Voloshin A.E., Rudneva E.B., Manomenova V.L., Vasilyeva N.A., Kovalev S.I., Grigorieva M.S., Emelchenko G.A., Masalov V.M., Zhokhov A.A.</u> .....	84
A MATHEMATICAL MODEL OF FINITE-SIZE EFFECTS IN THIN FILM CRYSTALLIZATION Kozyukhin S., <u>Vorobyov Y.</u> , Lazarenko P., Sybina Yu., Ermachikhin A., Sherchenkov A.....	85
FORMATION MECHANISMS OF HEMATITE CONCAVE NANOCUBES <u>Wang Z.</u> .....	86
FINITE SIZE AND PROXIMITY EFFECTS IN ULTRA THIN EPITAXIAL TRANSITION METAL SUPERLATTICES <u>Wolff M.</u> .....	87
RELATIONSHIP OF Mg <sub>2</sub> Si PHASE-CONTENT AND THERMAL EXPANTION PROPERTIES OF Mg-Si AND Mg-Si-Ca ALLOYS <u>Wu Sh., Guo T., An P., Zhou X., Lü Sh.</u> .....	88
MOLECULAR DYNAMICS SIMULATION OF Ti CRYSTAL GROWTH PROCESS WITH CRYSTAL-LIQUID CONFIGURATION METHOD <u>Yang X.</u> .....	89
INFLUENCE OF PREFORMED NUCLEI ON CRYSTAL NUCLEATION KINETICS IN SODA-LIME-SILICA GLASS <u>Yuritsyn N.S.</u> .....	90
NUCLEATION AND GROWTH OF CRYSTALS IN SODA-LIME-SILICA GLASSES <u>Yuritsyn N.S.</u> .....	91
PREPARATION AND STUDY OF WATER-SOLUBLE COBALT AND NICKEL SALTS <u>Zainullin O.B., Komornikov V.A., Timakov I.S.</u> .....	92
<b>SESSION “New methods and approaches to the description of growth and the investigation of different properties of wide-bandgap semiconductors” .....</b>	<b>93</b>
LOW-TEMPERATURE SYNTHESIS OF α-SiC NANOCRYSTALS Nussupov K.Kh., <u>Beisenkhanov N.B.</u> , Bakranova D.I., Keiinbay S., Turakhun A.A., Sultan A.A.....	93
AROMATIC-LIKE CARBON NANOSTRUCTURES CREATED ON THE VICINAL SiC SURFACES <u>Benemanskaya G., Timoshnev S., Kukushkin S.</u> .....	94
BULK GROWTH OF GaN. HOW TO OVERCOME THE EQUILIBRIUM CRYSTAL SHAPE? <u>Bockowski M.</u> .....	95

GROWTH AND STUDY OF ALLOYED GaP NANOWIRE HETEROSTRUCTURES <u>Bolshakov A.</u> , Fedorov V., Mozharov A., Sibirev N., Kryzhanovskaya N., Cirlin G., Mukhin I. ....	96
BORON NITRIDE EPILAYERS GROWN ON AlO <sub>x</sub> N <sub>y</sub> AND Al <sub>2</sub> O <sub>3</sub> BUFFER LAYER <u>Caban P.A.</u> , Michalowski P., Gaca J., Wojcik M., Ciepiewski P., Mozdzonek M., Teklinska D., <u>Dumiszewska E.</u> , Firek P., Baranowski J.M. ....	97
III-V NANOWIRES GROWN BY MBE ON Si AND SiC SUBSTRATES <u>Cirlin G.</u> .....	98
MBE GROWTH, STRUCTURAL AND OPTICAL PROPERTIES OF GALLIUM ARSENIDE PHOSPHIDE NITRIDE HETEROSTRUCTURES ON SILICON <u>Fedorov V.</u> , Bolshakov A., Koval O., Sapunov G., Kirilenko D., Mozharov A., Mukhin I. ....	99
IMPROVEMENT OF CRYSTALLINE QUALITY OF AlGaIn BY NUCLEATION GROWTH AND ULTRAVIOLET LASER APPLICATION <u>Iwaya M.</u> , Sato K., Takeuchi T., Kamiyama S., Akasaki I., Miyake H.....	100
CONSTITUENTS OF THE GROWTH OF GaN NANOWIRE ARRAYS: NUCLEATION, RADIUS SELF-REGULATION, HEIGHT SELF-EQUILIBRATION, BUNDLING, ELASTIC AND PLASTIC RELAXATION <u>Kaganer V.</u> , Fernández-Garrid S., Sabelfeld K., van Treeck D., Geelhaar L., Brandt O.....	101
FORMATION AND STUDY OF THE PROPERTIES OF INGAN POLYTYPE STRUCTURES GROWN BY LOW-TEMPERATURE MOLECULAR-BEAM EPITAXY <u>Kotlyar K.</u> , Reznik R., Lihachev A., Kirilenko D., Soshnikov I., Cirlin G.....	102
SITE-SPECIFIC MICRO CROSS SECTIONING BY A FIB-SEM. ADVANTAGES FOR INVESTIGATION OF THIN FILMS <u>Lukashova M.V.</u> , Dergachev A.I. ....	103
NUCLEATION OF THE GRAPHENE-LIKE Si <sub>3</sub> N <sub>3</sub> LAYER ON THE Si (111) STUDIED BY STM <u>Mansurov V.G.</u> , Galitsyn Yu.G., Malin T.V., Milakhin D.S., Teys S.A., Zhuravlev K.S.....	104
GaN NANOCRYSTALS FORMATION ON THE GRAPHENE-LIKE g-AlN AND g-Si <sub>3</sub> N <sub>3</sub> SURFACES <u>Milakhin D.S.</u> , Malin T.V., Mansurov V.G., Galitsyn Yu.G., Zhuravlev K.S., Lebiadok Ya.V., <u>Razumets A.A.</u> .....	105
CONTROL OF THE POLARITY OF GaN EPITAXIAL LAYERS GROWN ON SiC/Si TEMPLATES <u>Mizerov A.</u> , Kukushkin S., Timoshnev S., Sharofidinov S., Bouravlev A. ....	106
GROWTH OF AlN AND GaN BULK CRYSTALS BY SUBLIMATION SANDWICH- METHOD <u>Mokhov E.N.</u> , Wolfson A.A., Kazarova O.P.....	107
GROWTH OF HIGH PURITY 3 INCH SiC CRYSTALS WITH HIGH STRUCTURAL PERFECTION <u>Nagalyuk S.</u> , Mokhov E., Ta Ching H. ....	108
IMPURITY EFFECTS ON NUCLEATION AND GROWTH OF SiC CLUSTERS AND LAYERS ON Si(100) AND Si(111) <u>Pezoldt J.</u> , Lubov M.N., Kharlamov V.S.....	109
TWO DIMENSIONAL ELECTRON GAS FORMATION AT AlGaIn/GaN INTERFACES <u>Caban P.</u> , Thorpe R., Feldman L., Michalowski P., Nielsen S., Julsgaard B., Pedersen K., <u>Popok V.N.</u> .....	110
MBE GROWTH AND PROPERTIES OF III-V AND NITRIDE NANOWIRES ON HYBRID SiC/Si SUBSTRATES. SI DIFFUSION INTO GaN NANOWIRES <u>Reznik R.</u> , Kukushkin S., Osipov A., Talalaev V., Kotlyar K., Cirlin G. ....	111

GaN SELECTIVE EPITAXY IN SUB-MICRON WINDOWS FORMED BY ION BEAM NANOLITHOGRAPHY <u>Rodin S.N.</u> , Lundin W.V., Tsatsulnikov A.F., Sakharov A.V., Usov S.O., Mitrofanov M.I., Levitskii I.V., Evtikhiev V.P. ....	112
SEMIPOLAR GaN ON A NANOSTRUCTURED Si(100) SUBSTRATE: THE TECHNOLOGY AND THE PROPERTIES <u>Rodin S.N.</u> , Bessolov V.N., Kompan M.E., Konenkova E.V., Orlova T.A., Pantelev V.N., Sereдова N.V., Scheglov M.P. ....	113
THE INFLUENCE OF SILICON SUBSTRATE ORIENTATION WITH A BUFFER SUBLAYER OF SILICON CARBIDE ON THE GROWTH AND POLAR PROPERTIES OF THIN ALUMINUM NITRIDE FILMS <u>Sergeeva O.N.</u> , Solnyshkin A.V., Kiselev D.A., Kukushkin S.A., Sharofidinov S., Kaptelov E.Yu., Pronin I.P. ....	114
BULK LAYERS OF POLAR AND SEMIPOLAR AlN, GaN AND AlGaN GROWN BY THE HVPE METHOD ON SI PLATES 2 'IN DIAMETER WITH A BUFFER LAYER OF NANO-SiC SYNTHESIZED BY THE ATOMIC SUBSTITUTION METHOD <u>Sharofidinov Sh.Sh.</u> , Kukushkin S.A. ....	115
NUCLEATION AND GROWTH MECHANISM OF MOISSANITE - NATURAL SiC <u>Shiryaev A.A.</u> , Pavlushin A.D. ....	116
DISLOCATION REACTIONS IN SEMI-POLAR GAN EPITAXIAL LAYERS GROWN ON SI(001) OFFCUT SUBSTRATE USING AlN AND 3C-SiC BUFFER LAYERS <u>Sorokin L.M.</u> , Gutkin M.Yu., Myasoedov A.V., Kalmykov A.E., Bessolov V.N., Osipov A.V., Kukushkin S.A. ....	117
SYNCHROTRON-BASED PHOTOEMISSION STUDY OF ELECTRONIC STRUCTURE OF GaN GROWN BY PLASMA ASSISTED MOLECULAR BEAM EPITAXY <u>Timoshnev S.</u> , Mizerov A., Benemanskaya G., Kukushkin S., Bouravleuv A. ....	118
<b>SESSION "Nonlinear and collective phenomena in the process of crystal growth" .....</b>	<b>119</b>
NON-LINEAR EFFECTS IN ELECTRODEPOSITION OF SEMICONDUCTOR NANOSTRUCTURES IN IONIC LIQUIDS <u>Borisenko N.</u> , Lahiri A., Endres F. ....	119
CLUSTERING AND MELTING IN 2D CUPRATE-LIKE LAYERS <u>Chetverikov A.</u> , Ebeling W., Velarde M. ....	120
IN SITU RECONSTRUCTION OF CRYSTAL SHAPE GROWN IN AN AXISYMMETRIC KYROPOULOS SYSTEM <u>Duffar T.</u> , Sen G., Braescu L. ....	121
<b>SESSION "Physics, chemistry, and mechanics of crystal surfaces" .....</b>	<b>122</b>
GAUSSIAN BEAM SPHERE OPTICS IN CONDENSED MATTER RESEARCH <u>Bredikhin V.</u> .....	122
TWO STEP ANNEALING NiO <sub>x</sub> PROMOTE THE GROWTH OF PEROVSKITE CRYSTAL TOWARD HIGH PERFORMANCE AMBIENT STABLE PEROVSKITE SOLAR CELL <u>Chen Ch.-P.</u> .....	123
STRESS-ASSISTED PHASE AND CHEMICAL TRANSFORMATIONS IN SOLIDS VIA CHEMICAL AFFINITY TENSOR <u>Freidin A.B.</u> , Morozov A.V., Muller W.H., Poluektov M., Figiel Ł., Sharipova L.L. ....	124
INVESTIGATION OF ELASTIC PROPERTIES OF NANO SiC GROWN ON Si BY ATOMIC SUBSTITUTION <u>Grashchenko A.S.</u> , Kukushkin S.A., Osipov A.V. ....	125

USING RECOVERED SILICON NANOPARTICLES FROM SILICON WIRE SAWING TO MODIFY THE SURFACE OF GRAPHENE NANOSHEETS FOR Li <sup>-</sup> ION BATTERIES ANODE APPLICATION	
<u>Hecini M.</u> , Beddek S., Drouiche N., Aoudj S., Palahouane B. ....	126
CRYSTAL GROWTH OF LARGE ANISOTROPIC La <sub>2</sub> NiO <sub>4+δ</sub> PLATELETS VIA MOLTEN-FLUX	
<u>Hinterding R.</u> , Zhao Z., Zhang C., Feldhoff A. ....	127
SURFACE OXIDATION EFFECT ON PHOTO-REACTIVITY OF TOPOLOGICAL INSULATOR Bi <sub>2</sub> Se <sub>3</sub> THIN FILMS AS A FUNCTION OF AIR EXPOSURE TIME	
<u>Hong S.-B.</u> , Chae J., Kim D.-K., Jeong K., Kim H., Yoo B., Cho M.-H. ....	128
HIGH RESOLUTION ANALYSIS ON Ni/Au/Ni/Au Ohmic CONTACT TO p-AlGaIn/GaN SEMICONDUCTOR	
<u>Hu Z.-F.</u> , Li X.-Y., Zhang Y. ....	129
CHEMICAL CHARACTERISTICS OF STEAM-INDUCED HYDROXIDE COMPOSITE FILM SURFACE FORMED ON Mg ALLOYS	
Miyashita T., Inamura M., Serizawa A., <u>Ishizaki T.</u> .....	130
HIGH-SPEED FORMATION OF SINTERED BOND-LINE BY ADDITION OF 350 NM Cu OR Cu@Ag PARTICLES BETWEEN MICRON Cu@Ag PARTICLES	
<u>Jong-Hyun L.</u> , Sung Yoon K. ....	131
ENERGY BAND DIAGRAM ANALYSIS OF TiO <sub>2</sub> /ELECTROLYTE INTERFACE IN PHOTOELECTROCHEMICAL CELL	
Hien T.T., Quang N.D., Kim C., <u>Kim D.</u> ....	132
A STUDY ON RECOVERY OF HIGH PURITY VALUABLE MATERIALS FROM END-OF -LIFE THIN FILM PHOTOVOLTAIC PANELS	
<u>Kim T.Y.</u> , Cho S.Y., Lee W.G. ....	133
SIMULATION OF RADIATION-INDUCED SEGREGATION IN Fe–Cr–Ni ALLOYS	
Skorokhod R.V., <u>Koropov O.V.</u> .....	134
WAVE HEAT PROCESSES IN LOW-DIMENSIONAL MATERIALS	
<u>Krivtsov A.</u> .....	135
ADSORPTION INDUCED DEFORMATION AND PHASE TRANSFORMATIONS IN NANOPOROUS CRYSTALS	
<u>Neimark A.V.</u> .....	136
THE TENSILE STRENGTH OF SiC FIBERS WITH THIN ZIRCONIA COATINGS DERIVED BY DIFFERENT METHODS	
<u>Prokip V.E.</u> , Lozanov V.V, Morozova N.B., Baklanova N.I. ....	137
GROWTH OF A FACETED PORE IN CRYSTALLINE MEDIA VIA BURTON-CABRERA-FRANK MECHANISM	
<u>Redkov A.V.</u> , Kukushkin S.A. ....	138
DEPENDENCE OF PROPERTIES OF VARIABLE GRADIENT POROUS STRUCTURE OF SILICON ON THE METHOD OF FORMATION	
<u>Rubtsova K.</u> , Silina M. ....	139
LINE AND POINT ENERGY OF GRAPHENE	
<u>Rusanov A.I.</u> .....	140
GROWTH AND PROPERTIES OF NOVEL GRAPHENE-BASED MAGNETIC HETEROSTRUCTURES FOR SPINTRONIC DEVICE APPLICATIONS	
Li S., Yamauchi Y., <u>Sakai S.</u> .....	141

MECHANICAL PROPERTIES OF PVD DEPOSITED AL <sub>2</sub> O <sub>3</sub> THIN FILM ON A SINGLE-CRYSTAL SUBSTRATE <u>Shumilin A.I.</u> , Plotnikov M.V., Fomin A.A. ....	142
OPPORTUNITIES OF ATOMIC FORCE MICROSCOPY TO STUDY THE NUCLEATION OF THIN COATING FORMED IN THE MOLECULAR LAYERING PROCESS <u>Sosnov E.A.</u> .....	143
SYNTHESIS AND ASSEMBLY OF COLLOIDAL NANOCRYSTALS TOWARDS ADVANCED FUNCTIONALITIES <u>Striccoli M.</u> , Fanizza E., Panniello A., Depalo N., Ingrosso C., Comparelli R., Petronella F., Dibenedetto C.N., Triggiani L., Vischio F., Rizzi F., Agostiano A., Curri M.L.....	144
<b>SESSION “Origin and statistics of lattice defects and their effect on the properties and growth of crystals”.....</b>	<b>145</b>
THEORETICAL MODELLING OF OXYGEN VACANCY CHARACTERISTICS IN LEAD ZIRCONATE TITANATE PBZR <sub>1-x</sub> TI <sub>x</sub> O <sub>3</sub> (PZT). EFFECTS ON STRUCTURAL AND FERROELECTRIC PROPERTIES <u>Bogdanov A.</u> , Kimmel A.....	145
THE CORRELATION STUDY OF THE CRYSTAL STRUCTURE WITH OPTICAL PROPERTIES OF AMMONIUM HYDROGEN PHOSPHATE SINGLE CRYSTALS DOPED BY CHROMIUM AND TITANIUM <u>Bolshakova N.</u> , Efimov N., Bushinsky M., Mudryi A., Turchenko V., Efimov V.....	146
TRANSFORMATION OF LATTICE POINT DEFECTS UNDER INFLUENCE OF LIGHT PULSES IN IRRADIATED LiF CRYSTALS <u>Bryukvina L.I.</u> .....	147
INFLUENCE OF DISLOCATIONS AND TOPOLOGICAL DEFECTS IN THIN SMECTIC FILMS ON STRUCTURE AND POLAR CHARACTERISTICS <u>Dolganov P.V.</u> , Shuravin N.S., Dolganov V.K., Fukuda A.....	148
ATOMIC SCALE TUNING OF QUANTUM DOT NUCLEATION AND EPITAXIAL GROWTH WITH STRAIN INDUCED TECHNIQUES <u>Dvurechenskii A.</u> , Smagina Zh.V., Zinoviev V.A., Rudin S.A., Nenashev F.V., Novikov P.L., Rodyakina E.E., Fomin B.I. ....	149
STRAIN-DRIVEN SELF-ASSEMBLY OF PLASMONIC NANO-VOIDS AND DOTS IN SiGeSn/Si MULTILAYERS <u>Gaiduk P.</u> .....	150
GROWTH OF Ho <sub>0,9</sub> Er <sub>0,1</sub> Fe <sub>3</sub> (BO <sub>3</sub> ) <sub>4</sub> FROM SOLUTIONS BASED ON Bi <sub>2</sub> Mo <sub>3</sub> O <sub>12</sub> AND Li <sub>2</sub> WO <sub>4</sub> <u>Gudim I.</u> , Demidov A., Eremin E., Shukla D.K.....	151
NUCLEATION AND EQUILIBRIUM DENSITY OF MISFIT DISLOCATION LOOPS IN CORE-SHELL NANOWIRES Kolesnikova A.L., Chernakov A.P., <u>Gutkin M.Yu.</u> , Romanov A.E. ....	152
PARTITIONING AND SEGREGATION IN 12Cr Fe-BASE OXIDE DISPERSION STRENGTHENED STEEL <u>Jang J.</u> , Mao X., Oh K.H., Rogozhkin S.V., Han C.H., Kim T.K. ....	153
SYNTHESIS, GROWTH AND STRUCTURAL FEATURES OF NEW RARE EARTH BORATE KCaNd(BO <sub>3</sub> ) <sub>2</sub> <u>Kononova N.G.</u> , Kuznetsov A.B., <u>Shevchenko V.S.</u> , Uralbekov B.M., Bolatov A.K., Kokh A.E., Simonova E.A. ....	154



EFFECT OF DOPING WITH RARE-EARTH OXIDES ON THE STRUCTURAL AND MECHANICAL CHARACTERISTICS OF ZIRCONIA CRYSTALS PARTIALLY STABILIZED BY YTTRIA	
<u>Kulebyakin A.V.</u> , Alisin V.V., Borik M.A., Lomonova E.E., Milovich F.O., Myzina V.A., Osiko V.V., Ryabochkina P.A., Sidorova N.V., Tabachkova N. Yu. ....	155
GROWTH AND STRUCTURAL STUDY OF THE NEW LITHIUM BARIUM BORATE $\text{Li}_3\text{Ba}_4\text{Sc}_3\text{B}_8\text{O}_{22}$	
<u>Kuznetsov A.</u> , Ezhov D., Kononova N., Kokh A., Uralbekov B. ....	156
OPTICAL PROPERTIES OF DEFECTIVE CDMNSE EPITAXIAL FILMS	
<u>Mehrabova M.</u> , Nuriyev H., Hasanov N., Kazimova A., Safarov N., Sadigov R. ....	157
EFFECT OF GAMMA IRRADIATION ON CONDUCTIVITY OF CdFeTe	
<u>Mehrabova M.</u> , Nuriyev H., Orujov H., Kerimova T., Abdullayeva A., Hasanov N., Nazarov A. ....	158
EFFECT OF LOCAL CRYSTAL STRUCTURE AND PHASE COMPOSITION ON TRANSPORT PROPERTIES OF SOLID SOLUTIONS $\text{ZrO}_2\text{-Y}_2\text{O}_3$ AND $\text{ZrO}_2\text{-Gd}_2\text{O}_3$	
<u>Milovich F.</u> , Volkova T., Agarkova E. ....	159
LOW-TEMPERATURE THERMOCYCLING AS A NEW METHOD OF EXPULSION OF QUENCHING DEFECTS FROM THE PEIERLS CONDUCTOR ORTHORHOMBIC TANTALUM TRISULFIDE	
<u>Minakova V.E.</u> , Nikitina A.M., Zaitsev-Zotov S.V. ....	160
STRUCTURE, THERMOPHYSICAL AND ELECTROPHYSICAL PROPERTIES OF SINGLE CRYSTALS OF SOLID SOLUTIONS BASED ON ZIRCONIUM DIOXIDE, CO-DOPED WITH SCANDIUM, YTTRIUM AND CERIUM	
<u>Popov P.A.</u> , Borik M.A., Kulebyakin A.V., Lomonova E.E., Kuritsyna I.E., Milovich F.O., Myzina V.A., Tabachkova N. Yu. ....	161
PERSPECTIVE MATERIALS FOR PHOTONICS BASED ON $\text{LiBa}_{12}(\text{BO}_3)_7\text{F}_4$ FLUORIDE BORATES CRYSTALS GROWN IN THE Li, Ba, B // O, F QUATERNARY RECIPROCAL SYSTEM	
<u>Simonova E.</u> , Kokh A., Kononova N., Kuznetsov A., Schevchenko V., Svetlichny V. ....	162
EFFECTIVE CHARGE IN $\text{LiNbO}_3$ FILMS FABRICATED BY RADIO-FREQUENCY MAGNETRON SPUTTERING METHOD	
Dybov V., Serikov D., Belonogov E., <u>Sumets M.</u> ....	163
STRUCTURAL AND OPTICAL RESEARCH OF A GaAs LAYER GROWN ON A $\text{Si}/\text{Al}_2\text{O}_3$ SUBSTRATE	
<u>Sushkov A.A.</u> , Pavlov D.A., Shengurov V.G., Denisov S.A., Chalkov V.Yu., Baidus N.V., Rykov A.V., Kryukov R.N. ....	164
CROSS-SECTIONAL STUDIES OF HEXAGONAL Ge INCLUSIONS IN THE Ge/Si (001) STRUCTURE	
<u>Sushkov A.A.</u> , Pavlov D.A., Krivulin N.O., Kochugova E.S., Murtazin R.I. ....	165
INFLUENCE MECHANISM OF TEMPERATURE ON THE LATTICE MISFIT AND ELASTIC MODULE IN Mo-RICHEN $\text{Ni}_3\text{Al}$ BASED SINGLE CRYSTAL SUPERALLOY	
<u>Zeng X.</u> ....	166
CHARACTERISTICS OF THE COMPOSITION, PURITY AND HOMOGENEITY OF SUBSTANCES IN THE MATERIAL SCIENCE	
<u>Zlomanov V.P.</u> , Gaskov A.M. ....	167
<b>SESSION “Fundamental problems (nucleation theory, phase transitions etc.) ”</b> .....	<b>168</b>
LOW DIMENSIONAL NANOSTRUCTURE GROWTH ON ANISOTROPIC SILICON (110) RECONSTRUCTION SURFACE	
<u>Asaoka H.A.</u> ....	168

IDEAL AND ULTIMATE TENSILE STRENGTH OF SOLIDS: MOLECULAR DYNAMICS MODELING <u>Baidakov V.G.</u> .....	169
ATOMISTIC MODELING OF SOLID-STATE PHASE TRANSITIONS IN POLY(3-ALKYLTHIOPHENES): FROM FORM II TO FORM I POLYMORPHS <u>Casalegno M.</u> , Nicolini T., Famulari A., Raos G., Po R., Meille S.V.....	170
MICRO-CANONICAL DESCRIPTION OF GROWTH AND THERMAL DECOMPOSITION OF ALUMINA CLUSTERS <u>Chemin A.</u> , Allouche A.-R., Melinon P., Miyajima K., Mafuné F., Amans D. ....	171
A FLOW EFFECT ON DISTRIBUTION OF SUPERCRITICAL NUCLEATION CENTERS DURING THE CRYSTALLIZATION PROCESS ILLUSTRATED BY THE EXAMPLE OF BORON CARBIDE-REINFORCED ALUMINUM <u>Eydelman E.D.</u> , <u>Durnev M.A.</u> .....	172
THE EVOLUTION OF POST-CRITICAL NUCLEATION CENTERS OF THE CRYSTALLIZATION PROCESS AT THE CENTRIFUGAL-CASTING METHOD FOR DESIGN OF GRADIENT COMPOSITES OF ALUMINUM AND GRAPHITE <u>Eydelman E.D.</u> , <u>Durnev M.A.</u> .....	173
THE CRYSTALLIZATION PROCESS IN THE PRESENCE OF A FLOW <u>Eydelman E.D.</u> , <u>Durnev M.A.</u> .....	174
STRIATION IN MELT-GROWN CRYSTALS AS A SELF-OSCILLATING PROCESS <u>Fedorov P.P.</u> , <u>Kuznetsov S.V.</u> , <u>Konyushkin V.A.</u> , <u>Nakladov A.N.</u> , <u>Chernova E.V.</u> .....	175
NON-CLASSICAL CRYSTAL GROWTH OF FLUORIDES AND OXIDES <u>Fedorov P.P.</u> , <u>Kuznetsov S.V.</u> , <u>Mayakova M.N.</u> , <u>Maslov V.A.</u> , <u>Baranchikov A.E.</u> , <u>Gaynutdinov R.V.</u> , <u>Ivanov V.K.</u> , <u>Osiko V.V.</u> .....	176
A MODEL OF SHAPES OF LIQUID CYLINDRICAL INCLUSIONS MIGRATING THROUGH A CRYSTAL, AND ITS APPLICATIONS FOR STUDYING KINETICS OF CRYSTALLIZATION (DISSOLUTION) <u>Garmashov S.</u> .....	177
KINETIC MODEL FOR CONDENSATION-INDUCED RESTRUCTURING OF ATMOSPHERIC SOOT AGGREGATES <u>Gor G.</u> , <u>Enekwizu O.</u> , <u>Khalizov A.</u> .....	178
NUCLEATION EFFECTS IN RECEPTORS CLUSTERING ON A T-CELL'S SURFACE <u>Prihodko I.V.</u> , <u>Guria G.Th.</u> .....	179
THE FASTEST CRYSTAL FORMATION MECHANISM <u>Kashchenko M.</u> , <u>Kashchenko N.</u> , <u>Chashchina V.</u> .....	180
NUCLEATION AND GROWTH OF NEW PHASE NUCLEI IN HETEROGENEOUS REACTIONS <u>Kortsenshteyn N.M.</u> .....	181
DYNAMICS OF NON-STATIONARY GROWTH OF BUBBLES AT DEGASSING OF LIQUID SOLUTION WITH CAPILLARY AND VISCOUS EFFECTS <u>Kuchma A.E.</u> , <u>Shchekin A.K.</u> .....	182
METHOD OF CHEMICAL SUBSTITUTION OF ATOMS IS A NEW METHOD OF GROWING LOW-DEFECTIVE EPITAXIAL FILMS. NANOSCALED SILICON CARBIDE ON SILICON: A NEW BANDGAP MATERIAL FOR MICRO- AND OPTOELECTRONICS <u>Kukushkin S.A.</u> , <u>Osipov A.V.</u> .....	183
PROFESSOR V.V. SLEZOV IS ONE OF THE FOUNDERS OF THE KINETIC THEORY OF FIRST-ORDER PHASE TRANSITIONS <u>Kukushkin S.A.</u> .....	184

CRYSTAL STRUCTURES AND PHASE TRANSITIONS OF ALUMINA AT NANOSCALE: A THEORETICAL STUDY BASED ON A BENCHMARKING OF EMPIRICAL POTENTIALS <u>Laurens G.</u> , Amans D., Allouche A.-R. ....	185
CRYSTAL NUCLEATION- AND CRYSTAL GROWTH-CONTROLLED FORMATION OF BULK METALLIC GLASSES <u>Louzguine-Luzgin D.V.</u> .....	186
SIMULATION OF NUCLEATION BY FREE ENERGY DENSITY FUNCTIONAL METHOD <u>L'vov P.E.</u> , Svetukhin V.V., Bulyarskii S.V. ....	187
CRYSTALLINE NUCLEATION IN AMORPHOUS MATERIALS UNDER SHEAR DEFORMATION <u>Mokshin A.V.</u> , Galimzyanov B.N. ....	188
AB INITIO METHODS IN THE DESCRIPTION OF PHASE TRANSITIONS AND INTERMEDIATE AND TRANSITION STATES <u>Kukushkin S.A.</u> , <u>Osipov A.V.</u> .....	189
DYNAMICS OF CRYSTAL NUCLEATION IN DEEPLY SUPERCOOLED METALLIC MELT <u>Pisarev V.V.</u> , Kirova E.M. ....	190
AMENDING CRYSTALLISATION DRIVING FORCE TO ASSESS THE GLASS FORMING ABILITY OF MELTED METALLIC GLASSES <u>Roula A.</u> , <u>Ikhlef E.</u> .....	191
CRYSTALLIZATION OF GLASS-FORMING MELTS: NEW ANSWERS TO OLD QUESTIONS <u>Schmelzer J.W.P.</u> .....	192
NUCLEATION OF Sb <sub>2</sub> S <sub>3</sub> IN THIN FILM Ge-Sb-S <u>Martinková S.</u> , <u>Shánelová J.</u> , <u>Málek J.</u> .....	194
MOLECULAR COMPONENT OF THE DISJOINING PRESSURE IN DROPLETS AT HETEROGENEOUS NUCLEATION <u>Shchekin A.</u> , <u>Lebedeva T.</u> , <u>Suh D.</u> .....	195
SUPERFAST DOMAIN WALL MOTION AND GROWTH OF DENDRITE DOMAINS IN FERROELECTRICS. ANALOGY WITH CRYSTAL GROWTH <u>Shur V.Ya.</u> , <u>Akhmatkhanov A.R.</u> , <u>Esin A.A.</u> , <u>Chuvakova M.A.</u> .....	197
MODEL OF NUCLEATION LIMITED BY ANOMALOUS GRAIN-BOUNDARY DIFFUSION <u>Sibatov R.</u> , <u>Svetukhin V.</u> .....	198
DOPING LIMIT IN GaAs:Te AS A DISORDER TO (PARTIAL LOCAL) CHEMICAL SHORT-RANGE ORDER TRANSITION IN CRYSTALLINE ALLOY - ELECTRICAL AND DIFFUSE X-RAY SCATTERING STUDIES USING ANNEALING <u>Slupinski T.</u> .....	199
UNUSUAL TEMPERATURE INDUCED SHORTENING OF C(sp <sup>3</sup> )-C(sp <sup>3</sup> ) BOND LENGTH IN BIBENZYL COMPOUNDS IN CRYSTAL STATE: OBSERVATION AND EXPLANATION <u>Smirnov A.</u> , <u>Odintsova O.</u> , <u>Shirin O.</u> , <u>Starova G.</u> , <u>Solovyeva E.</u> .....	200
WATER CONDENSATION AND ATMOSPHERIC PHENOMENA <u>Smirnov B.M.</u> .....	201
PREPARATION AND FORMATION MECHANISM OF NANO-Mg MATERIALS PREPARED BY PHYSICAL VAPOR DEPOSITION <u>Song X.</u> , <u>Su H.</u> , <u>Liu J.</u> , <u>Zhang B.</u> .....	202
EFFECT OF DIFFUSION ON NUCLEATION OF DISLOCATION LOOPS <u>Sorokin M.</u> .....	203
VAPORIZATION AND THERMODYNAMIC PROPERTIES OF OXIDE SYSTEMS AND MATERIALS: FROM BORATE TO HAFNATE	

<u>Stolyarova V.</u> .....	204
STRUCTURAL CHANGE OF AGGREGATES OF MAGNETIC NANOPARTICLES IN ROTATING MAGNETIC FIELD	
<u>Storozhenko A.</u> , Stannarius R., Shabanova I., Arefyev I. ....	205
SELF-ASSEMBLY PROCESSES OF ARRAYS OF CdS NANOCRYSTALS SYNTHESIZED USING THE LANGMUIR-BLODGETT METHOD	
<u>Svit K.</u> , Duda T., Kozhuhov A., Zhuravlev K. ....	206
THERMODYNAMICS OF NANOSIZED SESSILE DROPLETS ON SOLID SUBSTRATE: CONTACT ANGLE, ADSORPTIONS AND LINE TENSION	
<u>Tatyanenko D.V.</u> , Shchekin A.K. ....	207
ANISOTROPY IN THE ELASTICITY OF CRYSTALS: FUNDAMENTAL SOLUTION, DEFECTS, NONLINEARITIES, HARDNESS, HETEROSTRUCTURES – APPROXIMATIONS, AB INITIO AND FINITE-ELEMENT STUDIES	
<u>Telyatnik R.S.</u> .....	209
METHOD OF MATCHED ASYMPTOTIC EXPANSIONS TO CALCULATE THE RADIUS OF A DISPERSED PARTICLE IN THE PROCESS OF ITS HOMOGENEOUS GROWTH	
<u>Tropp E.A.</u> , Galaktionova N.E., Galaktionov E.V. ....	210
BIFURCATION THEORY OF PLASTICITY, DAMAGE AND FAILURE	
<u>Umantsev A.R.</u> .....	211
DIFFUSE $\alpha$ - $\beta$ PHASE TRANSITION IN THE SURFACE LAYERS OF QUARTZ	
<u>Vettegren V.I.</u> , Mamalimov R.I., Sobolev G.A., Ponomarev V.A., Kulik V.B. ....	212
DETERMINATION OF THE CRITICAL NUCLEI SIZE OF POLYMER FOLDED CHAIN CRYSTALS VIA A MICROSCOPIC KINETICS MODEL	
Zhang S.J., Guo B.H., <u>Xu J.</u> .....	213
UNIFIED TEMPERATURE SCALE FOR DESCRIPTION OF CRYSTALLIZATION KINETICS IN SUPERCOOLED LIQUIDS AND GLASSES	
<u>Yarullin D.T.</u> , Galimzyanov B.N., Mokshin A.V. ....	214
ON THE PROBABILITY-FREE MECHANISM OF MACROSCOPIC IRREVERSIBILITY AND MICROSCOPIC FOUNDATION OF THERMODYNAMICS	
<u>Zakharov A.Yu.</u> .....	215
PHASE DIAGRAM CALCULATION IN THE GENERALIZED LATTICE MODEL	
<u>Zakharov M.A.</u> .....	216
PHASE FIELD SIMULATION OF LITHIUM DIFFUSION AND DIFFUSION-INDUCED STRESSES IN BATTERY ELECTRODES WITH CONSIDERATION OF PHASE SEPARATION	
Song Y., <u>Zhang J.</u> .....	217
THE FLUCTUATION STAGE OF PHASE TRANSITION: NON - EQUILIBRIUM KINETICS	
<u>Zmievsckaya G.I.</u> .....	218
SHEAR INDUCED MARTENSITIC TRANSFORMATIONS IN CRYSTALLINE POLYETHYLENE: DIRECT MD SIMULATION	
Strelnikov I.A., <u>Zubova E.A.</u> .....	219
ON THE THEORY OF NUCLEATION AND GROWTH IN HIGH-TEMPERATURE SYNTHESIS OF COLLOIDAL QUANTUM DOTS	
Razumov V.F., <u>Tovstun S.A.</u> .....	220
TRAVELLING WAVE SOLUTIONS FOR THE PENROSE-FIFE PHASE FIELD MODEL	
Mchedlov-Petrosyan P. O., <u>Davydov L. N.</u> .....	221
CONTROLLED NUCLEATION OF NANOPORES IN GLASS OPTICAL FIBERS UNDER POWERFUL LIGHT ILLUMINATION AND TENSILE STRESS	
<u>Shlyagin M.</u> , Kukushkin S.A.....	222
AUTHORS INDEX .....	
	237

## AUTHORS INDEX

### A

Abdullayeva A. ....	158
Abramov A.S. ....	71
Afanas'ev M. ....	19
Agarkova E. ....	159
Agostiano A. ....	144
Akasaki I. ....	100
Akhmatkhanov A.R. ....	197
Aleksandrova O.A. ....	45
Alekseev A.S. ....	5
Alikin D.O. ....	71
Alisin V.V. ....	155
Allouche A.-R. ....	171, 185
Amans D. ....	171, 185
An P. ....	88
Andrianov R. ....	49
Angeluts A.A. ....	48
Anton A.M. ....	49
Antonova I.V. ....	40
Aoudj S. ....	126
Arefyev I. ....	205
Asaoka H.A. ....	168
Ashkinazi E. ....	70
Atanova A.V. ....	6

### B

Baidakov V.G. ....	169
Baidus N.V. ....	164
Baik M. ....	38
Baklanova N.I. ....	137
Bakranova D.I. ....	59, 93
Baran N. ....	33
Baranchikov A.E. ....	176
Baranovskii S.D. ....	7
Baranowski J.M. ....	97
Baturin I.S. ....	71
Beddek S. ....	126
Beisenkhanov N.B. ....	59, 93
Belonogov E. ....	163
Belysheva D.N. ....	82
Benemanskaya G. ....	94, 118
Berdnikov Y. ....	8
Berdnikov Y.S. ....	72
Berezner A. ....	9
Beskrovnyi A. ....	9
Bessolov V.N. ....	113, 117
Bityurin N. ....	12
Bockowski M. ....	95
Bogdanov A. ....	145
Bogdanov S.P. ....	67
Bolatov A. ....	39
Bolatov A.K. ....	154
Bolshakov A. ....	70, 96, 99
Bolshakova N. ....	146
Borik M.A. ....	155, 161
Borisenko N. ....	119
Borshchev O.V. ....	50, 52, 63
Bounar N. ....	10
Bouravleuv A. ....	11, 106, 118

Braescu L. ....	121
Brandt O. ....	101
Bredikhin V. ....	12, 122
Bryukvina L.I. ....	147
Bulyarskii S.V. ....	187
Bushinsky M. ....	146

### C

Caban P. ....	110
Caban P.A. ....	97
Carino A. ....	78
Casalegno M. ....	170
Cervellino A. ....	78
Chae J. ....	128
Chalkov V.Yu. ....	164
Chashchina V. ....	180
Chemin A. ....	171
Chen Ch.-P. ....	123
Cherkashin N. ....	13
Chernakov A.P. ....	152
Chernev I.M. ....	28
Chernov A.A. ....	14
Chernova E.V. ....	175
Chetverikov A. ....	120
Chezganov D.S. ....	71
Chilyasov A.V. ....	15
Cho M.-H. ....	38, 128
Cho S.Y. ....	133
Chuvakova M.A. ....	197
Ciepielewski P. ....	97
Cirlin G. ....	96, 98, 102, 111
Cirlin G.E. ....	46
Comparelli R. ....	144
Courac A. ....	16
Curri M.L. ....	144

### D

Dai B. ....	70
Das Mahapatra S. ....	18
Davydov L.N. ....	221
Demchenko P.S. ....	54
Demidov A. ....	151
Demina P. ....	51
Denisov S.A. ....	164
Denisyuk I.Yu. ....	48
Depalo N. ....	144
Đerek V. ....	33
Dergachev A.I. ....	103
Derkatchenko L.I. ....	37
Dibenedetto C.N. ....	144
Dolganov P.V. ....	148
Dolganov V.K. ....	148
Domnin I.N. ....	5
Dorokhin M. ....	51
Drouiche N. ....	126
Dubrovskii V.G. ....	17
Duda T. ....	206
Duffar T. ....	121
Dumiszewska E. ....	97
Durnev M.A. ....	172, 173, 174

Dutta I. ....	18
Dvurechenskii A. ....	149
Dybov V. ....	163

---

## **E**

Ebeling W. ....	120
Efimov N. ....	146
Efimov V. ....	146
Egorov E. ....	19
Egorov N.N. ....	22
Egorov V. ....	19
Emelchenko G.A. ....	66, 83, 84
Endres F. ....	119
Enekwizu O. ....	178
Ensinger W. ....	57, 58
Eremin E. ....	151
Ermachikhin A. ....	85
Erofeeva I. ....	51
Esin A.A. ....	197
Evstigneev V.S. ....	15
Evtikhiev V.P. ....	112
Eydelman E.D. ....	172, 173, 174
Ezhov D. ....	156

---

## **F**

Faizullin M.Z. ....	20
Famulari A. ....	170
Fanizza E. ....	144
Fedorov P.P. ....	175, 176
Fedorov V. ....	9, 96, 99
Fedorov V.A. ....	21
Fedotov S.D. ....	22
Feldhoff A. ....	127
Feldman L. ....	110
Fernández-Garrid S. ....	101
Figiel L. ....	124
Filimonov S.N. ....	30
Firek P. ....	97
Fokina M.I. ....	48
Fomin A.A. ....	142
Fomin B.I. ....	149
Freidin A.B. ....	124
Fukuda A. ....	148
Fursova T. ....	9

---

## **G**

Gaca J. ....	97
Gaiduk P. ....	23, 150
Galaktionov E.V. ....	24, 25, 210
Galaktionova N.E. ....	24, 25, 210
Galimzyanov B.N. ....	188, 214
Galitsyn Yu.G. ....	44, 104, 105
Gangrskaya E.S. ....	65
Garmashov S. ....	26, 177
Gaskov A.M. ....	167
Gaynutdinov R.V. ....	176
Gebavi H. ....	33
Geelhaar L. ....	101
Gerasimenko A.V. ....	28
Glas F. ....	27

Golubkov S.A. ....	22
Gor G. ....	178
Gouralnik A.S. ....	28
Grashchenko A.S. ....	125
Grebenev V.A. ....	43
Grebenev V.V. ....	42, 48, 52, 53, 66, 79
Grigorieva M.S. ....	84
Gudim I. ....	151
Guo B.H. ....	213
Guo T. ....	88
Guria G.Th. ....	179
Gurin V.N. ....	37
Gusarov V.V. ....	29
Gutakovskii A.K. ....	28
Gutkin M.Yu. ....	117, 152

---

## **H**

Han C.H. ....	153
Hasanov N. ....	157, 158
Hecini M. ....	126
Hervieu Yu.Yu. ....	30
Heya A. ....	60
Hien T.T. ....	132
Hinterding R. ....	127
Hong S.-B. ....	128
Hu K. ....	71
Hu Z.-F. ....	129

---

## **I**

Ievlev V.M. ....	31
Igo A.V. ....	32
Ikhlef E. ....	191
Ilkiv I. ....	11
Inamura M. ....	130
Ingrosso C. ....	144
Ishizaki T. ....	130
Ivanda M. ....	33
Ivanov A.B. ....	5
Ivanov V.K. ....	176
Ivanova A. ....	34
Iwai H.I. ....	35
Iwaya M. ....	100

---

## **J**

Jang J. ....	153
Jeong K. ....	128
Jong-Hyun L. ....	131
Julsgaard B. ....	110

---

## **K**

Kablukova N.S. ....	54
Kadivar E. ....	36
Kaganer V. ....	101
Kalashnikov E.V. ....	37
Kalmykov A.E. ....	117
Kaminskii A.A. ....	48
Kamiyama S. ....	100
Kanasugi K. ....	68

Kang H.-K.	38
Kaptelov E. Y.	64
Kaptelov E. Yu.	114
Karyev L.G.	21
Kashchenko N.	180
Kashchenko M.	180
Kazarova O.P.	107
Kazimova A.	157
Keiinbay S.	59, 93
Kerimova T.	158
Khalizov A.	178
Kharlamov V.S.	109
Khelfane A.	77
Khmelenin D.N.	6
Khodzitsky M.K.	54
Khomich A.	70
Khrapova E.K.	29
Kim C.	132
Kim D.	132
Kim D.-K.	128
Kim H.	128
Kim J.-H.	38
Kim T.K.	153
Kim T.Y.	133
Kimmel A.	145
Kirilenko D.	99, 102
Kirova E.M.	190
Kiselev D.A.	64, 114
Kochugova E.S.	165
Kokh A.	39, 156, 162
Kokh A.E.	154
Kokh K.	39
Kokh K.A.	40
Koldaeva M.V.	66
Kolesnikova A.L.	152
Kolobov A.Yu.	41
Komlenok M.	70
Komornikov V.A.	42, 43, 79, 92
Kompan M.E.	113
Konenkova E.V.	113
Konfederatova K.A.	44
Kononova N.	39, 156, 162
Kononova N.G.	154
Konyushkin V.A.	175
Korepanov O.A.	45
Koropov O.V.	134
Koryakin A.A.	46, 47
Kossack W.	49
Kotlyar K.	102, 111
Kotlyar K.P.	46, 47
Kortsenshteyn N.M.	181
Koval O.	99
Kovalev S.I.	84
Kovalyov S.I.	53, 55
Koverda V.P.	20
Kozhuhov A.	206
Kozlova N.N.	48
Kozyukhin S.	85
Krasilin A.A.	29
Kremer F.	49
Krivtsov A.	135
Krivulin N.O.	165
Kryukov R.N.	164
Kryzhanovskaya N.	96
Kuchma A.E.	182

Kukushkin S.	11, 94, 106, 111, 118
Kukushkin S.A.	46, 65, 114, 115, 117, 125, 138, 183, 184, 189
Kulebyakin A.V.	155, 161
Kulik V.B.	212
Kulishov A.A.	50, 52, 63
Kuritsyna I.E.	161
Kustov D.A.	40
Kuznetsov A.	39, 156, 162
Kuznetsov A.B.	154
Kuznetsov S.V.	175, 176
Kuznetsov Y.	51

---

## L

Lahiri A.	119
Latyshev A.	61
Laurens G.	185
Lazarenko P.	85
Lebedeva T.	195
Lebedev-Stepanov P.V.	52
Lebiadok Ya.V.	105
Ledentsov N.	13
Lee E.-H.	38
Lee W.G.	133
Leshchenko E.D.	47
Lesnikov V.	51
Levitskii I.V.	112
Li S.	141
Li X.-Y.	129
Lihachev A.	102
Liu J.	202
Lomonova E.E.	155, 161
Louzguine-Luzgin D.V.	186
Lozanov V.V.	137
Lü Sh.	88
Lubov M.N.	109
Lukashova M.V.	103
Lundin W.V.	112
L'vov P.E.	187
Lyasnikova M.S.	50, 52, 53, 63, 66

---

## M

Mafuné F.	171
Makarova E.S.	54
Makarova I.P.	42
Málek J.	194
Malin T.V.	44, 104, 105
Mamalimov R.I.	212
Manomenova V.L.	48, 53, 55, 66, 83, 84
Mansurov V.G.	44, 104, 105
Mao X.	153
Martinková S.	194
Masalov V.M.	66, 83, 84
Maslov V.A.	176
Matsuo N.	60
Mayakova M.N.	176
Mazing D.S.	45
Mchedlov-Petrosyan P. O.	221
Mehrabova M.	157, 158
Meille S.V.	170
Melinon P.	171

Michalowski P.	97, 110
Mikac L.	33
Milakhin D.S.	44, 104, 105
Milovich F.	159
Milovich F.O.	155, 161
Minakova V.E.	160
Mitrofanov M.I.	112
Miyajima K.	171
Miyake H.	100
Miyashita T.	130
Mizerov A.	106, 118
Mizutani T.	56
Mohammed A.S.A.	78
Moiseev A.N.	15
Mokhov E.	108
Mokhov E.N.	107
Mokshin A.V.	188, 214
Morozov A.V.	124
Morozova N.B.	137
Moshabaki A.	36
Moshnikov V.A.	45
Mozdzonek M.	97
Mozharov A.	96, 99
Mudryi A.	146
Muench F.	57, 58
Mukhin I.	96, 99
Muller W.H.	124
Murtazin R.I.	165
Myasnikova A.	69
Myasoedov A.V.	117
Myzina V.A.	155, 161

## **N**

Nagalyuk S.	108
Nakamura R.	60
Nakladov A.N.	175
Nazarov A.	158
Nebogatikova N.A.	40
Nebol'sin V.A.	74
Neimark A.V.	136
Nenashev F.V.	149
Nevedomskiy V.	13
Nicolini T.	170
Nielsen S.	110
Nikanorov S.P.	37
Nikitina A.M.	160
Nikolaev A.	13
Novikov P.L.	149
Novotelnova A.V.	54
Numakura H.	60
Nuriyev H.	157, 158
Nussupov K.Kh.	59, 93

## **O**

Odinets A.	81
Odintsova O.	200
Oh K.H.	153
Okuda K.	56
Okugawa M.	60
Orlova T.A.	113
Orujov H.	158

Osiko V.V.	155, 176
Osipov A.	111
Osipov A.V.	117, 125, 183, 189
Osipov V.V.	64
Ostrovskaya A.A.	63
Ozheredov I.A.	48

## **P**

Palahouane B.	126
Panniello A.	144
Panteleev V.N.	113
Parkhomchuk E.V.	80
Pavlikov A.	9
Pavlov D.A.	164, 165
Pavlushin A.D.	116
Pedersen K.	110
Petronella F.	144
Petrov A.	61
Pezoldt J.	109
Pil'nik A.A.	14
Pirogov E.	11
Pisarev V.V.	190
Plotnikov M.V.	142
Plusnin N.I.	62
Po R.	170
Poluektov M.	124
Ponomarenko S.A.	50, 52, 63
Ponomarev V.A.	212
Popok V.N.	110
Popov P.A.	161
Postnikov V.A.	50, 52, 63
Prikhodko I.V.	179
Prizhimov A.S.	31
Prokip V.E.	137
Pronin I.P.	64, 114
Pronin V.P.	64

## **Q**

Quang N.D.	132
------------	-----

## **R**

Ralchenko V.	70
Raos G.	170
Razumets A.A.	105
Razumov V.F.	220
Redkov A.V.	65, 138
Reznik R.	102, 111
Reznik R.R.	46
Ristić D.	33
Rizzi F.	144
Rodin S.N.	112, 113
Rodyakina E.E.	149
Rogilo D.	61
Rogozhkin S.V.	153
Romanov A.E.	152
Roula A.	191
Rubtsova K.	139
Rudin S.A.	149
Rudneva E.B.	48, 53, 55, 66, 83, 84
Rupasov A.	69



Rusakov A.....	69
Rusanov A.I.....	140
Ryabochkina P.A.....	155
Rykov A.V.....	164

---

## S

Sabelfeld K.....	101
Sadigov R.....	157
Safarov N.....	157
Sakai S.....	141
Sakharov A.....	13
Sakharov A.V.....	112
Sapunov G.....	99
Sato K.....	100
Scheglov M.P.....	113
Shevchenko V.....	162
Schick C.....	49
Schmelzer J.W.P.....	192
Selezneva E.V.....	42, 79
Sen G.....	121
Senkevich S.V.....	64
Seredova N.V.....	113
Seregin D.S.....	6
Sergeeva N.M.....	67
Sergeeva O.N.....	114
Serikov D.....	163
Serizawa A.....	68, 130
Shabanova I.....	205
Shalaev A.....	69
Shánelová J.....	194
Sharipova L.L.....	124
Sharofidinov S.....	11, 106, 114
Sharofidinov Sh.Sh.....	115
Shchekin A.....	195
Shchekin A.K.....	182, 207
Shchukin V.....	13
Sheglov D.....	61
Shendrik R.....	69
Shengurov V.G.....	164
Sherchenkov A.....	85
Shevchenko V.....	39
Shevchenko V.S.....	154
Shevlyagin A.V.....	28
Shirin O.....	200
Shiryaev A.A.....	116
Shkurinov A.P.....	48
Shlyagin M.....	222
Shu G.....	70
Shukla D.K.....	151
Shumilin A.I.....	142
Shur V.Ya.....	71, 197
Shuravin N.S.....	148
Sibatov R.....	198
Sibirev N.....	8, 96
Sibirev N.V.....	72
Sibirev V.N.....	72
Sidorova N.V.....	155
Sigov A.S.....	6
Silina M.....	139
Simonova E.....	162
Simonova E.A.....	154
Sinelshchikova O.Y.....	82
Skorokhod R.V.....	134

Slupinski T.....	199
Smagina Zh.V.....	149
Smirnov A.....	200
Smirnov B.M.....	201
Sobolev G.A.....	212
Sobolev M.....	11
Solnyshkin A.V.....	114
Solovyeva E.....	200
Solyankin P.M.....	48
Song J.-D.....	38
Song X.....	71, 202
Song Y.....	217
Sorokin L.M.....	117
Sorokin M.....	203
Sorokina N.I.....	48, 50, 52, 63, 66
Soshnikov I.....	102
Sosnov E.A.....	143
Spitsyn B.V.....	73
Stannarius R.....	205
Starova G.....	200
Statsenko V.N.....	22
Stepko A.S.....	52
Stolyarova V.....	204
Storozhenko A.....	205
Strelnikov I.A.....	219
Striccoli M.....	144
Su H.....	202
Suh D.....	195
Sultan A.A.....	59, 93
Sumets M.....	163
Sung Yoon K.....	131
Surin N.M.....	50, 52
Sushkov A.A.....	164, 165
Svetlichny V.....	162
Svetlichnyi V.....	39
Svetukhin V.....	198
Svetukhin V.V.....	187
Svidchenko E.A.....	50, 52
Sviridov S.I.....	82
Svit K.....	206
Swaikat N.....	74
Sybina Yu.....	85
Sycheva G.A.....	41, 75, 76

---

## T

Ta Ching H.....	108
Tabachkova N.Yu.....	155, 161
Tablaoui M.....	77
Takeuchi T.....	100
Talalaev V.....	111
Tanabe M.....	68
Tatyanenko D.V.....	207
Teklinska D.....	97
Telyatnik R.S.....	209
Tereshchenko O.E.....	40
Testino A.....	78
Teys S.A.....	104
Thorpe R.....	110
Timakov I.S.....	42, 43, 79, 92
Timoshnev S.....	94, 106, 118
Tiuliukova I.A.....	80
Tomin A.S.....	20
Tovstun S.A.....	220

Triggiani L. ....	144
Tropp E.A. ....	24, 25, 210
Tsatsulnikov A. ....	13
Tsatsulnikov A.F. ....	112
Tukmakova A.S. ....	54
Tumarkin A. ....	81
Tumarkin A.V. ....	82
Turakhun A.A. ....	59, 93
Turchenko V. ....	146
Turygin A.P. ....	71
Tyurnina N.G. ....	82
Tyurnina Z.G. ....	82

---

## U

Ubyivok E. ....	11
Ubyivok E.D. ....	46
Umantsev A.R. ....	211
Uralbekov B. ....	39, 156
Uralbekov B.M. ....	154
Usov S.O. ....	112

---

## V

van Treeck D. ....	101
Vasilyeva N.A. ....	66, 83, 84
Vaskevich A. ....	57
Velarde M. ....	120
Verin I.A. ....	66
Vettegren V.I. ....	212
Vinogradov A.V. ....	20
Vischio F. ....	144
Volkova T. ....	159
Voloshin A.E. ....	48, 50, 52, 53, 55, 66, 83, 84
Vorobyov Y. ....	85
Vorotilov K.A. ....	6

---

## W

Wang Z. ....	86
Wojcik M. ....	97
Wolff M. ....	87
Wolfson A.A. ....	107
Wu Sh. ....	88

---

## X

Xu J. ....	213
------------	-----

---


## Y

Yagovkina M.A. ....	37
Yamauchi Y. ....	141
Yang X. ....	89
Yarullin D.T. ....	214
Yasuda H. ....	60
Yoo B. ....	128
Yuritsyn N.S. ....	90, 91

---

## Z

Zainullin O.B. ....	79, 92
Zaitsev-Zotov S.V. ....	160
Zajnullin O.B. ....	42, 43
Zakharov A. Yu. ....	215
Zakharov M.A. ....	216
Zeng X. ....	166
Zhang B. ....	202
Zhang C. ....	127
Zhang J. ....	217
Zhang S.J. ....	213
Zhang T. ....	71
Zhang Y. ....	71, 129
Zhao Z. ....	71, 127
Zhigalina O.M. ....	6
Zhokhov A.A. ....	66, 83, 84
Zhou X. ....	88
Zhu J. ....	70
Zhuravlev E. ....	49
Zhuravlev K. ....	206
Zhuravlev K.S. ....	44, 104, 105
Ziane M.-I. ....	77
Zinoviev V.A. ....	149
Životkov D. ....	33
Zlomanov V.P. ....	167
Zlygostov M. ....	81
Zmievskaia GI. ....	218
Zubova E.A. ....	219
Zulina N.A. ....	48



**MECHANISMS AND NON-LINEAR  
PROBLEMS OF NUCLEATION AND  
GROWTH OF CRYSTALS AND  
THIN FILMS**  
2019